UNIVERSITY OF COPENHAGEN
FACULTY OF HEALTH AND MEDICAL SCIENCES

PhD Thesis

Jens Rithamer Jakobsen

The myotendinous junction: morphology, molecular composition and response to exercise

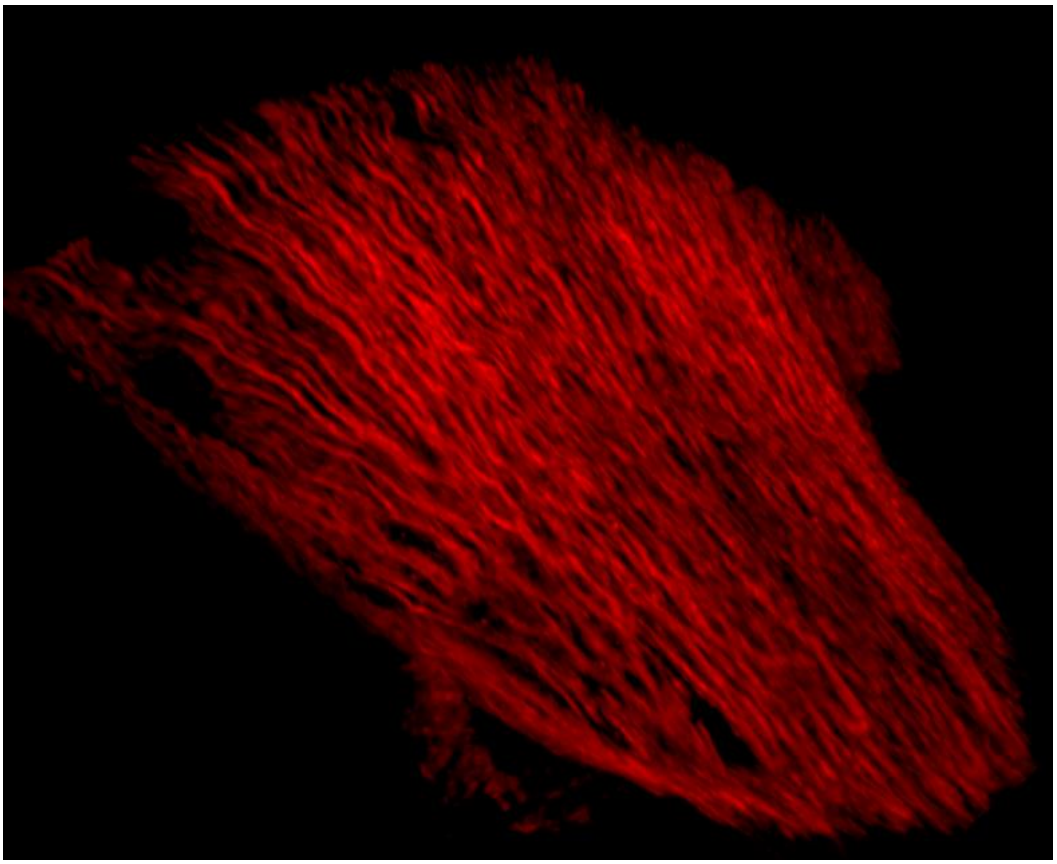

Supervisors: Michael Rindom Krogsgaard and Abigail Mackey

This thesis has been submitted to the Graduate School of Health and Medical Sciences,
University of Copenhagen August 20th, 2021

PhD Thesis

Jens Rithamer Jakobsen
Section of Sports Traumatology, M51, Bispebjerg and Frederiksberg hospital, Copenhagen, Denmark.
Contact details: jens.rithamer.jakobsendk@regionh.dk

Academic supervisors:

Professor Michael Rindom Krogsgaard.
Section of Sports Traumatology, M51, Bispebjerg and Frederiksberg hospital, Copenhagen, Denmark.

Abigail Mackey
Institute of Sports Medicine, Department of Orthopaedic Surgery M, Bispebjerg and Frederiksberg Hospital and Department of Biomedical Sciences, Faculty of Health and Medical Sciences, University of Copenhagen, Denmark.

Assessment Committee

Chair:

Professor Bo Sanderhoff Olsen
Department of Clinical Medicine, Faculty of Health and Medical Sciences, University of Copenhagen, Denmark

Opponents:

Professor Truls Raastad
Department of Physical Performance, Norwegian School of Sport Sciences, Oslo, Norway

Professor Richard Lieber
Department of Physical Medicine and Rehabilitation, Northwestern University, Chicago, IL, USA

Table of contents

Acknowledgements

The work behind this thesis includes work from a lot of talented researchers with different backgrounds. In order to gain insight into the mysteries behind the human MTJ it was necessary to put together a strong team. Therefore, even though I have been front person I think this thesis shows what can be achieved if good collaborations are formed.
My investigations of the human myotendinous junction started back in 2012 where Andreas Knudsen introduced me to this field and his project. I would therefore like to thank Andreas for letting me in on the team and passing the baton to me. Luckily a brilliant supervisor, Michael Krogsgaard, had initiated the project and took me under his wings.
I'm very honored to have worked together with such an intelligent and motivating researcher and doctor as Michael Krogsgaard. Things have not always been easy due to frustrating reviewer comments and grant rejections, but Michaels positive mind and curiosity have inspired me to continue through troublesome times. I hope one day I can be able to teach and inspire young doctors in the same way.
A department is nothing without a good secretary, so therefore I would like to thank Pia Andersen for helping me through the years with everything from salary to egg boilers.

I would also like to thank Michael Kjær for letting me be a part of the environment at the Institute of Sports Medicine Copenhagen (ISMC) and always trusting me and supporting my work. Abigail Mackey for being my co-supervisor and mentor when it comes to muscle research, immunohistochemistry, imaging etc. I have learned a lot since the first time we sat together with a microscope and I hope I can continue to use this knowledge in a meaningful way. Even though things have not always been easy with our projects I have always enjoyed your company and I couldn't have wished for a better co-supervisor.
Also, a great thanks to the other researchers and doctors at ISMC and especially the researchers in "Team Muscle" for bearing over with me through endless hours of horrible myotendinous junction papers in journal club. I have the deepest respect for you and the research you are doing.
Even though it has ruined some of my faith in research and have made it almost impossible to cite any myotendinous junction papers without biting my tongue off, I would like to thank Peter Schjerling for teaching me some valuable lessons about research and statistics.
I would also like to thank Anja and Ann-Christina for helping me in the lab. You made the countless of washing and incubation periods during immunohistochemistry staining more enjoyable.

A special thanks to Jens Hannibal and colleagues from the Department of Clinical Biochemistry. Even though my exchange stay wasn't planned to be there it has meant a lot to me both personally but also to the project. We did something no one has ever done before. Even though it wasn't easy we tried to push the confocal system to the limits of what is physically possible with light microscopy without knowing whether we would succeed or not. That kind of optimism and stubbornness is incredibly inspiring, and I truly hope that our departments can continue to work together in the future.

I would also like to thank the participants who were willing to join the studies and put themselves through the demanding exercise sessions and donate some of their hamstring muscle. Without you this kind of research would not be possible. Also, a great thanks to the surgeons from the Section of Sports Traumatology at Bispebjerg Hospital for providing me with tissue for many years.

Finally, I would like to thank my family for staying by my side and remembering that life is more than research.

Resume (Dansk)

Skeletmuskulatur er et specielt organ bestående af hundredtusindvis af celler, kaldet muskelfibre, som hver især er længere end nogen anden celle i kroppen. I hver ende er muskelfibrene forbundet til bindevæv, oftest en sene. Denne overgang mellem muskelfiber og sene kaldes den myotendinøse overgang (på engelsk myotendinous junction, forkortet MTJ). I denne overgang udveksles kraft under muskelarbejde og bevægelse. Under idræt, og især i discipliner hvor sprint eller spark er involveret, ses en høj forekomst af fibersprængningsskader. Baglårene er særligt udsatte for disse skader, som udgør størstedelen af ikke-kontakt relaterede skader i fodbold. Fibersprængninger ses næsten udelukkende i MTJ og skyldes formentlig hårde og pludselige kraftudviklinger.

Heldigvis har kliniske studier vist, at en stor andel af disse skader kan forebygges ved hjælp af specialiseret excentrisk styrketræning. Det er dog endnu uvist hvorfor denne træningsform er så effektiv til at forebygge fibersprængninger. Derfor vil denne afhandling forsøge at komme et skridt nærmere en forklaring. Selve afhandlingen er baseret på fire selvstændige studier, der alle forsøger at belyse forskellige aspekter af MTJ. De fire studier er opsummeret selvstændigt i nedenstående tekst:

Studie 1: ***Fiber type differences in the surface area of the human myotendinous junction***

I den myotendinøse overgang er hver enkel muskelfiber i kontakt med senen. For at øge arealet af den samlede kontaktflade er muskelmembranen meget foldet i enderne. Disse foldninger fyldes ud af udvoksninger fra senen, der griber fast i muskelfiberen som en masse små fingre. Da disse foldninger øger arealet af kontaktfladen mellem de to væv, betyder det at der er et stort areal, hvor kraften mellem muskel og sene kan udveksles. Dette betyder teoretisk set, at en større mængde kraft kan tolereres, fremfor hvis overfladen var helt glat. Flere dyrestudier har vist at træning har en effekt på størrelsen af disse foldninger og har antydet, at det kan være igennem et øget kontaktfladeareal at excentrisk træning virker forebyggende på fibersprængninger. En ulempe ved disse studier er dog, at de alle har benyttet elektron mikroskopi til at visualisere MTJ. Ved elektron mikroskopi analyseres kun meget små udsnit af enkelte muskelfibre. Det betyder, at man skal fotografere rigtig mange snit for at sikre sig, at man har en repræsentativ måling for den individuelle fiber. Derudover er det tvivlsomt hvorvidt man ved elektron mikroskopi kan skelne mellem type I og II muskelfibre, som har forskellige egenskaber.

I vores studie har vi forsøgt at imødekomme disse metodiske problemer ved at bruge confokal mikroskopi til at scanne MTJ fra hele muskelfibre og efterfølgende foretage en rekonstruktion i 3D for at kunne måle på arealet af hele kontaktfladen i MTJ. På denne måde fås et mål for arealet af kontaktfladen i hele muskelfibre, samtidig med at vi kan skelne mellem langsomme (type I) og hurtige (type II) muskelfibre.

Formålet med studiet var først og fremmest at vise, at man kan bruge confokal mikroskopi til at analysere MTJ, der ellers udelukkende er visualiseret via elektron mikroskopi tidligere. Derudover ville vi også undersøge, om der var forskel på arealet af kontaktfladen i type I og II muskelfibre. Metoden viste sig at være brugbar til at undersøge MTJ fra hele muskelfibre, hvilket muliggør måling på et stort antal fibre. Samtidig var vi i stand til at vise, at kontaktfladen mellem muskel og sene var signifikant større for type I sammenlignet med type II fibre. Dette fund tyder på at type II fibre kan være mere udsatte for fibersprængningsskader end type I fibre. Det kunne derfor tænkes,

at fremtidige forebyggelsesinterventioner med fordel kunne tilpasse deres strategier, så de særligt træner type 2 fibre.

Studie 2: ***Adipocytes are present at murine and human myotendinous junction***

I dette studie ville vi bekræfte en tidligere upubliceret observation, hvor vi havde set forekomst af fedtlignende celler ved MTJ. Dette er aldrig tidligere er dokumenteret i mennesker. Fedtceller er ikke kendt for at være involveret i stabilitet eller kraftoverførsel i væv, snarere tværtimod. Da MTJ er et område, som strukturelt er tilpasset til kraftoverførsel, jf. studie 1, og samtidig er et område, hvor skader hyppigt opstår, er tilstedeværelsen af fedtceller ikke logisk ud fra et biomekanisk synspunkt. I tidligere undersøgelser har vi vist, at der er en kontinuerlig remodellering af muskelfibre tæt ved MTJ, og da det er kendt, at fedtceller andre steder i kroppen er i stand til både at bidrage med energi og også udsende signalmolekyler, kunne det tænkes at fedtcellerne ved MTJ er involveret i dette.
Ved at inkludere biopsier fra både mus og mennesker ville vi kortlægge, om fedtceller var til stede i MTJ i begge arter og hos alle individer. Da de humane forsøgspersoner havde indgået i et træningsprojekt, inden prøverne blev taget, valgte vi også at undersøge, hvorvidt træning havde en påvirkning på antallet af disse celler ved MTJ.
Vi fandt fedtceller ved MTJ i alle vores forsøgspersoner og forsøgsdyr og kunne derfor konkludere, at fedtceller er en del af den normale anatomi af MTJ. Men vi kunne ikke se nogen forskel på antallet af fedtceller hos trænede sammenlignet med utrænede personer.
Tilbage står det åbenlyse spørgsmål: Hvad laver fedtcellerne i MTJ? I andre væv er det foreslået, at fedtceller kan være af betydning for opbygning af væv efter en skade via deres kontakt med immunsystemet, hvor de kan udsende signaler, der tiltrækker bl.a. makrofager, og dermed kan de bidrage til en gendannelse af det ødelagte væv. Da MTJ er et område, der hyppigt bliver skadet, samtidig med at det er et område med en konstant høj aktivitet af de celler, som er involverede i den konstante om- og genopbygning af muskelfibre, kunne det tænkes, at fedtceller findes ved MTJ for at hjælpe med disse processer.

Studie 3: RNA sequencing and immunofluorescence of ***the myotendinous junction of mature horses and humans***

Udover at have en meget speciel arkitektur har nyere studier indikeret, at MTJ indeholder specialiserede cellekerner, der producerer proteiner, som ikke ses andre steder i muskulaturen. Et eksempel på en af disse er collagen type 22, der kun ses ved vævsovergange, herunder MTJ, og som regnes for et protein af meget stor betydning for styrke og funktion af MTJ. Såfremt der er flere proteiner, som er unikke for MTJ, kan de ligeledes være af stor betydning at kende for forståelsen af MTJ, både ud fra et normal-fysiologisk perspektiv, men også i en skadesforebyggende og behandlende kontekst. Derfor valgte vi at undersøge om der findes gener for proteiner, der kun er udtrykt i MTJ og ikke i muskel og sene. Men da selve MTJ primært består af en blanding af muskel og sene, som har meget forskellige protein profiler, er det svært at isolere MTJ. For at imødekomme denne problemstilling, udviklede vi en metode til at opdele en prøve fra MTJ i dets respektive vævsfraktioner: muskel, MTJ og sene. På den måde kunne vi efterfølgende undersøge, om der var nogen gener udtrykt anderledes i MTJ end i de to andre fraktioner.
Til at undersøge dette blev der taget biopsier fra 20 heste. Prøverne blev opdelt i vævsfraktioner og efterfølgende blev niveauerne af de forskellige gener undersøgt ved RT-PCR. Herefter blev sæt af prøver fra de 5 heste, hvor der vurderet ved RT-PCR var bedst separation i henholdsvis muskel, MTJ og sene, udvalgt til videre analyse med RNA-sekventering.
Ved RNA-sekventering fandt vi ingen unikke gener i MTJ. Heller ikke genet kodende for collagen

22 var udtrykt udelukkende i MTJ. Selvom det kan skyldes, at generne ikke nødvendigvis er lokaliseret lige ved siden af de respektive proteiner, kunne der ved opdelingen af en enkelt biopsi i muskel, MTJ og sene komme lidt MTJ-væv med i både muskel og senefraktionerne, hvilket ville udviske eventuelle forskelle. Til trods for dette lykkedes det os at identificere en række gener, der ikke tidligere er observeret ved MTJ, herunder osteocrin, MNS1, lactase og ADAMTS8. Ved immunhistokemisk farvning med antistoffer rettet mod de identificerede proteiner fik vi bekræftet at periostin, nestin, osteocrin, MNS1 og lactase alle er lokaliseret i eller i nærheden af MTJ hos mennesker. Da funktionen af disse proteiner endnu ikke er kortlagt i skeletmuskulatur, er funktionen og dermed også indflydelsen af disse på MTJ fortsat uvis.

Studie 4: A single bout of eccentric exercise increases the expression of nestin and osteocrin in human myotendinous junctions

I det sidste studie valgte vi at bygge videre på de identificerede gener fra RNA-sekventeringen, og vi undersøgte, om ekspressionen af en række udvalgte gener blev påvirket af excentrisk træning. Excentrisk træning er vist i kliniske studier at være effektiv til at forebygge fibersprængninger i MTJ. Derfor var hypotesen, at excentrisk træning vil føre til øgede niveauer af specifikke gener, der på sigt ville føre til nydannelse af proteiner, som kunne have en beskyttende effekt overfor fibersprængningsskader.
Måden, dette blev undersøgt på, var ved at invitere 30 personer til at deltage i et forsøg, hvor de blev tilfældigt fordelt til enten at udføre én træningssession eller ingen træning. Træningssessionen var baseret på excentriske baglårsøvelser og inkluderede Nordic Hamstring, som er den mest benyttede øvelse i de kliniske studier, der undersøger effekten af træning på forekomsten af fibersprængninger. Ligesom hesteprøverne i studie 3 blev de humane prøver opdelt i vævsfraktioner indeholdende hhv. muskel, MTJ og sene og analyseret med RT-PCR.

Vi fandt højere niveauer af generne for nestin og osteocrin i MTJ og sene prøverne i de trænede personer sammenlignet med kontrol-personerne, men ingen forskelle for de øvrige gener. Funktionen af nestin og osteocrin i MTJ er endnu ikke klarlagt, men i fremtidige studier af, hvordan MTJ tilpasser sig til excentrisk træning, kunne man fokusere på disse proteiner.
Til trods for, at træningen var hård nok til, at der var omfattende død af muskelfibre i prøverne fra 3 forsøgspersoner i træningsgruppen, og at de resterende havde et signifikant højere niveau af makrofager i muskelvævet sammenlignet med kontrolpersoner, så vi ingen effekter af træning på antallet af muskelstamceller (satellitceller). Tidligere undersøgelser har ellers vist at disse celler stiger i antal som følge af træning, men vores studie samt et enkelt tidligere om MTJ har ikke kunnet bekræfte, at der er dette respons i MTJ. Det kunne tænkes, at årsagen til denne udeblivende stigning i antal af satellitceller er den store remodelleringsaktivitet, der er af muskelfibre ved MTJ, hvor satellitceller spiller en stor rolle. Det store behov for satellitceller kan derfor betyde, at så snart en celle har delt sig, fusionerer dattercellen med en muskelfiber, og dermed bidrager den ikke til antallet af satellitceller.

Abstract

Skeletal muscle is a specialized organ consisting of hundreds of multinucleated elongated cells called muscle fibers. Each muscle fiber is attached to connective tissue at each end, most often to a tendon, through the myotendinous junction (MTJ). During movement and muscle contraction, force is transmitted through this junction. In sports in general, but especially in disciplines involving sprinting or kicking, there is a high prevalence of strain injuries, and hamstring strain

injuries are the most common of these. This injury type is almost exclusively seen in the MTJ, and is thought to be caused by sudden and forceful contractions. Clinical studies have shown that these injuries can be prevented to a large extent by performing specialized eccentric strength training. However, it is not known why this type of exercise is particularly effective. This thesis aims to provide knowledge about the MTJ in general by investigating its composition and morphology and to examine how the MTJ adapts to eccentric exercise. The thesis is composed of four separate studies that cover various aspects of the MTJ. The four studies are summarized separately in the following:

Study 1: ***Fiber type differences in the interface area of human myotendinous junctions***

At the MTJ each muscle fiber is in contact with the tendon – or a connective tissue sheath. In order to enlarge the area of the interface between the muscle fiber and tendon the muscle membrane is highly folded at the end. Protrusions from the tendon fills these foldings grapping the muscle fiber like a myriad of small fingers. Since these foldings increase the area of the interface, force is exchanged between the muscle and tendon through a larger area compared to a model where the muscle fiber ends at a smooth surface. Theoretically, this means that a stronger force can be tolerated.
Several animal studies have shown that exercise affects the size of the foldings at the MTJ, and they have indicated that exercise could protect against strain injury by increasing the interface area of the MTJ. However, these studies have all used transmission electron microscopy (TEM) to visualize the MTJ. In TEM each slide represents a very small fraction of a muscle fiber, meaning that a large number of sections must be analyzed to obtain a representative measure of the individual muscle fiber. To overcome this disadvantage, the aim of this study was to design a method by which confocal microscopy is used to scan whole muscle fibers into thin sections, merge them to a 3D structure and later in specific software recreate a 3D surface of the muscle fiber, from which we can perform measurements. This allows us to measure the interface area of the MTJ in whole muscle fibers, and in addition it is possible to distinguish between slow (Type I) and fast (Type II) muscle fibers, which is challenging with TEM.

The aim of the study was to show that confocal microscopy can be used to examine MTJ and to investigate if there is a difference in the interface area between the two fiber types.
We found that the method was useful to analyze the interface area of the human MTJ, and that it can be easily applied to a large number of whole muscle fibers. We further showed that the interface area of type I fibers was significantly larger than type II fibers. The smaller interface area of the type II fibers could make them more susceptible to strain injury, and therefore prevention strategies could theoretically benefit from targeting these fiber types in particular.

Study 2: ***Adipocytes are present at murine and human myotendinous junction***

In this study we aimed to confirm a previous, unpublished observation of cells resembling adipocytes at the MTJ. There is no documentation in the literature that adipocytes are present at MTJ. Adipocytes are not known to provide mechanical stability or be able to transmit force in tissues, and since the MTJ is a region which is structurally specialized in force transmitted, and at the same time a region where strain injuries are frequent the presence of adipocytes are counterintuitive. Previous observations have shown a high rate of remodeling of the muscle fibers near the MTJ and since adipocytes are known to be able to provide energy as well as to secrete

signaling molecules, it is possible that the adipocytes at the MTJ are present to aid in the remodeling of muscle fibers.

By including samples from both mice and humans we aimed to analyze the presence of adipocytes in both species. The samples from human subjects were collected from a previous study testing the effects of 4 weeks of resistance exercise on the MTJ, and therefore it was also chosen to examine whether exercise had an effect on the number of these cells.
We found adipocytes present in samples from all subjects, both mice and humans, and we concluded that adipocytes are present in healthy MTJ from these two species as a normal phenomenon. However, there was no difference in the number of adipocytes at the MTJ between our trained and untrained human subjects.
In other tissues adipocytes are known to be important for the repair of tissue by activating the immune system through secretion of adipokines, which attract macrophages and other cells. Since the MTJ is a frequently injured tissue as well as a region with a high rate of remodeling of the muscle fibers and consequently a high activity of the cells involved in these processes, the adipocytes could be present at the MTJ to aid in the coordination and activity of these cells.

Study 3: ***RNA sequencing and immunofluorescence of the myotendinous junction of mature horses and humans***

Recent studies have shown that besides having a specialized structure, the MTJ contains specialized nuclei producing proteins which are not seen elsewhere in the skeletal muscle. An example is collagen type 22, which is only seen in tissue junctions. This collagen type is of great importance for the strength and integrity of the MTJ. Other genes could be unique for MTJ and important for the understanding of the MTJ, both from a basic physiologic perspective but also in an injury prevention and rehabilitation perspective..
Since the MTJ is composed of both muscle and tendon, contents of these tissues will influence the measurements of gene expression and proteins at the MTJ. Therefore, we developed a method in the current study to isolate the MTJ from muscle and tendon and aimed to analyze for unique genes at the MTJ by RNA-sequencing.
Samples were divided in three tissue fractions: muscle, MTJ and tendon and examined by RT-PCR. Set of samples from the 5 horses with the best separation of muscle, MTJ and tendon genes, respectively, were identified by RT-PCR and chosen for RNA-sequencing.
No unique genes were found at the MTJ by RNA-sequencing. This was surprising, in particular for Collagen XXII, which had previously been identified to be present uniquely at the MTJ. This finding could indicate that proteins are produced at other locations than where genes are expressed, or that the separation of the tissue fractions has been suboptimal, resulting in fragments of MTJ tissue in the muscle or tendon fractions.
However, we did identify a list of genes that was more highly expressed at the MTJ compared to tendon suggesting that they could be important for the MTJ. Some of these genes were confirmed to be present at the MTJ on a protein level in human samples by IHC, and they should be subject for further studies in order to fully understand their function at the MTJ.

Study 4: Effect of a single bout of eccentric exercise on gene expression in human MTJ

In the last study we aimed to use the findings from the RNA-sequencing to examine whether the expression levels of the genes, identified to be highly expressed at the MTJ, where affected by a

single bout of eccentric exercise. Clinical studies have shown that eccentric exercise is effective to prevent strain injuries at the MTJ and therefore it was hypothesized that eccentric exercise would induce changes in the synthesis of specific genes of relevance for protection against strain at the MTJ.
This was examined by enrolling 30 subjects randomized to either a single bout of eccentric exercise or no training. The exercise session was composed of eccentric hamstring exercises, including the Nordic Hamstring, which is the most often used exercise in the clinical studies on prevention of strain injuries. The method from study 3 was used to separate the samples into muscle, MTJ and tendon fractions and RT-PCR was used to measure expression levels of mRNA.
We found that the genes coding for osteocrin and nestin were more highly expressed in the exercised group compared to the control group, while no difference was seen for any of the other genes. The specific functions of osteocrin and nestin at the MTJ are not known, but these proteins could be important in the adaptive response of the MTJ to eccentric exercise, and their role should be examined in future studies.
Even though the exercise bout induced necrosis of a large number of muscle fibers in three subjects and a higher concentration of macrophages was seen in the muscle from the other exercised subjects, no effects were seen on the number of satellite cells. Satellite cells have previously been shown to proliferate and increase in number following exercise, however the current study together with one previous study have found that this increase does not occur at the MTJ. We speculate that it could be a dynamic phenomenon due to the high rate of remodeling of the muscle fibers at the MTJ, meaning that once a satellite cell has divided, the daughter cell fuses with a muscle fiber, and does not count in the pool of satellite cells.

General introduction

The function of muscle as a structure to create force is based on two specialized interfaces: The neuromuscular junction and the myotendinous junction (MTJ). At the MTJ individual muscle fibers are connected to the collagen fibrils in the tendon (Figure 1). This is where force is exchanged between muscle and tendon during movement. However, even though transmission of force is fundamental for motion, it is not clear exactly how this is generated. Generally, it is believed that most of the force is transmitted through the MTJ. This is supported by the fact that the MTJ has a unique morphology, which is advantageous for a structure that is specialized in force transmission. At the tip of the muscle fibers the muscle membrane is highly folded forming in-and evaginations with protrusion from the tendon, filling these invaginations (1).

Figure 1 *Scanning electron microscopy image of two muscle fibers approaching the tendon, forming the MTJ. From Tidball JG. Myotendinous junction: morphological changes and mechanical failure associated with muscle cell atrophy. Exp Mol Pathol. 1984 Feb;40(1):1-12.*

Like fingers in a glove the tendon holds the muscle fiber ensuring a large surface area as well as an optimal angle for force transmission. Through these foldings the actin filaments from the muscle is in contact with the collagen fibrils in the tendon providing a path for force transmission. This contact is primarily mediated by adherence of actin to dystrophin and ultimately the dystroglycan complex which attaches dystrophin to laminin on the extracellular side (2). Alternatively, actin is linked to laminin through the vinculin-talin-integrin complex (3).
Because of the large contact area between muscle and tendon these protein complexes are abundant at the MTJ. Previous studies have indicated that their presence is important for optimal function and force transmission through the MTJ by showing impaired transmission of force and high susceptibility towards injury in the absence of some of these proteins (4,5).

Despite this morphological specialization, the MTJ is still a region where injuries in the form of strain injuries are very frequent. In an athletic setting hamstring strain injuries are particular frequent, representing the most common non-contact injury in sports involving high speed running such as football, Australian rules football and athletics (6–8).
Because of this high incidence, there is much focus on prevention of these injuries, and eccentric training has shown to be particularly effective (9–11). However, little is known about how eccentric exercise affects the MTJ. Therefore, in order to explain the clinical observations, there is

need for more basic knowledge about the MTJ. Most studies investigating the MTJ have used animal muscles and have focused on the special morphology of the folded muscle membrane. Electron microscopy has been the preferred imaging technique, and as this thesis will discuss, this has limitations.
Only very few studies have examined the human MTJ and most of them have been published by our group (1,12–14). This is surprising, since there is much focus on MTJ in sports medicine because of the high incidence of hamstring strain injuries.
The reason for this lack of human studies is multifactorial, but one important reason is that a safe method to obtain biopsies of the MTJ from healthy individuals has not been available. Furthermore, the MTJ is a complex region to analyze because it is a delicate mixture of two very distinct tissues, skeletal muscle and tendon. This is highlighted by previous studies reporting exercise induced increases in concentration and gene expression of some of the proteins involved in linking actin to the extracellular matrix, i.e. integrins (15,16). Here the MTJ was not isolated from the general muscle and since these proteins are also present in the costameres it is not possible to tell whether the increase is actually seen in the MTJ . Therefore, in order to apply the more commonly known techniques such as RT-PCR, western blots, proteomics etc., the MTJ must be isolated, or the contribution from adjacent muscle and tendon must be quantified and considered in the interpretation of measurement results.

The aim of this PhD-study was to provide some answers to the issues mentioned above. More specifically to investigate the human MTJ in relation to composition and structure, methods to isolate the individual tissues, and how MTJ is affected by exercise. Furthermore, we aimed to investigate the expression of genes potentially unique to the MTJ as well as the effects of a single bout of exercise on some of the genes that are active at MTJ.

An aim of the PhD was to apply new techniques to how the MTJ is analyzed. Therefore, as much as this thesis will describe the knowledge of the MTJ as well as the newly discovered findings in the attached papers, it will also describe our effort to advance and improve the methods we know today to better and more accurately study the MTJ. This includes improved techniques to analyze the structure of the MTJ by imaging, as well as techniques to analyze composition and gene expression.

1.0 Study I (Fiber type differences in the surface area of the human myotendinous junction)

Injury to the MTJ occurs despite that the region is structurally optimized for force transmission, with the muscle membrane displaying a highly folded surface, increasing the area through which force is distributed. In close-up imaging using transmission electron microscopy (TEM) the muscle membrane forms invaginations, also named finger-like processes, that are filled with collagen fibrils approaching from the tendon (1,17). Due to these collagen-filled invaginations, the angle of force transmission is different compared to a situation where the muscle membrane is a smooth cone-shaped surface. This altered angle of force transmission results in more force transmitted as shear, or sliding, force which is more gentle on the tissue compared to tensile, or pulling force (18). Altogether the increased area and altered angle of force transmission theoretically reduces the stress on the MTJ.

The invaginations of the muscle membrane have been reported to be present in many different muscles from a variety of animals, and also in humans (1,19–25). The 3-dimensional structure has

been illustrated in a study on human hamstring muscles, showing that they form a rather complex network with multiple branching (1). It seems to be agreed on scientifically that following exercise interventions, with treadmill running being the preferred modality, the length and branching of the invaginations increase (20,26–30). The opposite is seen in most of the studies on immobilization in which the surface area decreases (19,31–35). The previous findings are summarized in Table 1.

Studies describing the effect of increased load on the MTJ

Author, year,species	Sample Size pr Group	Muscles/dominant fiber type	Intervention	Method of measurement	Results
Kojima,2008,rat	5	Gastrocnemius/ I Tibialis Ant./II	Running	Branching of fingers Angle of branching	↑
Curzi. 2012,rat	6	Gastrocnemius/ I EDL/II	Running	Branching of fingers	↑
Curzi. 2016. rat	3	EDL/II	Running	Interface length/baseline(IL/B ratio)	↑
Sierra. 2018. rat	3	Soleus/I	Swimming	Length and thickness of invaginations and evaginations	↑
Jacob. 2019. rat	5	Sternomastoid/II	Swimming	IL/B	
Neto J, 2020 rat	10	Plantaris/II	Loaded ladder climb	Length and thickness of invaginations and evaginations	↑

Studies describing the effect of unloading the MTJ

Author, year,species	Sample Size pr Group	Muscles/dominant fiber type	Intervention	Method of measurement	Results
Kannus, 1992. rat	8	Gastrocnemius/II Soleus/I	Immobilization 1 and 3 weeks	Length of surface area in relation to muscle fiber diameter	↓
Tidball 1992. rat	6	Plantaris/II	Space flight -4 davs	Folding factor	↓
Zamora. 1995. rat	2 5	Soleus/I Plantaris/II	Limb suspension for 8, 18 and 29 davs Space flight 14 days	No quantification	Only minor changes observed in Plantar is MTJ's. thinning and lengthening of the foldings at MTJ of Soleus MTJ s
Roffino, 1998. rat	8	Soleus/I	Space flight 14 days	IL B ratio-named normalized interface values by the authors.	↑
Roffino, 2006.monkey	2	Soleus/I +II	Space flight 14 days	No qualification	-
de Palma, 2011,human	12 Unloaded 3 controls	Gastrocnemius/ I+II	Bed rest (mean 60 months) in chronic diseased patients	Length of surface area n relation to muscle fiber diameter	↓
Curzi,2013,rat	4	Plantaris/II	Unloading	IL/B ratio Length of primary digits Brancing of fingers	↓

Table 1: *Studies describing the effects of loading and unloading on the surface area of the MTJ with a description of species used, muscles and muscle fiber types and the method used for measurements. From Jakobsen JR, Krogsgaard MR. The Myotendinous Junction-A Vulnerable Companion in Sports. A Narrative Review. Front Physiol. 2021 Mar 26;12:635561. doi: 10.3389* (36)

Growth of the invaginations increases the surface area further, meaning that force is distributed over an even larger area which theoretically increases the ability of the MTJ to withstand force and potentially lowers the risk of injury. However, a clinical effect on the incidence of strain injuries is seen after periods of heavy eccentric exercise in populations already accustomed to vigorous exercise, including high speed running (9–11). This suggests that this exercise results in different

adaptations than those induced by running, or that those adaptations are further amplified by exercise.

Therefore, future studies examining the effects of eccentric loading on the structure of the human MTJ are needed. The previous studies have used TEM to analyze the folded surface of the MTJ. This technique provides a very high resolution (around 1 nm) and thereby also a high level of detail. However, preparation of slides is time consuming so only a limited number of sections are imaged, meaning that only a small part of the total muscle fiber is measured in a limited number of fibers. Therefore, TEM might not provide imaging representative of the entire muscle fiber as well as all fibers in a muscle. Furthermore, is it questionable whether type I and type II muscle fibers can be clearly distinguished with TEM. While this might not be important in studies investigating murine muscles that have a very homogenous fiber type distribution, it is problematic in human muscles that are far more heterogeneous (37). Here the majority of muscles are composed of a mixture of both type I and type II fibers. Previous studies have indicated, that there is a difference in the anatomical construction of the MTJ surface between type I and type II muscle fibers (25,38,39). It might therefore be important to distinguish between type I and II fibers in analyses of the MTJ surface in species with a heterogeneous fiber type distribution. This can be achieved by analyzing the MTJ with immunohistochemistry (IHC) where the specific fiber types can be labelled with fluorescent antibodies. However, the resolution with regular widefield microscopy is not high enough to distinguish all the small invaginations seen at the MTJ.

Therefore, we aimed to perform a study that took all the aforementioned issues into account and made a method available that can analyze the interface between muscle and tendon in whole muscle fibers and by which it is possible to distinguish between fiber types and to perform the analysis in a blinded and standardized manner. Furthermore, we aimed to examine whether there is difference in the size of the interface area between muscle fiber types.

1.1 Methods (Study I)

The methods are described in detail in the attached manuscript entitled “Fiber type differences in the interface area of human myotendinous junctions” and will only briefly be explained here.

Samples were collected from 10 human subjects scheduled for reconstructive surgery of the anterior cruciate ligament (ACL) at Bispebjerg and Frederiksberg Hospital. During the surgery the semitendinosus tendon with attached muscle was harvested for the graft, and the tendon was used as graft. The MTJ that was in excess was used for this study. Quickly following dissection of the tissue, samples were prepared according to the single-fiber protocol, as described previously (40).

Individual fibers were imaged with a Spinning Disc Confocal microscope and later reconstructed in 3D where a surface-construction plugin in Imaris Bitplane was used to estimate the size of the

surface (see figure 2).

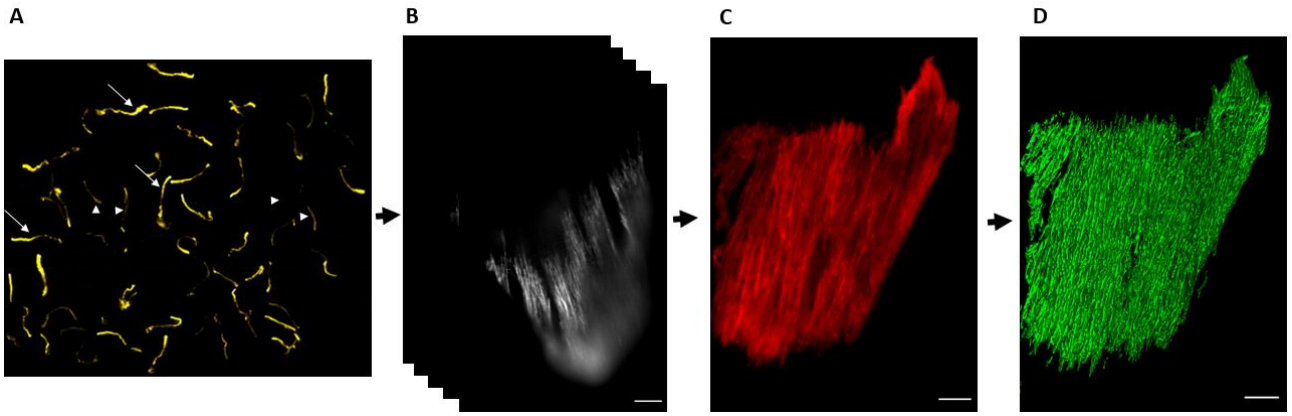

Figure 2:
The figure shows how the 3D-reconstructions were created. First an overview image of the MHC1 staining was taken to identify the typing of each fiber (A). Next a stack of images was taken using a spinning disc confocal microscope where only the collagen XXII staining was imaged (B). This stack of images was combined into a 3D structure (C) which was reconstructed using a specific software into a structure of which it was possible to measure the surface area (D). Scale bars are 10 µm.

Due to large variation in the interface area between the same fiber types from the same subjects Wilcoxon signed rank test was chosen to analyze differences between fiber types. Significance level was set to <0.05.

1.2 Results (Study I)

By 3D-reconstructing each muscle fiber end (figure 3) it was possible to estimate the interface area between muscle and tendon from 314 muscle fibers. The interface area of type I fibers was found to be 38.35 % larger compared to type II fibers (P=0.023) (See figure 4A).
The mean fiber diameter of the two fiber types was the same (53 µm) with a slightly higher percentage of type II fibers in the samples (58%) compared to type I (42%). When expressed relative to the fiber diameter for each fiber, the interface area of type I fibers was still significantly larger than of type II fibers (P= 0.008) (See figure 4B).

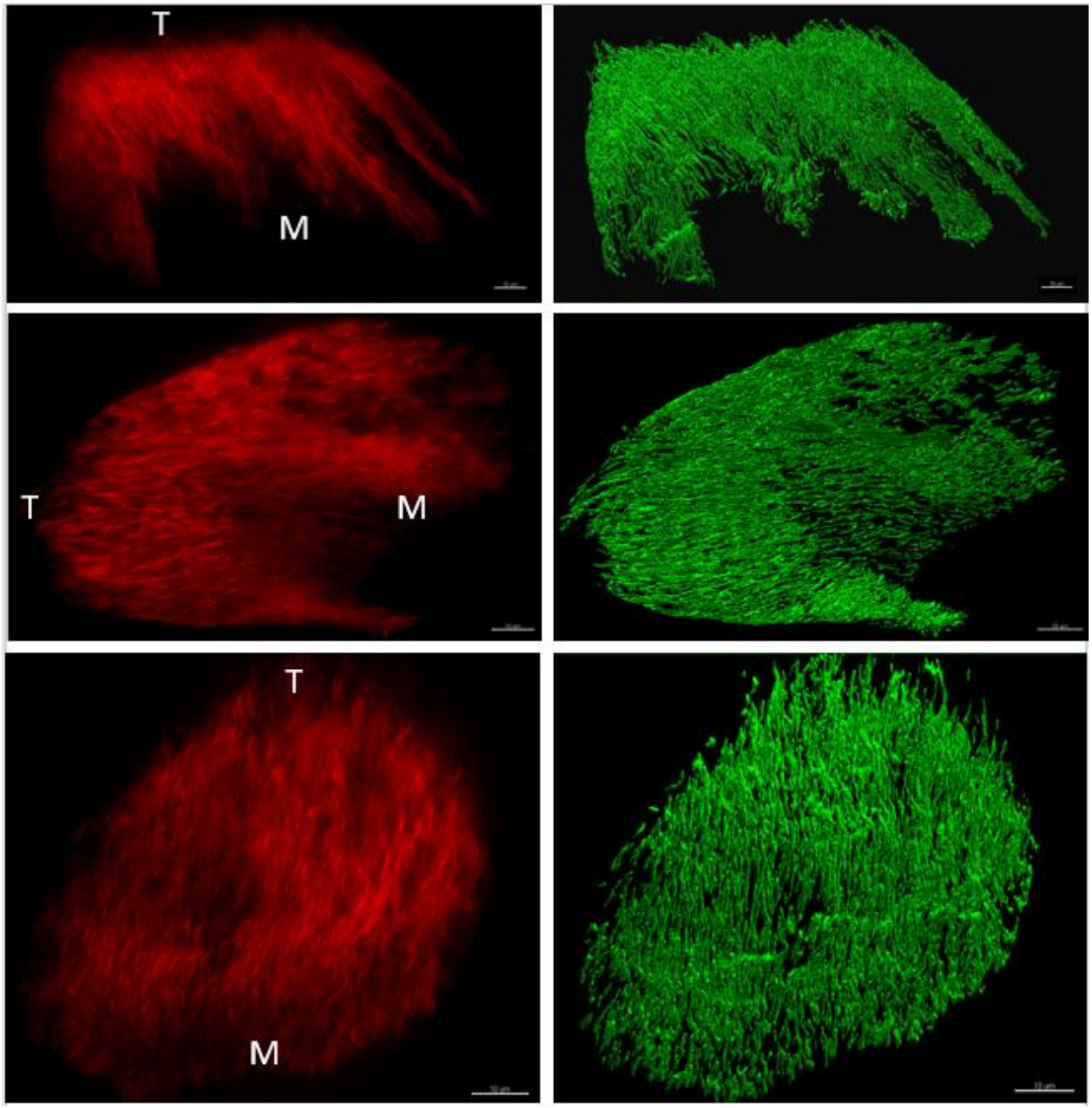

Figure 3
The figure shows the z-stack from three muscle fibers to the left labelled with collagen XXII. The left column shows the reconstructed surface of each of the fibers. Scale bars are 10 µm.

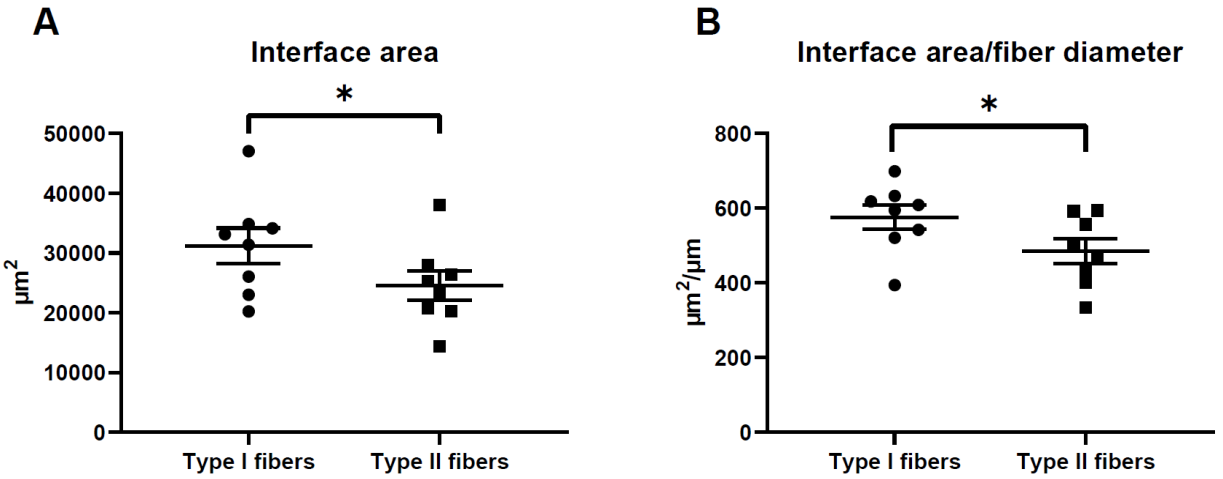

Figure 4:
Results from the measurements of the interface area.
*In A the measure of interface area is shown and individual median values are plotted as well as the median for each fiber type and SEM. In B the measurement of interface area is related to the diameter of each fiber and represented in the same way as A. * indicates significant differences (P<0.05)*

1.3 Discussion (Study I)

This study was the first study to investigate the surface area of the human MTJ from whole muscle fibers. Furthermore, was it the first to use confocal microscopy to analyze the complex interface which has previously been examined using TEM.
The main finding of the study was that type I fibers had a larger interface area compared to type II fibers. Furthermore, did we introduce a new method to analyze the morphology of the human MTJ from a large number of whole muscle fibers, and this could prove to be particularly useful for future studies.

Quantification using immunohistochemistry is complicated and the results can easily be affected by variations in the staining procedure or image acquisition and analysis. Therefore, a great effort was made to take these factors into account in this study. All fibers from all subjects were stained in the same batch using the same antibody dilution under the same environmental conditions. During the image acquisition the same setup was used with the same laser power and almost the same exposure time. Due to varying performance of the 568 nm laser, the exposure time could not be standardized and instead the time was adjusted in a window between 99-200mS in order to provide at least 10.000 grey values. Since the main outcome was not measures of pixel-intensity but instead surface area of staining this was not seen as a major issue. When analyzing the images, a macro was used for the settings behind the constructed surface so that all fibers were analyzed equally by an observer, blinded to the subject and fiber type.

The individual images obtained with the confocal system showed a very detailed surface which varied between fibers (Figure 5). This complexity was amplified when the individual images were stacked together in a z-stack which could be visualized in 3D. Even though there was a wide range

in the size of the interface area between fibers a significant difference was found when comparing the size of the interface area between type I and II fibers.
Interestingly, the interface area was larger in type I fibers compared to type II. Type I fibers are known to be more enduring and not capable of providing the same magnitude of force as the type II fibers which on the other hand are more easily fatigued (41,42). A high proportion of type II versus type I fibers have previously been speculated to be associated with an increased risk of strain injury (36,43,44). While the reason for this is probably multifactorial it could involve the combination of high force production in fibers that are easily fatigued (45). In addition, the smaller interface area of type II fibers found in the current study adds to this theory if the size of interface area affects the ability of the MTJ to tolerate loading, as suggested previously, and thereby also the susceptibility toward strain injury (17,28,46).

Differences in the size of surface area between fiber types have been sparsely investigated. Three studies from the same group have used stereology to compare the size of the MTJ surface between type I and II fibers in both mice, chicken and snake with different results (25,38,39). In chicken and mice the type II fibers were larger than type I whereas the opposite was seen in the snake muscles. The authors speculate that this variation could be because different animals were examined. However, it should be noted that a very limited number of fibers were analyzed from few animals in these studies meaning that the results might not be representable for the entire muscle.
Like in the previous EM studies where the foldings of the MTJ have been measured following exercise interventions, the stereology technique adjusts for the size of the fiber when calculating the interface area. The size of the interface area could be related to the size of the fiber and therefore the interface area was also expressed relative to fiber diameter in the current study. This did not affect the overall result. However, caution should be taken when expressing the size of interface area relative to fiber size in future studies since the fiber size is affected by changes in load (47,48). Since it is not known how quickly and to what extent the interface area adapts to loading, the results could reflect the changes in fiber size rather than the interface area.

The strength of the current study was the ability to examine a high number of whole muscle fiber ends. This means that the method would be useful for future studies wanting to examine the effects of loading/unloading on the area of the MTJ in humans.
The presented findings of a large interface area in type I compared to type II fibers indicate that type II fibers could be more vulnerable to injury, and future studies can examine whether the two fiber types are affected differently by exercise, and if the preventive effect of eccentric exercise is caused by adaptations in the type II fibers.

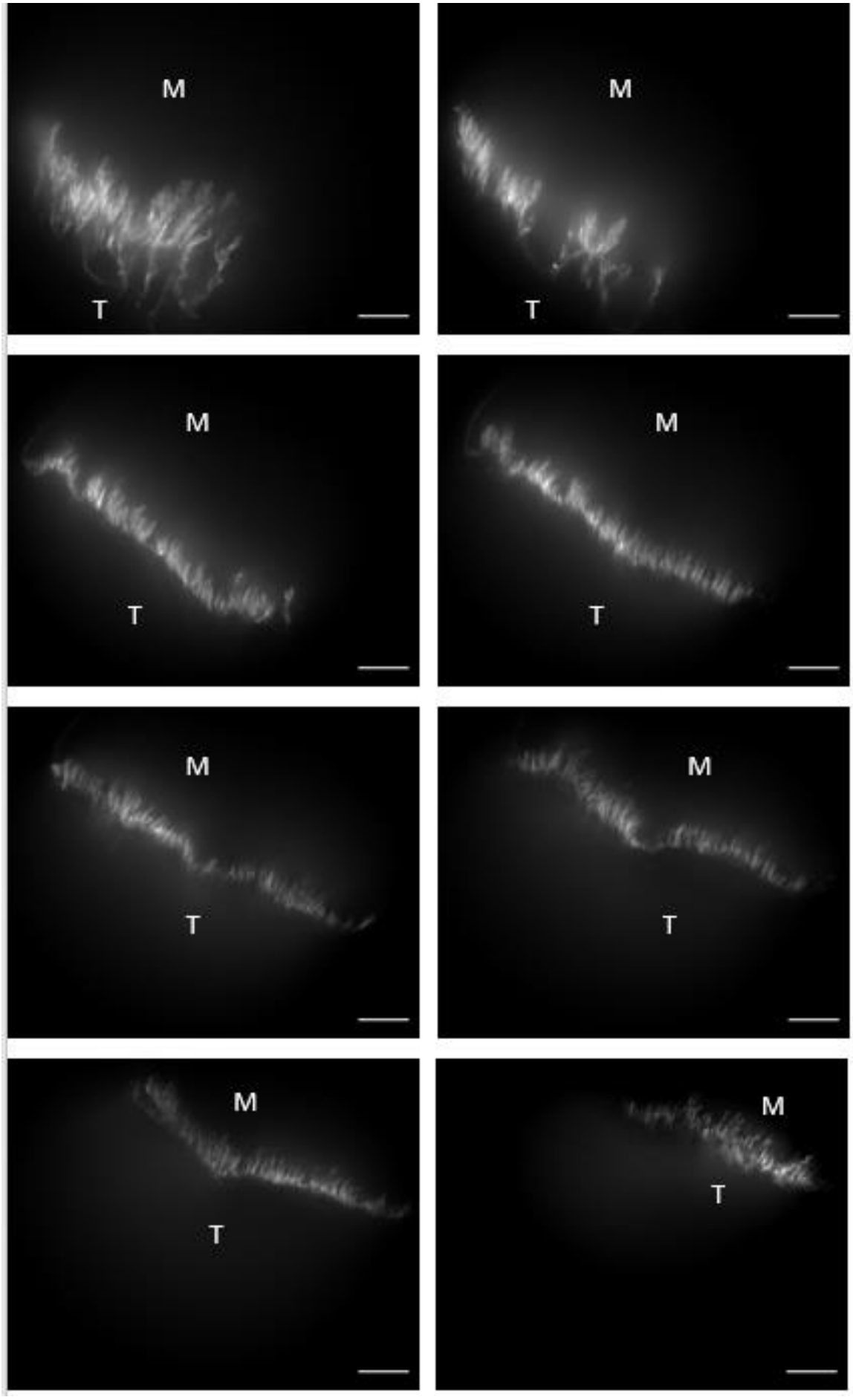
M
T
M
T
M
T
M
T
M
T
M
T
M
T
M
T

Figure 5:
Individual confocal images taken of human MTJ labelled with collagen XXII. The images are randomly picked from the Z-stack and shows the detailed foldings of the MTJ separating the muscle (M) from the tendon (T). Scale bars are 10 µm.

2.0 Study II (Adipocytes are present at murine and human myotendinous junction

For skeletal muscles to work during exercise, fuel is needed. Here carbohydrates as well as lipids are the main sources in aerobic conditions. Both carbohydrates and lipids are therefore stored in healthy skeletal muscles (49). However, in some metabolic diseases, such as diabetes and obesity, lipids are deposited inside the muscle fibers as lipid droplets and among the muscle fibers as adipose-like tissue. The latter is associated with an impaired muscle function whereas high levels of lipid droplets inside the muscle fibers is related to reduced insulin sensitivity (50,51). In skeletal muscles from athletes without reduced insulin sensitivity or muscle function the same phenomenon of a high intercellular lipid content is seen. This is known as the athletes' paradox and illustrates the complexity of lipids and adipocytes in skeletal muscle (50).

During our previous investigations of the MTJ we repeatedly noticed lipid containing holes in our sections of human MTJ's. Following specific IHC labelling we identified these holes as being adipocytes. In a study, exploring the capillary network near the MTJ of mouse diaphragm, the presence of adipocyte-like cells near the junction of this particular muscle has been reported (52). This observation has not been reported in any of the other animal or human studies looking at the ultrastructure of the MTJ.
Adipocytes are not known to be capable to transmit force and therefore their presence in this highly specialized region seems counter-intuitive at first sight. It could be speculated that these rather soft cells would negatively affect the strength of the MTJ. Therefore, a reduction of the number of adipocytes at the MTJ following resistance exercise would be beneficial in order to reduce the risk of strain injury. Because they are located outside of the muscle fibers, they are not directly available as an energy source for the muscles. Instead, their position near the region where high forces are exchanged between muscle and tendon might weaken this structure.
During a previous experiment we investigated the effects of 4 weeks of heavy resistance exercise on human subjects. Using those samples, we aimed to confirm the observation of adipocytes in healthy human MTJ as a general finding, and we also studied mice to analyze whether adipocytes are present through species, and we studied whether the number of adipocytes in human MTJs is affected by exercise.

2.1 Methods (Study II)

The method is described in detail in the attached article "Adipocytes are present at human and murine myotendinous junctions" and is briefly explained here (53).

Human samples were obtained from 10 subjects scheduled for anterior cruciate ligament reconstruction, as mentioned previously. The subjects were randomized preoperatively to either 4

weeks of heavy resistance exercise (n=5) or control (n=5). The exercise program is described in detail previously, but consisted of hamstring exercises including the Nordic hamstring (13). Following surgery samples collected from the semitendinosus muscle with the tendon included were cut, embedded in Tissue-Tek and frozen in liquid nitrogen cooled isopentane.

To analyze the presence of adipocytes in mouse MTJ's samples from 6 mice, bred to study neurotransmitters and circadian rhythm, were collected. Three were wild type mice whereas the others had knockouts of different receptors involved in circadian rhythm, none of which have been shown to affect overall activity patterns (54–56). The mice were perfusion fixed in Zamboni and the soleus and tibialis anterior muscles was dissected before they were immersed in Zamboni and cryoprotected in 30% sucrose in PBS before they were embedded in tissue-Tek and frozen like the human samples.

Samples from both species were sectioned and stained with IHC antibodies against perilipin-1 (PLIN1) to mark the adipocyte membrane, Collagen XXII and DAPI (Nuclei). Collagen XXII was used to indicate the MTJ, since this has been shown to be a valuable marker of this interface (57). For the human samples we wanted to quantify the number of adipocytes in relation to collagen XXII as well as the proportion of length of Collagen XXII+ MTJ with adjacent adipocytes (see figure 6).

To describe possible differences induced by training, Mann-Whitney's test was used. However, since no significant differences were seen the results were pooled.
The mice were included to show the presence of adipocytes at the MTJ and therefore no quantification was made on the number of cells.

From a single WT mouse, a soleus and a tibialis anterior muscle were prepared according to the single fiber protocol mentioned previously in the method section to paper 1. These muscles were dissected into smaller bundles containing the MTJ and stained with the same antibodies as the sections. A spinning disc confocal microscope was used to image the fiber-bundles (Figure 7).

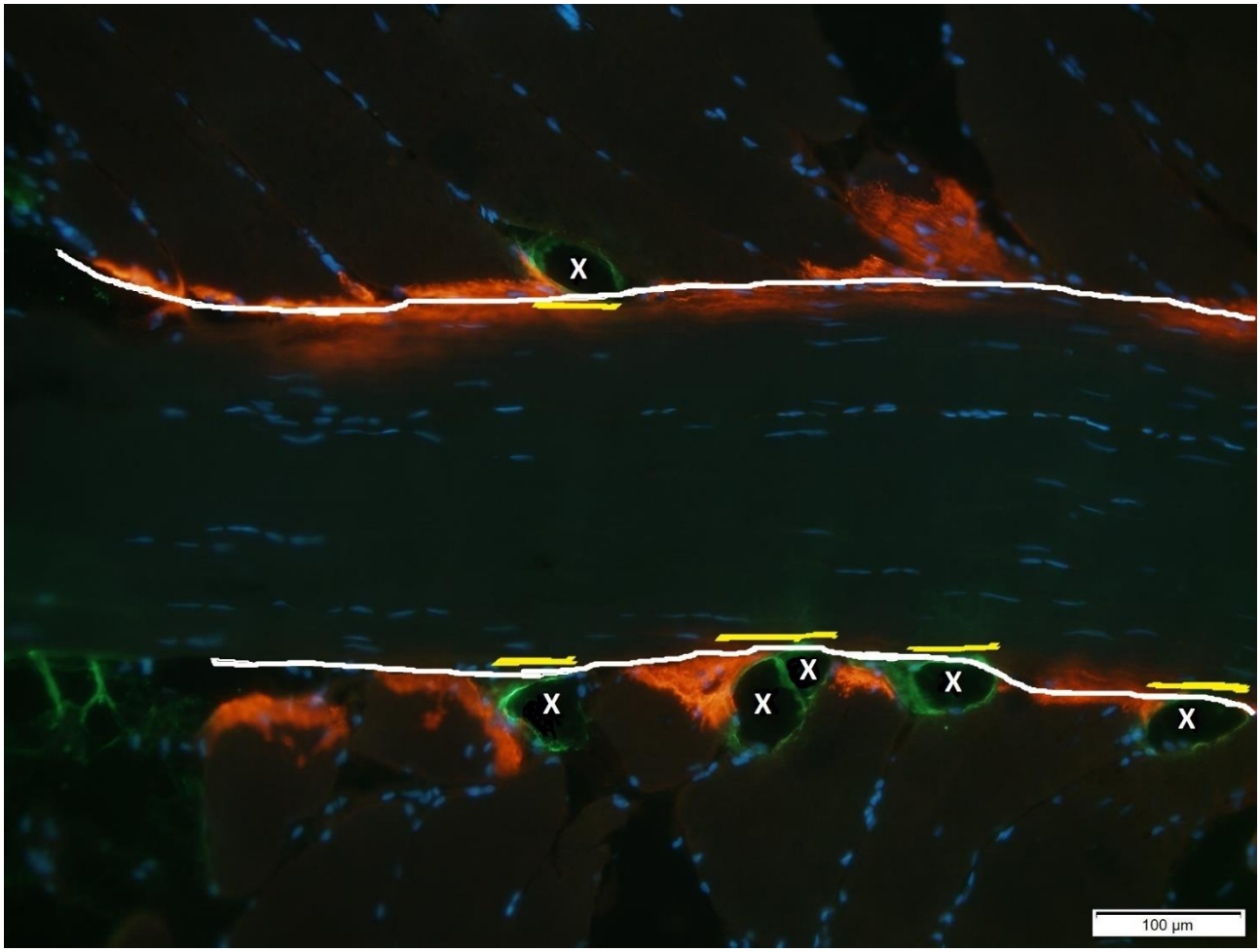

Figure 6:
Multichannel image of a section of human semitendinosus MTJ labelled with PLIN1 (green) and collagen XXII (red). The image shows the quantification of adipocytes (x) in relation to the length of the MTJ (White line) and the measure of MTJ with adjacent adipocytes (yellow lines).
From: Jakobsen, JR, Jakobsen, NR, Mackey, AL, et al. Adipocytes are present at human and murine myotendinous junctions. Transl Sports Med. 2021; 4: 223– 230.

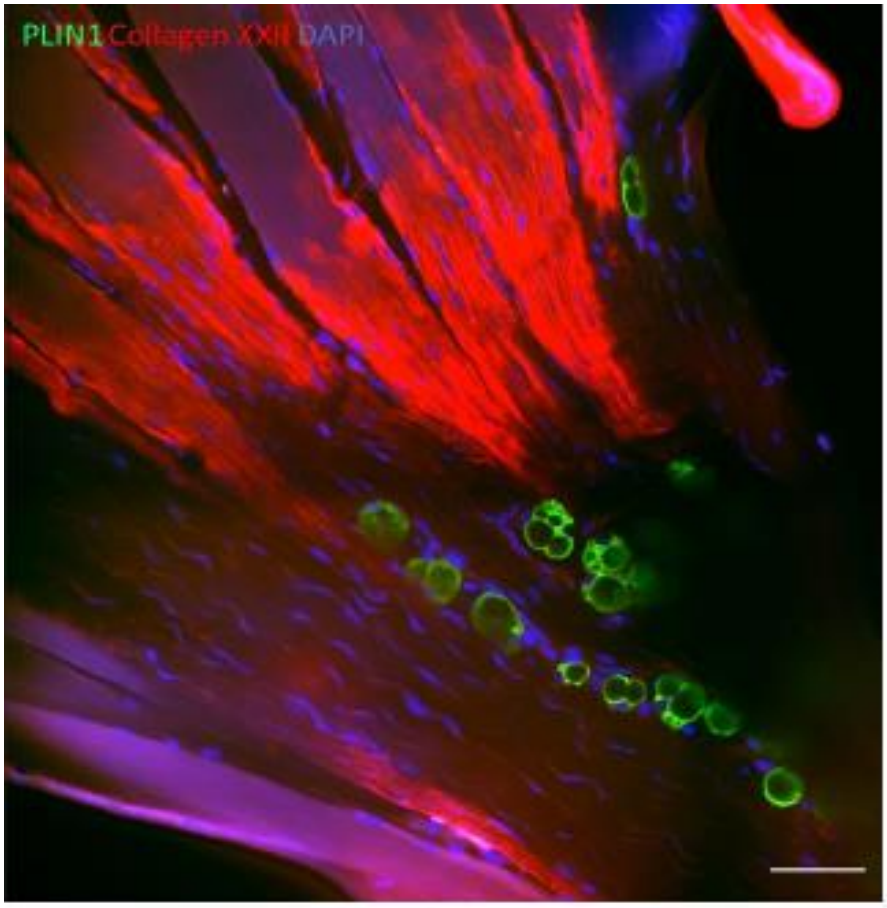

Figure 7: *Mouse MTJ imaged with confocal microscopy showing adipocytes at the MTJ indicated by Confocal image of a mouse soleus muscle showing PLIN1-labelled adipocytes (Green) near the collagen XXII labelled MTJ (red). Scale bar is 50 µm.*
From Jakobsen, JR, Jakobsen, NR, Mackey, AL, et al. Adipocytes are present at human and murine myotendinous junctions. Transl Sports Med. 2021; 4: 223– 230.

2.2 Results (Study II)

Adipocytes were found in all human subjects with no significant differences induced by training (see figure 8). Likewise, all mouse MTJs contained adipocytes. Where the adipocytes in human MTJs were mostly located between fibers near the collagen XXII+ muscle end, the distribution in mouse MTJs was different. Here adipocytes were also seen between fibers near collagen XXII but also in relation to the tendon on the opposite side of the MTJ (Figure 9).

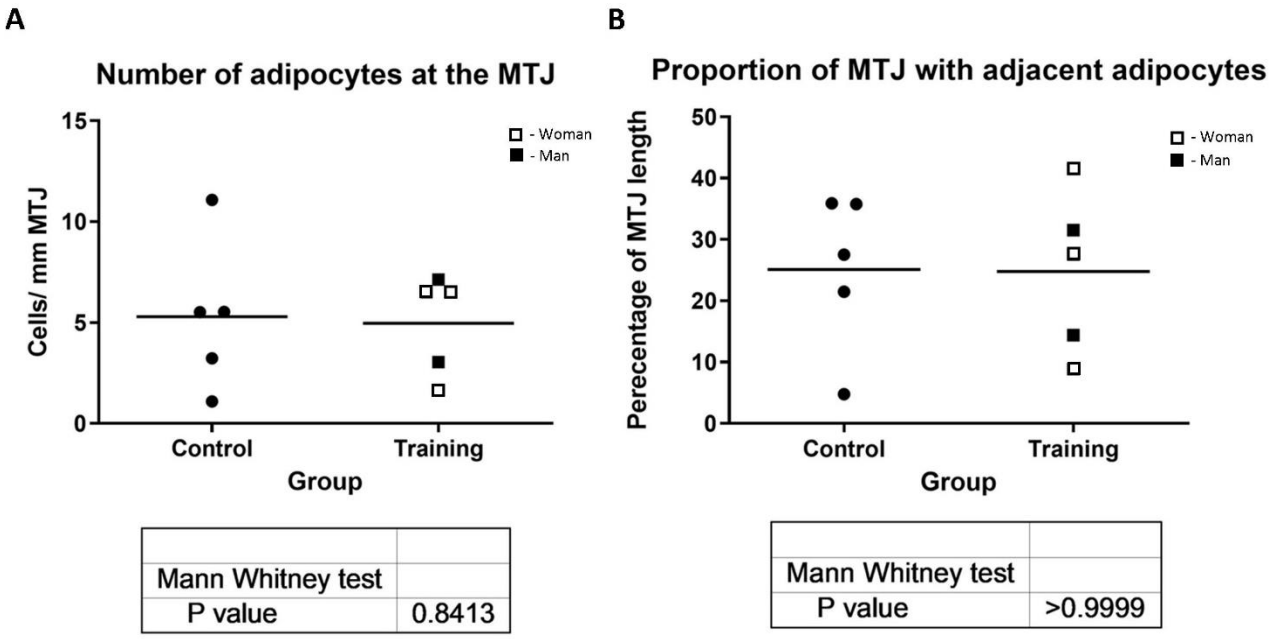

Figure 8

The graphs shows the quantification of adipocytes in human MTJ. A represent the number of adipocytes per length of MTJ wheras B represents the percentage of MTJ length with adjacent adipocytes.
From Jakobsen, JR, Jakobsen, NR, Mackey, AL, et al. Adipocytes are present at human and murine myotendinous junctions. Transl Sports Med. 2021; 4: 223– 230.

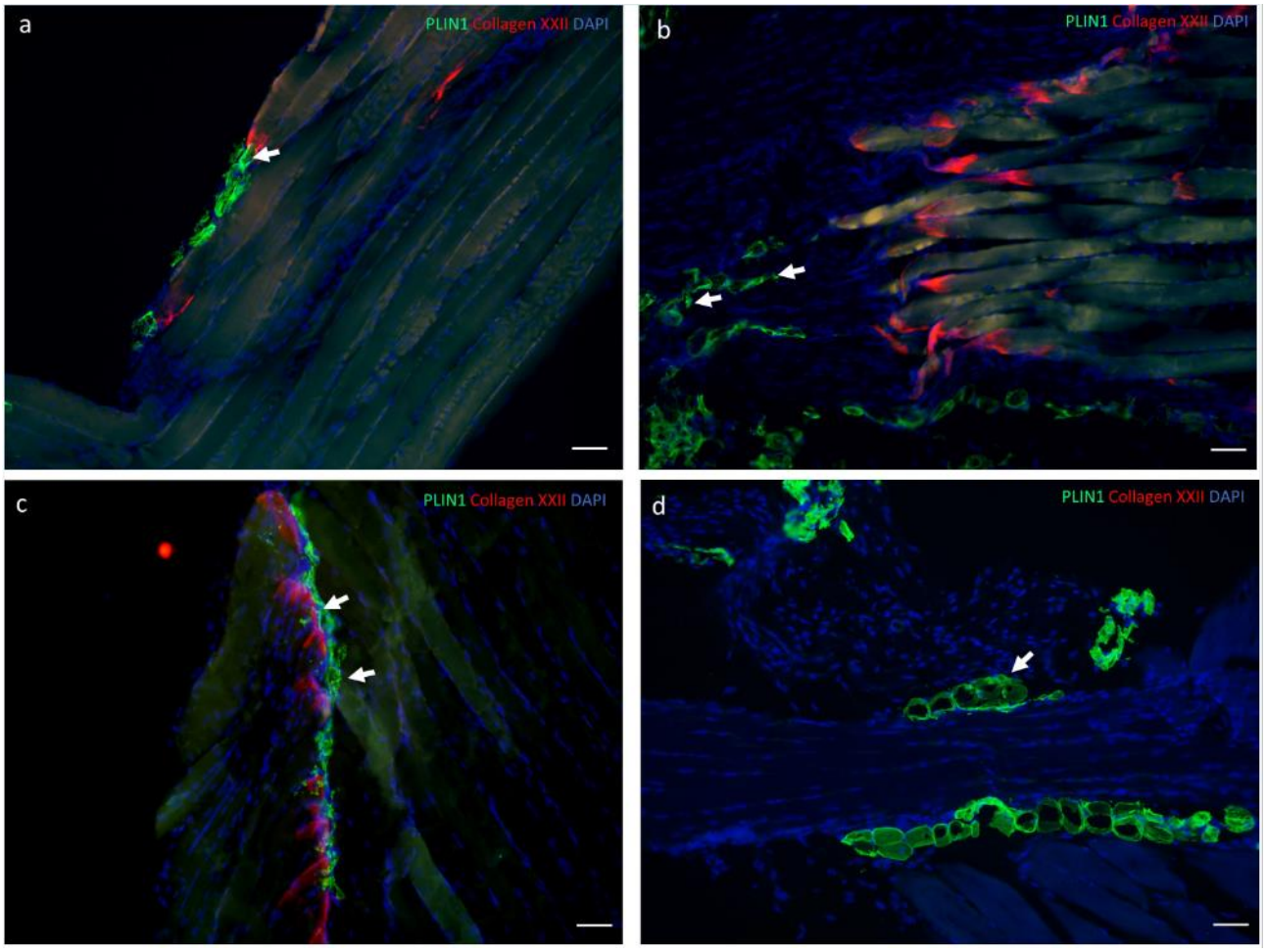

Figure 9

Representative images MTJs from mice labelled with antibodies against PLIN1 (green), collagen XXII (red) and DAPI (blue). The localization of adipocytes in mouse soleus muscle is shown in images Images a+b whereas c+d represent tibialis anterior muscle. In 5a and 5c adipocytes (arrows) are seen in close relation to the MTJ whereas 5b and 5d shows adipocytes located in the tendon substance. Scale bars are 50 µm.
From Jakobsen, JR, Jakobsen, NR, Mackey, AL, et al. Adipocytes are present at human and murine myotendinous junctions. Transl Sports Med. 2021; 4: 223– 230.

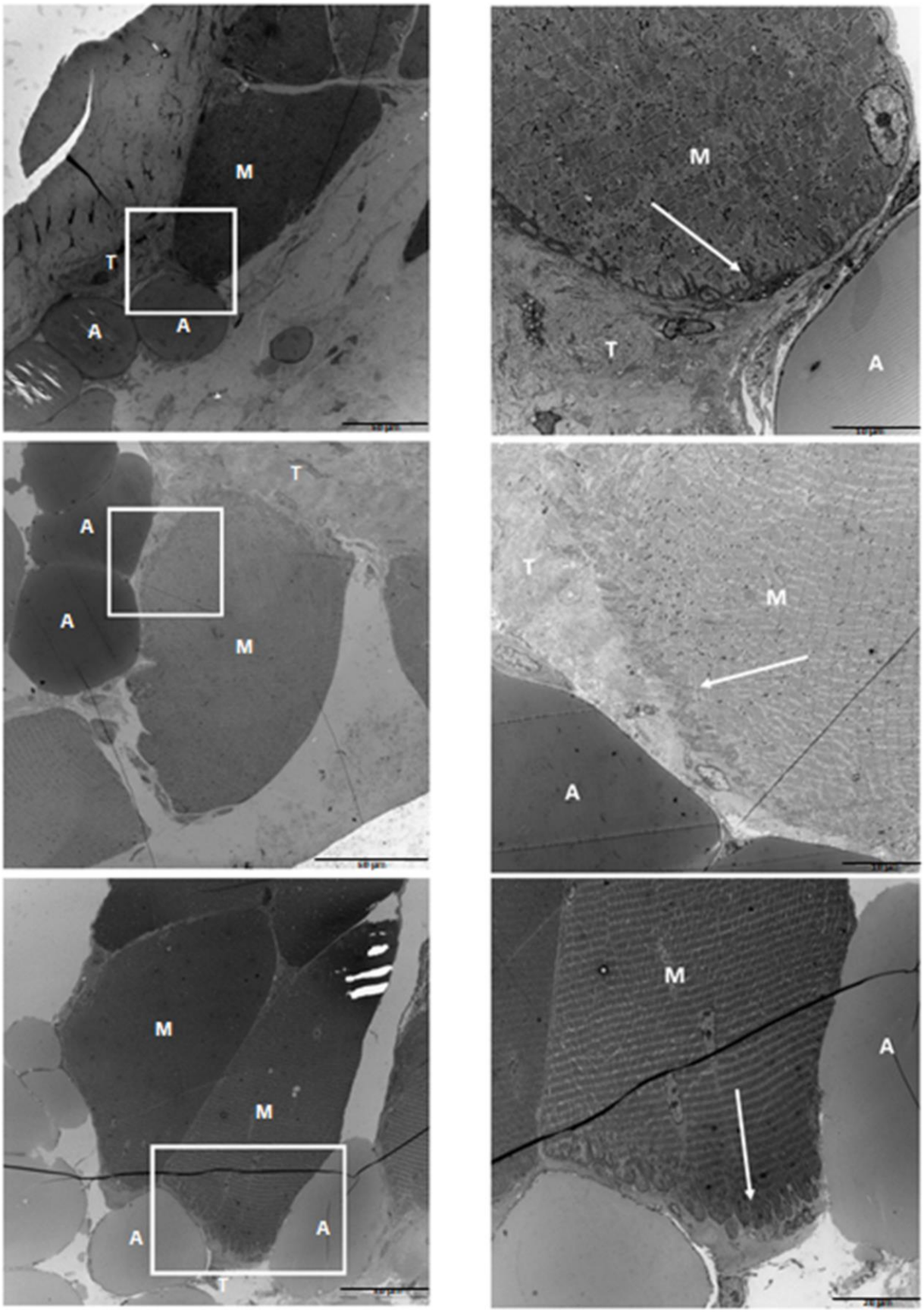

Figure 10: *Transmission electron microscopy image of human MTJ showing adipocytes (A) present at near the characteristic foldings at the MTJ (arrows). The images in right column are higher magnification images*

of the region marked by a square on the images in left column.
Scale bars are 50 μm in left column and 20 μm in the two upper images to the right and 10 μm in the bottom right image.
From Jakobsen, JR, Jakobsen, NR, Mackey, AL, et al. Adipocytes are present at human and murine myotendinous junctions. Transl Sports Med. 2021; 4: 223– 230.

2.3 Discussion (Study II)

The main finding in this study was that adipocytes are present in samples from both healthy humans and mice in very close relation to collagen XXII. By TEM the adipocytes were confirmed to be located close to the folded muscle membrane at the MTJ, through which force is thought to be transmitted (Figure 10). Whether this affects the ability of the MTJ to transmit or absorb force is not known.

The presence of adipocytes in the MTJ from mouse diaphragm muscles has been described previously (52). However, the numerous studies investigating the ultrastructure of the MTJ have not reported this. An explanation of this could be that the diaphragm is a special muscle which is different from other skeletal muscles used in the previous studies visualizing the MTJ. It could further be speculated that the deposition of adipocytes could be related to muscles with a specific muscle fiber type. To discard these theories, we included samples from the MTJ of mouse soleus and tibialis muscles which are composed of primarily type I and II fibers, respectively, and are used in previous studies (19,20,28). Adipocytes were seen in both muscles from all mice indicating that the presence of adipocytes is not related to a specific fiber typing or otherwise special muscle. However, in contrast to the human MTJs where adipocytes were mostly seen between muscle fibers near the MTJ, adipocytes were also seen in the tendon tissue with no relation to MTJ in mice.

Deposition of fibrosis and adipose tissue following injury is correlated with an increased risk of re-injury (58,59). The presence of adipocytes in previously injured MTJs would therefore be expected, however, none of the included subjects in this study had a previous history with hamstring strain injury. The adipocytes in un-injured MTJs could impair force transmission, though, and one of the potential effects of heavy eccentric exercise could therefore be a reduction of the number of adipocytes at the MTJ. To test this hypothesis, we had included samples from a previous study where subjects had performed heavy resistance exercise, including the Nordic Hamstring exercise, for 4 weeks. However, no significant differences were seen between the training and control groups. This might not necessarily mean that exercise does not influence the adipocytes. Instead of affecting the number of cells, exercise might influence the size or activity of the adipocytes. Unfortunately, the cell size is difficult to quantify on tissue sections by immunohistochemistry and would require serial sections of the same sample which could later be reconstructed and analyzed. We were not able to do that in the current study due to difficulties in sectioning the samples from the MTJ where the muscle and tendon are easily separated, meaning that many sections are discarded.

However, an interesting question is what the purpose of the adipocytes is. Given that the adipocytes are seen in "healthy" MTJs and are not affected by heavy resistance exercise, at least not to a degree that we could detect, it is likely that they have an important function at the MTJ. Theoretically, they could be present in this region to secure an optimal angle of insertion of the muscle fibers near the MTJ. This theory has been raised previously in a study reporting adipocytes

in the entheses at the tendon-bone junction in humans where they were seen to form adipose-like tissue with infiltrating blood-vessels and sensory nerve innervation (60). The authors speculated that the adipocytes could be present at the tendon-bone junction to facilitate movement between bone and tendon or to fill up room between fascicles in the tendon.

Previously the focus related to regenerating muscle fibers has been on the satellite cells, fibroblasts and macrophages. However, in recent years the complexity of adipocytes has been investigated showing various subtypes in different regions of the body, with multiple functions besides serving as a metabolic cell population (61,62). An example of this is the adipose tissue found in the palm and feet which serve as pressure regulator (63). In addition, adipocytes are also known to interact with their environment by secreting cytokines, known as adipokines, which have various effects throughout the body (64). Adipocytes located in the dermis layer of skin have been shown to affect both fibroblasts and macrophages following skin lesions. Following injury of the skin, adipocytes undergo lipolysis resulting in secretion of fatty acids which improves the migration of macrophages to the damaged area (65,66). An impairment of this interaction between adipocytes and macrophages causes suboptimal repair of the tissue. In addition to the suggested role of adipocytes in tissue repair, the common adipocyte and fibroblast precursor cells, the fibro-adipogenic cells (FAPs) have been shown to be important for myogenic proliferation following muscle injury (67–70).

Even though a direct interaction between adipocytes and macrophages or satellite cells has not been confirmed in skeletal muscle in relation to remodeling or regeneration of muscle fibers, it is interesting that they are located in this region of the skeletal muscle where injuries are most frequent and the ongoing remodeling is highest. Their ability to migrate to injured regions and contribute to the inflammatory process suggests that they should be included in models for the understanding of regeneration and remodeling at the MTJ (65,66,71).

Altogether, these findings indicate that adipocytes at the MTJ are of interest in the understanding of general homeostasis, remodeling and regeneration following injury to the MTJ. However, future research investigating the production of adipokines from the adipocytes located at the MTJ is needed in order to understand the functional role of these cells at the MTJ.

3.0 Study III (RNA sequencing and immunofluorescence of the myotendinous junction of mature horses and humans)

As mentioned previously, the distal part of the muscle fibers near the MTJ have been seen to undergo continues remodeling. This is demonstrated by immunoreactivity towards NCAM, which labels denervated, regenerating or newly formed muscle fibers, and supported by the finding of a high proportion of muscle fibers with centralized nuclei (40,72). Interestingly, this is not seen in the same muscle fiber a few hundred micrometers from the MTJ, indicating regional differences in the same cells. Recent studies have confirmed that specialized nuclei and particularly myonuclei are present at the MTJ with different gene expression than “regular” myonuclei (73–75). These nuclei are seen to express collagen XXII mRNA as well as NCAM1, among others. The specificity of this collagen type for the MTJ has been shown previously, and its importance for the tissue interface has been discussed (57). A knockout of the collagen XXII alpha-1 chain (COL22A1) in zebrafish resulted in significant impairment of the strength and function of the MTJ (76). Furthermore, mutations in the single-nucleotide polymorphisms (SNP’s) for COL22A1 have been correlated

with increased risk of strain injury in humans (77). Although this needs to be investigated further in order to draw certain conclusions, it highlights the importance of understanding the composition of the MTJ both from a basic research aspect and in relation to strain injury. In addition, an understanding of the gene expression at the MTJ would also improve the knowledge about the regeneration of the muscle fibers in the area as well as regeneration following injury. The latter is of great importance in a clinical context where previous injury is one of the most important risk factors for sustaining subsequent injury, probably due to suboptimal regeneration at the MTJ with formation of fibrosis.

The presence of myonuclei specific to the MTJ as well as the high rate of remodeling suggests a different transcriptional activity in this area which could be accompanied by a markedly increased expression of specific, and maybe unique, genes of high importance to the MTJ. However, the study of the composition of the MTJ is challenging due to the nature of the region being a mixture of muscle and tendon. Especially the muscle tissue makes it difficult to study the MTJ due to the high amounts of mRNA and protein in muscle fibers. Applying methods regularly used in skeletal muscle research such as western blots, PCR or proteomics would therefore most likely be unusable, due to the high signals from regular muscle. To overcome this issue, the MTJ needs to be separated from muscle and tendon. In a recent study this was done by isolating the MTJ, using a laser-capture microscope and analyzing the samples by proteomics (78). With this method a sample is sectioned as regularly performed for immunohistochemistry and each section dissected with a laser. The chosen region of interest is then captured for further analysis. Even though this is a very precise method with a high degree of control of what piece of tissue that is analyzed, it is also a very time-consuming process, since only regions from thin sections are cut at a time, meaning that many sections are needed. In addition, the laser cuts with very high temperatures, which could heat the tissue and thereby affect the proteins or genes.

Therefore, the current study had two aims. One was to develop a simple method to isolate larger pieces of MTJ tissue, separated from muscle and tendon without the need of special instruments. The other was to analyze the gene expression in the separated tissue fractions to find genes of interest for the MTJ.

3.1 Methods (Study III)

Samples were obtained from a study testing cardiac function and arrhythmia in 20 horses (7 geldings and 13 mares). A mixture of previous racing horses (n=11) and non-racing horses (n=9) were included (age 5-10 years).

All horses went through a range of tests not related to our study. These included three maximal effort running tests on treadmill on separate days. Unfortunately, due to differences in the time between these exercise sessions and collection of samples, we were not able to investigate potential effects of the tests on gene expression at the MTJ.
Quickly after slaughtering of each horse, one of the hindlimbs was removed and the superficial digitorum flexor muscles were dissected for further analysis in our study.
Samples containing muscle, MTJ and tendon were punched out using a 4 mm in diameter biopsy puncher. The samples were embedded in Tissue-Tek and an effort was made to place all samples in same manner with the tendon in the bottom and muscle on the top before freezing in liquid nitrogen-cooled isopentane.

The sectioning and collection of the various tissue fractions are described in detail in the attached paper (79). Briefly, the tissue block was sectioned from the top to bottom where 20 sections at a time were collected in each tube. Tubes representing the 6 fractions seen in figure 11 were chosen for further analysis.

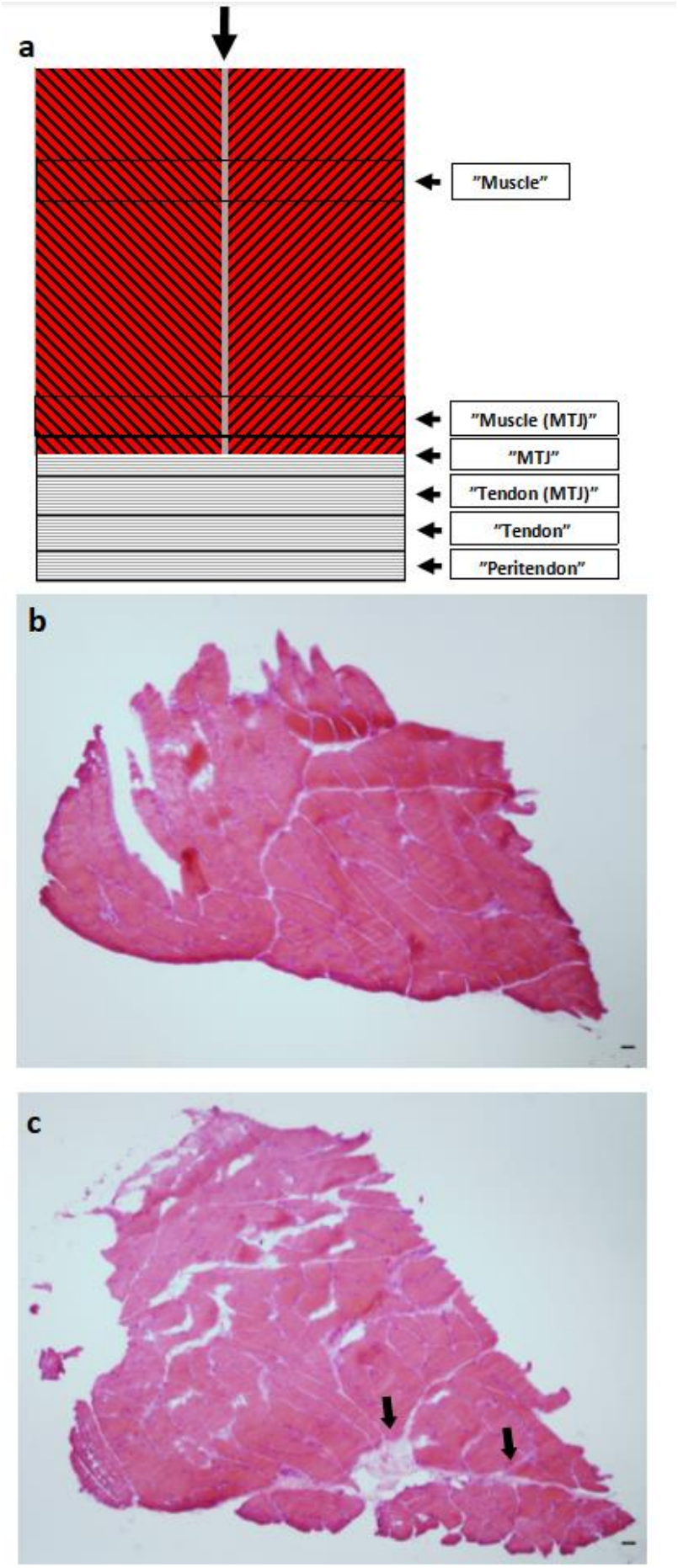
a
"Muscle"
"Muscle (MTJ)"
"MTJ"
"Tendon (MTJ)"
"Tendon"
"Peritendon"
b
c

Figure 11
a) Regions chosen for further analysis.
b) The control section stained with Hematoxylin and Eosin obtained before collecting tissue for the "muscle (MTJ)" tube.
c) The control section obtained before collecting tissue for the "MTJ" tube. Arrows mark regions of tendon tissue. Scale bars in b + c are 50 µm.

Gene expressions in the various fractions were analyzed using qRT-PCR looking at targets known from skeletal muscle, MTJ and tendon research. Based on these results samples from the "Muscle", "MTJ" and "Tendon" fractions from 5 horses were selected for RNA sequencing. Fractions from these horses exhibited the clearest separation into muscle-like, MTJ-like and tendon-like tissue.

By RNA-sequencing we tested for genes more highly expressed in MTJ tissue than in muscle and tendon.
However, despite the effort to isolate the MTJ fraction, it still consists of mostly muscle and some tendon tissue. Since the relative contribution from these tissues might affect the gene expression seen in the MTJ fractions we also tried to take the relative contribution of muscle and tendon to the MTJ fractions into account. This was done by identifying genes from muscle and tendon that were expressed at levels 10-fold greater than in the other tissue (muscle vs tendon) and from these expression levels the relative contribution of muscle and tendon to the MTJ fractions were estimated. The contribution from muscle and tendon were estimated to be 86-94% and 6-14%, respectively, to the MTJ samples. This was used to calculate expected gene expression levels in the MTJ fractions based upon the assumption that the MTJ is merely a mixture of muscle and tendon with no specific effect on gene expression levels. Discrepancies between the expected and measured values from the MTJ would be regarded as coming from the actual MTJ.

Immunohistochemistry

To confirm the presence of the targets revealed by RNA-sequencing at the MTJ, sections from human semitendinosus MTJ's were stained with commercially available immunofluorescent antibodies. Nine targets out of the list of 27 and 43 genes found to be enriched at the MTJ were chosen. The collection and preparation of the human tissue is as described previously in the thesis.

The chosen genes were: OSTN (musclin/osteocrin), CD52 (CAMPATH-1 antigen), LCT (lactase), ACTC1 (actin alpha cardiac muscle 1), NES (nestin), MNS1 (meiosis-specific nuclear structural protein 1), ADAMTS8 (ADAM metallopeptidase with thrombospondin type 1 motif 8), NEFM (neurofilament medium), POSTN (periostin), COL22A1 (collagen XXII), and NCAM1 (neural cell adhesion molecule.

Statistics
The statistics has been described in detail in the attached paper, but briefly the gene expression from the tissue fractions was compared in pairs between muscle vs MTJ, MTJ vs tendon and muscle vs tendon using Wilcoxon Signed-rank tests with Bonferroni corrections. The data from RNA-sequencing was analysed using DESeq where a false discovery rate < 0.05 and $\log2FC > 1$ was applied. To adjust for the contribution of muscle and tendon to the gene expression in the MTJ fractions the expected MTJ value was compared with the measured values using one-tailed t-tests with a false discovery rate < 0.1, $\log2FC > 1$.

3.2 Results (Study III)

RT-PCR

The results of the RT-PCR looking at expression levels of the tested gene targets in tissue fractions from all horses are displayed in figure 12. To compare the pure muscle, MTJ and tendon the gene expression levels from these fractions were analyzed statistically as displayed in figure 12b. No differences were seen between the trained and untrained horses.

COL22A1 was the only gene found to be more highly expressed in the MTJ compared to both muscle and tendon. In tendon ANGPTL4, UTRN and COMP expressions were higher than in both muscle and MTJ whereas GAPDH was the only target more highly expressed in muscle compared to the two other fractions.

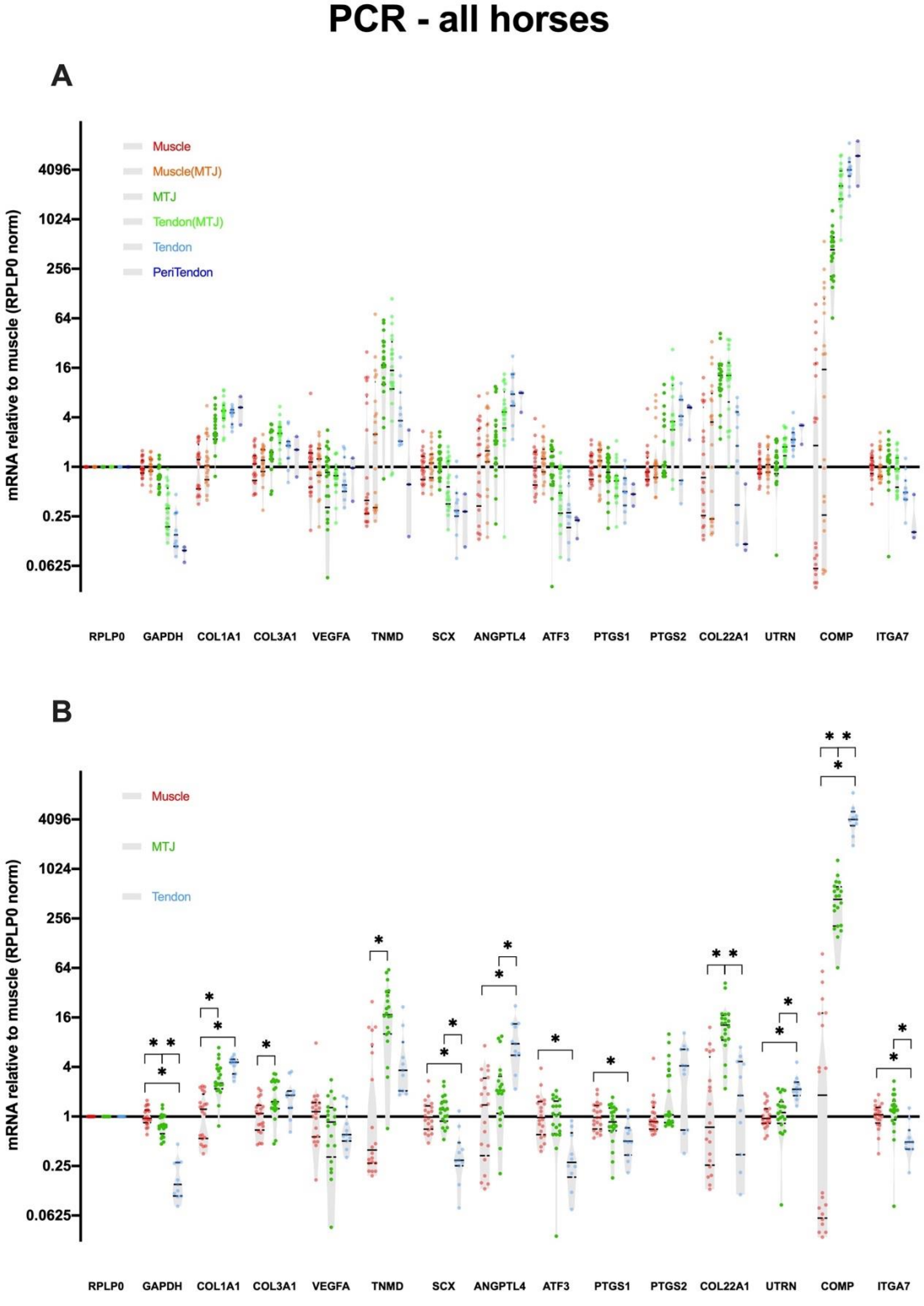

Figure 12

*The graphs show the results from the RT-PCR. In A all tissue fractions are included and the results from all genes shown separately In B only the "muscle", "MTJ" and "tendon" regions are shown. * indicates significant differences ($p<0.05$) between tissue fractions.*

From Jakobsen JR, Schjerling P, Svensson RB, et al RNA-sequencing and immunofluorescence of the myotendinous junction of mature horses and humans. Am J Physiol Cell Physiol. 2021 Jul 14. PMID: 34260300 (79).

RNA-sequencing

Based upon the RT-PCR data a Principal Component Analysis plot was made (Figure 13a). Here it is seen that the fractions begin to cluster together. Using the same data from the RT-PCR a t-distributed stochastic neighboring plot (t-SNE) was made to further look at these clusters (Figure 13b). In the t-SNE plot the tendon fractions are separated from the other, located close to the MTJ fractions. The MTJ fractions are seen close to each other with some muscle fractions nearby and others clustered far from the other fractions.

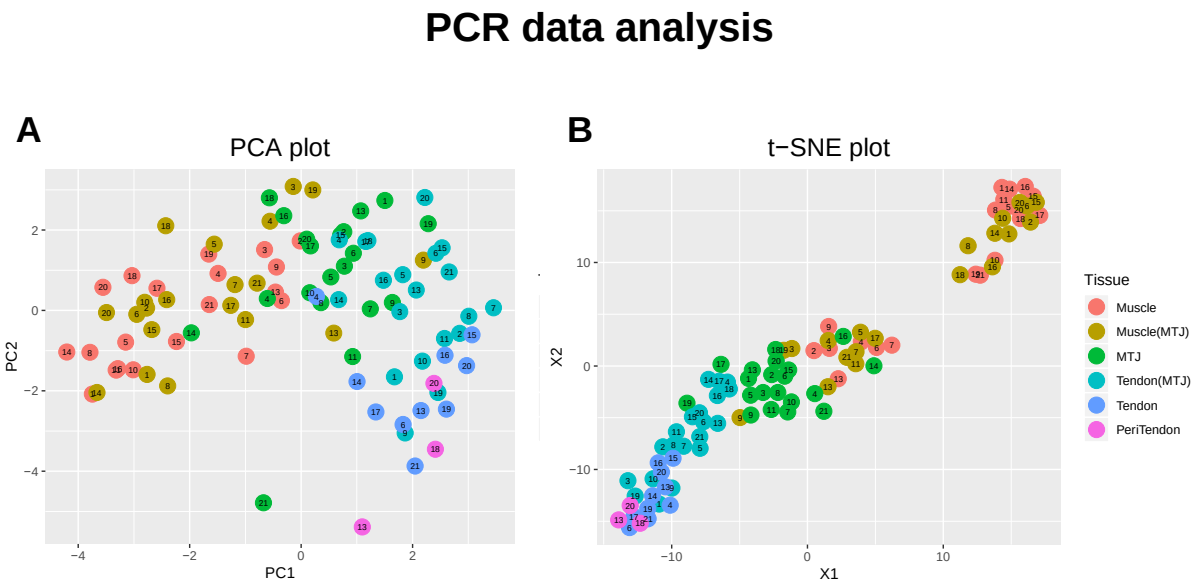

Figure 13
Principal Component Analysis (A) and t-distributed Stochastic Neighbor Embedding (t-SNE) plots (B), showing the distribution of the various tissue fractions represented by different colors from all the horses. Each horse is indicated by a number. Samples located close together reflect more similar mRNA levels. From Jakobsen JR, Schjerling P, Svensson RB, et al RNA-sequencing and immunofluorescence of the myotendinous junction of mature horses and humans. Am J Physiol Cell Physiol. 2021 Jul 14. PMID: 34260300.

Set of fractions from 5 horses showing the clearest separation between various fractions and thereby probably the best isolation, where chosen for RNA-sequencing.

When comparing the fractions: muscle, MTJ and tendon, no genes were found to be uniquely expressed at the MTJ. A list of 27 genes was found to be expressed significantly higher in the MTJ than both muscle and tendon (Figure 14c). Based upon the previously described assumption that the gene expression at the MTJ reflects the contributing muscle and tendon, 43 genes were more highly expressed than expected (Figure 15). COL22A1, NCAM1, POSTN, CNTNAP4, OSTN, ALDH3B1, MNS1, and CD52 were all found to be enriched at the MTJ using both techniques.

Among the 27 genes that were significantly higher in the MTJ than in the other fractions were COL22A1, NCAM1 and POSTN, all of which have been described in relation to the MTJ previously (76,80,81). Since the MTJ did not contain unique genes it could be viewed as a mixture of muscle and tendon without specialization. However, 43 genes were found to be more highly expressed at the MTJ than expected, based upon the previously explained assumption that the gene expression at the MTJ reflects the relative contribution from muscle and tendon. These 43 genes could therefore be more active at the MTJ. Interestingly, COL22A1, OSTN, ALDH3B1,

POSTN, CNTNAP4, NCAM1, MNS1, and CD52 were found to be enriched at the MTJ when employing both techniques. The GO and KEGG databases were checked and no significant pathways were identified. In general, the 27 and 42 genes could be grouped into proteins with relation to neural activity, immune system, cell assembly/adhesion, formation of extracellular matrix, cell-tissue interplay, metabolism and fluid regulation.

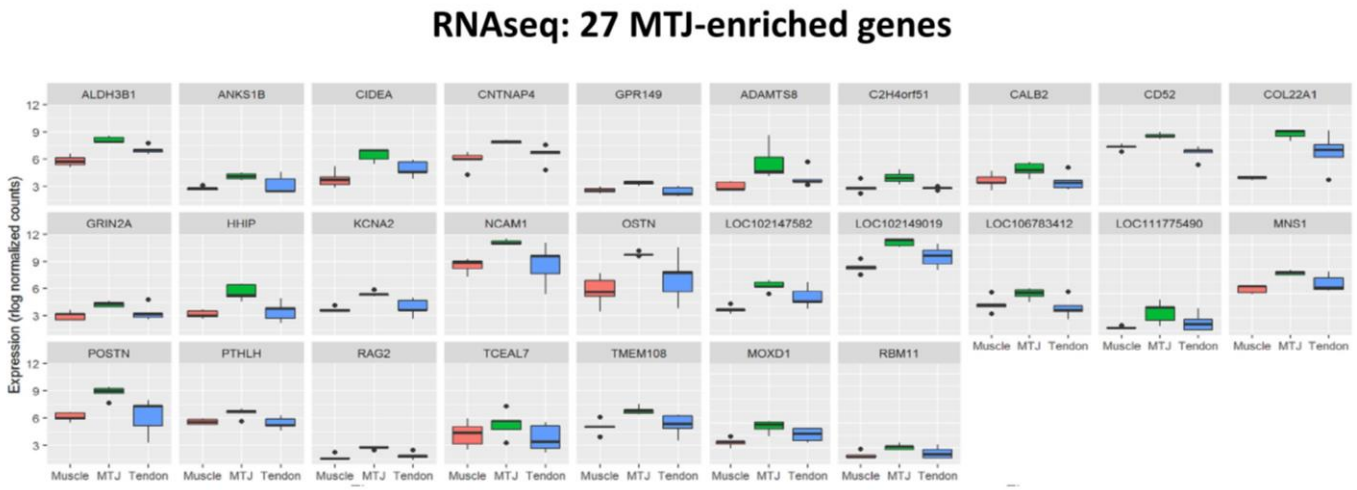

Figure 14
Box plots showing the levels of gene expression of the 27 "MTJ-enriched" genes in muscle, MTJ and tendon. From Jakobsen JR, Schjerling P, Svensson RB, et al RNA-sequencing and immunofluorescence of the myotendinous junction of mature horses and humans. Am J Physiol Cell Physiol. 2021 Jul 14. PMID: 34260300.

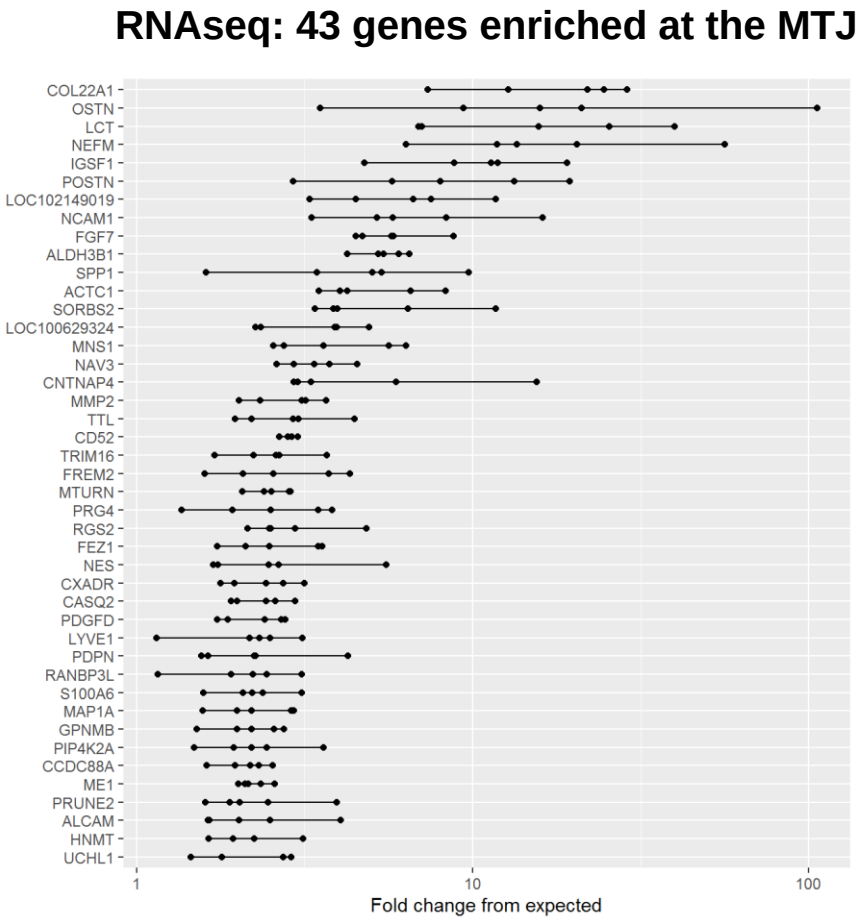

Figure 15
Genes identified to be enriched in the horse MTJ by RNA-seq. Each dot represents the mean fold difference compared to the expected value from each horse with the lines indicating the range.
From Jakobsen JR, Schjerling P, Svensson RB, et al RNA-sequencing and immunofluorescence of the myotendinous junction of mature horses and humans. Am J Physiol Cell Physiol. 2021 Jul 14. PMID: 34260300.

Immunohistochemistry

The presence of collagen XXII, NCAM, nestin, periostin, MNS1, osteocrin and lactase at the MTJ was confirmed on the protein level using immunofluorescence (See figures 16-18). It was not possible to confirm the presence of CD52, NEFM, ACTC1 and ADAMTS8 at the MTJ due to unconvincing staining of these targets.

NCAM, nestin and osteocrin were seen to stain the cytoplasm of the muscle, while osteocrin also stained some mononuclear cells between the muscle fibers. Collagen XXII and periostin were seen in close relation to each other at the tips of the muscle fibers. Lactase was expressed by mononuclear cells at the MTJ, and some myonuclei near the MTJ showed immunoreactivity against MNS1.

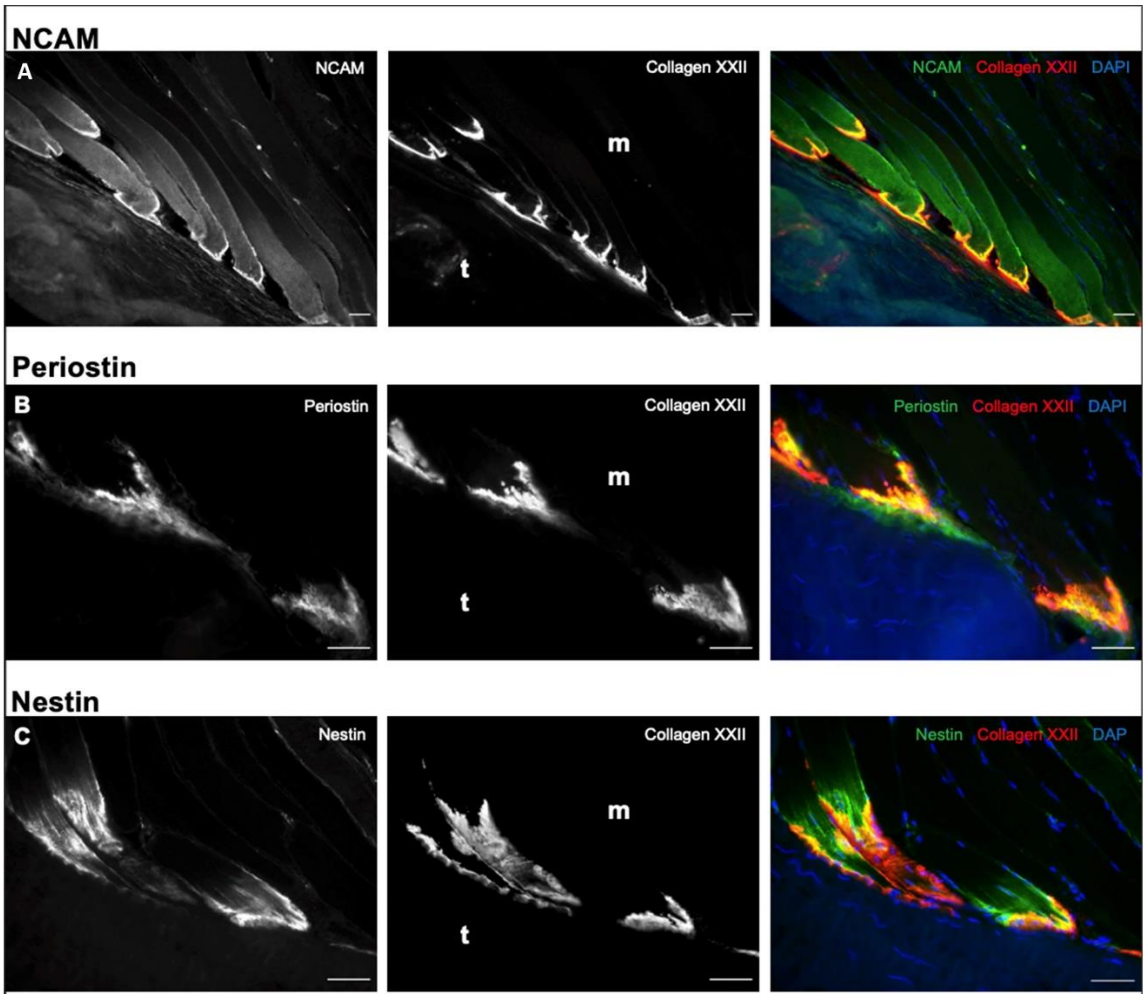

Figure 16
Representative images of staining of human MTJ samples against NCAM (A), Periostin (B) and Nestin (C) and co-stained with collagen XXII to identify the MTJ between muscle (m) and tendon (t). The two left columns show the individual channels in greyscale and to the right are merged images of the two channels with DAP included. All scale bars are 50 µm.
From Jakobsen JR, Schjerling P, Svensson RB, et al RNA-sequencing and immunofluorescence of the myotendinous junction of mature horses and humans. Am J Physiol Cell Physiol. 2021 Jul 14. PMID: 34260300.

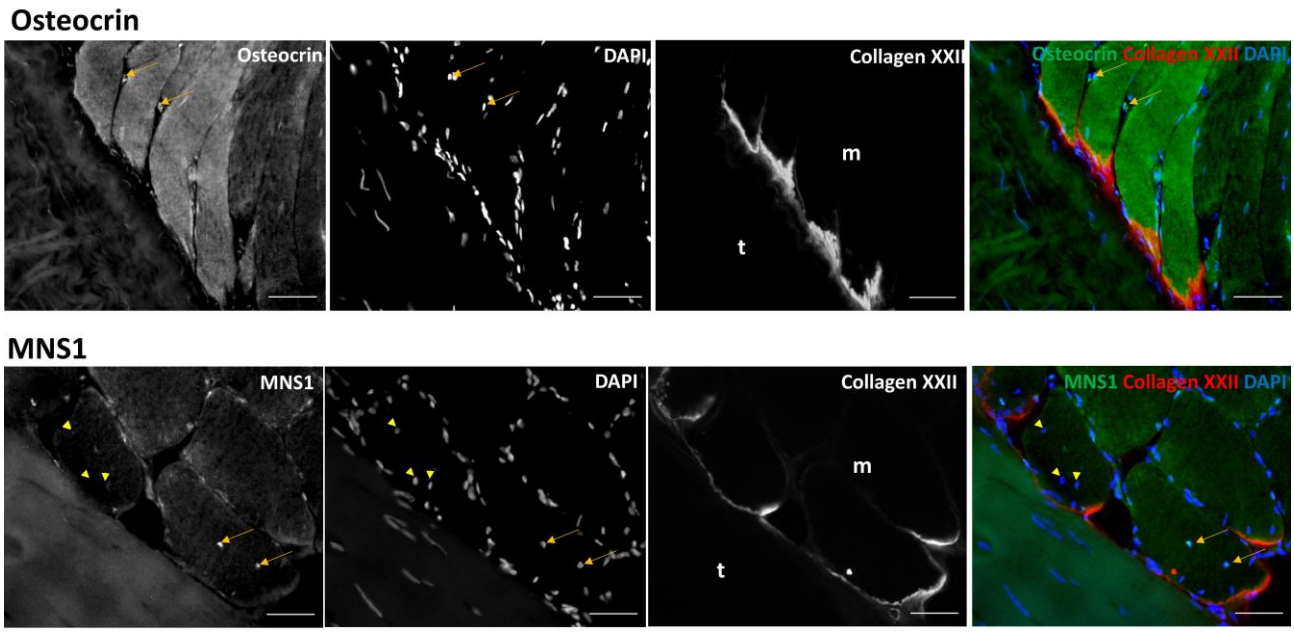

Figure 17
Representative images of staining of human MTJ samples against osteocrin and MNS1. Single grey-scale channels are shown in the first three columns with a merged image to the right. Osteocrin is seen to stain mononuclear cells near the MTJ (arrows) as well as the cytoplasm of muscle fibers. MNS1 is seen to stain some, but not all, myonuclei (arrows). Scale bars are 50 µm.
From Jakobsen JR, Schjerling P, Svensson RB, et al RNA-sequencing and immunofluorescence of the myotendinous junction of mature horses and humans. Am J Physiol Cell Physiol. 2021 Jul 14. PMID: 34260300.

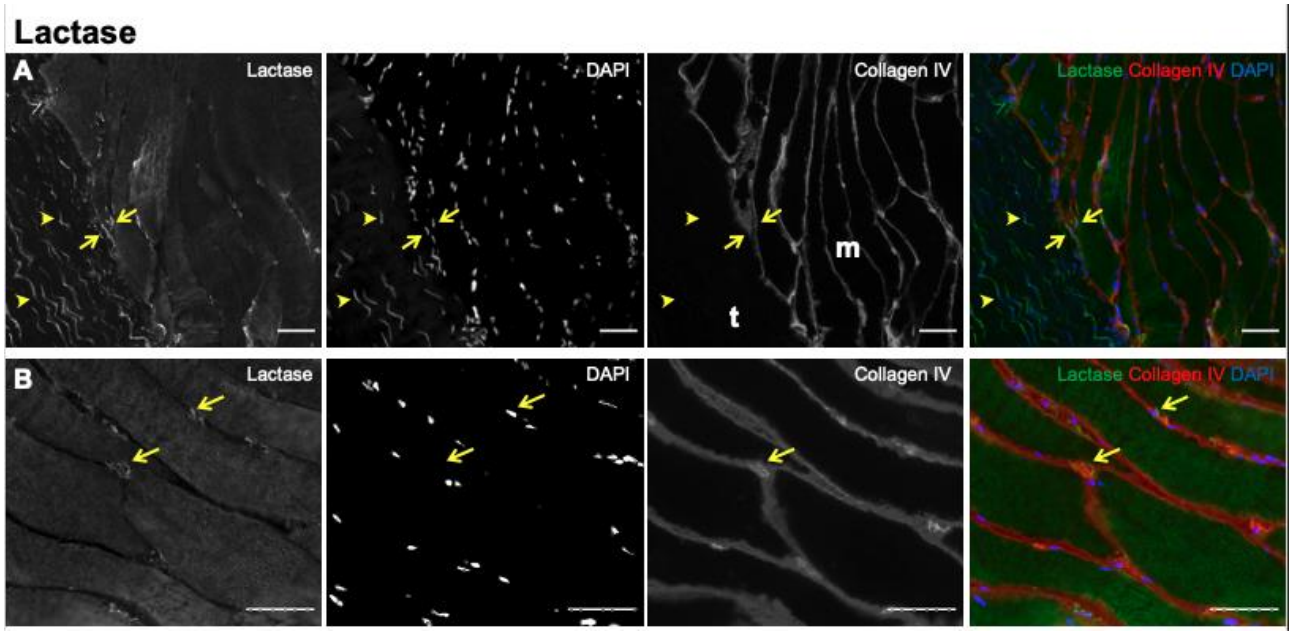

Figure 18
Representative images of staining of human MTJ samples against lactase showing mononuclear cells with immunoreactivity against lactase (arrows) near the MTJ (A) as well as between muscle fibers away from the MTJ (B). Single grey-scale channels are shown in the first three columns with a merged image to the right. Scale bars are 50 µm.

From Jakobsen JR, Schjerling P, Svensson RB, et al RNA-sequencing and immunofluorescence of the myotendinous junction of mature horses and humans. Am J Physiol Cell Physiol. 2021 Jul 14. PMID: 34260300.

3.3 Discussion (Study III)

The current study aimed to analyze the gene expression of the MTJ to identify potential unique genes or genes that were highly upregulated at the MTJ, and to develop a feasible method to isolate the MTJ from a sample containing muscle, tendon and MTJ.

Using RNA-sequencing the gene expression of the MTJ was analyzed. No genes were found to be uniquely expressed at the MTJ compared to the muscle and tendon fractions. This is surprising since several proteins have been shown to be unique to the MTJ, i.e. collagen XXII and Periostin (57,81). An explanation for the lack of unique genes could be that the mRNAs are produced at some distance from the MTJ. However, this is not the case for COL22A1 which have been shown by in situ hybridization to be produced close to the MTJ in zebra fish (76). The lack of unique genes at the MTJ could also be due to issues in isolating the MTJ leaving some MTJ tissue in the other tissue fractions, even though an effort was made to avoid this by analyzing the muscle fraction that was far from the MTJ. However, this was complicated by the architecture of the chosen muscle. In horse the superficial digitorum flexor muscle is the most frequently injured muscle and like the human hamstrings a location where strain injuries occur. It is also a muscle with a very special architecture and the muscle with the shortest muscle fibers and the highest pennation angle in horse (82). Because of these short fibers, of which many do not reach the tendon, several aponeuroses infiltrate the muscle and could create junction-like structures. This would significantly affect our ability to isolate the MTJ in the samples.

Despite this possible "contamination" of muscle and tendon fractions with MTJ-tissue it was possible to detect 27 genes that were expressed significantly higher at the MTJ compared to both muscle and tendon (Figure 14). Among these were COL22A1, NCAM1, NES and POSTN all of which have been described in relation to the MTJ previously (76,80,81), but also new targets were identified including OSTN, LCT and MNS1.
Since we did not find any unique genes at the MTJ it could be viewed as a region merely composed of a mixture of muscle and tendon without specialization. Using that assumption, we calculated an expected value for all genes based upon the relative contribution from muscle and tendon and found 43 genes to be more highly expressed at the MTJ than expected. Among these was Periostin (POSTN), which is grouped as a matricellular protein affecting connective tissues without being a structural protein in itself, and known to induce fibrosis in both skin, heart, lung and skeletal muscle as well as to contribute to several fibrotic diseases, probably through activation and migration of fibroblasts (83,84). In skeletal muscle POSTN mRNA expression increases rapidly following injury which is also the case for the expression of the periostin protein that is seen in relation to regenerating muscle fibers and myotubes (85). In addition to enriched expression of the POSTN gene at the MTJ we were also able to identify periostin on a protein level at the MTJ using immunohistochemistry. Co-staining with collagen XXII showed that Periostin is located distal to the muscle fiber on the "tendon side" of the MTJ. The finding is in line with previous studies showing both the presence of periostin at the MTJ in mice (81). Interestingly, in addition to POSTN, two growth factors known to be involved in various processes including formation of fibrosis, the fibroblast-growth factor 7 (FGF7) and Platelet Derived Growth Factor-D (PDGFD) were seen to be more highly expressed at the MTJ than in muscle and tendon. However, it was not found on the list of genes more highly expressed than expected at the MTJ.

PDGFD is poorly described in skeletal muscle but in cardiac muscle it has been shown to be involved in remodelling of the myocardium following infarction (86). Likewise, has FGF7 been shown to be induced following skeletal muscle injury where it is produced by myonuclei and affects the activity of fibroblasts (87). Together with periostin, FGF7, PDGFD and their resulting effects on both fibroblast activity could be of great interest in the understanding of the homeostasis of MTJ but also the regeneration following injury. Here deposition of fibrosis is of negative importance in an athletic setting, since increased fibrosis severely increases the risk of sustaining a re-injury. How to optimally regenerate damaged tissue without depositing excess amount of extracellular matrix is therefore a central element in the prevention of many strain injuries, and periostin could be an interesting asset in this.

The expression level of OSTN (Osteocrin) was also identified to be significantly higher at the MTJ compared to muscle and tendon. Osteocrin was initially identified as a bone-specific protein interacting with osteoblasts during bone-formation (88). However, it is also present in skeletal muscle where it has been renamed as "Musclin" and has very recently been shown to be expressed by myonuclei close to mouse MTJs by single-nuclei RNA-sequencing (74,75,89). In line with this, we found osteocrin to be more highly expressed in MTJ than in muscle and tendon in horse, and we were also able to confirm the presence of osteocrin on a protein level in relation to myonuclei near human MTJ. In skeletal muscle, osteocrin has been associated with mitochondrial function, and knockout of Osteocrin was shown to influence oxidative capacity negatively. This could indicate that the MTJ is a special region in the muscle when it comes to metabolism, which is supported by the finding of an increased concentration of mitochondria in muscle fibers near MTJ compared to further away (90). However, the functional implication of this is not known.
The same applies for the two other proteins lactase and MNS1, which we identified at the MTJ. Lactase is an enzyme which breaks down lactose in the intestines, and it has not been reported in skeletal muscle previously. Still we were able to identify small cells near the MTJ showing immunoreactivity against lactase. MNS1 was found to be expressed by some, but not all, myonuclei near the MTJ. This protein is thought to be involved in meiosis and seen in the maturing sperm cells and has previously not been related to muscle or tendon (91). However, the function and importance of MNS1 and lactase in skeletal muscle and MTJ is undescribed but could be of interest for future studies.

The purpose of the current study was also to function as a pilot study for study IV and other studies aiming to quantify issues of the MTJ without using image analysis. In order to successfully do that, the MTJ needs to be separated from the muscle and tendon with a somewhat evenly distribution of muscle and tendon in the MTJ fractions from all subjects.
Based on the RT-PCR data it is difficult to demonstrate whether we succeeded on that or not. However, in the data using a t-SNE plot some patterns could be identified. The t-SNE plot groups individual fractions based on their expression of the genes chosen for RT-PCR, so that fractions with similar expression values are grouped close together. On the t-SNE plot the tendon samples are seen to group together, without infiltration by any of the other fractions (Figure 13b). Most of the muscle samples are also forming a cluster different from the other fractions, but some muscle samples are located near the MTJ samples, indicating a high similarity between these. However, the most important finding in this context is the clustering of the MTJ samples. The close relation between all samples from the MTJ fraction indicate a high similarity between these, when it comes to the gene expression values found by RT-PCR. Because of this high similarity the employed

method of sectioning through a sample consisting of muscle, MTJ and tendon, separating these fractions, seem to be adequate, and the method can be used in future studies. The isolation is not perfect, though. Especially for some of the muscle samples, large differences are seen. These can also be identified in the diagram showing the expression of individual genes by RT-PCR. In this, the values from COMP are seen to differ to a very high degree between muscle samples, and collagen XXII is likewise seen not to be restricted to the samples from MTJ, even though it has been confirmed as a unique marker of the MTJ. COMP is known from cartilage but is also expressed in connective tissue. Together with the findings of collagen XXII in some of the muscle samples, which theoretically have been collected at some distance from the junction, this could indicate a high content of extracellular matrix and probably also MTJ in the samples. It may be because the isolation process is not effective enough. However, the explanation might be found in the anatomy of the muscle chosen for this study as explained previously

In conclusion, the current study reports a method to isolate the MTJ fraction from muscle and tendon. The high similarity between the isolated MTJ samples indicates that this method is useful for future studies examining the MTJ and the effects of interventions on the gene expression in this area. Furthermore, we identified 7 genes to be enriched at the MTJ and confirmed their presence at the MTJ on a protein level by immunohistochemistry indicating that these genes could be important in the understanding of the MTJ.

4.0 Study IV (A single bout of eccentric exercise increases the expression of nestin and osteocrin in human myotendinous junctions)

Clinically, the effect of eccentric exercise on the structure and metabolism of the MTJ is of interest to study, since this type of exercise is particularly effective to reduce the risk of strain injuries, as described previously. The main focus of studies on adaptations at the MTJ following exercise has been on the ultrastructure, and only a very limited number of studies have looked at how expression of specific genes or the protein content is influenced by exercise. At the MTJ the actin in the last sarcomere is linked to various cytoskeletal protein-complexes, which provide a transmembrane linkage to the collagen fibrils in the tendon. These include the transmembrane vinculin-talin-integrin complex and the dystrophin-glycoprotein complex (92). The importance of dystrophin for muscle function is well known due to Duchennes muscular dystrophy, in which a mutation in the dystrophin gene causes severely impaired muscle function. Besides suffering from impaired force transmission these patients are also very vulnerable to muscle damage, probably due to the absence of this strong adhesion of the sarcomeres to the membrane complexes (5). Interestingly, animal models have shown that upregulation of a specific integrin, integrin alpha 7, ameliorates some of the reduction in muscle force caused by the dystrophin-knockout (93,94). Additionally, knockout of integrin alpha 7 result in a special myopathy, affecting the strength of the MTJ, indicating an important role for this integrin at the MTJ (95).

It has been speculated whether increases in proteins, such as integrin alpha 7, at the MTJ would lead to an increase in strength and thereby have a preventive effect on strain injuries, and whether these adaptations can be induced by eccentric exercise. Increases in expression of mRNA for both alpha 7 integrin, talin and vinculin have been reported following eccentric loading regimes suggesting that a cytoskeletal adaptation of the MTJ to eccentric exercise may exist (15,96). However, none of these studies have isolated the MTJ fraction, meaning that the results reflect the

whole muscle and not necessarily the MTJ. Isolation of the MTJ is particularly important for these cytoskeletal proteins since many of them are present along the myofiber where it attaches laterally to the endomysium through costameres (97–99).

Therefore, the aim of this project was to evaluate the effect of eccentric exercise on the gene expression of human hamstring MTJ. Using the isolation method used in the horse-study we isolated the MTJ fraction and analyzed gene expression levels of both cytoskeletal genes and genes previously found to be of interest at the MTJ.

Our aim was to show whether there is a higher expression in patients who have trained of specific genes which could result in a protein synthesis, that would strengthen the MTJ and contribute to the reduction in susceptibility toward injury.

4.1 Method (Study IV)

Subjects planned for reconstruction of the ACL and did not participate in regular resistance exercise involving the hamstring muscles were used as described in study I. In this study subject who did not perform resistance exercise involving the hamstring muscles were enrolled. Due to possible effects on mRNA expression, smokers and subjects with BMI>30 were excluded. A total of 30 subjects were randomized to either a control group (n=16) or a training group who trained once, 7 days before the scheduled surgery (n=14). Unfortunately, five (3 exercise, 2 controls) subjects had to be excluded due to factors related to the surgery and not the study itself (cancelled surgery, tendon rupture during surgery and additional knee trauma).

Exercise intervention

The training program was built on three eccentric hamstring exercises and is described in detail in the supplements for the attached paper IV. Briefly it consisted of The Nordic Hamstring, lying leg curl and stiff-legged deadlift. All of which was composed of 3 sets of 6-8 repetitions until exhaustion with 2 minutes between each set. In addition to the hamstring exercises, the participants also did two exercises targeting the quadriceps muscles in order to train both the front and back thigh muscles. Here the seated leg extension and leg press was included and placed between the hamstring exercises in order to give the participants a longer break from the very intensive eccentric work. The participants were allowed not to go too hard on these exercises, especially on the leg extension, because this exercise can be uncomfortable for some patients with ACL rupture due to the high loads exerted on the tibia.

Tissue collection

The human tissue was obtained during the ACL-reconstructive surgery as described previously and approved by The Research Ethics Committees of the Capital Region of Denmark (ref. H-18022988) and conforming to the standards set by the Declaration of Helsinki. Briefly, the semitendinosus tendon and muscle was harvested from all participants and the tendon was used as ACL-graft. Excess tissue from the semitendinosus that contained muscle, tendon and MTJ was used in this project. Multiple samples from each subject were cut from the excess tissue, embedded in Tissue-Tek and frozen in liquid nitrogen-cooled isopentane.

From each subject one sample was prepared for immunohistochemistry and a separate one for RT-qPCR. For immunohistochemical evaluation the samples were aligned to give optimal sections containing MTJ with cross-sectionally cut muscle fibers.

Prior to PCR processing the samples were isolated into the various fractions using the approach described in study III.

Immunofluorescence

To investigate the cellular response to exercise, sections from all subjects were stained with antibodies against Neural Cell Adhesion molecule (NCAM) to label satellite cells, and CD68 to label macrophages.

Image analysis

To manually count the number of satellite cells and macrophages several images were stitched together using a macro in ImageJ. Here three channels were stitched together creating one image. All cells were counted by a person blinded to the intervention. A CD56 + cell located inside of laminin+ muscle membrane and containing a nucleus seen as DAPI-signal was defined as a satellite cell (Figure 19). Similarly, was a macrophage defined as a CD68+ cell with a DAPI-signal located between the muscle fibers but outside of the laminin+ muscle fibers (Figure 20).

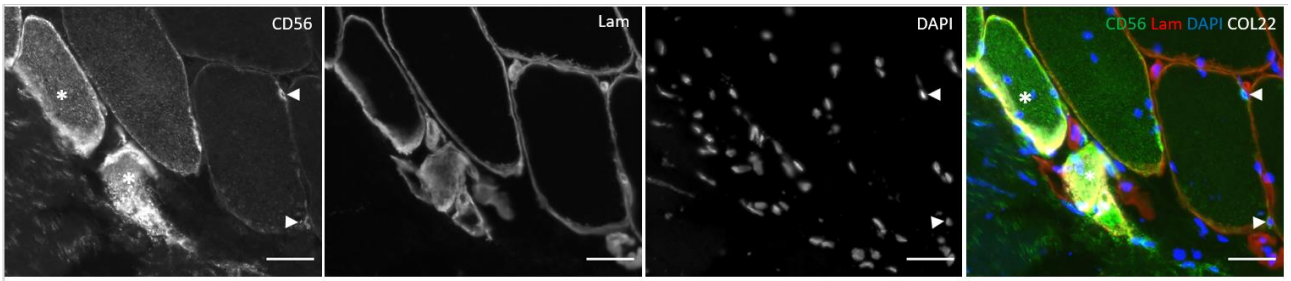

Figure 19:
Representative images of satellite cells (arrows) and muscle fibers near the MTJ (asterix) labelled with CD56 (green). Single grey-scale channels are shown in the first three columns with a merged image to the right. Scale bars are 50 µm.

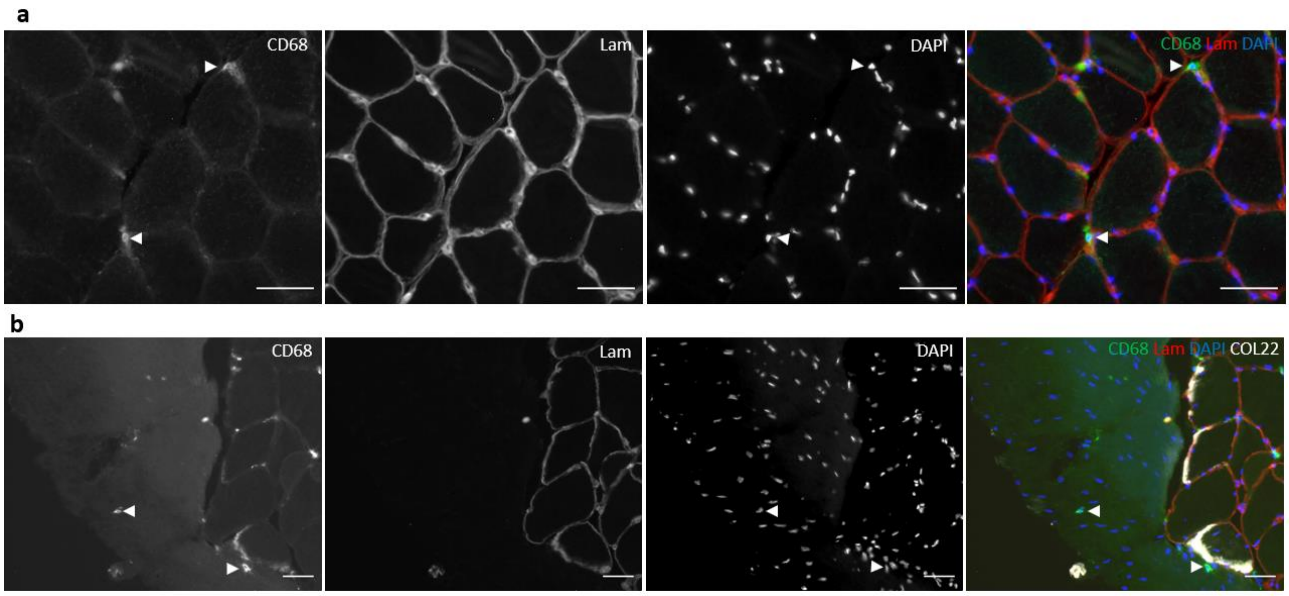

Figure 20:
Representative images of macrophages (arrowhead) in muscle (a) and tendon (b) labelled with CD68 (green). Single grey-scale channels are shown in the first three columns with a merged image to the right. Scale bars are 50 µm.

The concentration of macrophages was expressed both relative to area of muscle or tendon and relative to the number of muscle fibers.
A high number of muscle fibers showed signs of necrosis in samples from three subjects. These subjects were excluded from the analysis because the presence of necrosis made it difficult to estimate both satellite cells and macrophages properly (Figure 21)

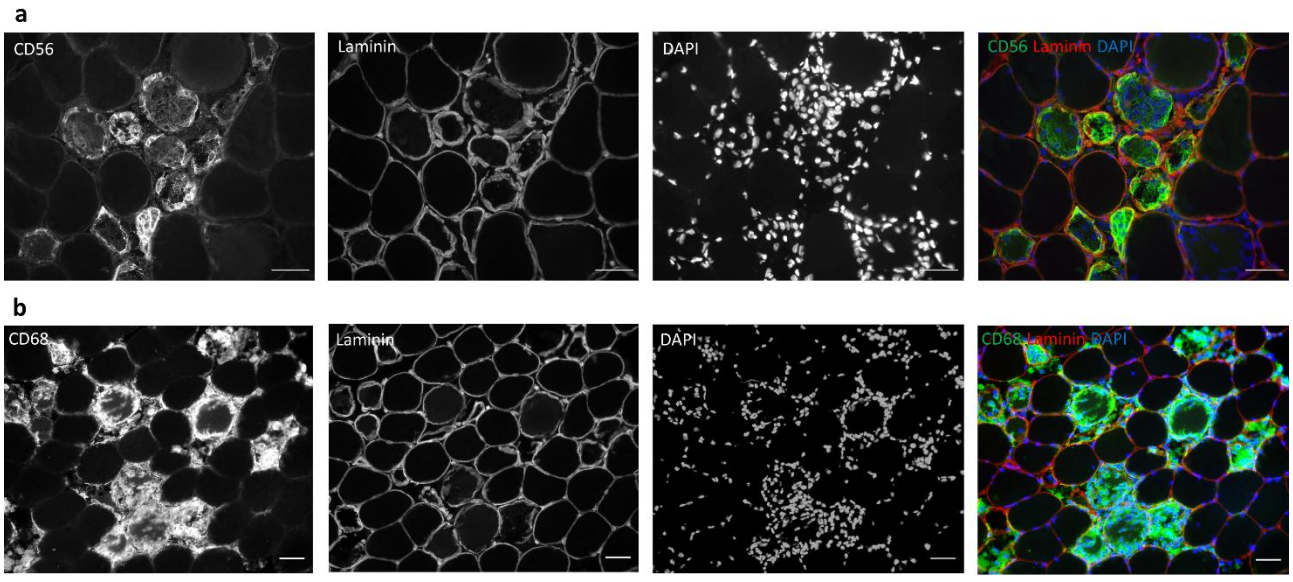

Figure 21
Representative images of a sample from an exercised subject showing signs of necrosis of the muscle fibers. In a) CD56+ muscle fibers that are either newly formed, denervated or under remodeling is seen together with

an indication of the intact muscle membrane (laminin). In b) the necrotic muscle fibers are labelled with CD68 which marks the infiltrating muscle macrophages. Single grey-scale channels are shown in the first three columns with a merged image to the right. Scale bars are 50 µm.

To express the RT-PCR data relative to tissue volume, the control sections mounted on glass slides prior to the collection of tissue for each tissue fraction was stained with Haematoxylin and Eosin before being imaged and analysed using ImageJ. By multiplying the area of the section with the number of sections collected, a measure of the volume was provided.

The RNA extraction, Real-time PCR and primer list is described in detail in the attached manuscript.

Statistics

To analyze satellite cell proliferation and macrophage infiltration unpaired t-test was used.

Data from RT-PCR was first normalized to control muscle means and expressed relative to RPLP0 (Shown in supplemental file in paper IV). However, the low number of cells in tendon meant that this normalization wasn't representative. Neither was the normalization to GAPHD. Therefore, data was expressed relative to tissue volume. Due to unevenly distributed variance in the data muscle vs MTJ and MTJ vs tendon was examined separately using Two-way repeated measures ANOVA where tissue and exercise was the two factors. The level of significance was set to < 0.05.

Graphs are made with the software GraphPad Prism 8.4.3.

4.2 Results (Study IV)

Macrophages and satellite cells

Significant higher concentrations of macrophages were seen in the exercised muscle compared to control (Figure 22b-c). However, an effect of exercise was not seen in the concentration of satellite cells in muscle. Macrophages were detected in the tendon but the concentration of these was not affected by exercise. In samples from three subjects more than 10% of the muscle fibers showed signs of necrosis. These samples were excluded from the analysis but are shown as separate values in figure 22.

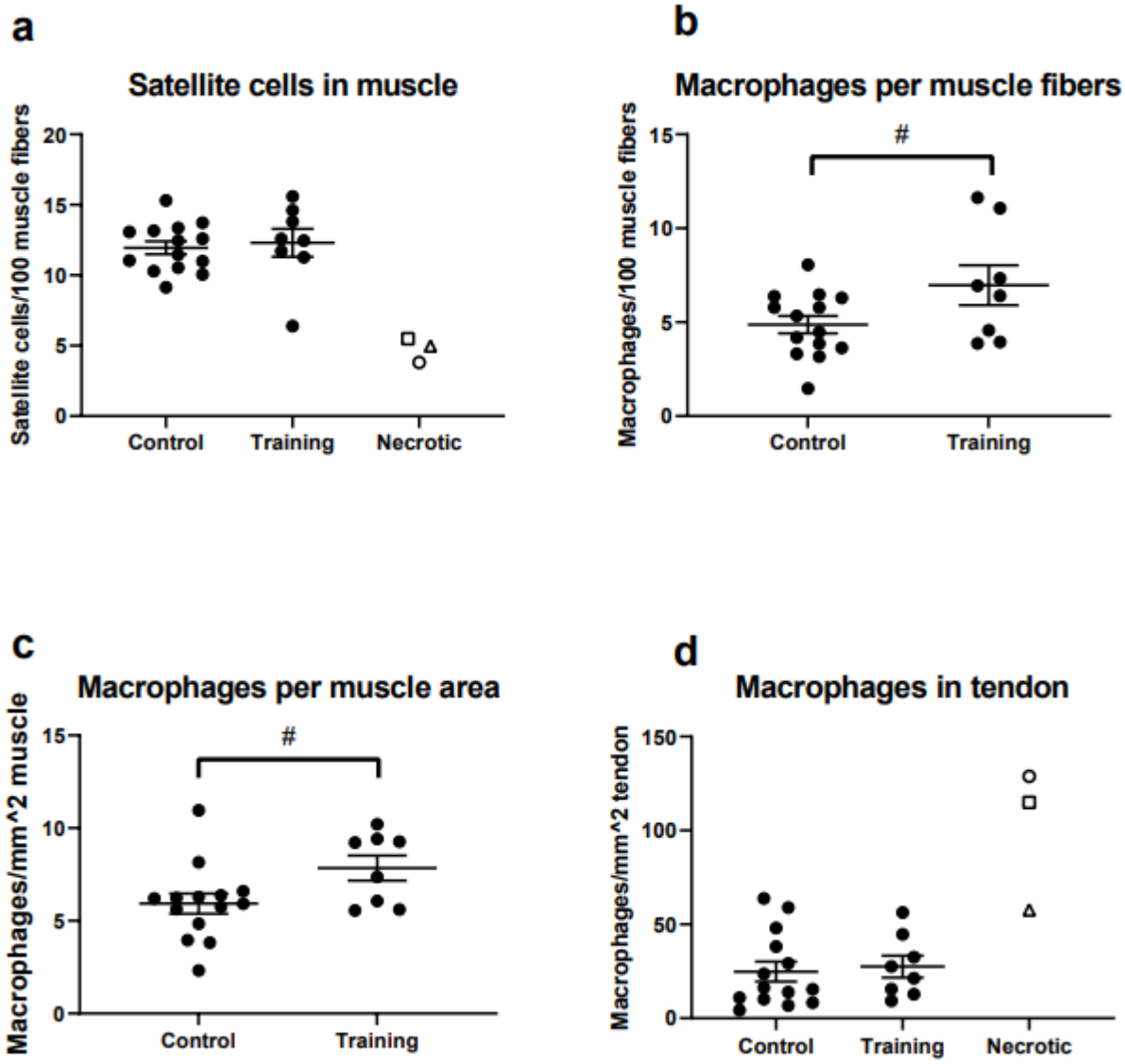

Figure 22
The effects of exercise on the satellite cell proliferation and macrophage infiltration in muscle and tendon is shown. The circles represents individual values with the open circles indicating the necrotic samples which was not included in the statistics. The lines indicate mean and SEM.
*In a) the number of satellite cells relative to number of muscle fibers are shown. The number of macrophages relative to number of muscle fibers (b) or to muscle area (c) is shown where d) illustrates the number of macrophages in tendon. * indicates significant differences ($p<0.05$).*

RT-PCR

Figure 23 shows the effect of exercise and tissue on the chosen genes. NES and OSTN were both expressed in higher levels in exercised MTJ and tendon fractions compared to control. Most of the chosen targets were more highly expressed in the MTJ than both muscle and tendon. These

included the previously identified "MTJ-specific" targets: COL22A1, NCAM1, POSTN, NES, MNS1, OSTN, ADAMTS8 and ITGA7.

Samples from subjects showing a high degree of necrosis of the muscle fibers were excluded from the analysis but are shown in figure 23.

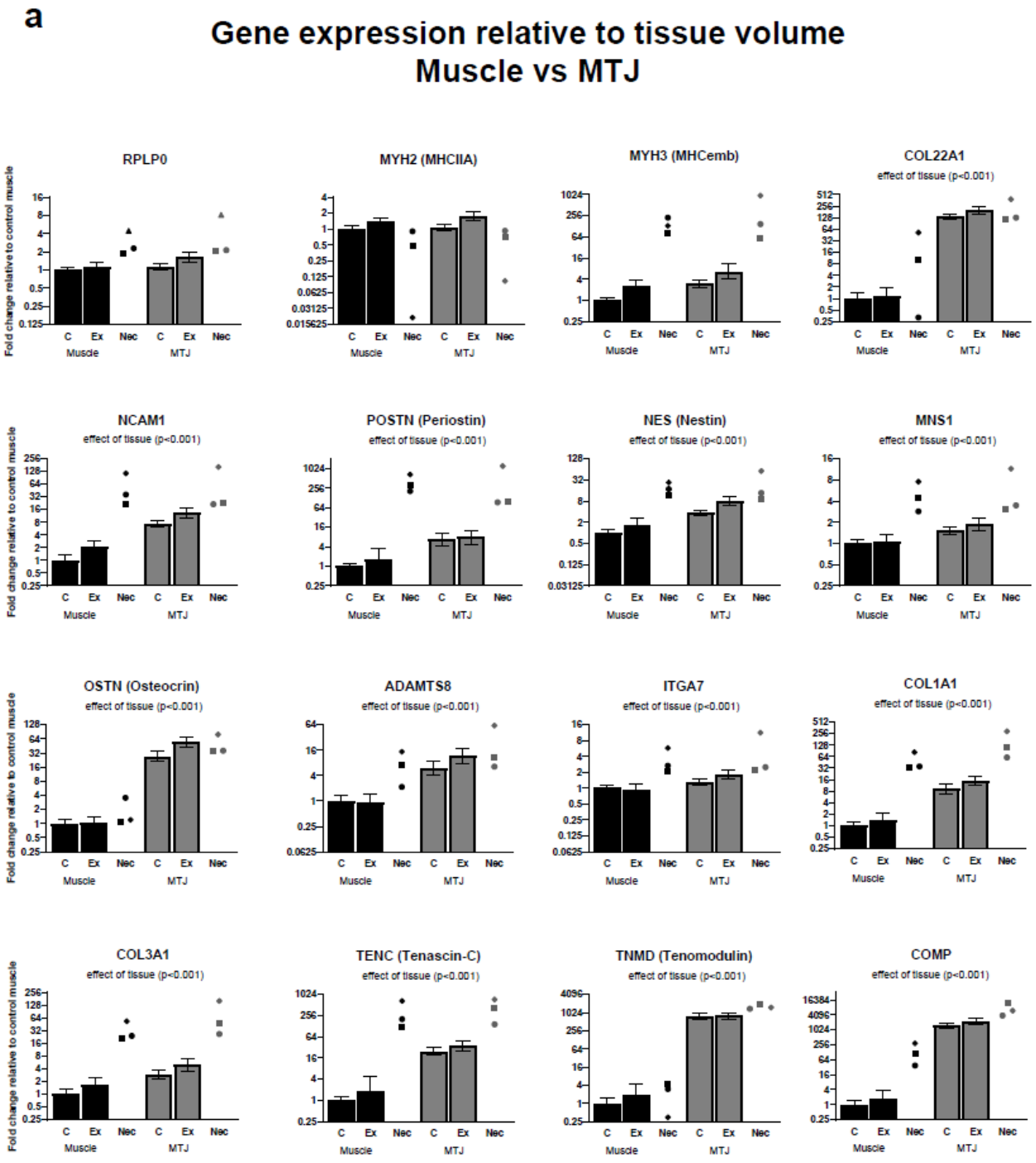

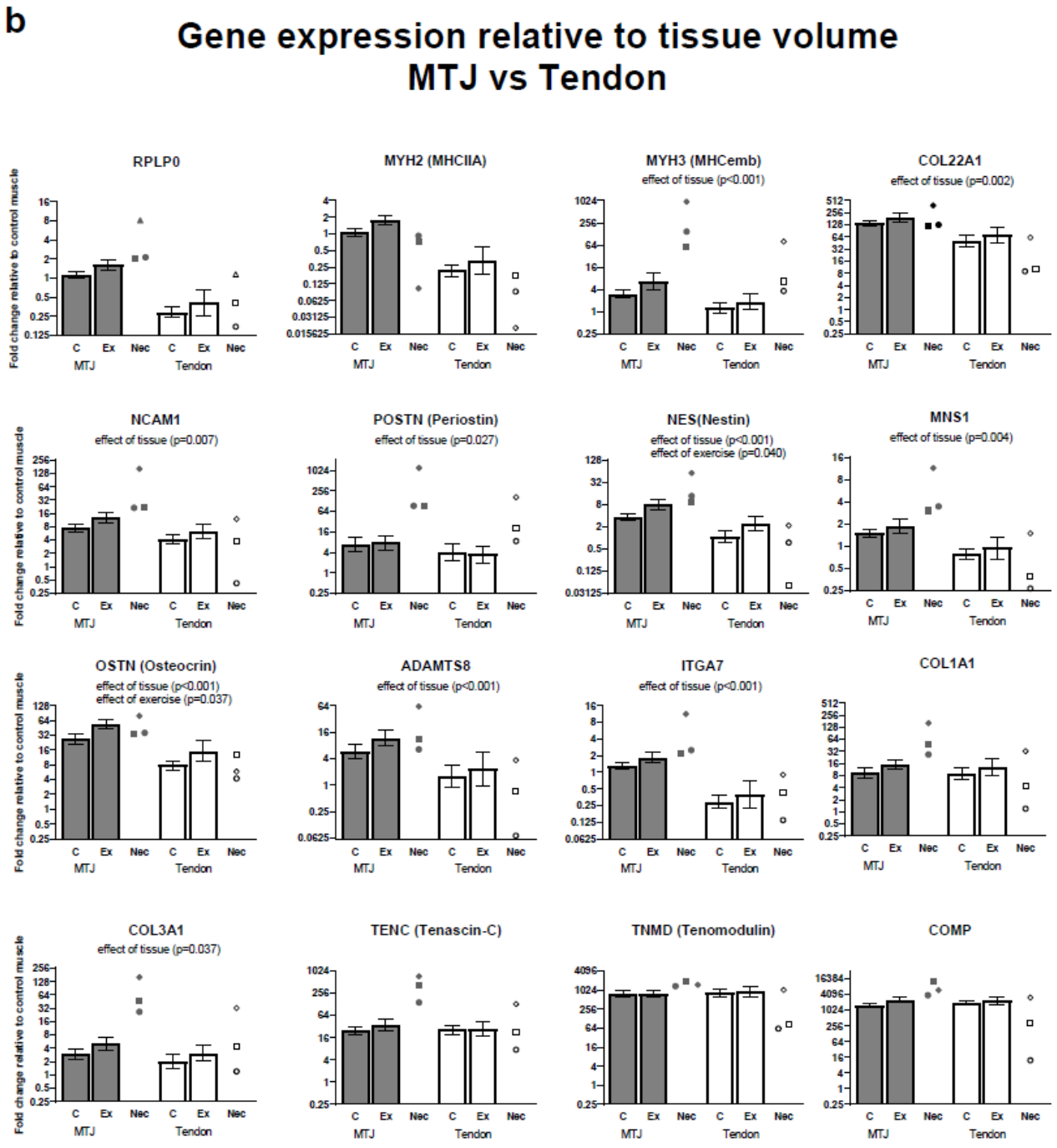

Figure 23:
The result of the PCR-analysis comparing muscle vs MTJ (a) and MTJ vs tendon (b) is shown in the figure. Data is normalized to tissue volume and expressed relative to the mean of control muscle. P-values from two-way repeated measures ANOVA examining effects of exercise and tissue is shown under each target. Values from the necrotic samples are shown as individual values. These were excluded from the analysis.

To investigate the expression of the chosen genes in relation to distance from the MTJ all fractions from three subjects were analyzed. These included 7 muscle samples in varying distance from the MTJ, 1 MTJ sample and 1 tendon sample.

A gradient was seen for many of the targets where the expression level decreased the further the fraction was from the MTJ (Figure 24).

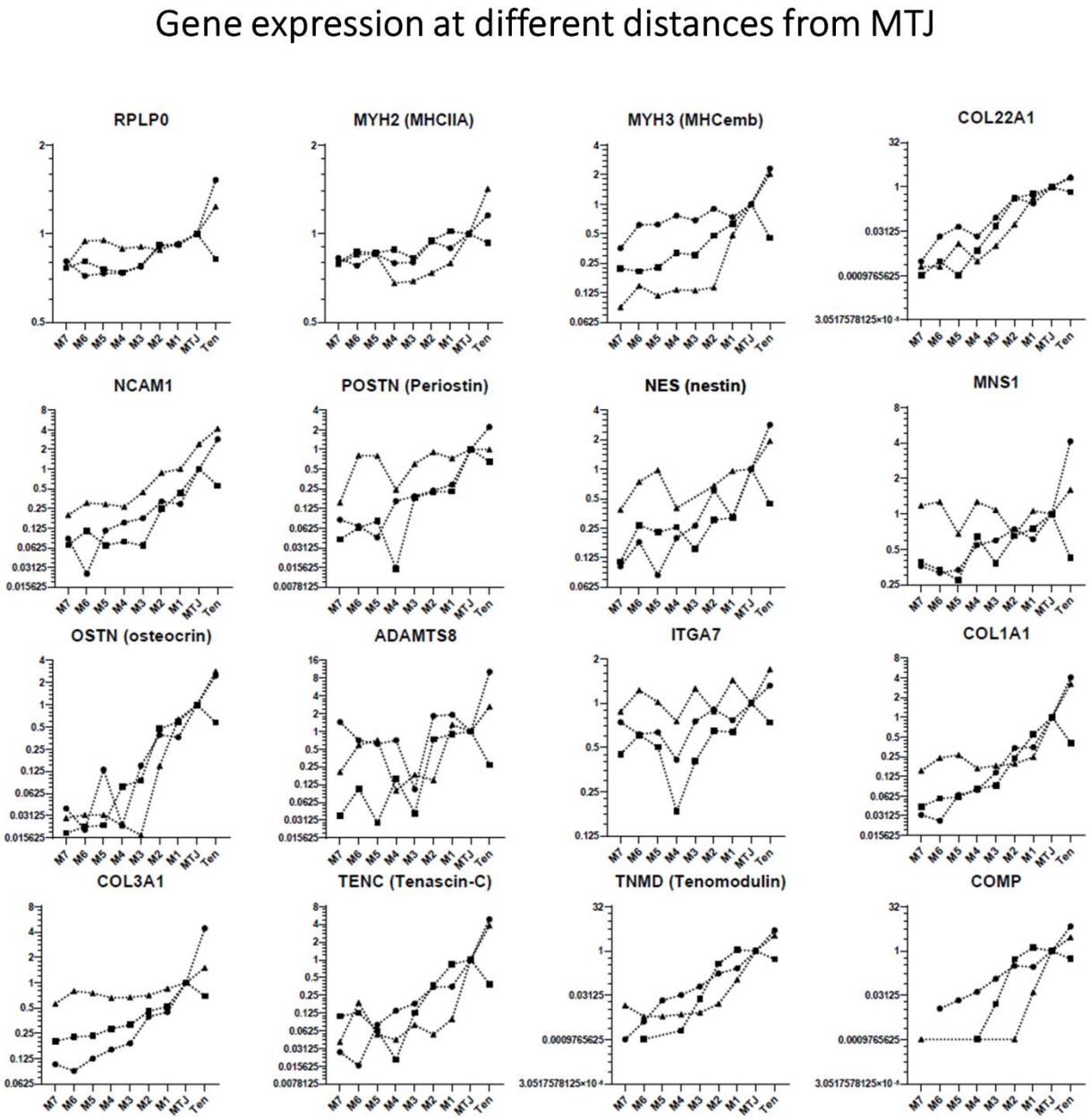

Figure 24

The graph shows the effect of distance to the MTJ on the RT-PCR values collected from 3 subjects. "M1-7" represents the muscle fractions where "M1" is the fraction closest to the MTJ.

4.3 Discussion (Study IV)

The main finding of the current study was that a single bout of eccentric exercise induced higher levels of OSTN and NES expression indicating that these genes are responsive to eccentric exercise in the MTJ. This was accompanied by infiltration of macrophages, but not satellite cells, in the

skeletal muscle. This was also the first study to investigate the effects of eccentric exercise on gene expression in human MTJ.

Osteocrin is a natriuretic peptide predominantly linked with bone research, but is also known from muscle research under the name "musclin" (100). The specific function of osteocrin is still not understood but it has been suggested to be involved in metabolism and mitochondrial processes (89,101–103). Osteocrin has previously been shown to increase in concentration following aerobic exercise and together with findings of impaired oxidative capacity of osteocrin-knockout mice this suggests a role of osteocrin in the mitochondrial adaptations to exercise (102). Osteocrin was also identified at the MTJ in horses and humans in study III. However, apart from that finding osteocrin has not been described in relation to the MTJ before. Therefore, the role of osteocrin at the MTJ is still uncertain, but it can be speculated that since the MTJ has been shown to be a region with a high remodeling activity, osteocrin could be involved in the metabolic processes that are needed for this process.

The high degree of remodulation or regeneration of fibers seen at the MTJ could also explain the finding of nestin at the MTJ. Nestin was also one of the genes found to be higher expressed at the MTJ by the RNA-sequencing of horse muscles. It has previously been shown to be upregulated following muscle injury (104,105) and involved in proliferation and muscle regeneration (106–108) as well as in the embryonic development of MTJs (106,109). This suggests that nestin could be involved in the adaptive response of the muscle fibers near the MTJ following eccentric exercise.

TENC ITGA7, COL1A1 and COL3A1 has all been shown to increase in expression following an exercise bout (110,111). However, these were not affected by exercise in any of the three tissue fractions in the current study. This lack of increase is probably due to the timing of sampling where samples in the current study are collected seven days post-exercise. This timepoint was chosen because exercise sessions were not carried out during weekends, and because it is the time where changes in satellite cells, macrophages and some mRNA can be detected (111,112). However, it is not optimal to study all mRNAs since some are known to respond rapidly and return to baseline again before the 7-day timepoint (i.e. Tenascin-C and ITGA7) (15,113).

While the exercise bout induced infiltration of macrophages in the muscle tissue it did not induce a detectable proliferation of satellite cells. As described previously satellite cells are muscle progenitor cells capable of proliferate and fuse with muscle fibers to provide additional nuclei or to form myotubes and subsequently new muscle fibers (112,114). This proliferation is normally seen in response to exercise (114,115). However, the current study is the second study from our group, in which a higher concentration of satellite cells in the muscle near the MTJ was not seen when compared to controls, following resistance exercise (80). In the distal ends of muscle fibers a high number of centralized nuclei are seen together with NCAM immunoreactivity (14). This could indicate that this region has a high turnover and therefore also a high request for satellite cells. If the need for satellite cells is high enough the lack of increase in satellite cell concentration could be a dynamic phenomenon, by which the newly formed daughter cells immediately fuse with a muscle fiber and thereby not add to the total satellite cell pool.
Furthermore, the current study investigates the semitendinosus muscle where most of the previous studies on satellite cells in human muscle have used vastus lateralis muscle.

While the effects of exercise on gene expression values were absent for most of the targets, there was a difference between the three tissues for a wide range of targets. Generally, most of the

targets were higher expressed in the MTJ compared to muscle, including the targets identified to be of importance for the MTJ by RNA-sequencing in study III. However, only ITGA7, MHCemb and NCAM1 were expressed to a greater extent in MTJ compared to tendon. While this could be due to many of the chosen genes being highly expressed in tendon, i.e. COL1A1, COMP, Tnmd, it could also indicate that the tendon fraction might not be pure. By inspection of the control sections mounted on glass-slides before collecting tissue for RT-PCR, it was seen that many of the tendon fractions also contained some muscle fibers. Therefore, the tendon fractions cannot be viewed as pure tendon, but may to some degree contain a mixture of tendon and MTJ.

Lactase was identified as a MTJ related gene by RNA-seq. in paper III. The expression of lactase was also measured in the current study, but it was not found consistently in the MTJ. It was found in the MTJ fractions from some subjects, but also in the muscle fractions from others. This could indicate that lactase is only expressed in some subjects but could also be because it is expressed by cells passing by skeletal muscle and thereby randomly being caught by the PCR.

In samples from three subjects we analyzed the effect of distance from the MTJ on the gene expression levels and found most genes to be more highly expressed closed to the MTJ, compared to expression in tissue fractions furthest from the MTJ. This means that the distance to the MTJ has a large effect on results and should be considered when measuring on samples obtained closed to the MTJ. Interestingly, COL22A1, which is considered a MTJ "specific" gene, was also seen in the muscle fractions at some distance from the MTJ. This is in contrast with a previous study showing the presence of COL22A1 close to the MTJ using in situ hybridization (57). However, it could indicate that COL22A1 is near the MTJ but to some degree diffuse in the muscle cytoplasm away from the junction.

In conclusion, a single bout of eccentric exercise was found to induce higher expression levels of nestin and osteocrin in the MTJ compared to controls. Furthermore, was the presence of the genes identified to be of interest for the MTJ in horses confirmed to be significantly higher in human MTJs than muscle.
These findings suggest that nestin and osteocrin could be of interest in future studies aiming to understand how eccentric exercise affects the human MTJ.

5. General discussion

The purpose of this PhD study and thesis was to gain knowledge about the MTJ with particular emphasis on human MTJ and changes induced by exercise. Even though some parts of the original plan had to be changed and some aspects were not included, the studies forming the thesis cover a broad spectrum of MTJ research. The majority of previous studies examining the MTJ have focused on ultrastructure, using TEM. In study I we introduced a new method to visualize the structure of the MTJ by confocal microscopy. We suggest this as a gold standard instead of electron microscopy for studies including quantification of the MTJ interface. Although this technique has a lower image resolution than electron microscopy, the number of fibers that it is possible to analyze and the possibility to measure the interface area is a great advantage compared to techniques that have been reported previously. Furthermore, the finding of a difference in surface area between fiber types indicates that electron microscopy is not optimal for this type of analysis, as fiber types cannot easily be distinguished with TEM. TEM is unique to analyze fine structures at the MTJ, but in the pursuit of an answer as to how eccentric exercise affects the size of the folded surface at the

MTJ, EM is of very limited help. For this purpose, it is paramount that many fibers are analyzed and that fiber types are easily distinguished since it is not known whether the fiber types adapt to exercise in the same way. The finding of a larger interface area of the MTJ from type I fibers compared to type II fibers is novel. The dominant theory in previous studies has been that the size of the interface area correlates with the ability to transmit and withstand forces without injury. The difference in interface area between fiber types indicates that loading might be tolerated differently, depending on fiber type. It has previously been speculated whether a particular fiber type distribution, with a large proportion of type II fibers, increases the risk of strain injury (45). If the size of the surface area is correlated to the ability to withstand stress, this might be true. However, this needs to be analyzed in future studies in order to draw any conclusion.

Eccentric exercise is of now the most effective method to prevent strain injuries. However, the mechanism of this effect is not clear. In relation to hamstring strain injury, the Nordic Hamstring exercise has the most promising effect, and it is also the most widely used exercise to prevent strain injuries. A key feature is that it applies high loads to the eccentricly working hamstring muscles. According to the size principle, where recruitment of more and larger motor-units are depending on the magnitude of force needed for the given task, this type of exercise would recruit a large amount of muscle fibers of both fiber types (116). It could be hypothesized that the clinical effect of Nordic Hamstring on strain injury risk is based on the ability of heavy eccentric exercise to recruit a large proportion of type II fibers, resulting in adaptations at the MTJ in these fibers. However, future studies are needed to confirm whether this is actually the case and if the interface area of the MTJ is able to adapt to exercise at all. The measurements of the interface area of the MTJ in study I was based on collagen XXII labelling of the folded surface. A larger interface area would therefore theoretically contain a higher total amount of collagen XXII compared to a smaller surface with shorter and fewer membrane foldings. Since a difference of almost 40% in the surface area between type I and II fibers was found, large differences in the protein concentration of collagen XXII could exist between the two fiber types.
If the foldings increase in length and number of branching following a loading regime as suggested from the earlier TEM quantifications on animal muscles, this could be accompanied by an increase in the amount of collagen XXII. Whether this increase would be equal between fiber types is not known, however, difference in surface area between fiber types suggest that the distribution of these should be considered when the contents of collagen XXII is quantified. A quantification of collagen XXII at the MTJ following a loading intervention has not yet been performed. However, in study III we measured the expression levels of collagen XXII mRNA (COL22A1) following an acute bout of eccentric exercise. Although mRNA levels are not equal to protein synthesis, it can be an indication of a possible increase in protein synthesis. Even though high levels of COL22A1 was found in the MTJ fraction, no differences were seen between the exercised and control group. This could indicate that eccentric exercise does not lead to an increase in the surface area of human MTJ, which is in line with a previous study of the effect of heavy resistance exercise on the MTJ interface area using TEM (12). However, the absence of an increase in COL22A1 expression could also be because of the timing of the sampling, since it is not known how quickly this collagen type responds to loading and for how long time the response is effective. Furthermore, could it be speculated whether the exercise bout induced similar adaptations between fiber types and whether the fiber type distribution between subjects could have an impact on the mRNA levels of COL22A1. The finding of different size of the interface area at the MTJ between the two muscle fiber types is so far the only knowledge we have about characteristics of the individual fiber types at the MTJ. Given the heterogeneity of fiber types in relation to cytoskeletal composition, energy supply systems and the contractile properties it is possible that

differences also exist in how the muscle fiber types function at the MTJ (117). Whether variations in exercise induced adaptations at the MTJ between fiber types influenced the results in study III on mRNA levels at the MTJ following an acute bout of eccentric exercise, is not known. However, future studies are needed to make further conclusions on this.

In addition to collagen XXII, eccentric exercise could also affect the concentration of other proteins specific to the MTJ. To investigate genes coding for proteins of potential importance for the MTJ, RNA-sequencing was performed on samples from the MTJ. These were isolated into fractions consisting of muscle, MTJ and tendon tissue. A total of 43 different genes were found to be more highly expressed in the MTJ compared to muscle and tendon, suggesting that they could be of interest in future studies on the MTJ. When grouped depending on their function, most of the 43 genes are related to the extracellular matrix or the cytoskeleton.

Based on these findings we investigated the effect of exercise on some of these identified genes. Nestin and osteocrin were both seen to be more highly expressed in exercised compared to control participants. Their presence was also confirmed at the protein level in sections of human hamstring MTJ, showing that nestin was located intracellularly, but only in the most distal part of the muscle fiber, whereas osteocrin was distributed in the muscle cytoplasm, as well as in mononuclear cells between the muscle fibers.
Nestin has previously been mentioned in relation to the MTJ, but the function of this protein as well as of osteocrin in the MTJ is yet unknown.

The protein CIDEA (Cell death activator) was one of the genes more highly expressed in the MTJ than in the two other fractions. CIDEA is expressed by adipocytes but in higher concentrations in brown adipocytes, and it has been suggested to be involved in browning of adipose tissue (101,118). While the presence nuclei expressing CIDEA at the MTJ confirms our finding from study II where we report adipocytes in human and murine MTJs it questions whether they are white or brown adipocytes. Since osteocrin has been suggested to be involved in browning of adipose tissue, this could be a potential function of the high expression of osteocrin at the MTJ (101). However, it has not been documented whether the adipocytes seen at the MTJ are white or brown, and it is not known, if the high expression of osteocrin following exercise leads to a browning of the adipocytes at the MTJ. There is much focus on browning of adipose tissue since the brown adipocytes differ from the white by the fact that they regulate body temperature and the production of heat through nonshivering thermogenesis by uncoupling of the electron transport chain from ATP in the mitochondria (101,118–120). In contrast to white adipose tissue, which is an energy storage, brown adipose tissue consumes energy. Browning of white adipose tissue has been shown to occur in response to various stimuli, such as cold exposure and exercise (118). However, it is still questionable to what extent this occurs in adult humans.

One group of genes identified to be higher expressed at the MTJ by the RNA-seq. analysis was related to the nervous system and nerve remodeling. The idea that the MTJ could contain a wide variety of sensory nerves is not new (121). The presence of sensory nerves at the MTJ is interesting since sensory nerves have several functions. They are capable of sensing pain and stretch but can also induce inflammation through secretion of proinflammatory cytokines that initiates inflammation through macrophages (122).
During the course of this PhD an attempt was made to analyze the presence of nerves at the MTJ. A large variety of antibodies known to target different nerve markers were tested. However, no signal was seen in sections of human MTJs. While this could indicate that the selected targets were

not present at the MTJ, it is also likely that the lack of signal was a consequence of methodological problems related to the application of staining protocols and antibodies, used in studies of the CNS in mice onto human muscle sections. In an attempt to stain nerve fibers in skeletal muscle, sections of mouse muscles were used, since the antibodies are validated in this species and the muscles are much smaller, meaning that the chance of catching a sensory nerve fiber in a thin section is higher than in human sections. In mice it was seen that nerve fibers expressing immunoreactivity against the two sensory neurotransmitters, substance P (Sub.P) and calcitonin gene-related peptide (CGRP) were present near the MTJ (Figure 25). CGRP and Sub.P are involved in sensation of pain, but they are also capable of inducing neurogenic inflammation (122–125). However, these have not previously been described in relation to the MTJ and their function in this region is therefore unconfirmed.

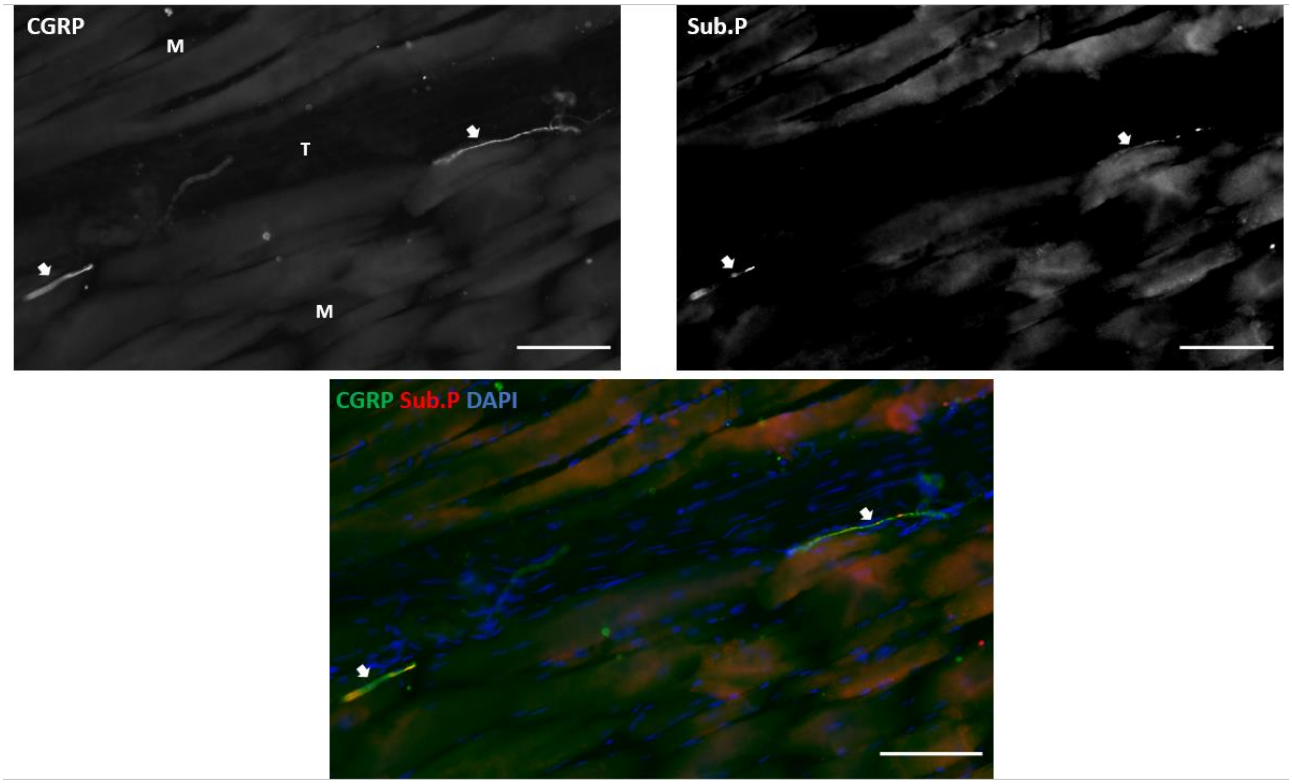

Figure 25:
Images of a section of mouse gastrocnemius muscle stained with immunofluorescent antibodies against calcitonin gene-related peptide (CGRP) and substance P (Sub.P) The first two images are signal channel images showing the CGRP and Sub.P staining, respectively. In the bottom a merged image of the two channels + a DAPI staining is shown. The tendon (T) is seen in the middle of the muscle (M) with two sensory nerve fibers positive for both CGRP and Sub.P (arrows) near the MTJ.
Scale bars are 50 µm.

6. Conclusions

The thesis shows a new method, in which confocal microscopy, using a spinning disc, can be used to analyze the size of the folded interface between muscle and tendon. The ability to easily distinct fiber types as well as analysis of whole muscle fibers in high abundance means, that this method should be considered the new golden standard to evaluate the interface area of the MTJ in humans. The importance of distinguishing between fiber types is highlighted by the fact that a larger interface of the MTJ was found for type I fibers compared to type II. The finding has relevance for determining risk factor for strain injury and for planning of the training in strain injury prevention programs.

Using both IHC and EM we confirm the presence of adipocytes in the MTJ from healthy human and murine muscles, located in very close relation to the foldings, through which force is suggested to be transmitted. The number of adipocytes at the MTJ was not seen to be influenced by resistance exercise to any high extent.

Additionally, we show a new method to isolate the MTJ from the surrounding muscle and tendon tissue, and this is valuable for studies aiming to quantify gene expression, protein concentration etc. at the MTJ. By applying the isolation method, a panel of genes was found to be significantly higher expressed at the MTJ and some were also confirmed to be present at the MTJ on a protein level. These genes could be of interest for future studies, seeking to understand the MTJ. Among these were NCAM and COL22A, both of which have previously been known to be enriched at the MTJ, but also POSTN and NES.
The latter was found in higher concentrations in subjects exposed to a single bout of eccentric exercise compared to controls. The timing of sampling could have led to some targets not being highly expressed at the specific time point. However, the increased expression of POSTN and NES suggests that these targets are of relevance in future studies of the MTJ, as well as I relation to the effect of exercise in this region.

7. Perspectives and future studies

The MTJ has been suggested to be the site of injury in most strain injuries, but a more thorough understanding of the dynamics and anatomy of these injuries is needed. It has been speculated that rapid stretch combined with a forceful contraction of the sarcomeres result in strains (126). However, it is not known which factors influence the tolerance of the sarcomeres and the linked structures in relation to stretch. Neither is it known where the actual breaking point is on a molecular level. MRI of strain injuries shows a heterogeneous group of injuries, ranging from

affection of both the muscle fibers at the MTJ to the connective tissue including the intramuscular tendon (Figure 26) (127–129).

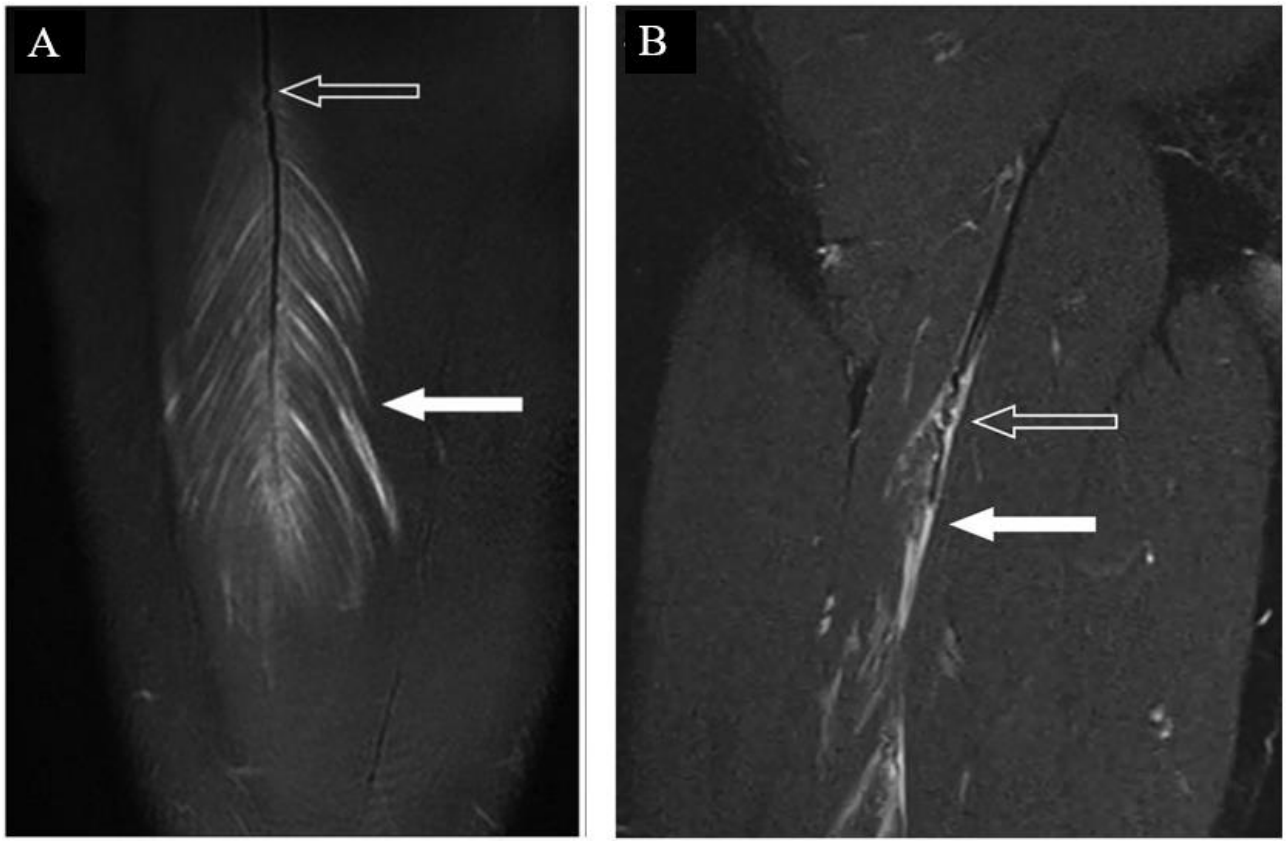

Figure 26: Strain injuries of MTJ and intramuscular tendon
MRi scans illustrating two different hamstring strain injuries. In A a strain injury of the myotendinous junction of the proximal biceps femoris is seen. The feather-like appearance characteristic for this type of injury is seen as white edema (white arrow) between the muscle fibers that attaches at the intramuscular tendon (open arrow) which is seen to be intact.
In B an injury of the intramuscular tendon is shown. The tendon is seen as a wavy structure (open arrow) and a defect in the tendon is seen which is filled with white edema (white arrow). Borrowed from Brukner P, Connell D. 'Serious thigh muscle strains': beware the intramuscular tendon which plays an important role in difficult hamstring and quadriceps muscle strains. Br J Sports Med. 2016 Feb;50(4):205-8. doi: 10.1136/bjsports-2015-095136. Epub 2015 Oct 30. PMID: 26519522.

Although it is speculative, strain injuries might therefore be a heterogeneous group, spanning from small intramuscular ruptures of the sarcomeres, or other related structures, to large ruptures involving the connective tissue scaffold. If that is the case, it would be interesting to know whether they all start as small displacements in the sarcomeres or have different mechanics. The studies of strain injuries are limited by the imaging produced by MRI and Computed Tomografi scans that are used to identify the site of injury. Most often the injuries are seen as edema and potentially also tissue retraction, however it is not possible to identify the exact structure that is damaged, at a microscopic level. This would require analysis of biopsies from the site of injury. A method to obtain larger pieces of tissue from injured MTJ's in living humans has not previously been described. In a recent study, small biopsies were taken from subjects with a strain injury in the calf and hamstring muscles using a Bard Magnum Biopsy Instrument. Ultrasound was used to identify

the location of injury, and a biopsy was obtained randomly from the hypo/hyperechoic area in the muscle (130). The relation to MTJ was not controlled in this study and biopsies for the study of MTJ would ideally require an open biopsy method. During this PhD we did develop such a method but did not get any opportunity to test it on athletes with a strain injury (see appendix). We hope to be able to do this in the future as knowledge of exactly where the injury occurs will be essential for future research on MTJ.

The recovery of a strain injury is, as described previously, depending on both the magnitude of injury but probably also the effectiveness of the inflammatory process and the following repair and degree of fibrosis. This repair process is affected by a wide range of cells and cytokines. Some of these are neurotransmitters that can activate an inflammatory process. Although it was not documented on human sections, we were able to document the presence of two sensory neurotransmitters, CGRP and Sub.P, at the MTJ, both of which are known to be involved in neurogenic inflammation. However, future studies are needed to understand the involvement of these neurotransmitters in the acute phase and the following repair process after injury to the MTJ.

As described regarding paper II, adipocytes have also previously been shown to be involved in the repair and fibrotic process following skin lesions. In the thesis we documented the presence of adipocytes at the MTJ. While the function of these cells at the MTJ is not known, it can be mentioned (unpublished) that the adipocytes were also easily identified when single fibers were dissected for the confocal analysis. Inspired by the observation of large numbers of adipocytes seen during the manual dissection in the stereomicroscope, we tried to set up a way to dissect and isolate the cells in order to analyze their gene expression later. However, we did not succeed in this, mainly because adipocytes could not be isolated without risk for contamination with other cells, such as fibroblasts, satellite cells and macrophages. Since we hypothesize that these adipocytes could have a different gene expression profile compared to adipocytes that are present in other organs, it is of course essential to be sure, that the samples are not contaminated with other cells. Time did not permit this technical issue to be solved during this PhD. Hopefully future studies will provide evidence regarding the adipocytes and their function at the MTJ.

Another important step towards understanding strain injuries, their mechanics and how to prevent them is to know how force is actually distributed and transmitted at the MTJ. The classic view on force transmission is the linear force pathway from sarcomeres directly to the tendon. However, some studies have indicated that this is not the only pathway since connections also exists spreading laterally from the sarcomeres to the endomysium through costameres (99,131,132). The magnitude of lateral force transmission could theoretically affect the overall stress on the MTJ to an important degree and increasing lateral force transmission could make the MTJ more resistant to heavy loading. However, it is not known whether lateral force transmission is a "trainable" or a static phenomenon, responsible for tightening the connective tissue surrounding the muscle fibers during contractions. We plan to study lateral force transmission in future projects.

Generally, long-term exercise studies using eccentric exercise to study adaptations in the MTJ are needed to boost the field and approach an answer as to why exercise prevents strain injury. In this thesis a panel of genes which could be of importance for the MTJ are identified as well as two genes, osteocrin and nestin, which have been shown to be responsive to eccentric exercise. These genes should be included in studies aiming at understanding the MTJ in relation to injury and exercise. Since gene expression levels not always reflect later protein synthesis, it is also needed to

confirm whether osteocrin and nestin are actually increased at a protein level following eccentric exercise.
A fiber type distribution with a higher proportion of type II vs type I fibers has already been associated with higher risk of strain injury. As suggested in the current thesis this risk could in part be due to a smaller interface area of the MTJ of type II compared to type I fibers. However, whether exercise interventions induce different adaptations in type I and II fibers is not known but could be a topic for research in the future. More specifically, it would be relevant to known if an eccentric exercise regimen consisting of the Nordic Hamstring exercise is capable of inducing greater adaptations in type II fibers compared to other regimes. Hopefully, these questions will be answered in the future and provide knowledge about the MTJ which would be useful to solve the clinical issue regarding strain injury prevention and rehabilitation.

8. References:

1. Knudsen AB, Larsen M, Mackey AL, Hjort M, Hansen KK, Qvortrup K, et al. The human myotendinous junction: an ultrastructural and 3D analysis study. Scand J Med Sci Sport. 2014/04/11. 2015;25(1):e116-23.
2. Henderson CA, Gomez CG, Novak SM, Mi-Mi L, Gregorio CC. Overview of the muscle cytoskeleton. Compr Physiol. 2017 Jul 1;7(3):891–944.
3. Shear CR, Bloch RJ. Vinculin in subsarcolemmal densities in chicken skeletal muscle: localization and relationship to intracellular and extracellular structures. J Cell Biol. 1985 Jul;101(1):240–56.
4. Hakim CH, Burkin DJ, Duan D. Alpha 7 integrin preserves the function of the extensor digitorum longus muscle in dystrophin-null mice. J Appl Physiol. 2013 Nov 1;115(9):1388–92.
5. Guo C, Willem M, Werner A, Raivich G, Emerson M, Neyses L, et al. Absence of alpha 7 integrin in dystrophin-deficient mice causes a myopathy similar to Duchenne muscular dystrophy. Hum Mol Genet. 2006 Mar 15;15(6):989–98.
6. Orchard J, Seward H. Epidemiology of injuries in the Australian Football League, seasons 1997-2000. Br J Sports Med. 2002;36(1):39–44.
7. Opar DA, Drezner J, Shield A, Williams M, Webner D, Sennett B, et al. Acute hamstring strain injury in track-and-field athletes: A 3-year observational study at the Penn Relay Carnival. Scand J Med Sci Sports. 2014 Aug;24(4):e254-9.
8. Ekstrand J, Hägglund M, Waldén M. Injury incidence and injury patterns in professional football: The UEFA injury study. Br J Sports Med. 2011 Jun;45(7):553–8.
9. Petersen J, Thorborg K, Nielsen MB, Budtz-Jorgensen E, Holmich P. Preventive effect of eccentric training on acute hamstring injuries in men's soccer: a cluster-randomized controlled trial. Am J Sport Med. 2011/08/10. 2011;39(11):2296–303.
10. Van Der Horst N, Smits DW, Petersen J, Goedhart EA, Backx FJG. The Preventive Effect of the Nordic Hamstring Exercise on Hamstring Injuries in Amateur Soccer Players: A Randomized Controlled Trial. Am J Sports Med. 2015 Jun 3;43(6):1316–23.

11. Arnason A, Andersen TE, Holme I, Engebretsen L, Bahr R. Prevention of hamstring strains in elite soccer: an intervention study. Scand J Med Sci Sport. 2007/03/16. 2008;18(1):40–8.

12. B. Knudsen A, Mackey AL, Jakobsen JR, Krogsgaard MR. No demonstrable ultrastructural adaptation of the human myotendinous junction to immobilization or 4 weeks of heavy resistance training. Transl Sport Med. 2021 Mar 13;tsm2.243.

13. Jakobsen JR, Mackey AL, Knudsen AB, Koch M, Kjær M, Krogsgaard MR. Composition and adaptation of human myotendinous junction and neighboring muscle fibers to heavy resistance training. Scand J Med Sci Sport. 2017;27(12).

14. Jakobsen JR, Jakobsen NR, Mackey AL, Koch M, Kjaer M, Krogsgaard MR. Remodeling of muscle fibers approaching the human myotendinous junction. Scand J Med Sci Sport. 2018;

15. Boppart MD, Volker SE, Alexander N, Burkin DJ, Kaufman SJ. Exercise promotes alpha7 integrin gene transcription and protection of skeletal muscle. Am J Physiol Regul Integr Comp Physiol. 2008 Nov;295(5):R1623-30.

16. Frenette J, Côté CH. Modulation of structural protein content of the myotendinous junction following eccentric contractions. Int J Sports Med. 2000;21(5):313–20.

17. Tidball JG. Force transmission across muscle cell membranes. J Biomech. 1991;24 Suppl 1:43–52.

18. Huijing PA. Muscle as a collagen fiber reinforced composite: a review of force transmission in muscle and whole limb. J Biomech. 1999/04/23. 1999;32(4):329–45.

19. Roffino S, Carnino A, Chopard A, Mutin M, Marini JF. Structural remodeling of unweighted soleus myotendinous junction in monkey. C R Biol. 2006/03/21. 2006;329(3):172–9.

20. Kojima H, Sakuma E, Mabuchi Y, Mizutani J, Horiuchi O, Wada I, et al. Ultrastructural changes at the myotendinous junction induced by exercise. J Orthop Sci. 2008/06/06. 2008;13(3):233–9.

21. Tidball JG. Myotendinous junction: Morphological changes and mechanical failure associated with muscle cell atrophy. Exp Mol Pathol. 1984;40(1):1–12.

22. Charvet B, Malbouyres M, Pagnon-Minot A, Ruggiero F, Le Guellec D. Development of the zebrafish myoseptum with emphasis on the myotendinous junction. Cell Tissue Res. 2011 Dec;346(3):439–49.

23. Nielsen KB, Lal NN, Sheard PW. Age-related remodelling of the myotendinous junction in the mouse soleus muscle. Exp Gerontol. 2018 Apr 1;104:52–9.

24. Tidball JG, Lin C. Structural changes at the myogenic cell surface during the formation of myotendinous junctions. Cell Tissue Res. 1989 Jul;257(1):77–84.

25. Trotter JA, Baca JM. A stereological comparison of the muscle-tendon junctions of fast and slow fibers in the chicken. Anat Rec. 1987;218(3):256–66.

26. Curzi D, Salucci S, Marini M, Esposito F, Agnello L, Veicsteinas A, et al. How physical exercise changes rat myotendinous junctions: an ultrastructural study. Eur J Histochem. 2012/06/13. 2012;56(2):e19.

27. Curzi D, Sartini S, Guescini M, Lattanzi D, Di Palma M, Ambrogini P, et al. Effect of Different Exercise Intensities on the Myotendinous Junction Plasticity. PLoS One. 2016;11(6):e0158059.

28. Rissatto Sierra L, Fávaro G, Cerri BR, Rocha LC, de Yokomizo de Almeida SR, Watanabe I-S, et al. Myotendinous junction plasticity in aged ovariectomized rats submitted to aquatic training. Microsc Res Tech. 2018 Aug;81(8):816–22.

29. Jacob CDS, Rocha LC, Neto JP, Watanabe IS, Ciena AP. Effects of physical training on sarcomere lengths and muscle-tendon interface of the cervical region in an experimental model of menopause. Eur J Histochem. 2019;63(3):131–5.

30. Pimentel Neto J, Rocha LC, Barbosa GK, Jacob C dos S, Krause Neto W, Watanabe I sei, et al. Myotendinous junction adaptations to ladder-based resistance training: identification of a new telocyte niche. Sci Rep. 2020 Dec 1;10(1).

31. Tidball JG, Quan DM. Reduction in myotendinous junction surface area of rats subjected to 4-day spaceflight. J Appl Physiol. 1992/07/01. 1992;73(1):59–64.

32. Kannus P, Jozsa L, Kvist M, Lehto M, Järvinen M. The effect of immobilization on myotendinous junction: an ultrastructural, histochemical and immunohistochemical study. Acta Physiol Scand. 1992 Mar;144(3):387–94.

33. Zamora AJ, Carnino A, Roffino S, Marini JF. Respective effects of hindlimb suspension, confinement and spaceflight on myotendinous junction ultrastructure. Acta Astronaut. 1995;36(8–12):693–706.

34. Curzi D, Lattanzi D, Ciuffoli S, Burattini S, Grindeland RE, Edgerton VR, et al. Growth hormone plus resistance exercise attenuate structural changes in rat myotendinous junctions resulting from chronic unloading. Eur J Histochem. 2013 Nov 13;57(4):e37.

35. Roffino S, Carnino A, Charpiot P, Marini JF. Increase in rat soleus myotendinous interface after a 14-d spaceflight. C R Acad Sci III. 1998 Jul;321(7):557–64.

36. Jakobsen JR, Krogsgaard MR. The Myotendinous Junction—A Vulnerable Companion in Sports. A Narrative Review. Front Physiol. 2021 Mar 26;12:635561.

37. Polgar J, Johnson MA, Weightman D, Appleton D. Data on fibre size in thirty-six human muscles. An autopsy study. J Neurol Sci. 1973 Jul 1;19(3):307–18.

38. Trotter JA, Samora A, Hsi K, Wofsy C. Stereological analysis of the muscle-tendon junction in the aging mouse. Anat Rec. 1987 Jul;218(3):288–93.

39. Trotter JA, Baca JM. The muscle-tendon junctions of fast and slow fibres in the garter snake: ultrastructural and stereological analysis and comparison with other species. J Muscle Res Cell Motil. 1987 Dec;8(6):517–26.

40. Mackey AL, Kjaer M. The breaking and making of healthy adult human skeletal muscle in vivo. Skelet Muscle. 2017 Nov 7;7(1).

41. Harridge SDR, Bottinelli R, Canepari M, Pellegrino MA, Reggiani C, Esbjörnsson M, et al. Whole-muscle and single-fibre contractile properties and myosin heavy chain isoforms in humans. Pflugers Arch Eur J Physiol. 1996;432(5):913–20.

42. Gollnick PD, Armstrong RB, Sembrowich WL, Shepherd RE, Saltin B. Glycogen depletion pattern in human skeletal muscle fibers after heavy exercise. J Appl Physiol. 1973;34(5):615–8.

43. Hägglund M, Waldén M, Ekstrand J. Previous injury as a risk factor for injury in elite football: A prospective study over two consecutive seasons. Br J Sports Med. 2006 Sep;40(9):767–72.

44. Mair SD, Seaber A V., Glisson RR, Garrett WE. The role of fatigue in susceptibility to acute muscle strain injury. Am J Sports Med. 1996;24(2):137–43.

45. Garrett WE, Califf JC, Bassett FH. Histochemical correlates of hamstring injuries. Am J Sports Med. 1984;12(2):98–103.

46. Tidball JG. The geometry of actin filament-membrane associations can modify adhesive strength of the myotendinous junction. Cell Motil. 1983;3(5):439–47.

47. Dirks M, Wall B, van de Valk B, Holloway T, Holloway G, Chabowski A, et al. One Week of Bed Rest Leads to Substantial Muscle Atrophy and Induces Whole-Body Insulin Resistance in the Absence of Skeletal Muscle Lipid Accumulation. Diabetes. 2016 Oct 1;65(10):2862–75.

48. Kadi F, Schjerling P, Andersen LL, Charifi N, Madsen JL, Christensen LR, et al. The effects of heavy resistance training and detraining on satellite cells in human skeletal muscles. J Physiol. 2004 Aug 1;558(Pt 3):1005.

49. Spriet LL. New insights into the interaction of carbohydrate and fat metabolism during exercise. Sports Med. 2014 May;44 Suppl 1(Suppl 1):S87-96.

50. Goodpaster BH, He J, Watkins S, Kelley DE. Skeletal Muscle Lipid Content and Insulin Resistance: Evidence for a Paradox in Endurance-Trained Athletes. J Clin Endocrinol Metab. 2001 Dec;86(12):5755–61.

51. Tuttle LJ, Sinacore DR, Mueller MJ. Intermuscular adipose tissue is muscle specific and associated with poor functional performance. J Aging Res. 2012;2012:172957.

52. Stuelsatz P, Keire P, Almuly R, Yablonka-Reuveni Z. A Contemporary Atlas of the Mouse Diaphragm: Myogenicity, Vascularity, and the Pax3 Connection. J Histochem Cytochem. 2012 Sep;60(9):638–57.

53. Jakobsen JR, Jakobsen NR, Mackey AL, Knudsen AB, Hannibal J, Koch M, et al. Adipocytes are present at human and murine myotendinous junctions. Transl Sport Med. 2020 Dec 8;tsm2.212.

54. Colwell CS, Michel S, Itri J, Rodriguez W, Tam J, Lelièvre V, et al. Selective deficits in the circadian light response in mice lacking PACAP. Am J Physiol - Regul Integr Comp Physiol. 2004 Nov;287(5 56-5).

55. Hannibal J, Ding JM, Chen D, Fahrenkrug J, Larsen PJ, Gillette MU, et al. Pituitary adenylate cyclase-activating peptide (PACAP) in the retinohypothalamic tract: A potential daytime regulator of the biological clock. J Neurosci. 1997;17(7):2637–44.

56. Riedel CS, Georg B, Fahrenkrug J, Hannibal J. Altered light induced EGR1 expression in the SCN of PACAP deficient mice. PLoS One. 2020 May 1;15(5).

57. Koch M, Schulze J, Hansen U, Ashwodt T, Keene DR, Brunken WJ, et al. A novel marker of tissue junctions, collagen XXII. J Biol Chem. 2004 May 21;279(21):22514–21.

58. Nikolaou PK, Macdonald BL, Glisson RR, Seaber A V, Garrett Jr. WE. Biomechanical and histological evaluation of muscle after controlled strain injury. Am J Sport Med. 1987/01/01. 1987;15(1):9–14.

59. Croisier JL. Factors associated with recurrent hamstring injuries. Vol. 34, Sports Medicine. Sports Med; 2004. p. 681–95.

60. Benjamin M, Redman S, Milz S, Büttner A, Amin A, Moriggl B, et al. Adipose tissue at entheses: the rheumatological implications of its distribution. A potential site of pain and stress dissipation? Ann Rheum Dis. 2004 Dec 1;63(12):1549–55.

61. Zwick RK, Guerrero-Juarez CF, Horsley V, Plikus M V. Anatomical, Physiological, and Functional Diversity of Adipose Tissue. Vol. 27, Cell Metabolism. Cell Press; 2018. p. 68–83.

62. Min SY, Desai A, Yang Z, Sharma A, DeSouza T, Genga RMJ, et al. Diverse repertoire of human adipocyte subtypes develops from transcriptionally distinct mesenchymal progenitor cells. Proc Natl Acad Sci U S A. 2019 Sep 3;116(36):17970–9.

63. Fontanella CG, Nalesso F, Carniel EL, Natali AN. Biomechanical behavior of plantar fat pad in healthy and degenerative foot conditions. Med Biol Eng Comput. 2016 Apr 1;54(4):653–61.

64. Ronti T, Lupattelli G, Mannarino E. The endocrine function of adipose tissue: An update. Vol. 64, Clinical Endocrinology. 2006. p. 355–65.

65. Shook BA, Wasko RR, Mano O, Rutenberg-Schoenberg M, Rudolph MC, Zirak B, et al. Dermal Adipocyte Lipolysis and Myofibroblast Conversion Are Required for Efficient Skin Repair. Cell Stem Cell. 2020 Jun 4;26(6):880-895.e6.

66. Sohn JH, Lee YK, Han JS, Jeon YG, Kim JI, Choe SS, et al. Perilipin 1 (Plin1) deficiency promotes inflammatory responses in lean adipose tissue through lipid dysregulation. J Biol Chem. 2018 Sep 7;293(36):13974–88.

67. Joe AWB, Yi L, Natarajan A, Le Grand F, So L, Wang J, et al. Muscle injury activates resident fibro/adipogenic progenitors that facilitate myogenesis. Nat Cell Biol. 2010 Feb;12(2):153–63.

68. Heredia JE, Mukundan L, Chen FM, Mueller AA, Deo RC, Locksley RM, et al. Type 2 innate signals stimulate fibro/adipogenic progenitors to facilitate muscle regeneration. Cell. 2013 Apr 11;153(2):376–88.

69. Biferali B, Proietti D, Mozzetta C, Madaro L. Fibro–Adipogenic Progenitors Cross-Talk in Skeletal Muscle: The Social Network. Vol. 10, Frontiers in Physiology. Frontiers Media S.A.; 2019.

70. Wosczyna MN, Rando TA. A Muscle Stem Cell Support Group: Coordinated Cellular Responses in Muscle Regeneration. Vol. 46, Developmental Cell. Cell Press; 2018. p. 135–43.

71. Schmidt BA, Horsley V. Intradermal adipocytes mediate fibroblast recruitment during skin wound healing. Dev. 2013 Apr 1;140(7):1517–27.

72. Jamali AA, Afshar P, Abrams RA LR. Differential expression of neural cell adhesion molecule (NCAM) after tenotomy in rabbit skeletal muscle. J Orthop Res. 2002;20(2):364–9.

73. Kim M, Franke V, Brandt B, Lowenstein ED, Schöwel V, Spuler S, et al. Single-nucleus transcriptomics reveals functional compartmentalization in syncytial skeletal muscle cells. Nat Commun. 2020 Dec 1;11(1).

74. Dos Santos M, Backer S, Saintpierre B, Izac B, Andrieu M, Letourneur F, et al. Single-nucleus RNA-seq and FISH identify coordinated transcriptional activity in mammalian myofibers. Nat Commun. 2020 Dec 1;11(1).

75. Petrany MJ, Swoboda CO, Sun C, Chetal K, Chen X, Weirauch MT, et al. Single-nucleus RNA-seq identifies transcriptional heterogeneity in multinucleated skeletal myofibers. Nat Commun. 2020 Dec 1;11(1).

76. Charvet B, Guiraud A, Malbouyres M, Zwolanek D, Guillon E, Bretaud S, et al. Knockdown of col22a1 gene in zebrafish induces a muscular dystrophy by disruption of the myotendinous junction. Development. 2013/10/18. 2013;140(22):4602–13.

77. Miyamoto-Mikami E, Kumagai H, Kikuchi N, Kamiya N, Miyamoto N, Fuku N. EQTL variants in COL22A1 are associated with muscle injury in athletes. Physiol Genomics. 2020 Dec 1;52(12):588–9.

78. Can T, Faas L, Ashford DA, Dowle A, Thomas J, O'Toole P, et al. Proteomic analysis of laser capture microscopy purified myotendinous junction regions from muscle sections. Proteome Sci. 2014 May 7;12(1).

79. Jakobsen JR, Schjerling P, Svensson RB, Buhl R, Carstensen H, Koch M, et al. RNA-sequencing and immunofluorescence of the myotendinous junction of mature horses and humans. Am J Physiol Physiol. 2021 Jul 14;

80. Jakobsen JR, Jakobsen NR, Mackey AL, Koch M, Kjaer M, Krogsgaard MR. Remodeling of muscle fibers approaching the human myotendinous junction. Scand J Med Sci Sports. 2018 May 8;

81. Jacobson KR, Lipp S, Acuna A, Leng Y, Bu Y, Calve S. Comparative Analysis of the Extracellular Matrix Proteome across the Myotendinous Junction. J Proteome Res. 2020 Oct 2;19(10):3955–67.

82. Brown NAT, Kawcak CE, McIlwraith CW, Pandy MG. Architectural properties of distal forelimb muscles in horses,Equus caballus. J Morphol. 2003 Oct;258(1):106–14.

83. Walker JT, McLeod K, Kim S, Conway SJ, Hamilton DW. Periostin as a multifunctional modulator of the wound healing response. Vol. 365, Cell and Tissue Research. Springer Verlag; 2016. p. 453–65.

84. Hara M, Yokota K, Saito T, Kobayakawa K, Kijima K, Yoshizaki S, et al. Periostin Promotes Fibroblast Migration and Inhibits Muscle Repair After Skeletal Muscle Injury. J Bone Joint Surg Am. 2018 Aug 15;100(16):e108.

85. Özdemir C, Akpulat U, Sharafi P, Yildiz Y, Onbaşilar I, Kocaefe Ç. Periostin is temporally expressed as an extracellular matrix component in skeletal muscle regeneration and differentiation. Gene. 2014 Dec 15;553(2):130–9.

86. Zhao W, Zhao T, Huang V, Chen Y, Ahokas RA, Sun Y. Platelet-derived growth factor involvement in myocardial remodeling following infarction. J Mol Cell Cardiol. 2011 Nov;51(5):830–8.

87. Tanaka Y, Yamaguchi A, Fujikawa T, Sakuma K, Morita I, Ishii K. Expression of mRNA for specific fibroblast growth factors associates with that of the myogenic markers MyoD and proliferating cell nuclear antigen in regenerating and overloaded rat plantaris muscle. Acta Physiol. 2008 Oct;194(2):149–59.

88. Thomas G, Moffatt P, Salois P, Gaumond MH, Gingras R, Godin É, et al. Osteocrin, a

Novel Bone-specific Secreted Protein That Modulates the Osteoblast Phenotype. J Biol Chem. 2003 Dec 12;278(50):50563–71.

89. Nishizawa H, Matsuda M, Yamada Y, Kawai K, Suzuki E, Makishima M, et al. Musclin, a Novel Skeletal Muscle-derived Secretory Factor. J Biol Chem. 2004 May 7;279(19):19391–5.

90. Eisenberg BR, Milton RL. Muscle fiber termination at the tendon in the frog's sartorius: A stereological study. Am J Anat. 1984;171(3):273–84.

91. Furukawa K, Inagaki H, Naruge T, Tabata S, Tomida T, Yamaguchi A, et al. cDNA cloning and functional characterization of a meiosis-specific protein (MNS1) with apparent nuclear association. Chromosom Res. 1994 Mar;2(2):99–113.

92. Matsumura K, Campbell KP. Dystrophin-glycoprotein complex: Its role in the molecular pathogenesis of muscular dystrophies. Muscle Nerve. 1994 Jan;17(1):2–15.

93. Burkin DJ, Wallace GQ, Nicol KJ, Kaufman DJ, Kaufman SJ. Enhanced expression of the alpha 7 beta 1 integrin reduces muscular dystrophy and restores viability in dystrophic mice. J Cell Biol. 2001 Mar 19;152(6):1207–18.

94. Hakim CH, Burkin DJ, Duan D. Alpha 7 integrin preserves the function of the extensor digitorum longus muscle in dystrophin-null mice. J Appl Physiol. 2013 Nov 1;115(9):1388–92.

95. Mayer U, Saher G, Fässler R, Bornemann A, Echtermeyer F, Von Der Mark H, et al. Absence of integrin α7 causes a novel form of muscular dystrophy. Nat Genet. 1997;17(3):318–23.

96. Frenette J, Côté CH. Modulation of structural protein content of the myotendinous junction following eccentric contractions. Int J Sports Med. 2000 Jul;21(5):313–20.

97. Mondello MR, Bramanti P, Cutroneo G, Santoro G, Di Mauro D, Anastasi G. Immunolocalization of the costameres in human skeletal muscle fibers: confocal scanning laser microscope investigations. Anat Rec. 1996 Jul;245(3):481–7.

98. Pardo J V., D'Angelo Siliciano J, Craig SW. A vinculin-containing cortical lattice in skeletal muscle: Transverse lattice elements ('costameres') mark sites of attachment between myofibrils and sarcolemma. Proc Natl Acad Sci U S A. 1983;80(4 I):1008–12.

99. Passerieux E, Rossignol R, Letellier T, Delage JP. Physical continuity of the perimysium from myofibers to tendons: involvement in lateral force transmission in skeletal muscle. J Struct Biol. 2007/04/17. 2007;159(1):19–28.

100. Moffatt P, Thomas GP. Osteocrin - Beyond just another bone protein? Vol. 66, Cellular and Molecular Life Sciences. 2009. p. 1135–9.

101. Jeremic N, Chaturvedi P, Tyagi SC. Browning of White Fat: Novel Insight Into Factors, Mechanisms, and Therapeutics. Vol. 232, Journal of Cellular Physiology. Wiley-Liss Inc.; 2017. p. 61–8.

102. Subbotina E, Sierra A, Zhu Z, Gao Z, Koganti SRK, Reyes S, et al. Musclin is an activity-stimulated myokine that enhances physical endurance. Proc Natl Acad Sci U S A. 2015 Dec 29;112(52):16042–7.

103. Shimomura M, Horii N, Fujie S, Inoue K, Hasegawa N, Iemitsu K, et al. Decreased muscle-derived musclin by chronic resistance exercise is associated with improved

insulin resistance in rats with type 2 diabetes. Physiol Rep. 2021 May 5;9(9).

104. Lindqvist J, Torvaldson E, Gullmets J, Karvonen H, Nagy A, Taimen P, et al. Nestin contributes to skeletal muscle homeostasis and regeneration. J Cell Sci. 2017 Sep 1;130(17):2833–42.

105. Singh DP, Lonbani ZB, Woodruff MA, Parker TJ, Steck R, Peake JM. Effects of topical icing on inflammation, angiogenesis, revascularization, and myofiber regeneration in skeletal muscle following contusion injury. Front Physiol. 2017 Mar 7;8(MAR):93.

106. Vaittinen S, Lukka R, Sahlgren C, Hurme T, Rantanen J, Lendahl U, et al. The expression of intermediate filament protein nestin as related to vimentin and desmin in regenerating skeletal muscle. J Neuropathol Exp Neurol. 2001;60(6):588–97.

107. Vaittinen S, Lukka R, Sahlgren C, Rantanen J, Hurme T, Lendahl U, et al. Specific and innervation-regulated expression of the intermediate filament protein nestin at neuromuscular and myotendinous junctions in skeletal muscle. Am J Pathol. 1999;154(2):591–600.

108. Sahlgren CM, Pallari HM, He T, Chou YH, Goldman RD, Eriksson JE. A nestin scaffold links Cdk5/p35 signaling to oxidant-induced cell death. EMBO J. 2006 Oct 18;25(20):4808–19.

109. Carlsson L, Li Z, Paulin D, Thornell LE. Nestin is expressed during development and in myotendinous and neuromuscular junctions in wild type and desmin knock-out mice. Exp Cell Res. 1999 Aug 25;251(1):213–23.

110. Hyldahl RD, Nelson B, Xin L, Welling T, Groscost L, Hubal MJ, et al. Extracellular matrix remodeling and its contribution to protective adaptation following lengthening contractions in human muscle. FASEB J. 2015 Jul 1;29(7):2894–904.

111. Jensen SM, Bechshøft CJL, Heisterberg MF, Schjerling P, Andersen JL, Kjaer M, et al. Macrophage Subpopulations and the Acute Inflammatory Response of Elderly Human Skeletal Muscle to Physiological Resistance Exercise. Front Physiol. 2020 Jul 24;11.

112. Kadi F, Charifi N, Denis C, Lexell J, Andersen JL, Schjerling P, et al. The behaviour of satellite cells in response to exercise: What have we learned from human studies? Vol. 451, Pflugers Archiv European Journal of Physiology. Pflugers Arch; 2005. p. 319–27.

113. Fluck M, Tunc-Civelek V, Chiquet M. Rapid and reciprocal regulation of tenascin-C and tenascin-Y expression by loading of skeletal muscle. J Cell Sci. 2000/10/06. 2000;113 (Pt 2:3583–91.

114. Crameri RM, Langberg H, Magnusson P, Jensen CH, Schrøoder HD, Olesen JL, et al. Changes in satellite cells in human skeletal muscle after a single bout of high intensity exercise. J Physiol. 2004 Jul 1;558(1):333–40.

115. Dreyer HC, Blanco CE, Sattler FR, Schroeder ET, Wiswell RA. Satellite cell numbers in young and older men 24 hours after eccentric exercise. Muscle Nerve. 2006 Feb;33(2):242–53.

116. Henneman E. Relation between size of neurons and their susceptibility to discharge. Science. 1957;126(3287):1345–7.

117. Schiaffino S, Reggiani C. Fiber Types in Mammalian Skeletal Muscles. https://doi.org/101152/physrev000312010. 2011 Oct;91(4):1447–531.

118. Stanford K, Middelbeek R, Goodyear L. Exercise Effects on White Adipose Tissue: Beiging and Metabolic Adaptations. Diabetes. 2015 Jul 1;64(7):2361–8.

119. Lo K, Sun L. Turning WAT into BAT: a review on regulators controlling the browning of white adipocytes. Biosci Rep. 2013;33(5):711–9.

120. Jankovic A, Golic I, Markelic M, Stancic A, Otasevic V, Buzadzic B, et al. Two key temporally distinguishable molecular and cellular components of white adipose tissue browning during cold acclimation. J Physiol. 2015 Aug 1;593(15):3267–80.

121. Jozsa L, Balint J, Kannus P, Järvinen M, Lehto M. Mechanoreceptors in human myotendinous junction. Muscle Nerve. 1993;16(5):453–7.

122. Scott A, Bahr R. Neuropeptides in tendinopathy. Front Biosci. 2009 Jan 1;14(6):2203–11.

123. Brain SD, Williams TJ, Tippins JR, Morris HR, MacIntyre I. Calcitonin gene-related peptide is a potent vasodilator. Nature. 1985;313(5997):54–6.

124. Russell FA, King R, Smillie SJ, Kodji X, Brain SD. Calcitonin gene-related peptide: physiology and pathophysiology. Vol. 94, Physiological reviews. American Physiological Society; 2014. p. 1099–142.

125. Bohnsack M, Meier F, Walter GF, Hurschler C, Schmolke S, Wirth CJ, et al. Distribution of substance-P nerves inside the infrapatellar fat pad and the adjacent synovial tissue: a neurohistological approach to anterior knee pain syndrome. Arch Orthop Trauma Surg. 2005 Nov;125(9):592–7.

126. Garrett WE. Muscle Strain Injuries. Vol. 24, The American journal of sports medicine. 1996.

127. De Smet AA, Fisher DR, Heiner JP, Keene JS. Magnetic resonance imaging of muscle tears. Skeletal Radiol. 1990 May;19(4):283–6.

128. Koulouris G, Connell D. Evaluation of the hamstring muscle complex following acute injury. Skeletal Radiol. 2003 Oct 1;32(10):582–9.

129. Brukner P, Connell D. "Serious thigh muscle strains": beware the intramuscular tendon which plays an important role in difficult hamstring and quadriceps muscle strains. Br J Sports Med. 2016 Feb 1;50(4):205–8.

130. Bayer ML, Hoegberget-Kalisz, M, Svensson R, Hjortshoej M, Olesen J, Nybing J, et al. Chronic Sequelae After Muscle Strain Injuries: Influence of Heavy Resistance Training on Functional and Structural Characteristics in a Randomized Controlled Trial. Am J Sports Med. 2021 Jul 15;3635465211026623.

131. Zhang C, Gao Y. Finite element analysis of mechanics of lateral transmission of force in single muscle fiber. J Biomech. 2012/06/12. 2012;45(11):2001–6.

132. Ramaswamy KS, Palmer ML, van der Meulen JH, Renoux A, Kostrominova TY, Michele DE, et al. Lateral transmission of force is impaired in skeletal muscles of dystrophic mice and very old rats. J Physiol. 2011 Mar 1;589(Pt 5):1195–208.

9. Appendix

How to make biopsies from the human semitendinosus myotendinous junction.
Biopsies from the semitendinosus myotendinous junction are made with the participant placed in a lying supine position, back-up. The semitendinosus MTJ is localized by ultrasound and the biopsy area is marked on the thigh 2-3 centimeters proximal to the most distal insertion of muscle to the tendon (14-20 cm proximal of the insertion of the tendon on the pes anserinus). Under sterile conditions and after subcutaneous injection of local analgesics, a small incision (1-2 cm) is made in the skin just superficial to the semitendinosus muscle/tendon, which is easily located by asking the participant to contract his hamstrings. Gently the subcutaneous tissue is pulled to the side and a small incision is made in the fascia covering the semitendinosus. When the semitendinosus MTJ is visualized, local analgesics are injected in the muscle proximal to the biopsy site, and one or two biopsies of 5 mm in diameter containing muscle, MTJ and tendon, is taken using a surgical biopsy puncher. Skin is closed with Vicryl Rapid.

From dissection it is obvious, that the biopsy is only a very small part of MTJ, and the risk of rupture in the post-biopsy period is negligible.

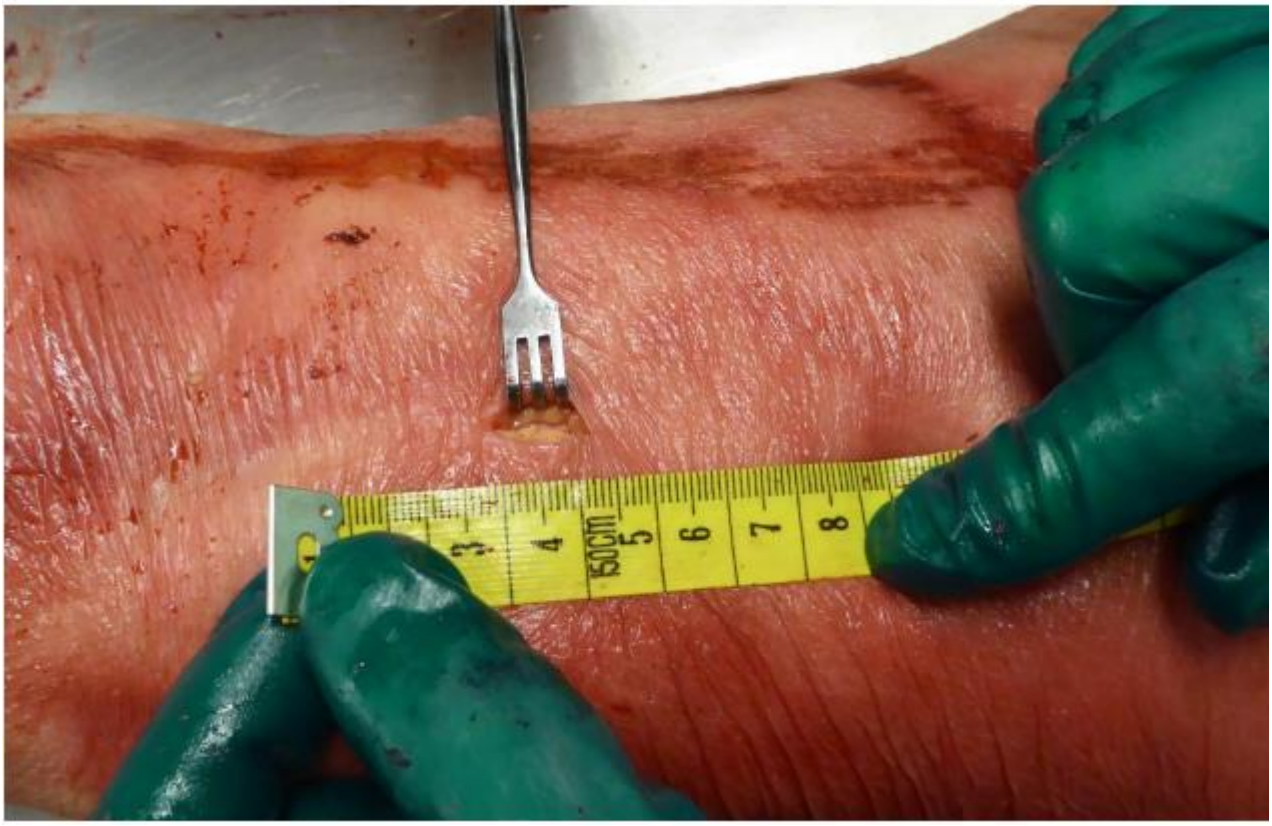

The skin incision needed for the biopsy.

The fascia over the tendon is incised longitudinally in order to reach the tendon beneath.

The tendon is visible after incision of the fascia

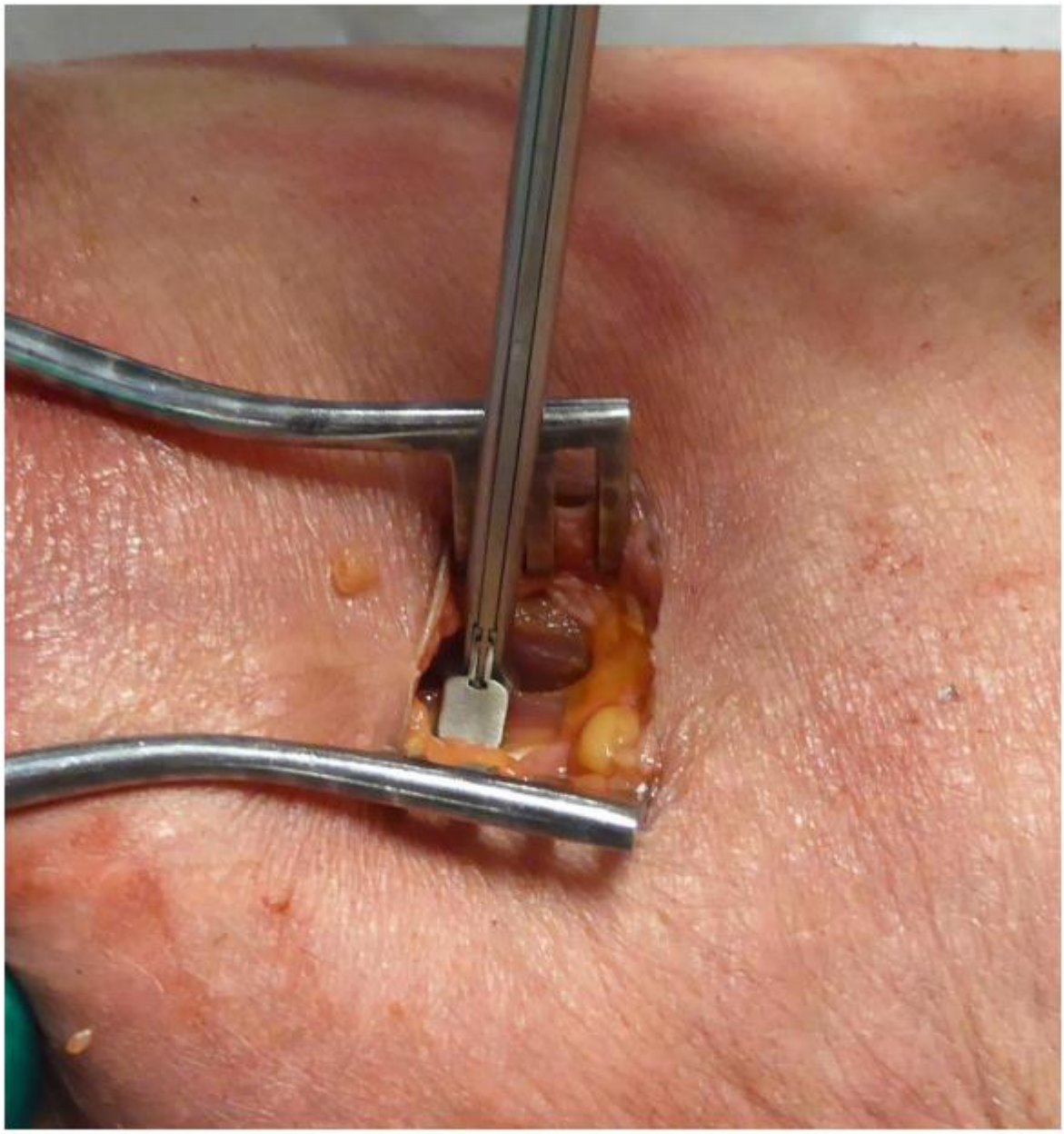

The MTJ is identified and a biopsy taken using a basket forceps.

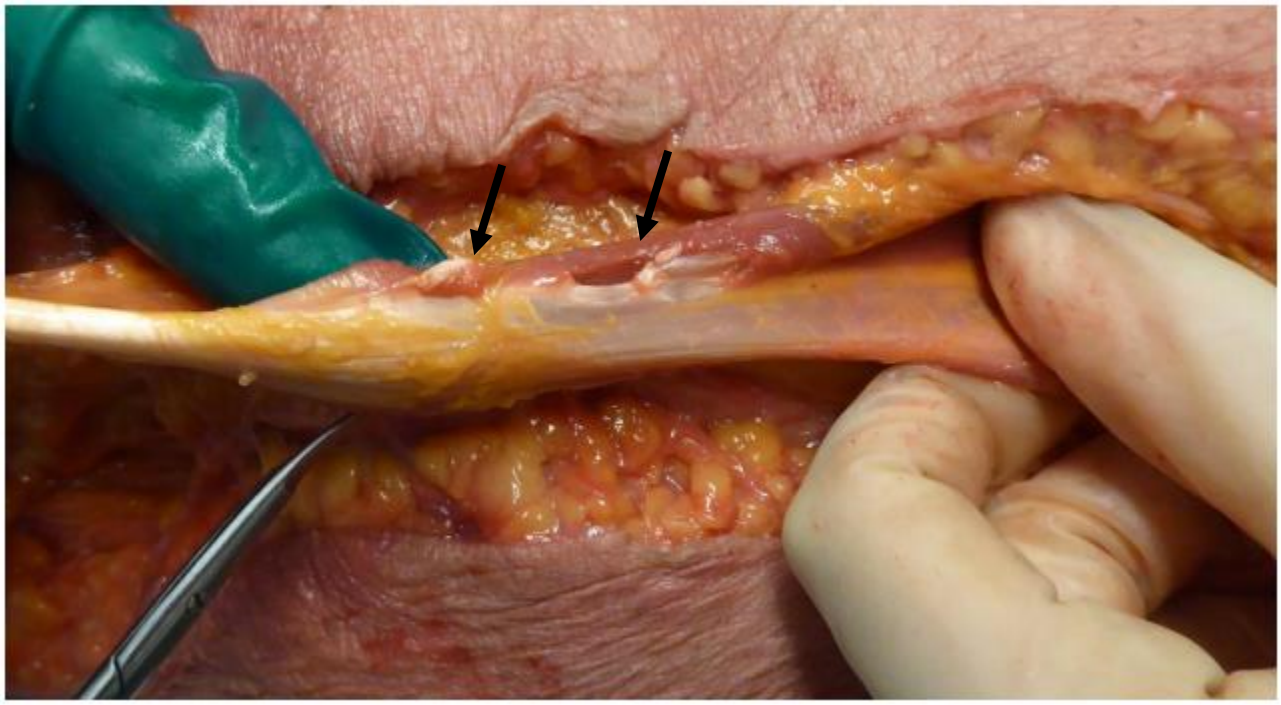

The semitendinosus muscle and tendon after two biopsies. Arrows indicates where the biopsies were taken.

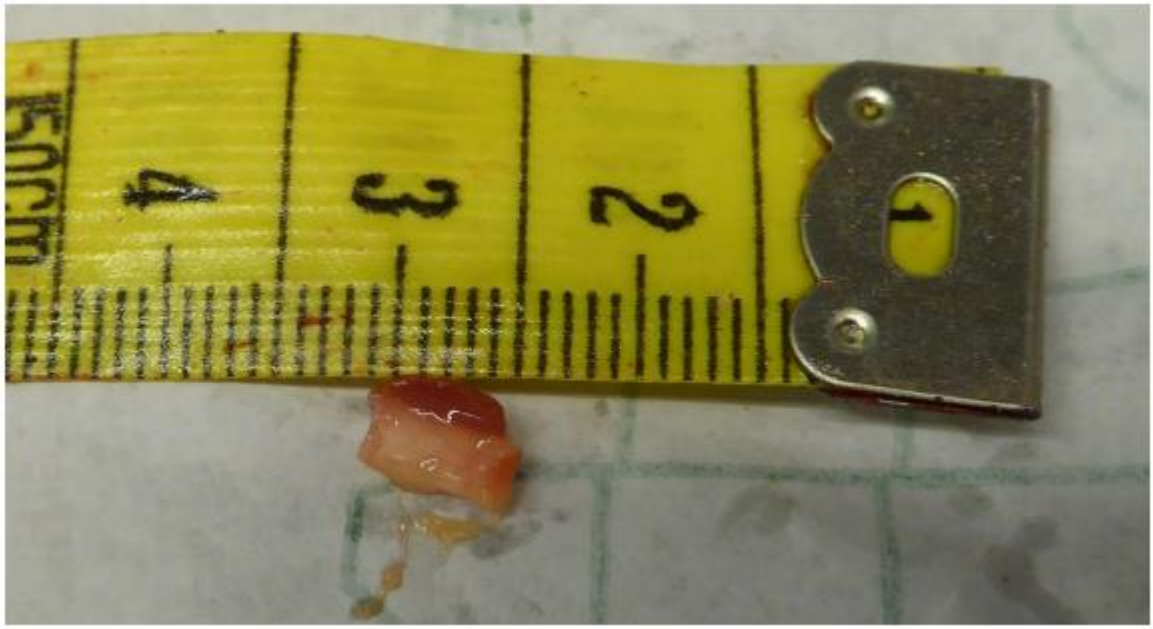

The size of the biopsy.

10. Papers

Paper I: Fiber type differences in the surface area of human myotendinous junction.
Status: Manuscript not submitted.

Paper II: Adipocytes are present at murine and human myotendinous junction
Status: Published in Translational Sports Medicine.

Paper III: RNA-sequencing and immunofluorescence of the myotendinous junction of mature horses and humans.
Status: Published in American Journal of Physiology – Cell Physiology.

Paper IV: A single bout of eccentric exercise increases the gene expression of nestin and osteocrin in human myotendinous junctions.
Status: Manuscript not submitted.

Fiber type differences in the surface area of the human myotendinous junction

Jens R. Jakobsen[1], Abigail L. Mackey[2,3], Manuel Koch[4,5], Jens Hannibal[6], Michael Kjær[2], Michael R. Krogsgaard[1].

[1]Section for Sports Traumatology M51, Department of Orthopaedic Surgery, Copenhagen University Hospital, Bispebjerg and Frederiksberg, Denmark*

[2]Institute of Sports Medicine, Department of Orthopaedic Surgery M, Copenhagen University Hospital, Bispebjerg and Frederiksberg, Denmark*

[3]Xlab, Center for Healthy Aging, Department of Biomedical Sciences, Faculty of Health and Medical Sciences, University of Copenhagen, Copenhagen, Denmark

[4] Institute for Dental Research and Oral Musculoskeletal Biology, and Center for Biochemistry, Medical Faculty, University of Cologne, Cologne, Germany

[5]Center for Molecular Medicine Cologne (CMMC), University of Cologne, 50931, Cologne, Germany

[6]Department of Clinical Biochemistry, Bispebjerg and Frederiksberg Hospital, Copenhagen, Denmark

*Departments are part of IOC Research Center Copenhagen.

Corresponding author
Jens Rithamer Jakobsen
Section of Sports Traumatology, M51, department of Orthopaedic Surgery M
Bispebjerg Hospital
Nielsine Nielsens Vej 3
Copenhagen 2400 NV
Denmark
Tel: (+45) 3863 5639
Email: jensjakobsendk@gmail.com

Conflict of Interest
The authors have declared that no conflict of interest exists.

Abstract

Background: The myotendinous junction (MTJ) is a region structurally specialized in force transmission and susceptible to strain injuries. Foldings are formed where muscle and tendon meet which increases the contact area between these two tissues and theoretically improves the ability of the MTJ to withstand loading. It is unknown, if the interface area of MTJ is the same in type I and type II muscle fibres.

Method: Samples were collected from human semitendinosus MTJs, and individual muscle fibres with intact MTJ were isolated by microscopic dissection and labelled with antibodies against collagen XXII (indicating MTJ) and type I myosin (MHCI). Using a spinning disc confocal microscope, the MTJs from all fibres were scanned and subsequently reconstructed in 3D-models. The interface area between muscle and

tendon was measured on this reconstruction by a blinded observer, and results were compared between type I and II fibres. The validity of measurements was assessed through blinded, repeated measurements in xxx fibres.

Results: By application of this method it was possible to analyse the entire MTJ from 314 muscle fibres. Type I muscle fibres had a 38.35% larger interface area of MTJ compared to type II fibres ($p<0.05$). This was also found when expressing the area relative to fiber diameter.

Conclusion: By applying a new method to analyse the structure of the MTJ from a large number of fibers it was found that the interface area between the muscle and tendon are higher in type I compared to type II fibers. This new method could prove useful for future studies wanting to quantify on differences in the structure of the MTJ between a large number of fibers.

Introduction

The myotendinous junction (MTJ) is the tissue structure through which force between muscle and tendon is transmitted. The morphology of in the contact area between the termination of each muscle fibre and the collagen fibrils from the tendon is highly specialized. The muscle membrane is intensively folded, forming invaginations consisting of collagen-rich protrusions from the tendon - visually like fingers penetrating the muscle fibre. Collagen type XXII is a useful marker of the MTJ(1), and transmission electron microscopy-imaging (TEM) has confirmed that this particular collagen is present in the protrusions from the tendon(1).

The angle of force transmission is different in an interface with such protrusions compared to a smooth cone-shaped interface (2,3). Consequently, a higher proportion of force is transmitted as shear- or sliding-force, which is more protective in relation to retain the tissue structure compared to tensile- or pulling-force (2). Theoretically, the large area for force transmission and the reduced angle between tissues lower the stress on the MTJ.

Despite its specialized structure, the MTJ is where strain injuries are most frequently seen (4). Strain injuries, and especially hamstring strain injuries, are among the most frequent non-contact injuries in many sports, and they are therefore common objects for research in sports medicine (5–8). Clinical studies have shown that eccentric exercise with the Nordic Hamstring exercise is very effective to reduce the risk of these injuries (9–13).

It has been hypothesized that the size of the foldings and thereby the area of the interface might affect the risk of injury (3,14). In animals, the effect of various loading regimes is an increasing size of the foldings and the overall interface area of MTJ, when measured on TEM-images (14–18). This theoretically increases the ability of the MTJ to transfer force and potentially lowers the risk of strain injury (2,3). In atrophic or unloaded muscle the opposite occurs (19–22): the foldings decrease in size, and this reduces the overall area by which force is transmitted. It has been suggested that there is a correlation between how much the MTJ is loaded through activity and the risk of strain injury, meaning that following periods with lower loading the risk of strain injury increases. This implies that plasticity of the foldings at the MTJ may be a key factor for the risk of strain injury (23).

An advantage of TEM is that very small structures are visualized due to the high resolution achieved with this technique, compared to regular light microscopy. The drawback is, that the very small regions analyzed by TEM might not be representative of the tissue. Furthermore, is the tissue preparation and image analysis very time consuming compared to regular immunohistochemistry.

It has been suggested that there might be differences in the structure of the foldings of the MTJ, dependent on muscle fiber type, as the surface area of type II fibers seems to be larger compared to type I fibers (24,25). While this is of less importance in studies on mice, in which most muscles consist almost exclusively of type I or II fibers, it must be considered in analysis of human muscles, because in general they are composed of both fiber types with no fixed ratio. Unfortunately, distinguishing between fiber types by TEM is not straightforward. For these reasons TEM is not an ideal method to analyze changes in the human MTJ, for instance in relation to exercise, or differences of the MTJ dependent on fiber type. Therefore, the current study aimed to develop a method for regular immunohistochemistry (IHC) by use of confocal microscopy to analyze larger, representative samples of the entire MTJ, and within a realistic time frame to analyze a higher number of samples, while at the same time determine the muscle fiber type. With such a method available, we also aimed to investigate possible differences in the surface area of the MTJ between type I and II muscle fibers, hypothesizing that type II fibers have a larger surface area of MTJ.

Methods

Participants

Samples were collected from 10 human subjects (3 females and 7 males, mean age 27.1 ± 6.3 and BMI 24.3 ± 1.6. All subjects were scheduled for ACL-reconstructive surgery at Bispebjerg and Frederiksberg Hospital and had not performed resistance exercise involving the hamstring muscles during the preceding 3 months. During the surgery the semitendinosus was harvested, and the tendon was used as graft. The excess tissue containing the MTJ, was used for this study. Quickly following dissection of the tissue, samples were prepared according to a single-fiber protocol, as described previously (26). Briefly, samples were pinned in a silicone-coated dish to keep the fiber length and incubated in Krebs-Henseleit buffer with procaine, followed by Zamboni fixative (indhold I detaljer) incubation overnight followed by storage in 50% Glycerol in PBS until dissection.

Using a stereo microscope, single muscle fibers were dissected from the tendon using a surgical scalpel. An effort was made to separate the tissues while keeping the tip of each muscle fiber intact. 50 fibers were dissected from each subject and placed in NUNC well-plates for IHC staining.

Staining protocol

The single fibers were pre-incubated for one hour in an Immunobuffer (IB) (PBS containing 50 mM glycine, 0.03% saponin, 0.25% BSA, 0.05% sodium azide and 0.1 %Triton-X to increase the permeability of the antibodies). Hereafter, a mixture of two primary antibodies was added and left for incubation at 5° for three days. Previous tests found this superior in relation to signal-to-noise ratio in the image analysis

afterwards compared to shorter incubation periods. The primary antibodies were: Guinea-pig anti-Collagen XXII diluted in IB 1:1000 (a kind gift from Manuel Koch University of Cologne, Germany) and mouse anti-MHC1 Alexa 649 1:100 (A4.951, Hybridoma Bank). Following washing in IB the fibers were incubated with secondary antibodies overnight at 5°. The following secondary antibodies were used: Goat Anti guinea pig Alexa 568, Goat Anti-mouse Alexa 647. Before mounting in glycerol-containing mounting medium with DAPI (Molecular Probes ProLong Gold anti-fade reagent, cat. no. P36935; Invitrogen A/S), the fibers were washed in IB and once in PBS. When using a coverslip, it was seen that the fibers were compressed and that the level of compression was different between fibers. Because it was not possible to find a method where the coverslip was mounted in a standardized manner with an equal compression of all fibers on all slides, it was chosen not to use coverslips and instead scan the fibers directly using immersion oil on the objective. This was not found to affect the image quality.

Confocal microscopy

The images of the muscle fibers were obtained using an iMIC microscope equipped with a wide field and a confocal unit (Till Photonic, FEI Munich, Germany) (27) . The microscope was equipped with appropriate filter settings for detecting DAPI, Texas Red/Alexa561/594 and CY5/ Alexa647. For confocal imaging, the iMIC used an Andromeda disk system (FEI, Germany) and a Hamamatsu 16-bit camera (Model C10600-10B-H, Hamamatsu Photonic, Japan) for recording. For wide field microscopy, the iMIC used a 12-bit camera (Model C84484-03G02, Hamamatsu Photonic, Japan) and the following objectives: x10, numerical aperture (NA) = 0.35 and ×60, NA = 1.46.
Using the x10 objective an wide field overview image of the entire slide was made using the Alexa 647 staining to distinguish type I and II fibers (Fig. 1A). The position of the MTJ of each fiber was marked in the system for easier navigation later and the presence of MHC1 staining noted. In some muscle fibers only specific regions of the fiber showed immunoreactivity against the MHC1 antibody. Therefore, a type I fiber was defined as a fiber showing immunoreactivity against MHC1 in any part of the fiber. (Figure 1A)

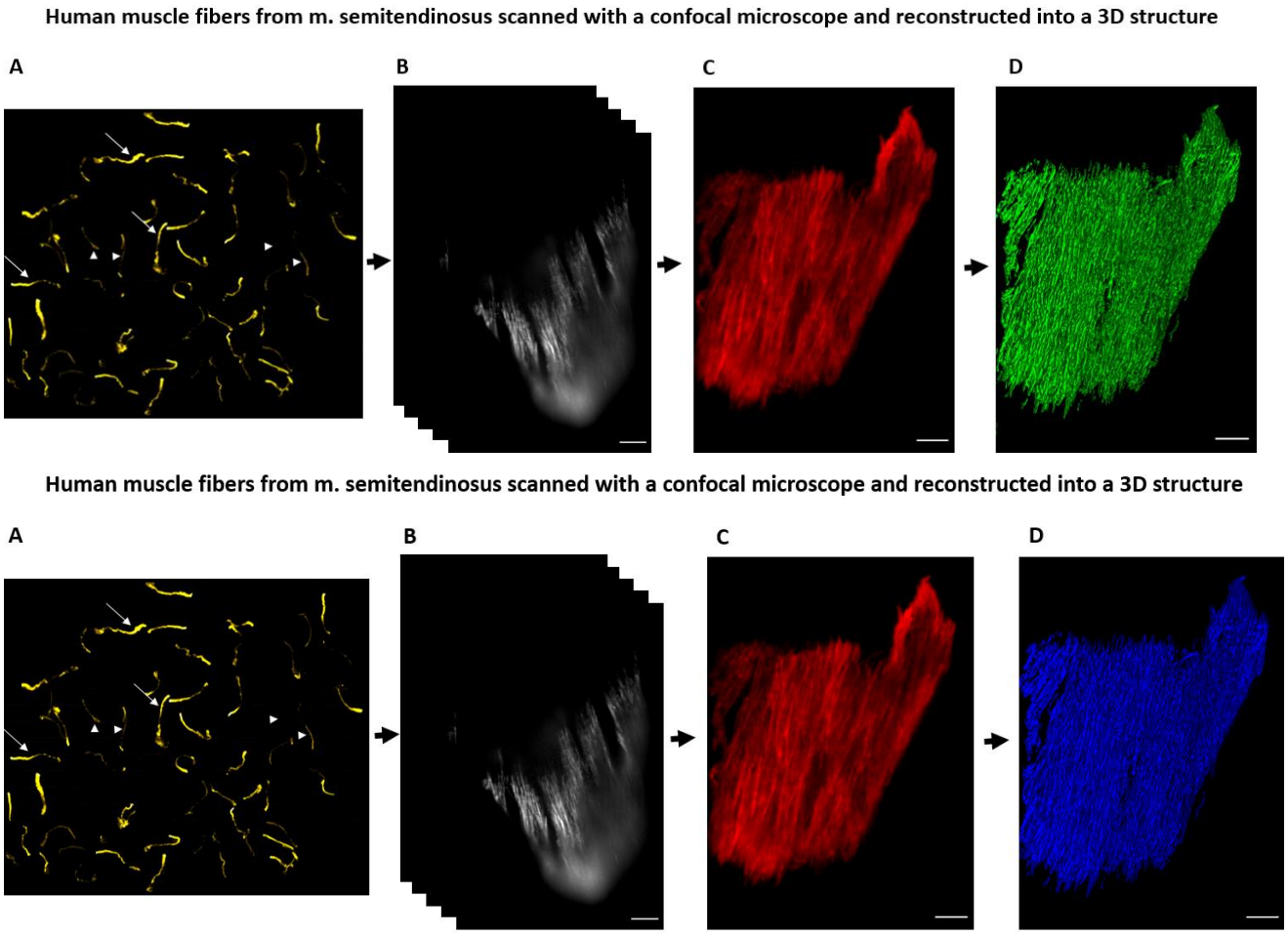

Figure 1:

The figure shows the workflow of the study starting by the widefield fluorescent image of all fibers from a subject where type I MHC is labelled and the fiber type is registered (type I arrow, type II arrowhead). Each fiber is also labelled with collagen XXII antibody and scanned using the confocal part of the microscope providing images through the depth of the fiber as shown in b). These images are merged in a z-stack (image c) which is used to create the 3D surface (d) from which the measurements are made. Scale bars are 10 µm.

Z-stacks of individual fibers were created using a 561 nm laser to image the collagen XXII staining in conjunction with oil immersion and the x60 objective. Based on the wavelength and the numerical aperture (NA) of the objective, a theoretical working resolution (smallest visual distance between two pixels) could be calculated: resolution = wavelength (λ /2* NA). In the current setup the theoretical resolution was ~192 nm with a Z-resolution of 200 nm.

Each fiber was scanned from bottom to top with a z-distance between images of 0.2 µm using the same laser intensity, but varying exposure time (between 99-200 mS) to get at least 10.000 grey values in all fibers. (Figure 2)

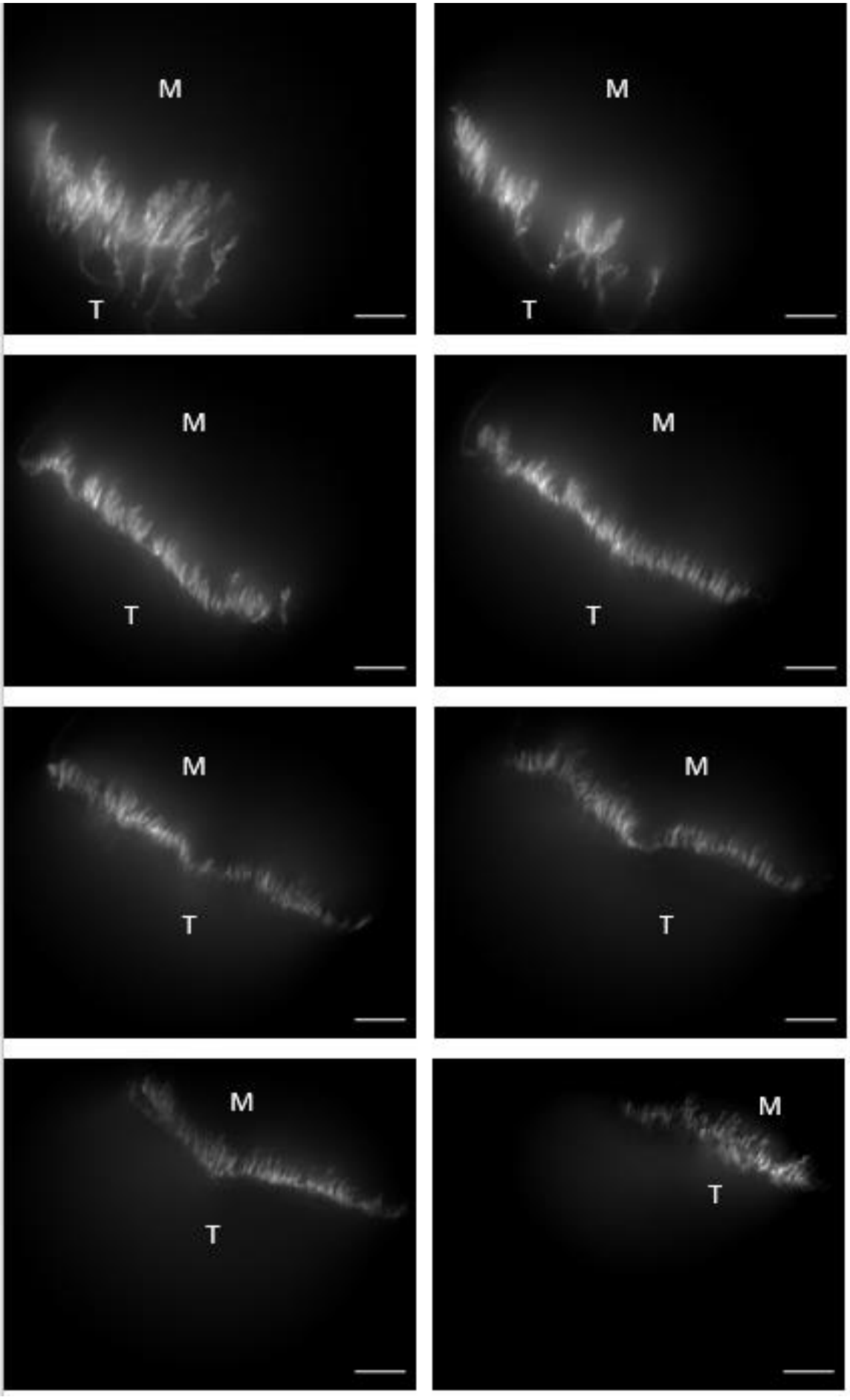
M
T
M
T
M
T
M
T
M
T
M
T
M
T
M
T

Figure 2:
The figure shows representative confocal images of the collagen XXII labelled MTJ separating the muscle (M) from the tendon (T). The images are randomly picked from the Z-stack used to make the 3D reconstruction. Scale bars are 10 µm.

All z-stack files were saved in the same folder and later re-arranged and re-labelled by a person not involved in the analysis, to blind the observer responsible for measuring the interface area regarding subject. The 647 nm channel type was not included in the z-stack, and therefore also blinded for the observer.

Image analysis

The z-stack of individual muscle fibers were analyzed using Imaris BitPlane 9.5 (RRID:SCR_007370)(Bitplane, Switzerland) Using the "Surfaces" plug-in to create an artificial surface based on a thresholding of the collagen XXII staining from which the area could be measured (see figure 1). The settings for creating the surfaces were identical for all fibers from all subjects. To test the reproducibility of the method multiple measurements of the same fibers were made and a variation of less than 1 % was found.

In some fibers the signal to noise ratio was too low for the software to create a useful surface and these fibers were therefore excluded.

During the dissection, staining and imaging some fibers were either lost or in a condition where they could not be analyzed. Some fibers appeared to have lost the end which could be an indication of poor dissection or damaging during the staining process. Others were lost while pipetting during staining or poorly stained resulting in poor image quality. From a total of 500 dissected fibers (50 fibers from each subject), 314 fibers were found suitable for image analysis.

Statistics

A pilot experiment was performed to obtain data to estimate the necessary sample size to distinguish a relevant difference in surface area between fiber types. In this, 28 fibers (14 of each fiber type) from a single subject were analyzed and the interface areas was found to be 27382 μm^2 (± 1460) for type I fibers and 23732 (±1821) for type II fibers. Based on this, at least 6 subjects were needed to be able to confirm that this is an actual difference with a power of 80 % and significance level of 0.05. Since the fiber type distribution might vary between subjects and some fibers would be lost during preparation, we chose to include 50 fibers from 10 subjects to be sure to have at least 10 fibers of each type from each subject.

Unfortunately, samples from two subjects did not have the minimum 10 fibers of each fiber type, and the subjects were excluded from the analysis. From each of the remaining 8 subjects a median of 15 type I (Range 11-20) and 20 type II fibers (Range 12-32) were analyzed.

In order to take fiber size into account the measurements of interface area were also expressed relative to the diameter of the fiber given as the size of the z-height of each fiber. Due to large variation in the interface area between same fiber type from the same subjects Wilcoxon signed rank test was chosen to analyze differences between fiber types. Significance level was set to <0.05.

Results

Using immunohistochemistry, it was possible to stain and identify type I and II fibers (Figure 1) and later imaged individual fibers using an iMIC spinning disc confocal microscope. Figure 2 shows representative images through the stack of images obtained from one fiber. A high complexity of the foldings is seen on all individual images but to an even greater extent on the collection of images in 3D z-stacks (Figure 3). Based on the z-stacks a reconstruction of the surface was created (figure 3) from which it was possible to measure the size of interface area between muscle and tendon. Generally, the appearance of the foldings at the fiber end was very heterogenous between subjects (figure 3) but also between fiber types where the interface area of type I fibers was found to be 38.35 % larger than type II fibers (P=0.023) (Figure 4A). Expressed relative to the fiber diameter the interface area of type I fibers was still significantly larger than type II (P=0.008) (Figure 4B). The mean diameter of both fiber types was 53 µm and the distribution of the fiber types showed a higher number of type II (58%) compared to type I (42%).

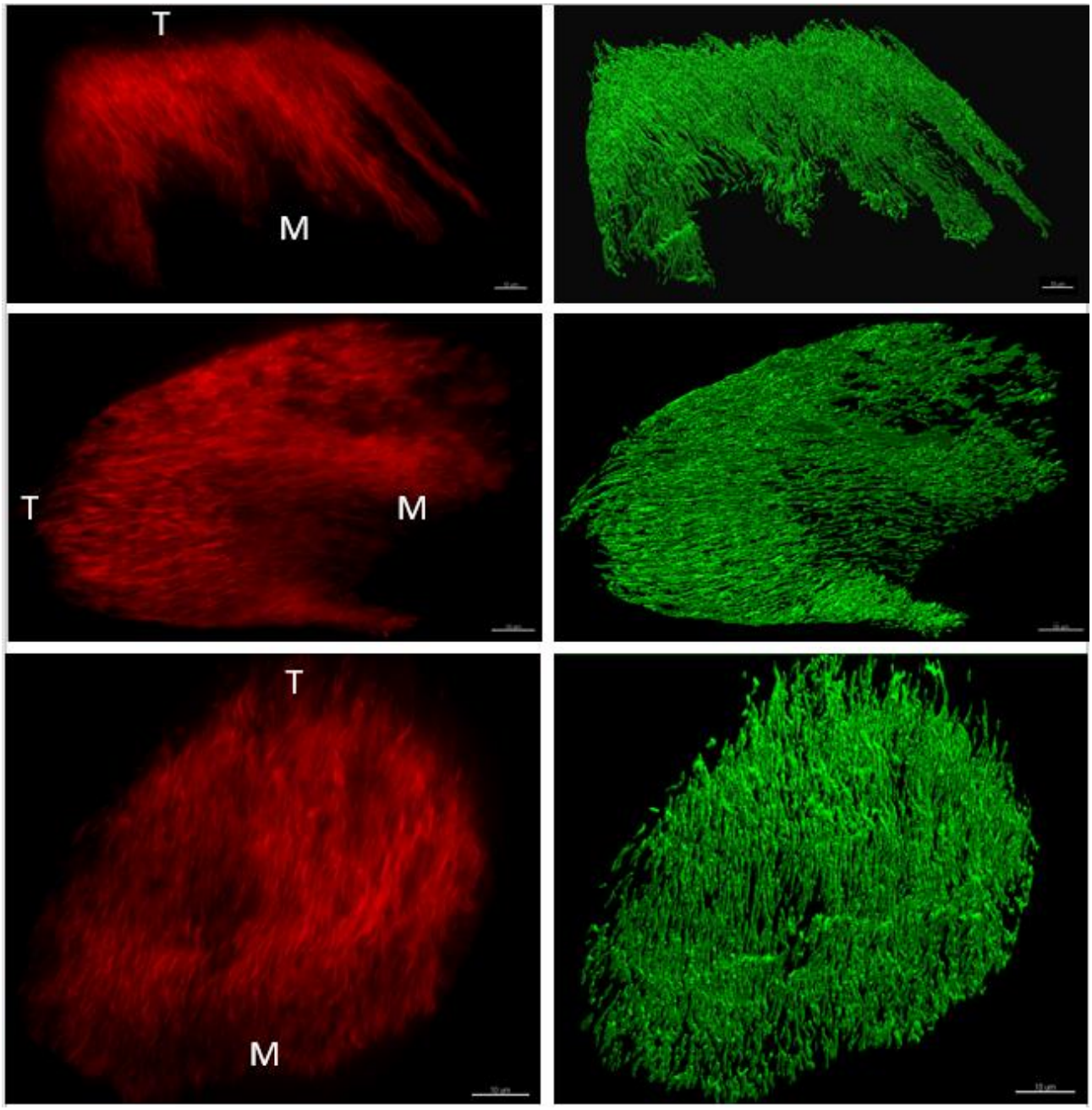

Figure 3:
The left column shows z-stacks of different muscle fiber ends with indication of the muscle (M) and tendon sides (T). The right column is the software constructed surface based on the z-stack from left column. Based on these constructed surfaces the interface area was calculated.
Scale bars are 10 μm.

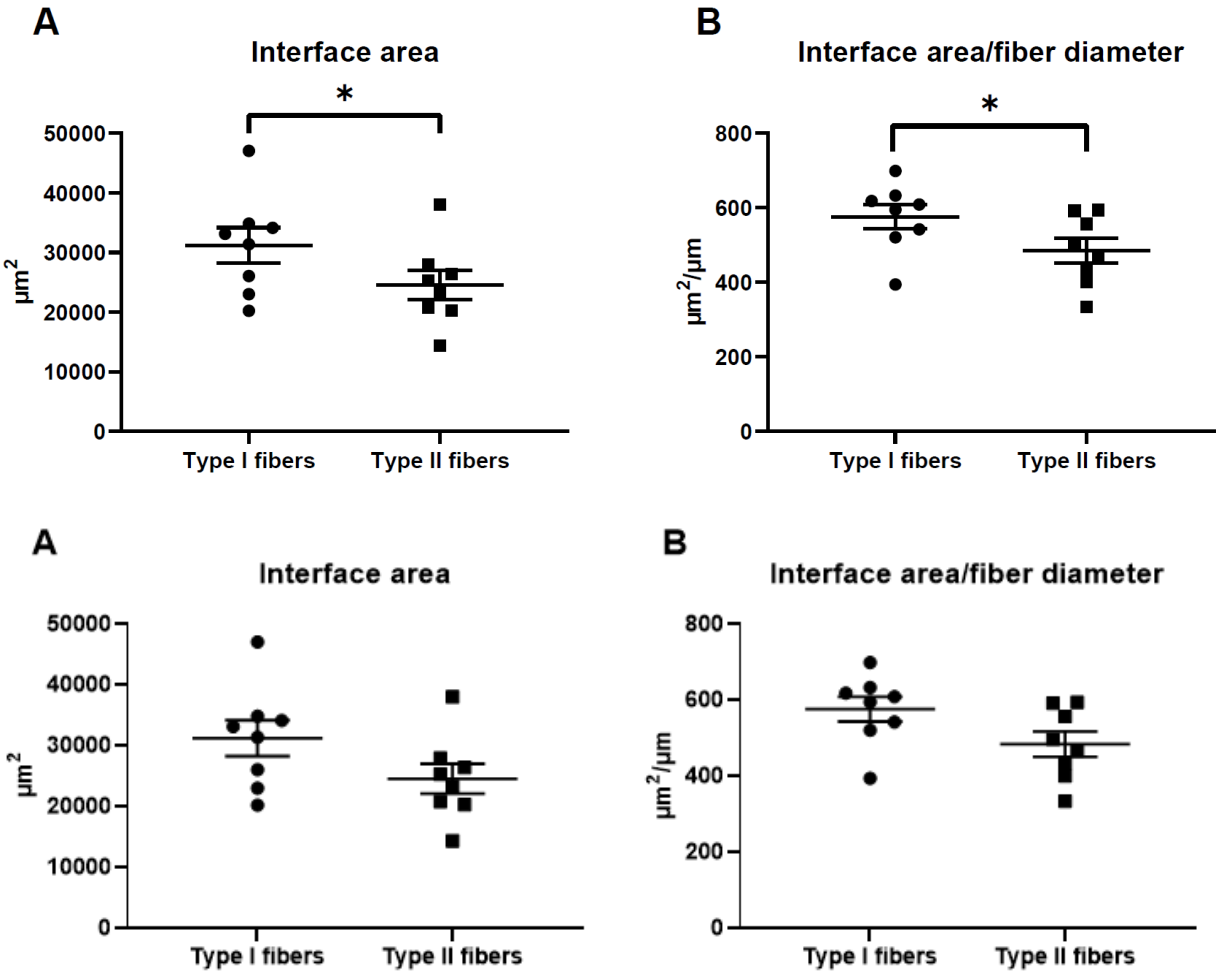

Figure 4:

The figure shows the result of the measurements of the interface area of MTJ type I and type II fibers-. In A) the interface area is plotted as individual median values as well as the median for all type I and II fibers. A significant difference is seen between the fiber types (P= 0.023). In B the interface area is expressed relative to the muscle fiber diameter of each fiber type per subject and the median for type I and II fibers are shown. A significant difference between fiber types is also seen here (P=0.008).

Discussion

This is the first study to analyze the size of the interface area between muscle and tendon in humans by a new technique based on confocal microscopy and fluorescence IHC. The main finding is that type I fibers from human semitendinosus muscles have a larger interface area compared to type II fibers from the same muscle. Furthermore, the new method described is introduced to analyze the entire MTJ of muscle fibres from a high number of samples and subjects, which could be particularly interesting for future studies examining the basic structure of the human MTJ as well as changed induced by exercise.

The unique structure of the MTJ has been subject for many studies previously, with the majority using transmission electron microscopy (TEM) as imaging technique (15,22,28–30). By TEM the highly folded surface of the MTJ and the complexity of these foldings has been demonstrated by 3D-reconstruction of MTJ from human samples (29). Only one study used light microscopy to analyze the foldings of the MTJ (31). In this, the muscle membrane at MTJ was labelled with dystrophin, and the size of the tendon foldings into muscle was calculated on the basis of a 3-D reconstruction, based on consecutive cross-sections of the muscle fibers approaching the MTJ.

In the current study a spinning disc confocal microscope was used to scan individual muscle fiber ends. Collagen XXII, which is known to exclusively be located at MTJ, was used to label the folded surface of each section and stack of sections was compiled to a 3D structure. The stacked images showed a very detailed organization of the foldings together with a large variation in both size and appearance between fibers. Interestingly, the interface area was found to be significantly higher for type I fibers compared to type II. If a larger interface area lowers the risk of injury during force transmission, as suggested previously (3,14,32), then the present findings suggest that type I fibers could be more resistant to load-induced injury than type II fibers.
Type II fibers are known to be capable of producing faster and stronger contractions compared to type I fibers which are more enduring and therefore also more resistant to fatigue (33–35). Among risk factors and biomechanics explaining strain injuries, fatigue seems to be important(35–37). Since type II fibers can produce high force but are also easily fatigued, it has been suggested that a high proportion type II/type I fibers in a muscle is correlated to a higher risk of strain injury (38). While this has not been validated thoroughly yet, it is interesting that some of the most frequently injured muscles, the hamstring muscles, generally contain a higher proportion of type II compared to type I fibers (38). The findings of the current study support this theory by showing a smaller area of force transmission between muscle and tendon in type II fibers from one of the hamstring muscles, the semitendinosus, compared to type I fibers.
Even though the etiology of strain injuries is complex and affected by multiple parameters, it may be essential that the foldings of the muscle membrane at the MTJ have a high degree of plasticity and are able to increase in size following loading. Based on this, targeting the type II fibers in a prevention program may be advantageous. In the clinical world this is well-known since the most effective prevention regimes involve heavy eccentric loading (9–11,13) which is thought to a higher degree to involve type II fibers. Whether the interface area of type II fibers increase more than in type I fibers following heavy eccentric loading is not known.

Two studies have compared the area of the MTJ between fiber types previously with different results in chicken and snake. A stereological approach was used to estimate the area of the MTJ on TEM sections and the muscles consisting of type II fibers were found to have larger area compared to the type I dominant muscle in chicken. However, the opposite was seen in muscles from snake by the same group. Here a larger area of type I fibers was found. Here the size of the fiber was also taken into account in the measures. This has also been done in most of the previous studies measuring on TEM-images where the surface of the MTJ is often expressed relative to diameter of the fiber. Theoretically, a larger fiber could have a larger interface area of the MTJ, however, in the current study it was seen that the size of the MTJ was instead determined by the morphology, where some MTJs had very short foldings and others ended in very long thread-like foldings (Figure 5). When analyzing the effects of a loading/unloading intervention caution should be taken

when expressing the MTJ surface area relative to fiber size since these interventions might induce hypertrophy/atrophy. It is not known whether the size of foldings changes as quick as the fiber size following i.e. atrophy and therefore this type of calculation would give an overestimate of the MTJ surface area.
In the current study the interface area of type I fibers was still significantly larger than type II fibers when the measurements were expressed relative to fiber diameter.

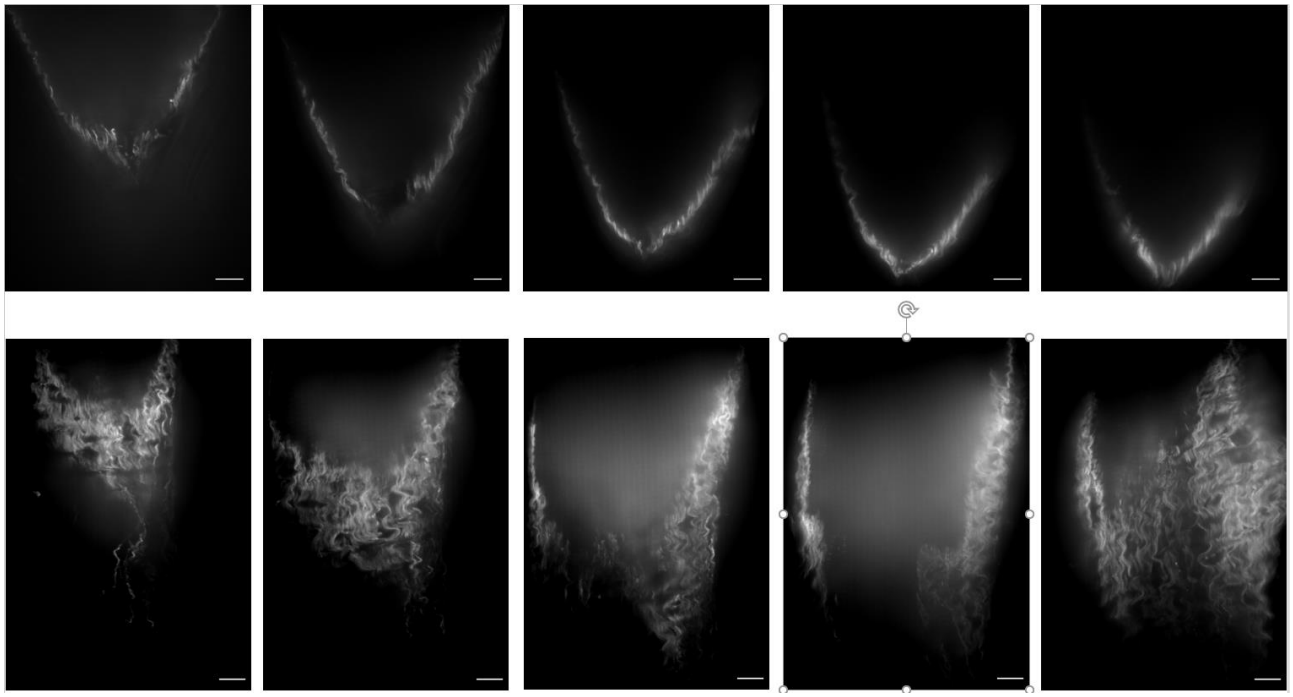

Figure 5:
The figure shows representative sections of two type II fibers which illustrates that the size of fiber not necessarily determines the interface area of the MTJ. The upper row shows 5 images randomly picked from the z-stack of the whole fiber with a total surface area of 20692 µm^2. The bottom row shows 5 images from a thinner fiber but with an interface area of the MTJ of 76759 µm^2.
Scale bars are 10 µm.

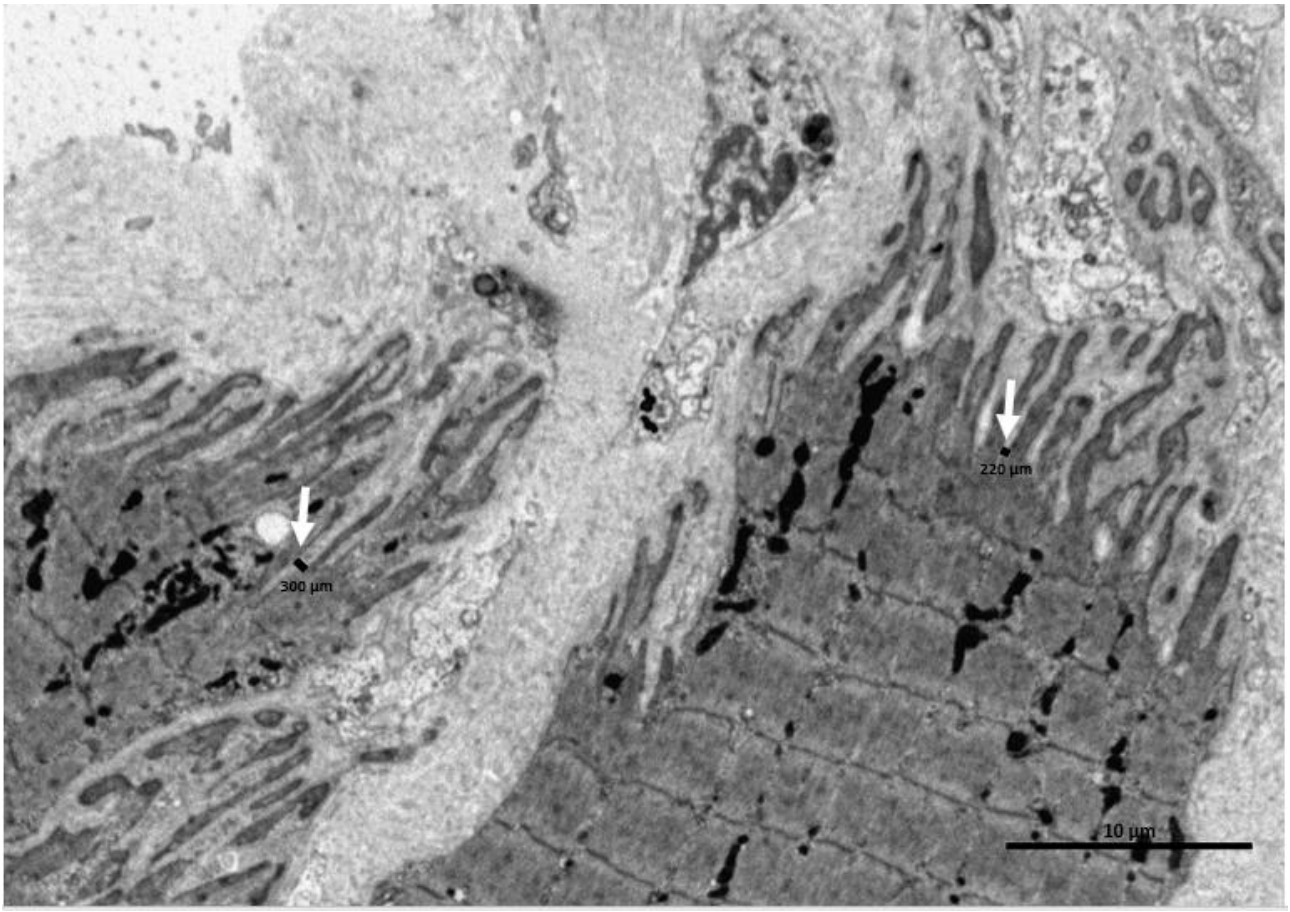

Figure 6:

Electron microscope image of human MTJ showing the size of the foldings (arrows and bars). Generally, the width of the foldings were between 220-400 µm.

Scale bar 10 µm.

Image acquired by Andreas Billa Knudsen, made at the Centre for Integrated Microscopy (CFIM) at the Panum Institute in Copenhagen, Denmark, used by permission.

Previous TEM-images from human MTJ's have shown that the thickness of the foldings ranges between ~220-400 nm (Figure 6). In the current setup a theoretical resolution of 200 nm was calculated and the actual resolution should be somewhere near this. Although some details might not have been visualized the current setup is probably enough to identify most of the details in the foldings although the resolution is far from the previously used TEM-images capable of resolutions around 1 nm. The advantage of present method, though, is that whole fibers are measured in a high number, making it possible to measure surface area of fibers and obtain a quantitative measure of this, which is essential and useful in future studies wanting to quantify on a high number of fibers.

In conclusion, this study has provided a method to analyze the entire interface area of the MTJ from human muscle fibers, making it possible to analyze a large number of fibers in many samples. Furthermore, was it shown that the interface area between muscle and tendon was higher for type I fibers compared to type II. Although future studies need to confirm this, it indicates that type II fibers might be more susceptible to

injury and that interventions aiming to prevent strain injury should focus on inducing adaptations in the type II fibers.

References:

1. Koch M, Schulze J, Hansen U, Ashwodt T, Keene DR, Brunken WJ, et al. A novel marker of tissue junctions, collagen XXII. J Biol Chem [Internet]. 2004 May 21 [cited 2015 Oct 10];279(21):22514–21. Available from: http://www.pubmedcentral.nih.gov/articlerender.fcgi?artid=2925840&tool=pmcentrez&rendertype=abstract

2. Huijing PA. Muscle as a collagen fiber reinforced composite: a review of force transmission in muscle and whole limb. J Biomech. 1999/04/23. 1999;32(4):329–45.

3. Tidball JG. Force transmission across muscle cell membranes. J Biomech [Internet]. 1991 [cited 2019 Nov 22];24 Suppl 1:43–52. Available from: http://www.ncbi.nlm.nih.gov/pubmed/1791181

4. Garrett Jr W. Muscle strain injuries [Internet]. Am J Sports Med. 1996 [cited 2021 Jan 5]. p. 2–8. Available from: https://pubmed.ncbi.nlm.nih.gov/8947416/

5. Ekstrand J, Hägglund M, Waldén M. Epidemiology of muscle injuries in professional football (soccer). Am J Sports Med. 2011;39(6):1226–32.

6. Orchard J, Seward H. Epidemiology of injuries in the Australian Football League, seasons 1997-2000. Br J Sports Med. 2002;36(1):39–44.

7. Hagel B. Hamstring injuries in Australian football [Internet]. Vol. 15, Clinical Journal of Sport Medicine. Clin J Sport Med; 2005 [cited 2021 Jan 6]. p. 400. Available from: https://pubmed.ncbi.nlm.nih.gov/16163004/

8. Hickey J, Shield a. J, Williams MD, Opar D a. The financial cost of hamstring strain injuries in the Australian Football League. Br J Sports Med [Internet]. 2014;48(8):729–30. Available from: http://bjsm.bmj.com/cgi/doi/10.1136/bjsports-2013-092884

9. Van Der Horst N, Smits DW, Petersen J, Goedhart EA, Backx FJG. The Preventive Effect of the Nordic Hamstring Exercise on Hamstring Injuries in Amateur Soccer Players: A Randomized Controlled Trial. Am J Sports Med. 2015 Jun 3;43(6):1316–23.

10. Petersen J, Thorborg K, Nielsen MB, Budtz-Jorgensen E, Holmich P. Preventive effect of eccentric training on acute hamstring injuries in men's soccer: a cluster-randomized controlled trial. Am J Sport Med. 2011/08/10. 2011;39(11):2296–303.

11. Seagrave RA, Perez L, McQueeney S, Toby EB, Key V, Nelson JD. Preventive Effects of Eccentric Training on Acute Hamstring Muscle Injury in Professional Baseball. Orthop J Sport Med [Internet]. 2014 Jun [cited 2019 Nov 22];2(6):2325967114535351. Available from: http://www.ncbi.nlm.nih.gov/pubmed/26535336

12. Al Attar WSA, Soomro N, Sinclair PJ, Pappas E, Sanders RH. Effect of Injury Prevention Programs that Include the Nordic Hamstring Exercise on Hamstring Injury Rates in Soccer Players: A Systematic

Review and Meta-Analysis [Internet]. Vol. 47, Sports Medicine. Springer International Publishing; 2017 [cited 2020 Oct 14]. p. 907–16. Available from: https://pubmed.ncbi.nlm.nih.gov/27752982/

13. Arnason A, Andersen TE, Holme I, Engebretsen L, Bahr R. Prevention of hamstring strains in elite soccer: an intervention study. Scand J Med Sci Sport. 2007/03/16. 2008;18(1):40–8.

14. Rissatto Sierra L, Fávaro G, Cerri BR, Rocha LC, de Yokomizo de Almeida SR, Watanabe I-S, et al. Myotendinous junction plasticity in aged ovariectomized rats submitted to aquatic training. Microsc Res Tech [Internet]. 2018 Aug [cited 2019 Nov 22];81(8):816–22. Available from: http://www.ncbi.nlm.nih.gov/pubmed/29689628

15. Curzi D, Salucci S, Marini M, Esposito F, Agnello L, Veicsteinas A, et al. How physical exercise changes rat myotendinous junctions: an ultrastructural study. Eur J Histochem. 2012/06/13. 2012;56(2):e19.

16. Curzi D, Sartini S, Guescini M, Lattanzi D, Di Palma M, Ambrogini P, et al. Effect of Different Exercise Intensities on the Myotendinous Junction Plasticity. PLoS One [Internet]. 2016 [cited 2019 Nov 22];11(6):e0158059. Available from: http://www.ncbi.nlm.nih.gov/pubmed/27337061

17. Kojima H, Sakuma E, Mabuchi Y, Mizutani J, Horiuchi O, Wada I, et al. Ultrastructural changes at the myotendinous junction induced by exercise. J Orthop Sci. 2008/06/06. 2008;13(3):233–9.

18. Jacob CDS, Rocha LC, Neto JP, Watanabe IS, Ciena AP. Effects of physical training on sarcomere lengths and muscle-tendon interface of the cervical region in an experimental model of menopause. Eur J Histochem. 2019;63(3):131–5.

19. Tidball JG, Quan DM. Reduction in myotendinous junction surface area of rats subjected to 4-day spaceflight. J Appl Physiol. 1992/07/01. 1992;73(1):59–64.

20. Kannus P, Jozsa L, Kvist M, Lehto M, Järvinen M. The effect of immobilization on myotendinous junction: an ultrastructural, histochemical and immunohistochemical study. Acta Physiol Scand [Internet]. 1992 Mar [cited 2019 Nov 22];144(3):387–94. Available from: http://www.ncbi.nlm.nih.gov/pubmed/1585821

21. Roffino S, Carnino A, Chopard A, Mutin M, Marini JF. Structural remodeling of unweighted soleus myotendinous junction in monkey. C R Biol. 2006/03/21. 2006;329(3):172–9.

22. Zamora AJ, Carnino A, Roffino S, Marini JF. Respective effects of hindlimb suspension, confinement and spaceflight on myotendinous junction ultrastructure. Acta Astronaut. 1995;36(8–12):693–706.

23. Bengtsson H, Ekstrand J, Waldén M, Hägglund M. Few training sessions between return to play and first match appearance are associated with an increased propensity for injury: a prospective cohort study of male professional football players during 16 consecutive seasons. Br J Sports Med [Internet]. 2019 Aug 29 [cited 2019 Nov 22]; Available from: http://www.ncbi.nlm.nih.gov/pubmed/31466941

24. B. Knudsen A, Mackey AL, Jakobsen JR, Krogsgaard MR. No demonstrable ultrastructural adaptation of the human myotendinous junction to immobilization or 4 weeks of heavy resistance training. Transl Sport Med [Internet]. 2021 Mar 13 [cited 2021 Apr 11];tsm2.243. Available from: https://onlinelibrary.wiley.com/doi/10.1002/tsm2.243

25. Trotter JA, Samora A, Hsi K, Wofsy C. Stereological analysis of the muscle-tendon junction in the aging mouse. Anat Rec [Internet]. 1987 Jul [cited 2020 May 12];218(3):288–93. Available from: http://www.ncbi.nlm.nih.gov/pubmed/3631543

26. Trotter JA, Baca JM. A stereological comparison of the muscle-tendon junctions of fast and slow fibers in the chicken. Anat Rec. 1987;218(3):256–66.

27. Mackey AL, Kjaer M. The breaking and making of healthy adult human skeletal muscle in vivo. Skelet Muscle. 2017 Nov 7;7(1).

28. Trotter JA, Samora A, Baca J. Three-dimensional structure of the murine muscle-tendon junction. Anat Rec. 1985;213(1):16–25.

29. Knudsen AB, Larsen M, Mackey AL, Hjort M, Hansen KK, Qvortrup K, et al. The human myotendinous junction: an ultrastructural and 3D analysis study. Scand J Med Sci Sport. 2014/04/11. 2015;25(1):e116-23.

30. Palma LD, Marinelli M, Pavan M, Bertoni-Freddari C. Involvement of the muscle-tendon junction in skeletal muscle atrophy: An ultrastructural study. Rom J Morphol Embryol. 2011;52(1):105–9.

31. Nielsen KB, Lal NN, Sheard PW. Age-related remodelling of the myotendinous junction in the mouse soleus muscle. Exp Gerontol [Internet]. 2018 Apr 1 [cited 2020 Dec 10];104:52–9. Available from: https://pubmed.ncbi.nlm.nih.gov/29421351/

32. Tidball JG. The geometry of actin filament-membrane associations can modify adhesive strength of the myotendinous junction. Cell Motil. 1983;3(5):439–47.

33. Harridge SDR, Bottinelli R, Canepari M, Pellegrino MA, Reggiani C, Esbjörnsson M, et al. Whole-muscle and single-fibre contractile properties and myosin heavy chain isoforms in humans. Pflugers Arch Eur J Physiol [Internet]. 1996 [cited 2021 May 27];432(5):913–20. Available from: https://pubmed.ncbi.nlm.nih.gov/8772143/

34. Gollnick PD, Armstrong RB, Sembrowich WL, Shepherd RE, Saltin B. Glycogen depletion pattern in human skeletal muscle fibers after heavy exercise. J Appl Physiol [Internet]. 1973 [cited 2021 May 27];34(5):615–8. Available from: https://pubmed.ncbi.nlm.nih.gov/4703734/

35. Hägglund M, Waldén M, Ekstrand J. Previous injury as a risk factor for injury in elite football: A prospective study over two consecutive seasons. Br J Sports Med [Internet]. 2006 Sep [cited 2020 Oct 5];40(9):767–72. Available from: https://pubmed.ncbi.nlm.nih.gov/16855067/

36. Mair SD, Seaber A V., Glisson RR, Garrett WE. The role of fatigue in susceptibility to acute muscle strain injury. Am J Sports Med [Internet]. 1996 [cited 2021 Jan 4];24(2):137–43. Available from: https://pubmed.ncbi.nlm.nih.gov/8775109/

37. Jakobsen JR, Krogsgaard MR. The Myotendinous Junction—A Vulnerable Companion in Sports. A Narrative Review. Front Physiol [Internet]. 2021 Mar 26 [cited 2021 Apr 11];12:635561. Available from: https://www.frontiersin.org/articles/10.3389/fphys.2021.635561/full

38. Garrett WE, Califf JC, Bassett FH. Histochemical correlates of hamstring injuries. Am J Sports Med [Internet]. 1984 [cited 2021 Jan 6];12(2):98–103. Available from: https://pubmed.ncbi.nlm.nih.gov/6234816/

Received: 30 July 2020 | Revised: 6 November 2020 | Accepted: 10 November 2020

DOI: 10.1002/tsm2.212

ORIGINAL ARTICLE

WILEY

Adipocytes are present at human and murine myotendinous junctions

Jens R. Jakobsen[1] | **Niels R. Jakobsen**[1] | **Abigail L. Mackey**[3,2] | **Andreas B. Knudsen**[1] | **Jens Hannibal**[4] | **Manuel Koch**[5] | **Michael Kjaer**[2] | **Michael R. Krogsgaard**[1]

[1]Department of Sports Traumatology M51, Bispebjerg and Frederiksberg Hospital, Copenhagen, Denmark

[2]Institute of Sports Medicine M81, Department of Orthopaedic Surgery M, Bispebjerg and Frederiksberg Hospital, Copenhagen, Denmark

[3]Center for Healthy Aging, Xlab, Department of Biomedical Sciences, Faculty of Health and Medical Sciences, University of Copenhagen, Copenhagen, Denmark

[4]Department of Clinical Biochemistry, Bispebjerg and Frederiksberg Hospital, Copenhagen, Denmark

[5]Institute for Dental Research and Oral Musculoskeletal Biology, and Center for Biochemistry, Medical Faculty, University of Cologne, Cologne, Germany

Correspondence
Jens R. Jakobsen, Department of Sports Traumatology M51, Bispebjerg and Frederiksberg Hospital, Vestre Længdevej 3, 2400 Copenhagen, Denmark.
Email: jensjakobsendk@gmail.com

Funding information
Lundbeckfonden; Sundhed og Sygdom, Det Frie Forskningsråd; International Olympic Committee; Nordea-fonden; Aase og Ejnar Danielsens Fond; Danish Biotechnology Center for Cellular Communcation; Deutsche Forschungsgemeinschaft

Abstract

The presence of adipocytes at the myotendinous junction (MTJ) has not previously been reported in mammals. However, during studies of the MTJ, our group has noticed the presence of adipocytes as a general and surprising phenomenon. The main aim of this study was to describe and quantify the presence of adipocytes in relation to the MTJ in healthy human subjects. In addition, we wanted to investigate whether adipocytes are also found at the MTJ in mice, which is a commonly used species in muscle and tendon research. Samples from the semitendinosus MTJ from 10 healthy human subjects and tibialis anterior and soleus from 6 mice were prepared for electron microscopy or for immunohistochemical labeling against perilipin (PLIN1, to identify adipocytes), collagen XXII (representing the myotendinous junction), and nuclei (DAPI). In all humans and mice, numerous adipocytes were present at the MTJ. Electron microscopy of human samples showed that adipocytes were located near the characteristic foldings of the muscle membrane at the MTJ. The large number of adipocytes at the MTJ in humans and mice suggests that they have an important function in the interplay between skeletal muscle and tendon in this region.

KEYWORDS

musculoskeletal system,

1 | INTRODUCTION

The myotendinous junction (MTJ) has been subject to increasing interest during the past decade, and the unique properties of this region have been revealed. Several studies, mainly on animals, have shown that the most distal part of the sarcolemma is folded and that these foldings are surrounded by tendon. This architecture increases the interface area of the

Department of Sports Traumatology M51, Bispebjerg and Frederiksberg Hospital, Copenhagen, Denmark and Institute of Sports Medicine M81, Department of Orthopaedic Surgery M, Bispebjerg and Frederiksberg Hospital, Copenhagen, Denmark, Departments are part of IOC Research Center Copenhagen.

MTJ.[1,2,3] Almost half of the muscle fibers contain centralized myonuclei and display NCAM-reactivity in the most distal part of the muscle fibers at the MTJ, suggesting an ongoing remodeling in this region.[4] However, the number of satellite cells, fibroblasts, and macrophages seems to be identical to what has been reported from the muscle belly.[4,5] This could be explained by a different transcriptional activity of these cells at the MTJ compared to the muscle belly.

In sports traumatology, there is particular focus on MTJ because of the large risk of strain injuries related to this structure, hamstring strain injuries being the most common.[6,7] A prevention strategy, targeting the hamstring muscles by slow, heavy eccentric resistance training with the Nordic Hamstring exercises, effectively reduces the risk of strain injury, and this could potentially be effected through ultra-structural adaptation or remodeling of the MTJ.[8,9,10]

Previous work by our group investigated the effects of heavy resistance training (HRT) on human MTJ. [4,5] During these studies, the presence of numerous adipocytes at the MTJ was identified. This phenomenon has not been described in literature, neither in humans nor in animals.

Accumulation of intramuscular lipid droplets is seen in patients with diabetes and has been suggested to be a predictor of insulin resistance.[11] Skeletal muscles use energy derived from both glycogen storages and intramuscular lipid droplets.[12] Interestingly, the concentration of intramuscular lipids has also been shown to increase following aerobic exercise in healthy insulin sensitive subjects, suggesting that lipids might be necessary for the function of exercising muscle.[11] In contrast, accumulation of adipocytes in intermuscular adipose-like tissue (IMAT) is normally correlated to obesity, diabetes, muscle disorders, inactivity, and trauma—all conditions with low muscle force production.[13]

Based on our observations in humans we hypothesized that adipocytes are occurring as a normal phenomenon in the mammalian MTJ.

The aim of this study was to confirm, and quantify in humans, the presence of adipocytes in relation to the MTJ in healthy human subjects and in mice, which is a commonly used species in muscle, tendon and myotendinous junction research.

2 | MATERIALS AND METHODS

2.1 | Human samples

The human samples for this study were obtained from a randomized controlled trial where the effects of heavy resistance training on the MTJ were studied.[5] The study was approved by The Research Ethics Committees of the Capital Region of Denmark (ref. H-4-2011-089) and was completed according to the standards of the Helsinki Declaration. All subjects provided written consent to participate.

The training regime has been described previously in detail,[5] but in summary it consisted of 3 weekly sessions for 4 weeks. Each session consisted of 4 hamstring exercises and 2 quadriceps exercises performed as 3 sets of 6-8 repetitions until exhaustion.

All subjects were healthy except for an isolated anterior cruciate ligament (ACL) rupture. Samples from 10 subjects (5 controls (5 males) and 5 trained (3 females and 2 males), average age 35.4 years, SD: 7.8) were collected. During reconstruction of the anterior cruciate ligament (ACL) the distal semitendinosus tendon, including its full MTJ, was stripped. Samples from the most proximal end of the stripped semitendinosus tendon were taken for this study before the tendon was prepared as graft for the ACL-reconstruction. Since the most proximal part of the semitendinosus tendon in this region continues as an intramuscular tendon, some samples had muscle fibers inserting from both sides of the tendon (Figure 1A). A small piece of muscle with attached tendon was cut for Electron Microscopy and fixated in 2% glutaraldehyde in 0.05 M phosphate buffer (pH 7.2) before the rest of the sample was embedded in Tissue-Tek *(*Sakura Finetek Europe, Zoeterwoude, Netherlands*)*, frozen in liquid nitrogen-cooled isopentane and stored at –80°C. 10 µm thick frozen sections were cut from each frozen specimen using a cryostat, and placed on glass slides (Superfrost Plus), which were stored at −80°C until immunohistochemical analysis.

2.2 | TEM preparations

After fixation in glutaraldehyde the samples were rinsed twice in 0.15 M sodium phosphate buffer (pH 7.2) and once in 0.12 M sodium cacodylate buffer (pH 7.2) before postfixation in 2% OsO4 with 0.05 M K3FeCn6 in 0.12 M sodium cacodylate buffer (pH 7.2) for 2 hours. Samples were en-bloc stained with 1% uranyl acetate overnight and subsequently rinsed three times of 10-15 minutes each in distilled water. Using ethanol, the samples were dehydrated according to standard procedures before being transferred to propylene oxide and embedded in Epon (Electron Microscopy Sciences, Hatfield, PA, USA). Ultrathin sections at the MTJ region were cut with a Reichert-Jung Ultracut E microtome (Leica Microsystems, Vienna, Austria), collected on one-hole copper grids with Formvar supporting membranes and stained with uranyl acetate and lead citrate.

The TEM images were acquired using a Philips CM 100 (Philips, Eindhoven, The Netherlands) transmission electron microscope operated at an accelerating voltage of 80 kV. Digital images were recorded with an OSIS Veleta, side

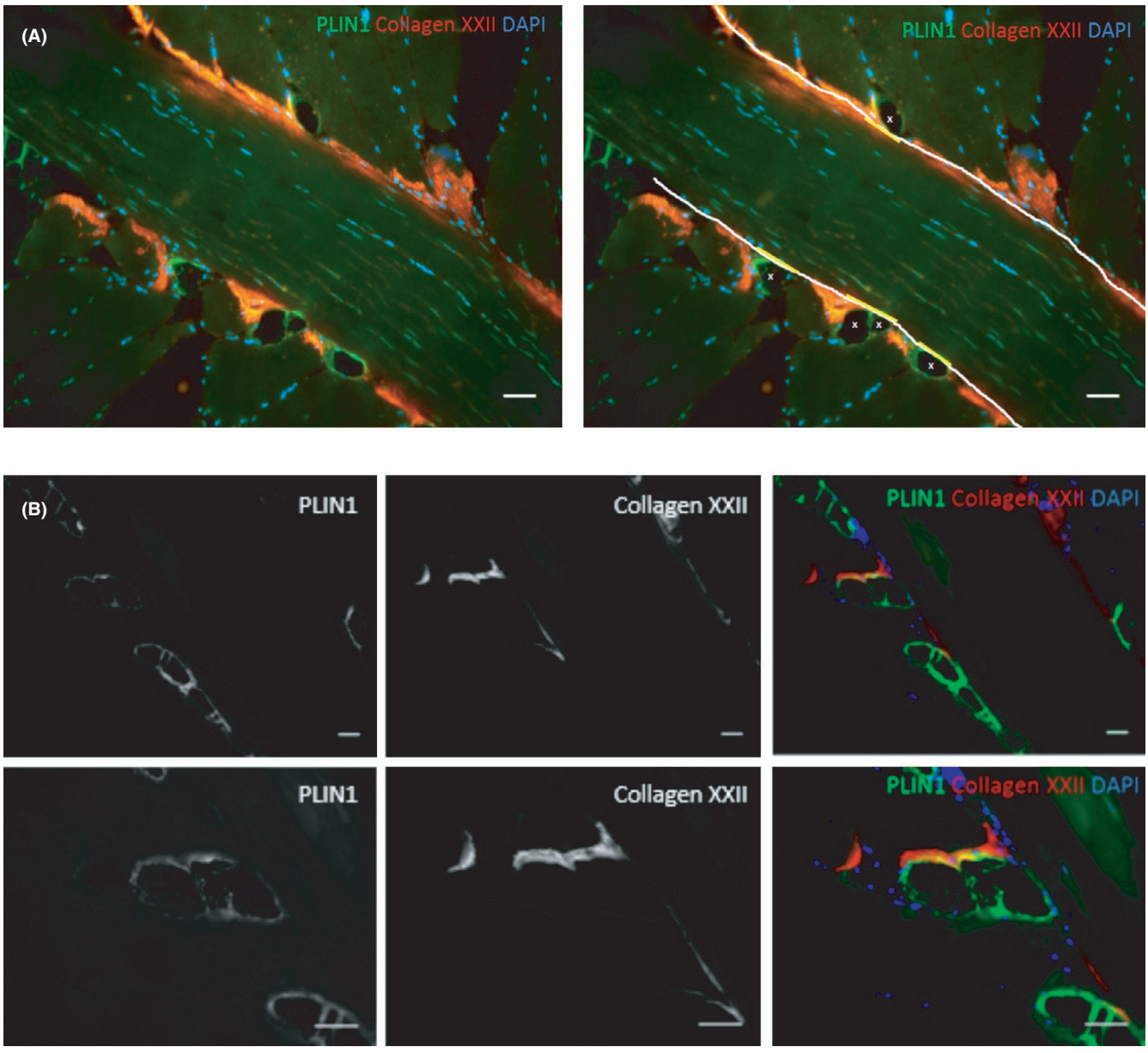

FIGURE 1 Immunohistological images of adipocytes at human MTJ. A, M-channel images of the human MTJ stained against collagen XXII (red), perilipin-1 (PLIN1, green) and DAPI/nuclei (blue), illustrating the measurement of the length of MTJ (white line) and the parts of MTJ with adjacent adipocytes (yellow line). Adipocytes are marked with a white x. The tendon is seen in the middle of the image with muscle fibers approaching from both sides. In this image the length of MTJ was 1.55 mm, 6 adipocytes counted, and 389 μm of the MTJ measured to have adjacent adipocytes. Scale bar is 50 μm. B, Separate channel images of human MTJ showing the close relation between the adipocytes and collagen XXII staining at the tip of muscle fibers. The first column shows PLIN1, the second column collagen XXII and the third column merged images of PLIN1 (green), collagen XXII (red), and DAPI/nuclei(blue). The images are obtained from the same area in the same section with the second row taken with higher magnification. Scale bars are 50 μm on all images

mounted digital slow scan 2k × 2k CCD camera (Olympus) and the AnalySIS ITEM software package (Olympus).

Both intramuscular lipid droplets and adipocytes express the protein perilipin (PLIN), which is member of a family of proteins that protects against lipases.[14] Whereas PLIN2 and 5 are normally seen in intramuscular lipid droplets, PLIN1 is only found in adipocytes.[14] Therefore, PLIN1 is useful for staining adipocytes in muscle tissue.

2.2.1 | Mouse samples

Samples were obtained from 6 healthy mice (Median age 12 weeks, range 9-37 weeks), from the C57 species, that had been fed a standard diet and had no history of injury, unloading or specific loading interventions. The mice were bred to study neurotransmitters and circadian rhythm. Three mice were wild type (WT) C57 male mice, one mouse had

a knockout of the Early Growth Response protein 1 (Egr-1), one had a knockout of the Vasoactive intestinal peptide receptor 2 (VPAC2) and one had a knockout of the Pituitary adenylate cyclase-activating polypeptide (PACAP). Neither of the knockouts have demonstrated any altered locomotor behavior. The knockouts of VPAC2 and PACAP have been shown not to affect the overall activity pattern of the mice.[15,16,17]

6 mice were anesthetized and perfusion fixed by a transcardial infusion of Zamboni fixative (2% formaldehyde, 0.15% picric acid) and had the hindlimb removed for dissection. The whole soleus and tibialis anterior muscles with tendons were removed and immersion fixed overnight in Zamboni fixative, followed by dehydration in 30% sucrose for 24 hours before they were frozen in Tissue-Tech using dry ice.[18] Longitudinal 10-20 μm thick sections were cut and mounted on glass slides. The experiment on mice was performed in accordance with the law on animal experiments in Denmark (publication #1306, November 23rd, 2007) and Directive 2010/63/EU with the license number 2017-15-0201-01364 issued to Jens Hannibal from Animal Experiments Inspectorate, Ministry of Justice, Denmark.

From these 6 mice, a soleus and tibialis muscle from one of the WT mice was prepared to visualize whole bundles of muscle fibers with the distal tendon attached as described previously.[19] Following the perfusion fixation and dissection, the muscles were pinned to keep the fiber length and immersed in Krebs-buffer with 0.1% procaine for 2 minutes followed by fixation in Zamboni fixative overnight. The following day Zamboni was replaced by 50% glycerol in PBS and kept at −20°C. Under a stereomicroscope the muscles were cut into bundles of fibers with pieces of tendon attached and transferred to a 12-well Nunc plate where they were washed in Immunobuffer (IB:PBS containing 50 mM glycine, 0.25% BSA, saponin, 0.05% sodium azide 0.03%) and incubated overnight with two primary antibodies (guinea pig anti-Collagen XXII, provided by Manuel Koch and anti-PLIN1, Sigma HPA024299) mixed in IB. Following another wash in IB, the samples were incubated for 2 hours with two secondary antibodies mixed in IB (A-11075:568 goat anti-guinea pig, A-11034:488 goat anti-rabbit) before they were carefully put on glass slides in a drop of mounting medium (Molecular Probes Prolong Gold mounting with DAPI, cat. no. P36931, Invitrogen).

2.2.2 | Immunohistochemistry protocol

Sections from both human and mice were allowed to air dry and were fixed with 5% formaldehyde (Histofix, Histolab, Gothenburg, Sweden, where after they were washed in PBS before incubation overnight with the primary antibodies to stain adipocytes (Perilipin-1, Sigma HPA024299) and collagen XXII (guinea pig anti-Collagen XXII, provided by Manuel Koch). This was followed by two secondary antibodies: A-11075:568 goat anti-guinea pig, A-11034:488 goat anti-rabbit. Nuclei were stained with a mounting medium containing DAPI (Molecular Probes ProLong Gold anti-fade reagent, cat. no. P36935; Invitrogen A/S). The sections were stained against collagen XXII because this collagen type is specific for tissue junctions, including the MTJ, and indicates the location of the MTJ in the sections.[20]

2.2.3 | Image analysis

Adipocytes from the human samples were counted by a person blinded to the intervention. Only intact adipocytes staining clearly for PLIN1 and in close contact with collagen XXII were counted. Adipocytes are vulnerable and easily pulled apart during preparation, and on many slides, it was not possible to measure the precise dimensions of the cells. Therefore, we could not analyze the volume of adipocytes, as this would require stacks of slices with intact adipocytes.

On each slide, 4-6 sections were mounted and the section with the longest MTJ, measured as length of collagen XXII, was chosen for further measurements. Since the whole length of MTJ from a single section could not fit into one image, several images were combined to visualize the entire MTJ, but only one such section per subject was analyzed. With ImageJ the total length of the MTJ in each section was measured using the "free hand line" tool and using the same technique, the length of MTJ adjacent to adipocytes was also measured and the number of adipocytes was counted (see Figure 1A).

All samples were analyzed using an Olympus BX51 microscope mounted with a digital camera (Olympus DP71, Olympus Deutschland GmbH), controlled by the software Cell^F (Olympus Soft Imaging Solutions, GmbH).

2.3 | Confocal imaging

Images were obtained using an iMIC confocal microscope (Till Photonics, FEI, Germany) equipped with appropriate filter settings for detecting DAPI, CY2/Alexa488 and Texas Red/Alexa561/594. For confocal imaging, the iMIC used an Andromeda spinning disk system (FEI) and a Hamamatsu 16-bit camera (Model C10600-10B-H, Hamamatsu Photonic) for recording.

2.4 | Statistics

Mann-Whitney's test was used to analyze for differences between the CON and HRT groups. Since no differences were observed between human groups data were pooled.

The samples from mice MTJ were included to study if adipocytes are present at the MTJ in this species, and therefore quantification of the number of adipocytes was not performed. Four to six sections from each sample were examined for the presence of adipocytes near collagen XXII, which was used as an indication of MTJ.

3 | RESULTS

In all human subjects, adipocytes were identified at the MTJ in close proximity to collagen XXII (Figure 1B). Transmission electron microscopic (TEM) images confirmed the presence of adipocytes close to the characteristic folding of the sarcolemma of the muscle fiber at the MTJ (Figure 2).

From each subject, a median of 1.84 mm (Range: 0.9-3.7) MTJ was analyzed.

There were large individual differences in both groups (Figure 3), but no significant difference between the control and HRT groups in the number of adipocytes pr mm MTJ ($P = .421$) or the percentage of MTJ covered by adipocytes ($P > .999$).

In all samples from mice (both the soleus and TA) adipocytes were seen in close vicinity to collagen XXII (see Figure 4) or in the tissue adjacent to the transition between muscle and tendon. The MTJ from mice show a much more

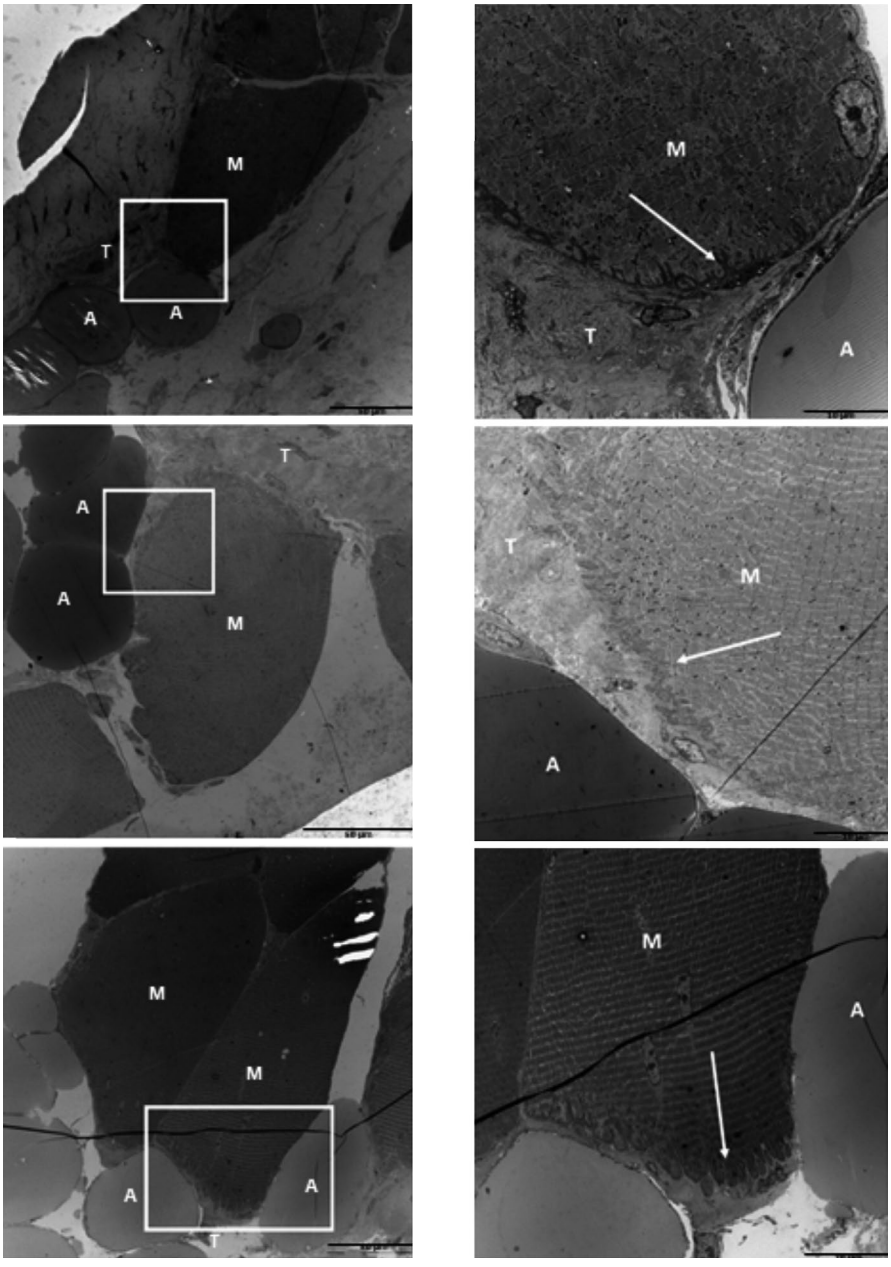

FIGURE 2 Electron microscope images of adipocytes at the MTJ. Images of human MTJ from three individuals. To the left are low magnification (scale bars are 50 μm) with a quadrant indicating the area of focus shown to the right at higher magnification (scale bars are 10 μm in the two upper images and 20 μm in the lower image). In all samples, the adipocytes (A) are located adjacent to the characteristic foldings of the MTJ (indicated by white arrow). Muscle is marked M. Rotation is slightly different on the higher magnification images [Colour figure can be viewed at wileyonlinelibrary.com]

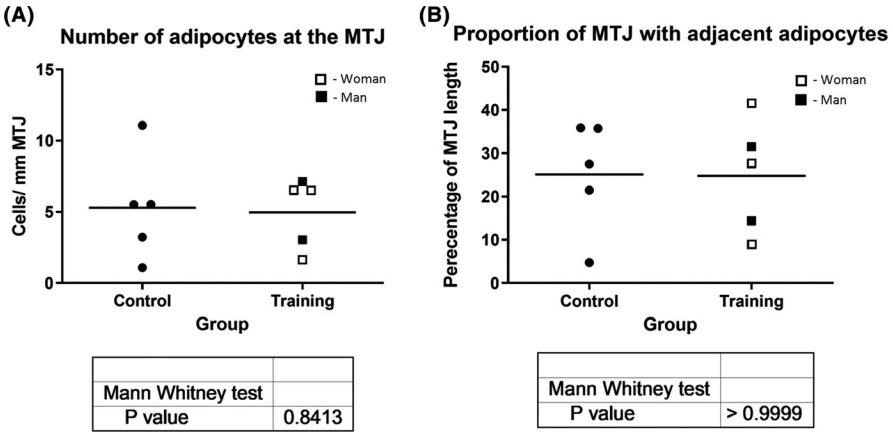

Mann Whitney test	
P value	0.8413

Mann Whitney test	
P value	> 0.9999

FIGURE 3 Quantification of adipocytes at the human MTJ: A shows the number of adipocytes pr mm MTJ in the control and the training group (individual values and mean). B shows the proportion (length) of MTJ with adjacent adipocytes

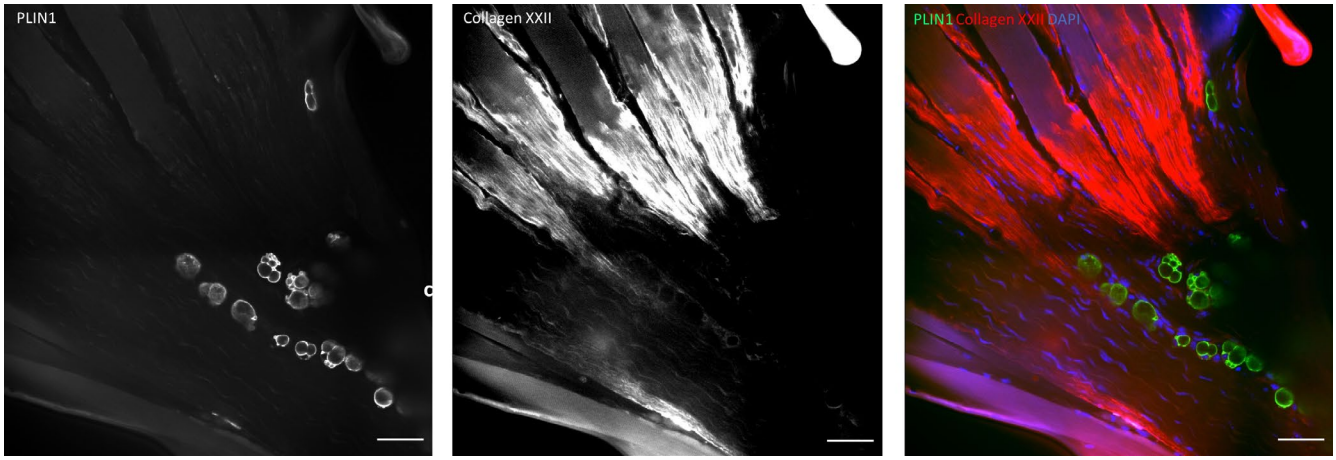

FIGURE 4 Confocal images of MTJ with adipocytes. Representative images of mouse soleus MTJ obtained by confocal microscopy. The first column shows PLIN1, the second column collagen XXII and the third column merged images of perilipin-1, collagen XXII, and DAPI/nuclei. The adipocytes are seen at the very end of the fibers next to collagen XXIII and extending into the tendon tissue. Scale bars are 50 μm [Colour figure can be viewed at wileyonlinelibrary.com]

scattered occurrence of proportion of collagen XXII compared to human samples, probably due to differences in the muscle architecture between the muscles, meaning that the muscle fiber tips are not visualized on all section even though the interface between muscle and tendon is seen. Therefore, it was impossible to quantify adipocytes in the same way as for the human MTJ. There was some difference between the samples in how adipocytes were clustering at and around MTJ in mice, and Figure 5 shows the various patterns.

4 | DISCUSSION

The purpose of this study was to confirm and further describe the presence of adipocytes at the mammalian MTJ. Adipocytes were found adjacent to the human MTJ in all subjects as well as in all mice. The ultrastructure of the MTJ has previously been studied in animals and humans.[1,2,3,21] However, adipocytes have never been reported in relation to the MTJ. TEM images revealed adipocytes very close to the characteristic foldings of the sarcolemma, which is precisely where force is transmitted from the muscle fiber to the collagen fibrils in the tendon. In the human MTJs adipocytes were mostly seen between terminating muscle fibers close to their insertion (as evidenced by the presence of collagen XXII). This was also the case for the mouse muscles where adipocytes in close relation to collagen XXII staining were seen in all mice (Figures 4, 5A, and C). In addition, adipocytes were also observed in the tendon tissue with no relation to MTJ (B and D) in mice. This was not found in the human samples. And the grouping of adipocytes into larger clusters, as seen in some of the mice samples, was not observed in humans where adipocytes were most often seen as single cells or two—three cells in a small group. Adipocytes have been reported in entheses at the tendon-bone junction in humans.[22] They were located in adipose-like tissue with sensory nerve innervation and

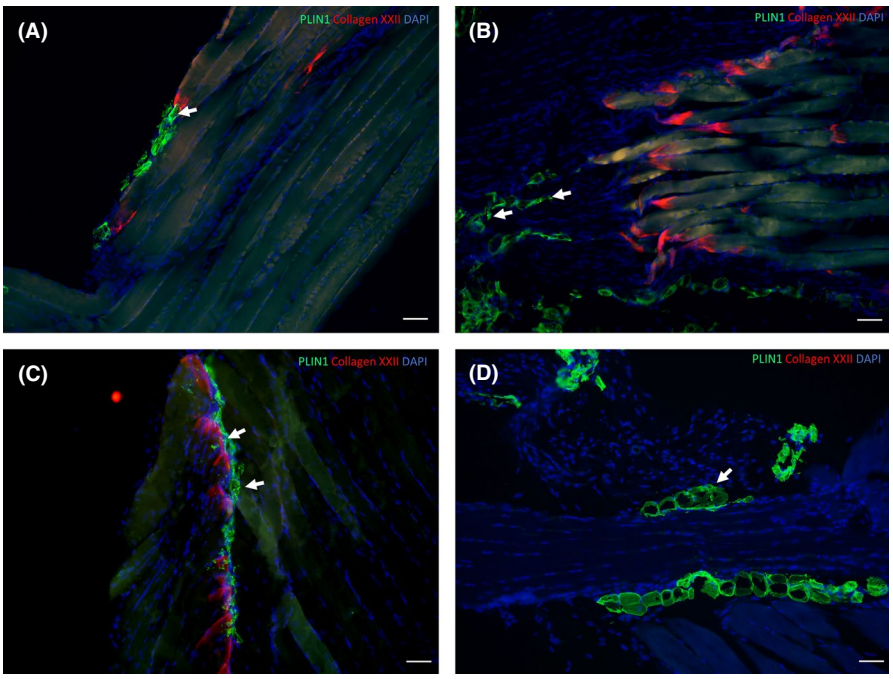

FIGURE 5 Distribution of adipocytes at the muscle-tendon interface. Representative images of mouse muscle stained against collagen XXII (red), PLIN1 (green), and DAPI (blue) showing various locations of adipocytes near the MTJ. Images A + B are obtained from soleus muscles from different mice and c + d from tibialis anterior muscles. A and C show adipocytes (arrows) in very close relation to the MTJ distal to collagen XXII staining. Besides the location adjacent to collagen XXII stained MTJ adipocytes (arrows) were also seen in the tendon tissue at some distance to the MTJ, as shown in B and D. In D no collagen XXII staining is visible even though the section has been stained against collagen XXII and muscle is seen close to tendon. Scale bars are 50 μm [Colour figure can be viewed at wileyonlinelibrary.com]

blood vessels in the tendon-bone junction.[22] The authors speculated that this adipose tissue might facilitate movement between tendon and bone and fill out empty space between the tendon fascicles.[22] Similarly, adipocytes at the MTJ could occupy space between muscle fibers and thereby provide the muscle fibers with an optimal angle of insertion to the tendon for the best transmission of force. However, these suggestions are speculative and require evidence to support them.

The human samples used in the present study were obtained from a study on the effect of HRT on the MTJ, and therefore an effect of this training program on the adipocytes should potentially show as difference between groups (training or no training) even though the sample size was quite small. Adipocytes are not known to have any force transmitting properties, and the presence of adipocytes in this region, where great forces are transmitted, could increase the susceptibility of strain at the MTJ when it is exposed to sudden high loads. However, there was no difference in the number or concentration of adipocytes at MTJ in patients who had performed HRT during the 4 weeks prior to sampling compared to controls.

The terminations of muscle fibers undergo continuous remodeling as they approach the MTJ.[4] This is a highly controlled process involving various cell-types including macrophages, fibroblasts, and satellite cells.[23,24] This extensive remodeling could be aided by adipocytes at the MTJ. Besides serving as energy storage, adipocytes secrete cytokines, also called adipokines, which have extensive effects on many aspects of metabolism. These cytokines include interleukin-6 (IL-6) and Tumor Necrosis Factor α (TNF-α) which affect inflammation and insulin resistance, and angiotensinogen and plasminogen activating inhibitor 1 (PAI-1) involved in the vascular system and blood clotting.[25] However, it is not known if the adipocytes at the MTJ secrete the same adipokines as adipocytes from the subcutaneous fat tissue, and the specific production of cytokines was not analyzed in this study.

5 | PERSPECTIVES

This study provides the novel evidence that adipocytes are abundantly present in close proximity to the MTJ in healthy human subjects as well as in mice. The MTJ is susceptible to strain injury and therefore the understanding of the ultrastructure and metabolism of this region is of relevance. It is the task of further studies to explain the role of adipocytes at the MTJ. They could be involved in force transmission, regeneration, and remodeling at the MTJ and therefore be important for prevention of strain injuries and involved in the regeneration of the MTJ following injury.

ACKNOWLEDGEMENTS

We would like to thank the Core Facility for Integrated Microscopy, Faculty of Health and Medical Sciences, University of Copenhagen, where the transmission electron images and The Lundbeck Foundation, Danish Medical Research Council, The Nordea Foundation (Healthy Aging Grant), IOC Research Centre for Sports Medicine Copenhagen, and Aase and Einar Danielsen's Foundation for financial support. Ma. K. was supported by the Deutsche Forschungsgemeinschaft (FOR2722). JH was supported by the Danish Biotechnology Center for Cellular Communication.

CONFLICT OF INTEREST

No conflicts of interests are declared by any of the authors.

ORCID

Jens R. Jakobsen https://orcid.org/0000-0002-9346-1046
Abigail L. Mackey https://orcid.org/0000-0002-2017-4580

REFERENCES

1. Curzi D, Salucci S, Marini M, et al. How physical exercise changes rat myotendinous junctions: an ultrastructural study. *Eur J Histochem*. 2012;56(2):e19.
2. Knudsen AB, Larsen M, Mackey AL, et al. The human myotendinous junction: an ultrastructural and 3D analysis study. *Scand J Med Sci Sport*. 2015;25(1):e116-e123.
3. Kojima H, Sakuma E, Mabuchi Y, et al. Ultrastructural changes at the myotendinous junction induced by exercise. *J Orthop Sci*. 2008;13(3):233-239.
4. Jakobsen JR, Jakobsen NR, Mackey AL, Koch M, Kjaer M, Krogsgaard MR. Remodeling of muscle fibers approaching the human myotendinous junction. *Scand J Med Sci Sport*. 2018;28(8):1859-1865.
5. Jakobsen JR, Mackey AL, Knudsen AB, Koch M, Kjaer M, Krogsgaard MR. Composition and adaptation of human myotendinous junction and neighboring muscle fibers to heavy resistance training. *Scand J Med Sci Sports*. 2017;27(12):1547-1559.
6. Sharafi B, Ames EG, Holmes JW, Blemker SS. Strains at the myotendinous junction predicted by a micromechanical model. *J Biomech*. 2011;44(16):2795-2801.
7. Taylor DC, Dalton JD, Seaber AV, Garrett WE. Experimental muscle strain injury. Early functional and structural deficits and the increased risk for reinjury. *Am J Sports Med*. 1993;21(2):190-194.
8. Arnason A, Andersen TE, Holme I, Engebretsen L, Bahr R. Prevention of hamstring strains in elite soccer: an intervention study. *Scand J Med Sci Sport*. 2008;18(1):40-48.
9. Mjolsnes R, Arnason A, Osthagen T, Raastad T, Bahr R. A 10-week randomized trial comparing eccentric vs. concentric hamstring strength training in well-trained soccer players. *Scand J Med Sci Sport*. 2004;14(5):311-317.
10. Petersen J, Thorborg K, Nielsen MB, Budtz-Jorgensen E, Holmich P. Preventive effect of eccentric training on acute hamstring injuries in men's soccer: a cluster-randomized controlled trial. *Am J Sport Med*. 2011;39(11):2296-2303.
11. Goodpaster BH, He J, Watkins S, Kelley DE. Skeletal muscle lipid content and insulin resistance: evidence for a paradox in endurance-trained athletes. *J Clin Endocrinol Metab*. 2001;86(12):5755-5761.
12. Spriet LL. New insights into the interaction of carbohydrate and fat metabolism during exercise. *Sports Med*. 2014;44(Suppl 1):S87-96.
13. Tuttle LJ, Sinacore DR, Mueller MJ. Intermuscular adipose tissue is muscle specific and associated with poor functional performance. *J Aging Res*. 2012;2012:172957.
14. MacPherson RE, Herbst EA, Reynolds EJ, Vandenboom R, Roy BD, Peters SJ. Subcellular localization of skeletal muscle lipid droplets and PLIN family proteins OXPAT and ADRP at rest and following contraction in rat soleus muscle. *Am J Physiol Integr Comp Physiol*. 2012;302(1):R29-36.
15. Colwell CS, Michel S, Itri J, et al. Selective deficits in the circadian light response in mice lacking PACAP. *Am J Physiol Regul Integr Comp Physiol*. 2004;287(5):R1194-201.
16. Hannibal J, Hsiung HM, Fahrenkrug J. Temporal phasing of locomotor activity, heart rate rhythmicity, and core body temperature is disrupted in VIP receptor 2-deficient mice. *Am J Physiol Regul Integr Comp Physiol*. 2011;300(3):R519-R530.
17. Riedel CS, Georg B, Fahrenkrug J, Hannibal J. Altered light induced EGR1 expression in the SCN of PACAP deficient mice. *PLoS ONE*. 2020;15(5):e0232748.
18. Hannibal J, Ding JM, Chen D, et al. Pituitary adenylate cyclase-activating peptide (PACAP) in the retinohypothalamic tract: a potential daytime regulator of the biological clock. *J Neurosci*. 1997;17(7):2637–44.
19. Mackey AL, Kjaer M. The breaking and making of healthy adult human skeletal muscle in vivo. *Skelet Muscle*. 2017;7(1):24.
20. Koch M, Schulze J, Hansen U, et al. A novel marker of tissue junctions, collagen XXII. *J Biol Chem*. 2004;279(21):22514-22521.
21. Tidball JG, Quan DM. Reduction in myotendinous junction surface area of rats subjected to 4-day spaceflight. *J Appl Physiol*. 1992;73(1):59-64.
22. Benjamin M, Redman S, Milz S, et al. Adipose tissue at entheses: the rheumatological implications of its distribution. A potential site of pain and stress dissipation? *Ann Rheum Dis*. 2004;63(12):1549–55.
23. Bentzinger CF, Wang YX, Dumont NA, et al. Cellular dynamics in the muscle satellite cell niche. *EMBO Rep*. 2013;14(12):1062-1072.
24. Murphy MM, Lawson JA, Mathew SJ, Hutcheson DA, Kardon G. Satellite cells, connective tissue fibroblasts and their interactions are crucial for muscle regeneration. *Development*. 2011;138(17):3625-3637.
25. Ronti T, Lupattelli G, Mannarino E. The endocrine function of adipose tissue: an update. *Clin Endocrinol (Oxf)*. 2006;64(4):355–65.

How to cite this article: Jakobsen JR, Jakobsen NR, Mackey AL, et al. Adipocytes are present at human and murine myotendinous junctions. *Transl Sports Med*. 2021;4:223–230. https://doi.org/10.1002/tsm2.212

american physiological society
AMERICAN JOURNAL OF PHYSIOLOGY
CELL PHYSIOLOGY

Am J Physiol Cell Physiol 321: C453–C470, 2021.
First published July 14, 2021; doi:10.1152/ajpcell.00218.2021

RESEARCH ARTICLE

RNA sequencing and immunofluorescence of the myotendinous junction of mature horses and humans

Jens R. Jakobsen,[1] Peter Schjerling,[2,3] Rene B. Svensson,[2,3] Rikke Buhl,[4] Helena Carstensen,[4] Manuel Koch,[5,6] Michael R. Krogsgaard,[1] Michael Kjær,[2,3] and Abigail L. Mackey[2,7]

[1*]*Section for Sports Traumatology M51, Department of Orthopaedic Surgery, Bispebjerg and Frederiksberg Hospital, Copenhagen University Hospital, Copenhagen, Denmark;* [2*]*Institute of Sports Medicine Copenhagen, Department of Orthopaedic Surgery, Bispebjerg and Frederiksberg Hospital, Copenhagen University Hospital, Copenhagen, Denmark;* [3]*Center for Healthy Aging, Department of Clinical Medicine, University of Copenhagen, Copenhagen, Denmark;* [4]*Department of Veterinary Clinical Sciences, University of Copenhagen, Copenhagen, Denmark;* [5]*Institute for Dental Research and Oral Musculoskeletal Biology, Center for Biochemistry, Medical Faculty, University of Cologne, Cologne, Germany;* [6]*Center for Molecular Medicine Cologne, University of Cologne, Cologne, Germany; and* [7]*Xlab, Center for Healthy Aging, Department of Biomedical Sciences, Faculty of Health and Medical Sciences, University of Copenhagen, Copenhagen, Denmark*

Abstract

The myotendinous junction (MTJ) is a specialized interface for transmitting high forces between the muscle and tendon and yet the MTJ is a common site of strain injury with a high recurrence rate. The aim of this study was to identify previously unknown MTJ components in mature animals and humans. Samples were obtained from the superficial digital flexor (SDF) muscle-tendon interface of 20 horses, and the tissue was separated through a sequential cryosectioning approach into muscle, MTJ (muscle tissue enriched in myofiber tips attached to the tendon), and tendon fractions. RT-PCR was performed for genes known to be expressed in the three tissue fractions and t-distributed stochastic neighbor embedding (t-SNE) plots were used to select the muscle, MTJ, and tendon samples from five horses for RNA sequencing. The expression of previously known and unknown genes identified through RNA sequencing was studied by immunofluorescence on human hamstring MTJ tissue. The main finding was that RNA sequencing identified the expression of a panel of 61 genes enriched at the MTJ. Of these, 48 genes were novel for the MTJ and 13 genes had been reported to be associated with the MTJ in earlier studies. The expression of known [COL22A1 (collagen XXII), NCAM (neural cell adhesion molecule), POSTN (periostin), NES (nestin), OSTN (musclin/osteocrin)] and previously undescribed [MNS1 (meiosis-specific nuclear structural protein 1), and LCT (lactase)] MTJ genes was confirmed at the protein level by immunofluorescence on tissue sections of human MTJ. In conclusion, in muscle-tendon interface tissue enriched with myofiber tips, we identified the expression of previously unknown MTJ genes representing diverse biological processes, which may be important in the maintenance of the specialized MTJ.

collagen XXII; extracellular matrix; myotendinous junction; RNA sequencing

INTRODUCTION

Muscle strain injury accounts for the majority of exercise-related injuries in skeletal musculature, but is also common in relation to work and military training, and represents a leading cause for long-term functional disability, pain, and economic burden (1). Strain injury occurs in connection with abrupt muscle movement at the interface between the muscle and tendon, and in many cases leads to a separation of these two tissues. One of the main clinical challenges in this field is that, despite thorough rehabilitation, substantial injury recurrence is common, and it is estimated that ~80% of reinjuries occur at the same site as the original injury (2–5). Together, this indicates suboptimal repair after strain injuries and highlights the importance of gaining detailed insight into the molecular composition of the myotendinous junction (MTJ).

Data related to tendon and cartilage indicate that these tissues have no, or very limited, capacity for tissue renewal after skeletal maturity (6, 7), in contrast to skeletal muscle, which has a high rate of renewal (6). However, skeletal muscle contains a large extracellular matrix component in addition to the myofibers, and many types of resident mononuclear cells, all of which have different rates of turnover. We have previously shown that expression of muscle connective tissue-associated proteins demonstrates a slower and more prolonged

*Section for Sports Traumatology M51 and Institute of Sports Medicine Copenhagen are part of the International Olympic Committee Research Center Copenhagen.
Correspondence: A. L. Mackey (abigailmac@sund.ku.dk).
Submitted 8 June 2021 / Revised 1 July 2021 / Accepted 7 July 2021

time course of adaptation to experimentally induced muscle injury when compared with the cells and proteins related to regeneration of the muscle fibers themselves (8–12). Interestingly, the sustained elevated expression of several extracellular matrix proteins was associated with protection against reinjury (9). Whether similar principles apply at the MTJ is unknown. As the MTJ is the connecting interface between muscle and tendon, it is reasonable to assume that dynamic protein activity on both sides of the MTJ is required for maintenance and repair of the MTJ. Current knowledge about the MTJ comes largely from rodents, chicks, fish, and frogs, and often during development when direct cell-cell contact between tendon and muscle precursor cells exists (13–20). In contrast, in the adult state, these cells are separated by the muscle fiber basement membrane, and most of the tendon cells are embedded in a dense collagen matrix. Thus, the formation of the MTJ during development is fundamentally different from MTJ injury repair in the mature organism.

Several molecules involved in the formation of the connection between the two tissues have been described, both at the tendon side and at the muscle side of the junction (13). For example, collagen XXII is found in the basement at the MTJ in animals (21) and humans (22), and in the developing zebrafish has been shown to be crucial for optimal MTJ mechanical resilience (13). Furthermore, it has recently been suggested that single-nucleotide polymorphisms related to collagen XXII a 1 chain (COL22A1) expression are associated with susceptibility to a muscle injury in humans (23). Recently, the application of single-nuclei RNAseq (snRNAseq) to mouse skeletal muscle has provided detailed pre-mRNA profiles of clusters of nuclei characterizing the MTJ (24–27), confirming this region to be a highly specialized domain. A few of the MTJ genes identified by snRNAseq have been verified on tissue sections. For example, the presence of mRNA for *Adamts20* (28), *Tigd4*, and *Ebf1* (26) was convincingly shown in the myonuclei at the fiber tips by fluorescence in situ hybridization (FISH). In further support of the MTJ being a specialized region of the myofiber, it was elegantly demonstrated using RNAscope that, during development (E15.5), mRNA for the slow myosin heavy chain type I (*Myh7*) emerges initially at the tips of the fibers, whereas the rest of the fiber body remains predominantly filled with transcripts for (neonatal) *Myh8* (12). Taken together, there is clear and mounting evidence for a specialized role for nuclei at the MTJ. However, we still lack studies using an unbiased systematic approach to analyze adult muscle, MTJ, and tendon, in tissue and region-specific manner while accounting for biological variation.

Here, we studied the muscle-tendon complex from the superficial digital flexor (SDF) muscle of the horse, due to its exposure to great strain during activity and a high incidence of injury in racing horses (29), and the hamstrings in humans, because they are the most common location for strain injury (30). The main aim of the study was to uncover unique, or enriched, expression patterns of genes at the MTJ (defined as the muscle tissue enriched with fiber tips, adjacent nonmuscle cells, and the layers of tendon closest to the MTJ) when compared with neighboring tendon and muscle tissue, using an unbiased tissue-specific analysis approach.

MATERIALS AND METHODS

Animal and Human Study Approval

Horse.

Samples were obtained from 20 horses (7 geldings and 13 mares) that were enrolled in a study investigating cardiac function and arrhythmia in response to exercise. All horses were between 5–10 yr of age and standardbred trotters. Nine had been sedentary for at least 1 year, and 11 had performed high-intensity training and racing for at least 3 years before inclusion in the study. The project was approved by the Animal Experiments Inspectorate in Denmark (2016-15-0201–01128) and the Ethical Committee at the Department of Veterinary Clinical Sciences, University of Copenhagen. All horses were subjected to a protocol testing their cardiac function. Over a 3-day period, they did three familiarization sessions of walking on a treadmill, followed by three maximal effort tests performed with 2–3 days recovery in between. All maximal effort tests were performed on a treadmill with 6% inclination and speed set to 7 m/s with increases in the speed of 0.5 m/s every 60 s until the horses could not keep up.

Human.

The human tissue was obtained from patients [2 females and 2 males, age: 24–35 yr, body mass index (BMI) < 25, nonsmokers, and with no known diseases] undergoing anterior cruciate ligament (ACL) reconstruction surgery with the use of the hamstring tendons, as previously described (31). Participation was approved by The Research Ethics Committees of the Capital Region of Denmark (Ref. H-3-2010-070) according to the standards set by the Declaration of Helsinki. All volunteers gave written informed consent before inclusion.

Tissue Collection

Two to eight days following the last exercise, the horses were premedicated with flunixin-meglumine 1.1 mg/kg, detomidine 0.01 mg/kg, acepromazine 0.03 mg/kg, morphine 0.06 mg/kg, and butorphanol 0.01 mg/kg intravenously (iv). General anesthesia was induced by intravenous administration of zolazepam combined with tiletamine (Zoletil, Virbac Denmark A/S, Kolding, Denmark, 1.5 mg/kg i.v.) and maintained by isoflurane inhalation (IsoFlo Vet., Orion Pharma Animal Health, Copenhagen, Denmark, 1.4%). During anesthesia, additional analgesia with 0.06 mg/kg morphine (Morfin DAK 20 mg/mL, Takeda Pharma A/S, Taastrup, Denmark) was performed every 3 h along with a continuous rate infusion of the muscle relaxant Rocoronium (Rocoronium, 10 mg/mL, Hameln Pharmaceuticals, Hameln, Germany, 0.3 mg/kg/h) were applied. Cardiac electrophysiology testing was performed during anesthesia, ending with exsanguination and the heart being removed for further processing in a different project not related to the outcomes of the current study.

From humans, the muscle-tendon interface of the semitendinosus was obtained in relation to the harvest of the tendon for ACL reconstruction. The unused interface tissue was donated for the study. The samples were mounted in TissueTek (Sakura Finetek Europe, Zoeterwoude, Netherlands),

frozen in liquid nitrogen-cooled isopentane, and stored at −80°C.

Sample Preparation

As soon as possible postmortem the left forelimb was cut off and transported on ice to the laboratory, where the SDF muscle was dissected and small samples of muscle with attached tendon were punched out using a 4-mm diameter biopsy puncher. The samples were mounted in TissueTeK, tendon side down, frozen in liquid nitrogen-cooled isopentane, and stored at −80°C until analysis.

To isolate the MTJ, these blocks of tissue were mounted in a cryostat (muscle face-up; Fig. 1) and sectioned in 10-μm thick slices. The first section was mounted onto a glass slide, serving as a control section to determine tissue composition (muscle/MTJ/tendon) and measuring the area of the section later. Twenty sections (200-μm total depth) were then cut and collected in an Eppendorf tube using a sterile technique. The first section after the collection of these 20 sections was also mounted onto the glass slide. This was repeated until the tendon began to be visible on the control sections (Fig. 1*D*). This assessment was made by viewing unstained sections immediately upon collection onto a glass slide, using a standard bright-field microscope. The subsequent sections were collected as the fraction termed "MTJ" until the point where only the tendon (i.e., no muscle) remained. Because some of the samples were cut at a slight angle, the number of sections in the MTJ fraction varied from 20 to 30 (200–300 μm). Collection of sections continued until no tissue remained. Based on evaluation of the control sections, six specific fractions from each sample were retrospectively identified for RT-PCR as illustrated in Fig. 1: *1*) "muscle": the second fraction collected (with the lowest risk of tendon contamination); *2*) "muscle-MTJ": the fraction collected just before the MTJ; 3) "MTJ": containing both muscle and tendon; *4*) "tendon-MTJ": the fraction collected immediately after the MTJ (potentially containing some muscle); *5*) "tendon": pure tendon tissue collected immediately after "tendon-MTJ"; *6*) "tendon(surface)": the part of the tendon furthest away from the MTJ, only collected from a small number of samples due to limited thickness of tendon tissue.

RNA Extraction

The cryosections were homogenized in 1 mL of TriReagent (Molecular Research Center, Cincinnati, OH) containing five stainless steel balls of 2.3 mm diameter (BioSpec Products, Bartlesville, OK) by shaking in a FastPrep-24 instrument (MP Biomedicals, Illkirch, France) at speed level 4 for 15 s. Following homogenization, bromochloropropane was added

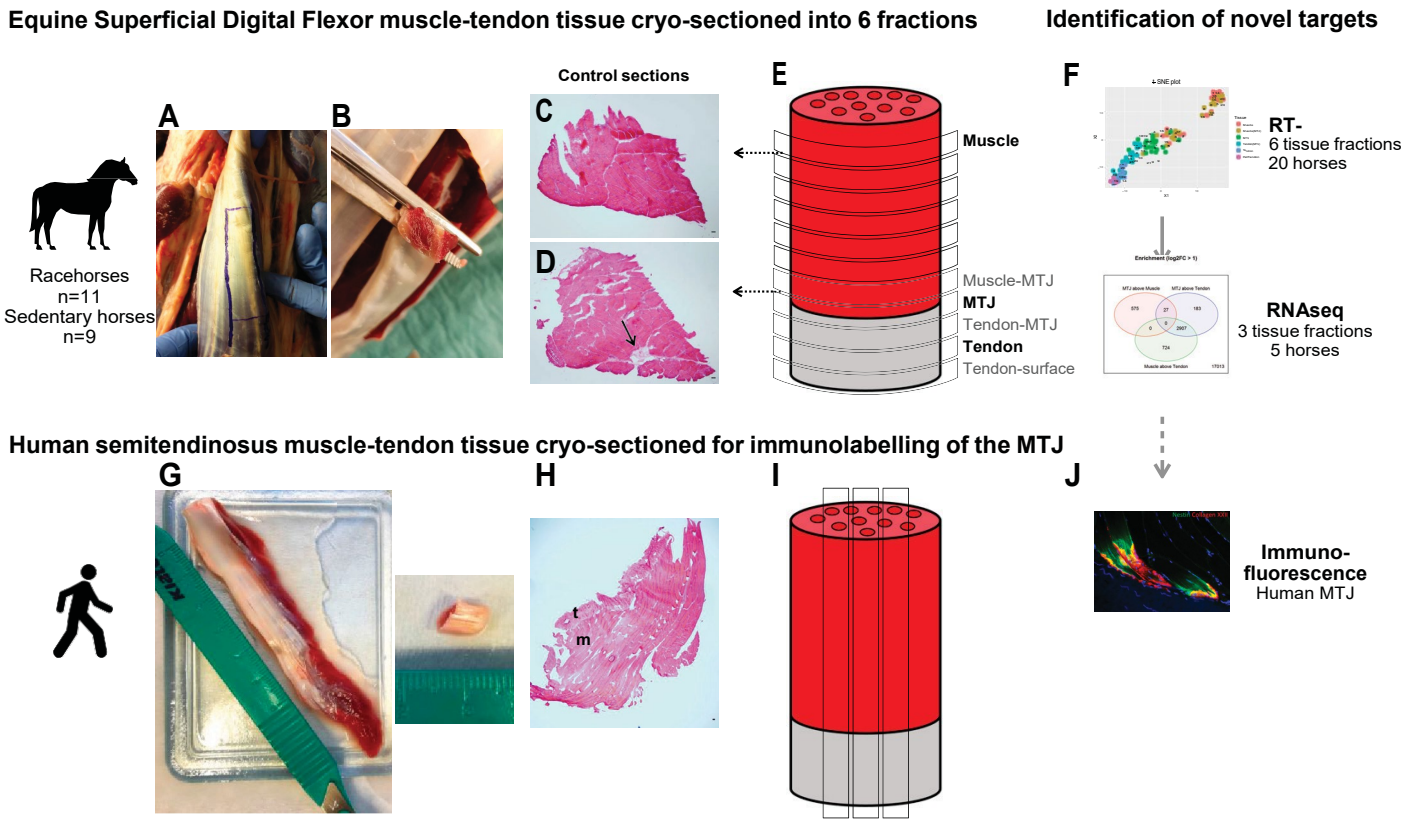

Figure 1. Study overview. A piece of horse SDF muscle-tendon complex (*A*, *B*) was frozen for cryosectioning. Control sections were examined before collecting sections of the six tissue fractions (*E*), e.g., the "muscle-MTJ" fraction (*C*) or "MTJ" (*D*, arrow points to tendon tissue emerging); Scale bar = 50 μm. For identification of novel targets (*F*), t-SNE plots of the RT-PCR data were used to select five horses for RNAseq. Human hamstring semitendinosus MTJ tissue was collected (*G*, ruler units in cm) and oriented for sectioning (*I*) to have both muscle (m) and tendon (t) present on the section (*H*). Targets enriched at the MTJ in the RNAseq data were selected for immunofluorescence (*J*). MTJ, myotendinous junction; RNAseq, RNA-sequencing; SDF, superficial digital flexor; t-SNE, t-distributed stochastic neighbor embedding.

to separate the samples into an aqueous and an organic phase. Following isolation of the aqueous phase, RNA was precipitated using isopropanol and 80 µg of glycogen (Invitrogen, Naerum, Denmark). The RNA pellet was then washed in ethanol and subsequently dissolved in 10-µL RNAse-free water. Total RNA concentrations were determined by Ribogreen assay (R11490, Life Technologies, Naerum, Denmark).

Real-Time RT-PCR

Total RNA (30 ng) was converted into cDNA in 20 µL using the OmniScript reverse transcriptase (QIAGEN, CA) and 1 µM poly-dT (Invitrogen, Naerum, Denmark) according to the manufacture's protocol (QIAGEN). For each target mRNA, 0.5 µL cDNA was amplified in a 25-µL SYBR Green polymerase chain reaction (PCR) containing 1× Quantitect SYBR Green Master Mix (QIAGEN) and 100 nM of each primer (Table 1). The amplification was monitored real time using the MX3005P Real-time PCR machine (Stratagene, CA). The Ct values were related to a standard curve made with known concentrations of cloned PCR products or DNA oligonucleotides (UltramerTM oligos, Integrated DNA Technologies, Inc., Leuven, Belgium) with a DNA sequence corresponding to the sequence of the expected PCR product. Undetected products set to one molecule (Supplemental Fig. S1; see https://doi.org/10.6084/m9.figshare.14748216.v1). The specificity of the PCR products was confirmed by melting curve analysis after amplification. RPLP0 mRNA was chosen as internal control.

RNA Sequencing

As the samples contain variable amounts of muscle, MTJ, and tendon, a principal component analysis (PCA)/t-SNE analysis of the RT-PCR data was performed in R to identify the most representative samples for muscle, MTJ, and tendon (32, 33). Based on the t-SNE-plot of the RT-PCR data, "muscle," "MTJ," and "tendon," fractions from five horses (one sedentary mare, one race gelding, and three race mares) were selected for RNA sequencing. Total RNA from these samples were sent to BGI for RNA sequencing (SE50, BGI Europe, Copenhagen, Denmark) using their Smart-seq II/DNBseq method. Approximately 25 million reads were obtained after quality filtering (>97% clean reads). The reads were mapped to the horse reference genome (EquCab3.0) using Rsubread (34) (restricted to unique alignments). It was possible to map 60%–73% of the reads uniquely to the genome and those were counted and assigned to the transcripts. The count data were analyzed with DESeq2 (35) (normalized rlog values used for PCA and expression measures). The full data are available in the Gene Expression Omnibus database (GSE166468).

Estimation of Muscle and Tendon Contribution to MTJ Fractions

Expression levels in MTJ fractions were estimated ("expected mix") based on the relative contribution from muscle and tendon tissue. From the muscle and tendon fractions, reference genes "specific" to muscle or tendon, respectively, were selected based on displaying at least a 10-fold difference between the two tissues, and having at least 100 counts within all samples of the tissue with the high expression levels (Supplemental Fig. S2; "Reference genes for MTJ prediction.xlsx"). For each horse, to estimate the relative amount of muscle in the MTJ fraction, the counts for each muscle-specific reference gene of the MTJ sample were divided by the counts for the same gene in the muscle fraction and the median used as an estimate, $Factor_{muscle}$. The relative amount of tendon ($Factor_{tendon}$) was determined in the same manner using the tendon-specific reference genes and normalizing to the tendon fraction. The expected contribution of muscle and tendon to the counts of each gene in the MTJ fraction was then calculated as $MTJ_{expected} = Factor_{muscle} \times Counts_{muscle} + Factor_{tendon} \times Counts_{tendon}$, where $Counts_{muscle}$ and $Counts_{tendon}$ refer to the counts of that gene in the muscle and tendon fractions, respectively. Before comparison with the real MTJ counts, all values below 10 were set to 10 and likewise for the real MTJ counts to prevent excessive noise from low counts.

Pathway Analyses

The measured and expected MTJ values were used to search for enriched pathways in MTJ by Generally Applicable Gene Set Enrichment (GAGE) (36) and Fast Gene Set Enrichment Analysis (FGSEA) (37) in R against the Kyoto Encyclopedia of Genes and Genomes (KEGG) and GO databases. Pathway analyses for enrichment in

Table 1. *Primers for real-time RT-PCR*

Name	NCBI/ENSEMBL ID	Sense	Antisense
RPLP0	NM_001252576.1	GAGACTGATTACACCTTCCCACTTGCT	ACAAATGCAGATGGATCAGCCAAGAA
GAPDH	NM_001163856.1	GCATTGCCCTCAACGACCACTTT	CATAAGGTCCACCACCCTATTGCTGT
COL1A1	XM_023652710.1	CGCTTCACCTACAGCGTCACCTAC	AGCGGGAGGTCTTGGTGGTTT
COL3A1	ENST00000317840.9	TTTGGTTTGGAGAATCTGTGGATGGT	TCAAGGACATCTTCAGGAAGGTCAGG
SCX	NM_001105150.1	GCACCTTCTGCCTCAGCAACC	CTCCGAATCGCCGTCTTTCTGT
TNMD	NM_001081822.1	GCGCCAGACAAGCAAGTGAAGA	TCTCATCCAGCATGGGGTCAAA
VEGFA	NM_001081821.1	GTGTGCCCCTGATGCGGTGT	TGTGTTGGCTTTGGTGAGGTTTG
ANGPTL4	XM_023644667.1	ACGACCTCCGCAGGGACAAG	TTGAAGAGGGATGGAGCGGAAG
ATF3	XM_005609809.3	AGCTGCCAAGTGCCGAAACAAG	TGGGCCTTCAGTTCAGCATTCAC
PTGS1	NM_001163976.1	GCATGAAGCCCTACGCCTCTTT	GCAGCCCAGGGTAGAACTCCAA
PTGS2	NM_001081775.2	ATGATGAACGCTTGTTCCAGACGA	CAGTTTGAAGTGATAGCCGCTCAGG
COL22A1	XM_014728097.2	GGCAGGTGGGTCTGGAAGGA	TCCCAGGAGGCCCCATCTCG
COL17A1	XM_014733101.2	TGGCTTTGCTGGAGGTCTGGA	CCTGGACAGTGTAGGCCATTCCTT
COMP	NM_001081856.1	CTATGGAAGGACCCCCGCAAC	ACCAGCTCAGGGCCCTCATAGAA
ITGA7	XM_023643743.1	TGATCGTCCGAGCCAACATCAC	CCACCGGGTCCAAGTATACCATC

MTJ versus tendon or muscle were not performed, as such analyses would be expected to simply yield muscle or tendon-specific pathways due to the mix in MTJ samples.

Immunofluorescence

Nine targets identified by RNAseq to be enriched at the MTJ were selected for further evaluation by immunofluorescence (IF) on cryosections of human semitendinosus MTJ: NES (nestin), OSTN (musclin/osteocrin), CD52 (CAMPATH-1 antigen), ACTC1 (actin a cardiac muscle 1), ADAMTS8 (A Disintegrin and Metalloproteinase with Thrombospondin type 1 motif 8), LCT (lactase), NEFM (neurofilament medium), POSTN (periostin), MNS1 (meiosis-specific nuclear structural protein 1), COL22A1 (collagen XXII), and NCAM1 (neural cell adhesion molecule 1). From the human samples, sections (10-μm thick) were cut with a cryostat and stored at −80°C. For the IF protocol, the sections were washed in TBS and incubated in TBS containing 1% bovine serum albumin (BSA), before being incubated overnight in a mixture of two primary antibodies (Table 2), diluted in TBS containing 1% BSA. The following day the slides were washed in TBS and incubated for 45 min in appropriate secondary antibodies (Table 2), diluted 1:500 in TBS containing 1% BSA. After washing in TBS, the slides were mounted with coverslips and mounting medium containing DAPI (Molecular Probes ProLong Gold antifade reagent, Cat. No. P36931, Thermo Fisher Scientific, Denmark). Initially, each antibody was stained in combination with collagen XXII. Based on staining patterns, a subsequent double stain was carried out with collagen IV for antibodies against lactase and ADAMTS8, to investigate whether staining was associated with capillaries. Initially, all antibodies were tested with fixation in Histofix (Histolab, Gothenburg, Sweden) for 8 min, either before application of the primary antibody or before mounting. For all antibodies except MNS1, the final protocol included fixation before the final wash (before mounting) for improved preservation of nuclei morphology. For MNS1, fixation was carried out before the wash step before incubation with the primary antibodies.

The M3F7 monoclonal antibody developed by Furthmayr was obtained from the Developmental Studies Hybridoma Bank, created by the NICHD of the NIH, and maintained at The University of Iowa, Department of Biology, Iowa City, IA.

Statistics

All PCR data were analyzed in Sigmaplot v. 14.0. Mann–Whitney Rank Sum tests were performed on the PCR data to investigate potential differences in mRNA levels between trained and untrained horses, within each tissue fraction. For the pooled (trained and untrained horses) PCR data, Wilcoxon Signed-rank tests with Bonferroni corrections were made for each target, comparing the fractions muscle with MTJ, MTJ with tendon, and tendon with muscle. The muscle-MTJ and tendon-MTJ fractions were not included in this analysis since they might represent a mixture of two tissue fractions. The tendon-surface region was also excluded because only a very limited number of samples were collected from this region. For RNAseq data, statistical differences between tissue types were determined using DESeq2 (35) (design = ~ HorseID + Tissuetype, lfcshrink/apegml) with false discovery rate (FDR) < 0.05 and log2FC > 1. For comparison between the MTJ measured and expected mix values, log-relative differences were tested using a one-tailed (increase) t test (FDR < 0.1, log2FC > 1). The reason for using a one-tailed test is that the expected counts are the sum of

Table 2. *Primary and secondary antibodies used for staining the sections of human muscle-tendon tissue*

Gene Name	Protein	Primary Antibody	Secondary Antibody
NES	Nestin	Mouse, sc-23927, Santa Cruz Biotechnology Dallas, Texas	Donkey anti-mouse, 715-545-152, Jackson Immunoresearch, Ely, UK
OSTN	Osteocrin/musclin	Rabbit, orb157918, Biorbyt, Cambridge, UK	Donkey anti-rabbit, 711-486-152, Jackson Immunoresearch
CD52	CAMPATH-1 antigen	Rabbit, 21809-1-AP, Proteintech, Rosemont, Illinois	Goat anti-rabbit, A-11034, Molecular Probes, Thermo Fisher Scientific, Denmark
ACTC1	Actin a cardiac muscle 1	Rabbit, sab2700789, Sigma Aldrich Denmark A/S	Goat anti-rabbit, A-11034, Molecular Probes
ADAMTS8	ADAM metallopeptidase with thrombospondin type 1 motif 8	Rabbit, hpa066349, Sigma Aldrich	Goat anti-rabbit, A-11034, Molecular Probes
LCT	Lactase	Rabbit, hpa007408, Sigma Aldrich	Goat anti-rabbit, A-11034, Molecular Probes
NEFM	Neurofilament medium	Mouse, amab91030, Sigma Aldrich	Goat anti-mouse, A-11029, Molecular Probes
POSTN	Periostin	Rabbit, ab14041, Abcam, Cambridge, UK	Donkey anti-rabbit, 711-486-152, Jackson Immunoresearch
MNS1	Meiosis-specific nuclear structural protein 1	Rabbit, PA5-59016, Thermo Fisher Scientific	Donkey anti-rabbit, 711-486-152, Jackson Immunoresearch
COL22A1	Collagen XXII	Guinea pig, provided by Manuel Koch	Goat antiguinea pig, A-11075, Molecular ProbesorDonkey anti-guinea pig, 706-585-148, Jackson Immunoresearch
NCAM1	Neural cell adhesion molecule / CD56	Mouse, 347740, Becton Dickinson	Goat anti-mouse, A-11029, Molecular Probes
COL4A1/ COL4A2	Collagen IV	Mouse, M3F7, Hybridoma Bank	Goat anti-mouse, A-11031, Molecular Probes

muscle and tendon contributions such that any contribution from the MTJ must be in addition to this value.

RESULTS

RT-PCR

Tissue-specific samples of the SDF muscle-tendon complex from the horses were collected by cryosectioning the tissue from the muscle side, through the MTJ, and ending at the tendon side, as illustrated in Fig. 1. To validate this sectioning approach in obtaining muscle, MTJ, and tendon tissue, RT-PCR was performed for genes that were likely to be differentially expressed in the muscle, MTJ, and tendon tissue fractions. mRNA levels for the racing and sedentary horses were compared within each tissue type. No statistically significant differences were found (Supplemental Fig. S3), so the data from all 19 horses were pooled. In Fig. 2, the RT-PCR results are displayed for the respective tissue fractions, for each of the genes. The results are expressed relative to the mean value from muscle and in this graph normalized to RPLP0. RPLP0 was chosen since the total amount of RNA varies between muscle and tendon tissue because of the larger number of cells in skeletal muscle. However, RPLP0 is more equally expressed in the different tissues resulting in a more reliable result when comparing gene expression relative to RPLP0 from the different tissues (Supplemental Fig. S1).

As can be seen in Fig. 2, a variety of patterns is evident from the 14 targets. For example, at the MTJ, COL22A1 was expressed at a greater level compared with both muscle and tendon, whereas tenomodulin was expressed to a greater extent in the MTJ than in muscle, but not compared with tendon. In muscle, GAPDH was found to be elevated compared with the two other regions. In tendon, higher levels of cartilage oligomeric peptide (COMP), but lower levels of scleraxis, were seen relative to muscle and MTJ.

Selection of Samples for RNAseq

To select the cleanest muscle, MTJ, and tendon samples for RNAseq, all the PCR data (all samples and all genes) were analyzed together by Principle Component Analysis (PCA) and t-distributed stochastic neighbor embedding (t-SNE). From the PCA (Fig. 3), most of the MTJ samples can be observed close to each other, but there are some outliers and "infiltration" of muscle and tendon tissue. The muscle and muscle-MTJ fractions are also separated from the others with a few outliers, but no clear separation is apparent between muscle-MTJ and muscle. The fractions-labeled tendon and tendon-surface are very distinct and located close to each other. In the t-SNE plot (Fig. 3), most of the MTJ fractions are clustered close together, separated from most of the tendon and muscle fractions. The tendon fractions have the most distinct separation and are clustered closely together with only one MTJ sample infiltrating the cluster. In the muscle fractions, two clusters can be observed. One of them is located close to the MTJ samples and the other further away. The two clusters contain a mixture of both the muscle and the muscle-MTJ fractions. From this t-SNE plot (Fig. 3), muscle, MTJ, and tendon samples from five horses were selected for RNA sequencing to gain unbiased insight into genes that might be enriched or uniquely expressed at the MTJ. The criteria for selection were good separation into the three tissue regions (muscle, MTJ, and tendon). The horses that were selected were one sedentary mare, one race gelding, and three race mares. These horses are indicated in Fig. 3*D*.

RNA Sequencing

From the RNAseq data, a PCA plot was made for samples from the five horses to illustrate that variation in gene expression was primarily due to the different tissue types and to a lesser extent the different horses (Fig. 4*A*). No clear effects of gender or previous activity status were seen in the PCA plot (Supplemental Fig. S4*A*). Comparing muscle with tendon, 3293 genes were more expressed in muscle, and 4239 in the tendon. In the MTJ fraction, 602 genes were more expressed compared with muscle, whereas 3117 were observed to be higher in MTJ compared with the tendon (Fig. 4*B*). Although no genes were uniquely expressed at the MTJ, 27 genes, including COL22A1, were observed to be significantly higher (>2fold difference) in MTJ than both tendon and muscle (Fig. 4*C*).

Since the MTJ tissue fractions consist of varying amounts of muscle and tendon tissue, a second approach was used to explore the RNAseq data. An estimate of the contribution of muscle and tendon tissue was calculated for all MTJ samples based on the expression levels of the most highly expressed genes specific to the muscle (219) and tendon (322). (For a list of genes see Supplemental Fig. S2; see "Reference genes for MTJ prediction.xlsx"). A high correlation was seen between the expected and measured values from the genes in the MTJ samples, where less than 1.5-fold differences were seen between the expected and measured values for more than 95% of the genes (Supplemental Fig. S4*B*). The estimated contribution of muscle and tendon was 86%–96% and 6%–14%, respectively. Using this approach, we detected 43 genes in the MTJ displaying higher expression levels than expected (Fig. 5; Supplemental Fig. S5). For the fold change from the calculated expected mix value for all 17013 genes, see Supplemental Fig. S6, "MTJ_changes.xlsx"). Represented in this set of genes were eight of the genes among the 27 identified in Fig. 6 (COL22A1, OSTN, ALDH3B1, POSTN, CNTNAP4, NCAM1, MNS1, and CD52). Of the 43 genes, five displayed at least 10-fold higher expression than expected, with COL22A1 demonstrating the greatest (17-fold) difference above expected levels.

A search for enriched pathways within the measured versus expected mix MTJ values was performed using GAGE and FGSEA. No significant pathways in GO or KEGG were found, except for four KEGG pathways that were downregulated in MTJ with GAGE analysis (Table 3). The KEGG pathway database represents knowledge on metabolism and function at the cell and organism levels, which can be linked to specific genes. The 27 and 43 genes identified from the two approaches are combined in Table 4.

Immunofluorescence

To investigate whether the expression of some of the MTJ-enriched genes (in Table 4) were also present at the protein level, immunofluorescence was performed. The presence of

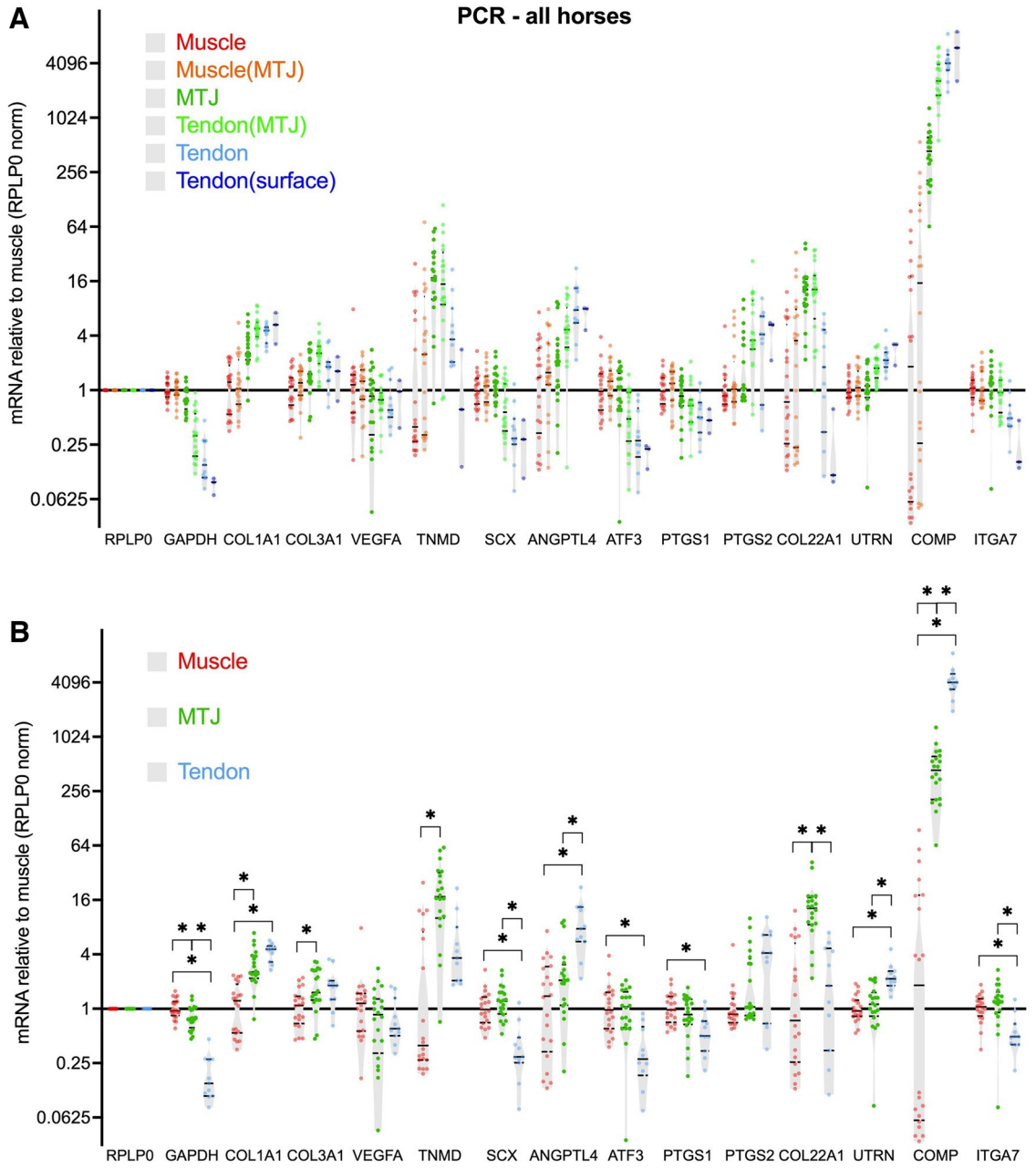

Figure 2. PCR data. The graph shows the mRNA results for each of the 14 targets. Each tissue fraction is indicated by a different color and each dot represents a horse (n = 19 horses). The values are expressed relative to muscle and normalized to RPLP0. In *A*, all regions are shown but no statistical analyses were carried out. In *B*, only the "muscle," "MTJ," and "tendon" fractions are shown since these displayed clearer separation between the tissue types. Comparisons were performed pairwise using the Wilcoxon Signed-rank test with Bonferroni correction. $^{*}P < 0.05$. MTJ, myotendinous junction.

collagen XXII, NCAM, periostin, osteocrin, nestin, MNS1, and lactase was confirmed in the human MTJ (Figs. 6, 7, and 8). Staining for CD52, NEFM, ADAMTS8, and ACTC1 was inconclusive. NCAM and nestin were present in the cytoplasm of the muscle fibers as they approached the tendon, whereas periostin was located distal to collagen XXII, at the tips of the fibers. MNS1 was expressed by myonuclei close to the MTJ and in mononuclear cells between muscle fibers close to the MTJ. Lactase was seen in mononuclear cells between the skeletal muscle fibers and distributed both between the distal parts of muscle fiber and at the interface between the muscle fiber and the tendon at the MTJ. Osteocrin immunoreactivity was observed in muscle fiber cytoplasm and also in mononuclear cells at the MTJ.

DISCUSSION

The main findings of the present study were the identification of genes demonstrating enriched expression at the injury-prone myotendinous junction (MTJ) of the adult horse SDF muscle. Although no genes were exclusively expressed at the MTJ, RNA sequencing revealed genes representing a wide range of biological processes that were highly expressed in the MTJ. This is the first unbiased approach to

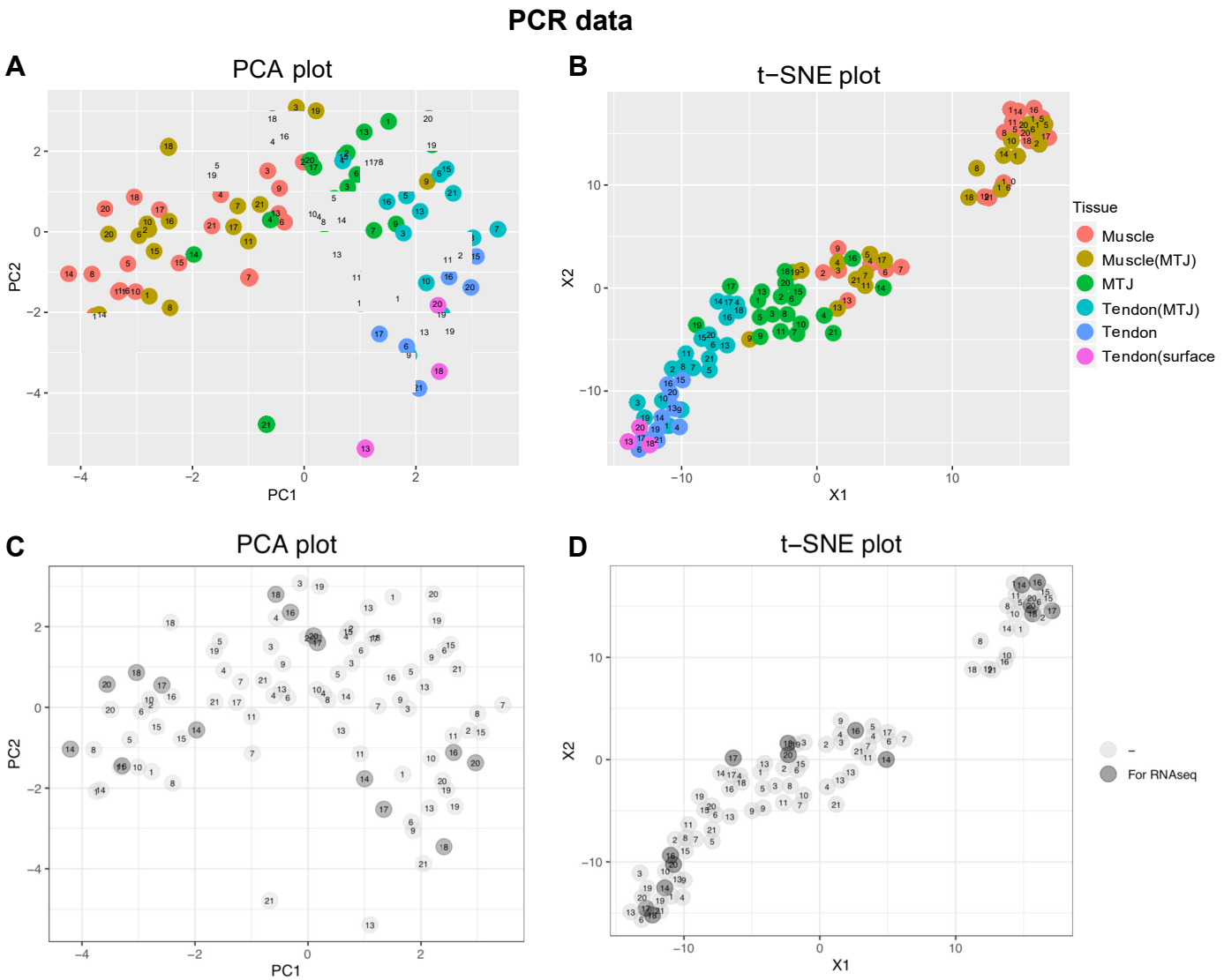

Figure 3. Distribution of PCR data in relation to tissue fractions. Principal component analysis (*A*) and t-distributed stochastic neighbor embedding (t-SNE) plots (*B*), showing the distribution of the various samples from all the horses ($n = 19$). Samples located close together reflect more similar mRNA levels. The numbers refer to the individual horse from which the tissue is taken. In *B*, the tendon tissue fractions are isolated and clustered together. The same is seen for most of the MTJ fractions, whereas the two different muscle regions are mixed. *C* and *D* contain the same data points as *A* and *B*, but with the five horses selected for RNAseq indicated. MTJ, myotendinous junction; RNAseq, RNA-sequencing.

explore this unique tissue interface in a large, mature mammal, where exposure to great mechanical strain is high and strain injury is frequent. Furthermore, immunofluorescent staining of human hamstring MTJ tissue demonstrated the presence of periostin, osteocrin, lactase, and MNS1 in the human MTJ for the first time. Together, these findings indicate the expression of previously unrecognized genes and proteins at the muscle-tendon interface, which may be important for maintaining plasticity in, and between, the myofiber and tendon ECM compartments.

The lack of difference in gene expression levels between the racehorses and sedentary horses can most likely be explained by the study protocol, as all horses performed treadmill exercises 2–8 days before tissue sampling. Therefore, gene activity is probably more determined by loading of the MTJ during the recent exercise than by the status of the horse as racing or sedentary. It is important to emphasize that these findings should not be interpreted as a lack of capacity for remodeling of the MTJ in response to exercise loading. As discussed elsewhere, loading and unloading lead to alterations in the folding morphology of the MTJ as well as changes in gene and protein expression levels (16, 19). Indeed, it is possible that differences between the racing and sedentary horses exist at the protein and/or structural level. A study with more stringent timing of exercise and tissue sampling is required to investigate this.

Collagen XXII is a protein uniquely expressed at tissue junctions, including the MTJ, where in situ hybridization clearly shows gene expression exclusively in the basement membrane of the muscle cells at the MTJ and aponeurosis (21). Our PCR and RNA sequencing data confirm that COL22A1 was expressed at significantly higher levels in the isolated MTJ fraction compared with the muscle and tendon. However, the detection of COL22A1 to some extent in the muscle and tendon samples indicates the incomplete

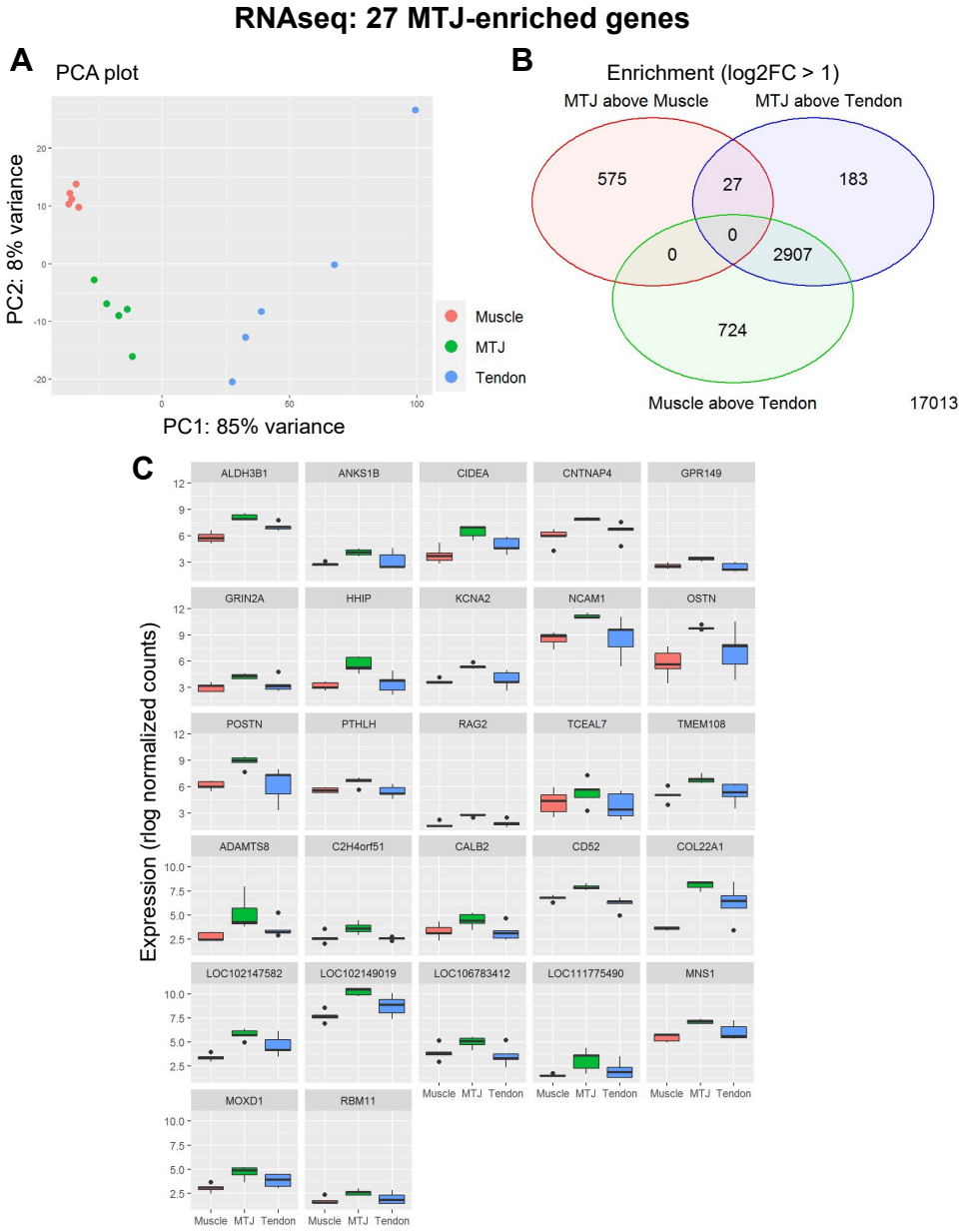

Figure 4. RNA-seq-27-enriched MTJ genes. Genes expressed at higher levels in MTJ than both muscle and tendon (n =5 horses). *A*: PCA plot based on the RNAseq data showing the distribution of the samples from 5 horses selected for RNAseq. The muscle and MTJ samples are clustered close together with larger differences between the tendon samples. *B*: Venn diagram illustrating the differences in gene expression between the three tissue types. Furthermore, 27 genes are more greatly expressed at the MTJ than both muscle (red circle) and tendon (blue circle), determined using DESeq2 with FDR < 0.05 and log2FC > 1. *C*: box plots showing the expression of the 27 genes in muscle, MTJ, and tendon. FDR, false discovery rate; MTJ, myotendinous junction; RNAseq, RNA-sequencing; PCA, principal component analysis.

separation of the three tissues, reducing the likelihood of detecting genes uniquely expressed at the MTJ. Nonetheless, the finding of COL22A1 as one of the most enriched genes at the MTJ in both RNA-sequencing approaches confirms that the method developed for this study to isolate MTJ-enriched tissue, muscle, and tendon can be used to analyze and compare the three tissues.

The first RNA-sequencing approach identified 27 genes that were expressed at significantly higher levels at the MTJ when compared with both muscle and tendon. The second approach took into account the relative contribution from muscle and tendon tissue to the MTJ samples, estimated to be between 86%–94% and 6%–14%, respectively, and calculated expected mix values based on these tissue proportions. Furthermore, 43 genes were expressed at higher levels than the expected mix values, where COL22A1 emerged as top of the list, expressing 17-fold greater levels than the expected mix. Using these data, GAGE enrichment analysis revealed a downregulation of four pathways (Parkinson's disease, ribosome, thermogenesis, and Huntington disease) in the MTJ tissue (Table 3), the significance of which remains obscure. Determining the correct analysis approach of the RNA sequencing data is not straightforward due to the MTJ representing a combination of muscle and tendon rather than an independent tissue that can be isolated. Interestingly, eight common genes were detected on both the 27-gene and the 43-gene lists (COL22A1, OSTN, ALDH3B1, POSTN, CNTNAP4, NCAM1, MNS1, and CD52), so we combined these into one list of 61 genes (Table 4). Although no GO or KEGG pathways enriched in MTJ were found, frequently appearing GO

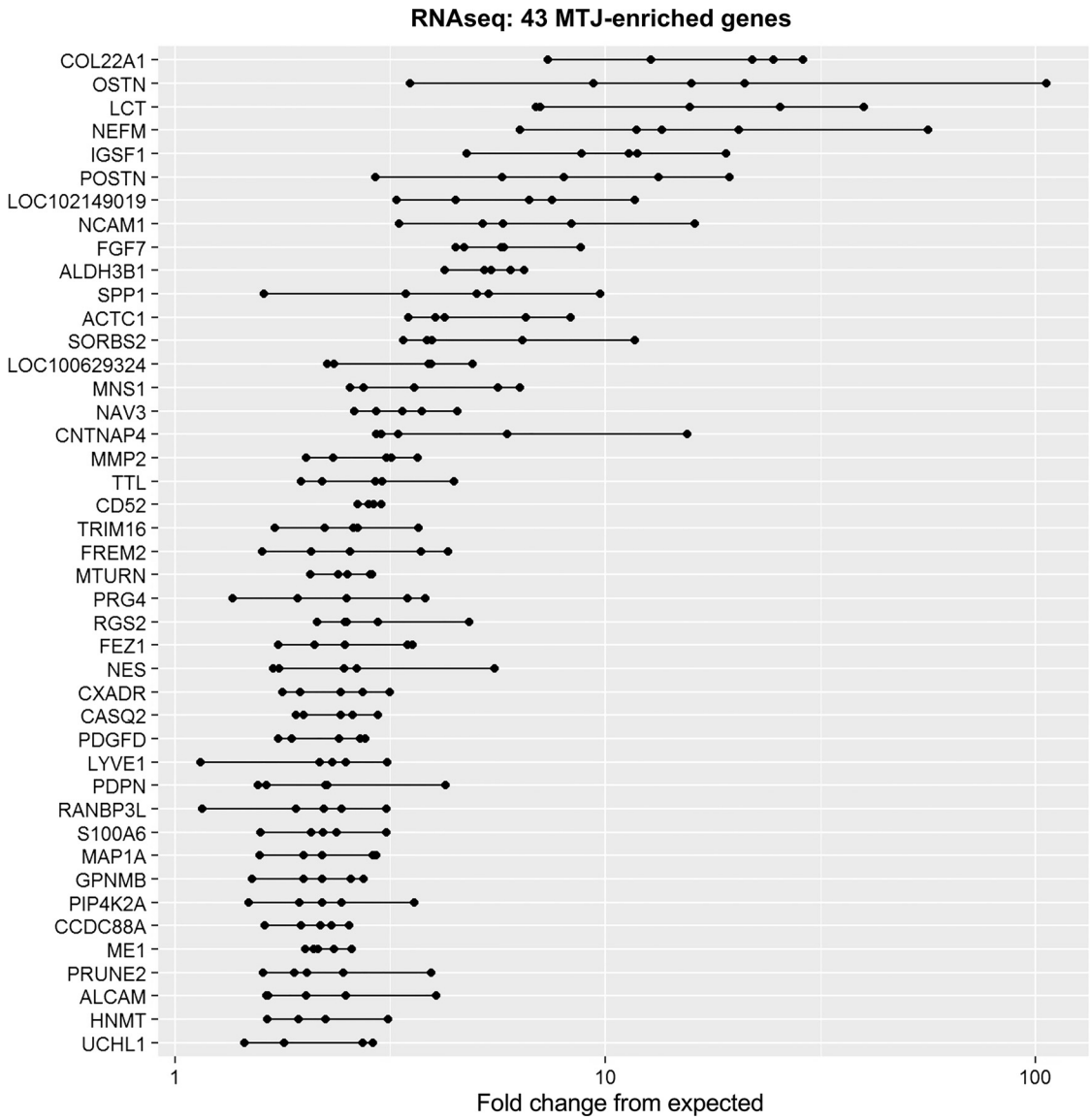

Figure 5. RNA-seq-43-enriched MTJ genes. List of genes from RNA sequencing of horse muscle, MTJ, and tendon tissue fractions showing 43 genes that are more highly expressed at the MTJ than expected mix values, based on the relative contribution of muscle and tendon, and using one-tailed (increase) *t* test (FDR < 0.1, log2FC > 1). Each dot represents the mean fold difference from the calculated expected mix value, for each horse ($n = 5$). The lines indicate the range. See Supplemental Fig. S5 for individual plots of genes in each tissue fraction. FDR, false discovery rate; MTJ, myotendinous junction; RNAseq, RNA-sequencing.

annotations for the 61 genes were related to neural activity, the immune system, cell adhesion, extracellular matrix, cytoskeleton, tissue repair, and metabolism, indicating great diversity in biological processes active at the MTJ.

Notably, neural-related genes were heavily represented among the enriched MTJ genes (e.g., FEZ1, GPR149, GRIN2A, NCAM1, NEFM, PRUNE2, and UCHL1), indicating that a strong neural component exists at the MTJ. The detection of NCAM1 in both data sets supports our earlier finding of NCAM at the protein level in the cytoplasm of myofibers as they approach the MTJ while being virtually absent throughout the rest of the myofiber cell (30). NCAM is known to be expressed by satellite cells, myotubes, and muscle fibers during development and regeneration (10, 37), in addition to denervated muscle fibers (38). These processes are also characterized by the presence of centrally positioned myonuclei, a feature we previously reported in fibers close to the MTJ in human muscle (30). Similar to the expression of NCAM, nestin was seen in the cytoplasm of muscle fibers as they were inserted at the MTJ. This expression of nestin has previously been described in animal and human tissue at the MTJ and also in relation to acetylcholine receptors at the neuromuscular junction (39, 40). In further support of a neural component at the MTJ, staining of the nerve-related acetylcholine esterase (AChE) has been observed on the muscle side of the MTJ in rats and fish (41–43), as well as a wide range of sensory nerve receptors, including Golgi tendon organs, Ruffini corpuscles, and free nerve endings (44, 45). However, the implications of these neural-related genes at the muscle-tendon interface remain unknown.

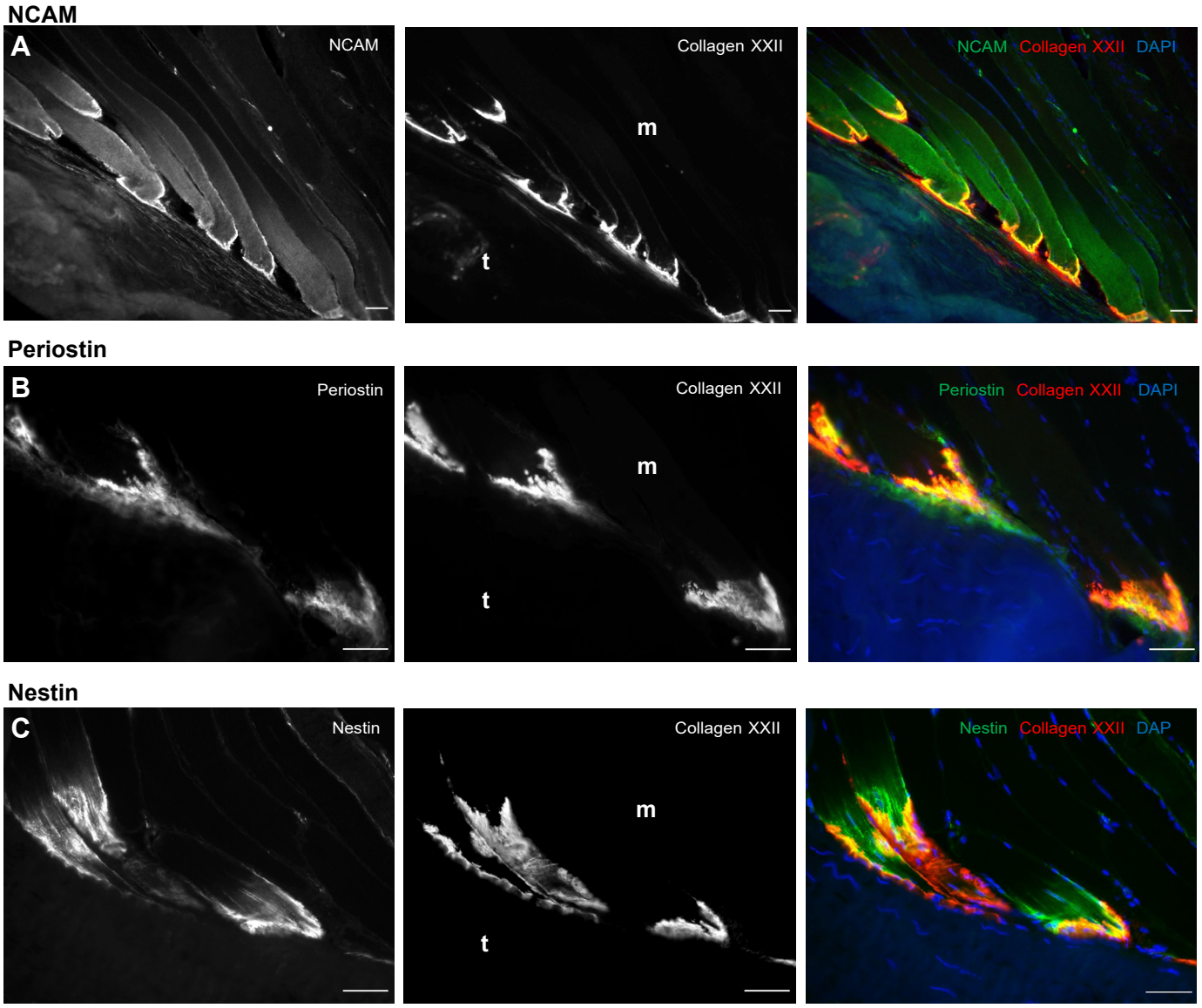

Figure 6. Microscopy images of NCAM (*A*), periostin (*B*), and nestin (*C*) staining in human MTJ. Muscle (m) and tendon (t) are seen on either side of the MTJ. Single grayscale images are displayed with a merged image to the *right*. NCAM is expressed in the muscle fiber cytoplasm at the fiber tips only, where the intensity of staining increases as the fibers approach the MTJ (collagen XXII). Periostin can be observed between the tendon and collagen XXII at the MTJ, as well in close association with collagen XXII. Nestin displays a similar staining pattern to NCAM, present in the muscle fiber cytoplasm as it approaches the MTJ. Scale bar = 50 μm. MTJ, myotendinous junction; NCAM, neural cell adhesion molecule.

Periostin (POSTN) was found to stain human MTJ tissue distal to collagen XXII in the ECM of the inserting fiber. Periostin is a matricellular protein, known to be involved in ECM remodeling and it increases in concentration following injury, suggesting a potential role for this protein in regeneration and repair of ECM (46, 47). Its presence at the MTJ has been documented recently by proteomics and immunohistochemistry (IHC) in mice (15), but, to our knowledge, the current study is the first to show periostin in human MTJ tissue. We suggest that it is present at the MTJ to support ECM plasticity and readiness for repair, whenever necessary. As an indication of ECM plasticity at the MTJ, we further identified FGF7 and PDGFD to be higher expressed at the MTJ than the muscle and tendon. Both of these growth factors are involved in the regulation of fibroblast activity and fibrosis. Although PDGFD is involved in progression of cancers and remodeling of the myocardium following infarction (48, 49), less is known about FGF7, especially in relation to skeletal

Table 3. *GAGE enrichment analysis for KEGG pathways on MTJ measured vs. expected mix values*

GAGE Analysis: Observed vs. Expected				
Direction	Mix	Statistic	Genes	Adj.Pval
Down	Parkinson disease (path:ecb05012)	−3.7623	82	3.7e-02
	Ribosome (path:ecb03010)	−3.5452	90	3.8e-02
	Thermogenesis (path:ecb04714)	−3.2323	137	5.0e-02
	Huntington disease (path:ecb05016)	−3.2293	109	5.0e-02

Only pathways identified as downregulated in MTJ were found. GAGE, Generally Applicable Gene Set Enrichment.

Table 4. *Overview of the two approaches (comparisons of two tissues, and observed vs. expected mix) to identify genes significantly enriched at the MTJ from the horse RNAseq data.*

				Pairwise Comparisons of Tissues										MTJ Observed vs. Expected Mix			
				Tendon vs. Muscle			MTJ vs. Muscle			MTJ vs. Tendon							
GeneID	Gene	Description	Grouping	Fold Diff	*P* Value	FDR	Fold Diff	*P* Value	FDR	Fold Diff	*P* Value	FDR			Fold Diff	*P* Value	FDR	Previously reported at MTJ
100057678	*ACTC1*	Actin a cardiac muscle 1	cytoskeletal	0.4	0.0190	0.0333	1.1	0.0127	0.1031	11.1	0.0000	0.0000		$	5.0	0.0003	0.0585	
100072682	*ADAMTS8*	ADAM metallopeptidase with thrombospondin type 1 motif 8	integrin binding	4.2	0.0013	0.0028	17.9	0.0000	0.0000	3.1	0.0011	0.0028	#		4.0	0.0559		(25)
100061848	*ALCAM*	activated leukocyte cell adhesion molecule	adhesion	2.2	0.0001	0.0003	2.1	0.0001	0.0017	1.0	0.8689	0.9040		$	2.2	0.0044	0.0858	
100053339	*ALDH3B1*	aldehyde dehydrogenase 3 family member B1	metabolism	2.7	0.0000	0.0000	5.9	0.0000	0.0000	2.1	0.0005	0.0014	#	$	5.4	0.0000	0.0124	
100052606	*ANKS1B*	ankyrin repeat and sterile a motif domain containing 1B	ephrin receptor binding	1.7	0.1171	0.1707	5.1	0.0001	0.0015	2.5	0.0048	0.0104	#		2.2	0.0061		
102150106	*C2H4orf51*	chromosome 2 C4orf51 homolog	uncharacterized	1.0	0.8740	0.9056	3.1	0.0009	0.0150	3.9	0.0001	0.0004	#		1.7	0.0528		
100068401	*CALB2*	calbindin 2	calcium handling	1.1	0.7756	0.8275	2.6	0.0033	0.0411	2.7	0.0051	0.0112	#		2.3	0.0200		
100059622	*CASQ2*	calsequestrin 2	calcium handling	0.5	0.0318	0.0532	1.1	0.1824	0.4812	4.0	0.0005	0.0013		$	2.3	0.0002	0.0559	
100052471	*CCDC88A*	coiled-coil domain containing 88 A	microtubule, cytoskeletal	1.2	0.1536	0.2162	1.9	0.0000	0.0002	1.6	0.0018	0.0044		$	2.1	0.0003	0.0594	(26)
111772400	*CD52*	CD52 molecule	immune cells	0.7	0.0227	0.0392	2.2	0.0000	0.0002	3.6	0.0000	0.0000	#	$	2.9	0.0000	0.0013	
100050546	*CIDEA*	cell death-inducing DFFA like effector a	lipid regulation	2.6	0.0102	0.0187	9.5	0.0000	0.0000	2.7	0.0076	0.0159	#		7.8	0.0023		
100055462	*CNTNAP4*	contactin-associated protein family member 4	adhesion	1.6	0.0966	0.1435	4.1	0.0000	0.0001	2.4	0.0018	0.0044	#	$	4.9	0.0038	0.0840	
100069427	*COL22A1*	collagen type XXII a 1 chain	ECM	16.6	0.0000	0.0000	59.2	0.0000	0.0000	2.3	0.0162	0.0316	#	$	17.1	0.0002	0.0460	(15, 21,22, 24–27)
100067795	*CXADR* CXADR Ig-like cell adhesion molecule		adhesion	0.4	0.0053	0.0103	1.1	0.1699	0.4634	4.9	0.0000	0.0001		$	2.4	0.0006	0.0639	
100049011	*FEZ1*	fasciculation and elongation protein zeta 1	neural	1.9	0.0013	0.0028	2.4	0.0000	0.0001	1.3	0.1184	0.1818		$	2.6	0.0013	0.0681	
100033961	*FGF7*	fibroblast growth factor 7	tissue repair	6.0	0.0000	0.0000	9.4	0.0000	0.0000	1.5	0.0287	0.0528		$	5.7	0.0001	0.0293	(25, 27)
100062675	*FREM2*	FRAS1-related extracellular matrix 2	ECM	0.6	0.1212	0.1757	1.1	0.1050	0.3598	3.6	0.0015	0.0036		$	2.7	0.0029	0.0808	(25)
100067870	*GPNMB*	glycoprotein nmb	integrin binding	3.7	0.0000	0.0000	2.6	0.0000	0.0002	0.8	0.1768	0.2552		$	2.2	0.0009	0.0639	
100054036	*GPR149*	G protein-coupled receptor 149	neural	0.9	0.6363	0.7101	2.5	0.0033	0.0411	4.1	0.0002	0.0006	#		1.4	0.0252		
100051329	*GRIN2A*	glutamate ionotropic receptor NMDA type subunit 2 A	neural	1.5	0.2449	0.3230	3.6	0.0008	0.0129	2.2	0.0170	0.0330	#		2.4	0.0016		
100062868	*HHIP*	hedgehog interacting protein	tissue repair	1.7	0.1512	0.2133	14.4	0.0000	0.0000	6.7	0.0000	0.0000	#		5.8	0.0035		
100051119	*HNMT*	histamine N-methyltransferase	metabolism	4.5	0.0000	0.0000	3.0	0.0000	0.0000	0.7	0.0043	0.0095		$	2.1	0.0012	0.0681	
100058129	*IGSF1*	immunoglobulin superfamily member 1	inhibin signaling	1.6	0.1014	0.1500	5.0	0.0018	0.0256	1.5	0.1349	0.2032		$	10.2	0.0003	0.0575	
100058705	*KCNA2*	potassium voltage-gated channel subfamily A member 2	ion channel	1.4	0.2427	0.3206	5.2	0.0000	0.0002	3.2	0.0003	0.0008	#		4.7	0.0000		
100055369	*LCT*	Lactase	metabolism	23.8	0.0000	0.0000	68.7	0.0000	0.0000	1.9	0.0437	0.0764		$	15.1	0.0007	0.0639	
100629324	*LOC100629324*	uncharacterized LOC100629324	uncharacterized	0.9	0.7522	0.8079	1.9	0.0062	0.0642	2.7	0.0023	0.0053		$	3.3	0.0008	0.0639	
102147582	*LOC102147582*	uncharacterized LOC102147582	uncharacterized	4.1	0.0002	0.0004	11.4	0.0000	0.0000	2.2	0.0077	0.0162	#		5.9	0.0006		
102149019	*LOC102149019*	uncharacterized LOC102149019	uncharacterized	2.3	0.0026	0.0053	6.2	0.0000	0.0000	2.4	0.0009	0.0023	#	$	6.1	0.0006	0.0639	
106783412	*LOC106783412*	uncharacterized LOC106783412	uncharacterized	0.8	0.4365	0.5238	2.4	0.0013	0.0193	3.8	0.0000	0.0001	#		2.7	0.0119		
111775490	*LOC111775490*	uncharacterized LOC111775490	uncharacterized	4.1	0.0325	0.0543	41.2	0.0000	0.0010	2.6	0.0156	0.0305	#		1.9	0.0454		
100055858	*LYVE1*	lymphatic vessel endothelial hyaluronan receptor 1	adhesion	4.5	0.0000	0.0000	2.9	0.0000	0.0000	0.7	0.0852	0.1365		$	2.1	0.0053	0.0895	
100070789	*MAP1A*	microtubule-associated protein 1 A	microtubule, cytoskeletal	0.6	0.0607	0.0950	1.4	0.0200	0.1367	2.8	0.0000	0.0001		$	2.3	0.0011	0.0681	
100070127	*ME1*	malic enzyme 1	metabolism	1.1	0.6131	0.6896	2.0	0.0000	0.0000	1.9	0.0000	0.0000		$	2.2	0.0000	0.0219	

Continued

AJP-Cell Physiol doi:10.1152/ajpcell.00218.2021 www.ajpcell.org

Table 4.— *Continued*

				Pairwise Comparisons of Tissues										MTJ Observed vs. Expected Mix			
				Tendon vs. Muscle			MTJ vs. Muscle			MTJ vs. Tendon							
GeneID	Gene	Description	Grouping	Fold Diff	*P* Value	FDR	Fold Diff	*P* Value	FDR	Fold Diff	*P* Value	FDR		Fold Diff	*P* Value	FDR	Previously reported at MTJ
100033948	*MMP2*	matrix metallopeptidase 2	ECM	3.5	0.0000	0.0000	3.5	0.0000	0.0000	1.0	0.9761	0.9841	$	2.8	0.0004	0.0594	(26)
100068954	*MNS1*	meiosis-specific nuclear structural 1	meiosis, cilium	1.6	0.0268	0.0455	3.7	0.0000	0.0000	2.3	0.0001	0.0002	# $	3.9	0.0009	0.0639	
100073103	*MOXD1*	monooxygenase DBH like 1	metabolism	2.5	0.0193	0.0339	7.3	0.0000	0.0003	2.2	0.0171	0.0331	#	2.9	0.0154		
100630214	*MTURN*	maturin, neural progenitor differentiation regulator homolog	tissue repair	4.2	0.0000	0.0000	3.5	0.0000	0.0000	0.8	0.0935	0.1481	$	2.5	0.0001	0.0293	
100050448	*NAV3*	neuron navigator 3	microtubule, cytoskeletal	6.7	0.0000	0.0000	5.9	0.0000	0.0000	0.9	0.4602	0.5592	$	3.4	0.0001	0.0417	(24–27)
100062164	*NCAM1*	neural cell adhesion molecule 1	tissue repair	1.3	0.4603	0.5475	3.9	0.0010	0.0162	2.7	0.0109	0.0221	# $	6.7	0.0010	0.0639	(24, 31)
100054129	*NEFM*	neurofilament medium	microtubule, cytoskeletal	53.7	0.0000	0.0000	122.3	0.0000	0.0000	1.3	0.3299	0.4279	$	16.3	0.0008	0.0639	
100064419	*NES*	Nestin	cytoskeletal	1.0	0.9057	0.9306	1.6	0.0099	0.0870	2.0	0.0070	0.0149	$	2.5	0.0060	0.0924	
100059841	*OSTN*	Osteocrin	tissue repair	2.3	0.0370	0.0609	21.5	0.0000	0.0000	3.5	0.0034	0.0076	# $	16.4	0.0037	0.0837	(25, 27)
100061488	*PDGFD*	Platelet-derived growth factor D	tissue repair	4.3	0.0000	0.0000	3.1	0.0000	0.0000	0.7	0.0252	0.0469	$	2.3	0.0005	0.0632	
102148273	*PDPN*	podoplanin	adhesion	3.8	0.0000	0.0000	2.7	0.0000	0.0002	0.8	0.2124	0.2979	$	2.2	0.0056	0.0910	
100066733	*PIP4K2A*	phosphatidylinositol-5-phosphate 4-kinase type 2 a	metabolism	0.9	0.6300	0.7049	1.7	0.0023	0.0302	2.1	0.0004	0.0011	$	2.2	0.0026	0.0805	(24,25)
100062608	*POSTN*	Periostin	ECM	1.2	0.5328	0.6161	5.1	0.0002	0.0048	3.7	0.0021	0.0049	# $	8.1	0.0016	0.0719	(15, 26)
100034016	*PRG4*	proteoglycan 4	ECM	5.3	0.0000	0.0000	3.8	0.0000	0.0000	0.7	0.0619	0.1037	$	2.4	0.0046	0.0872	
100063534	*PRUNE2*	prune homolog 2 with BCH domain	neural	1.6	0.0020	0.0042	2.1	0.0000	0.0000	1.4	0.0183	0.0353	$	2.3	0.0030	0.0811	
100033979	*PTHLH*	parathyroid hormone like hormone	tissue repair	0.9	0.5131	0.5980	2.0	0.0001	0.0023	2.4	0.0000	0.0000	#	2.5	0.0003		
100049881	*RAG2*	recombination activating 2	immune cells	1.7	0.1872	0.2564	11.3	0.0001	0.0030	4.3	0.0015	0.0037	#	1.2	0.0380		
100067588	*RANBP3L*	RAN binding protein 3 like	BMP signaling	12.7	0.0000	0.0000	5.4	0.0000	0.0000	0.5	0.0000	0.0000	$	2.1	0.0058	0.0916	
100068747	*RBM11*	RNA binding motif protein 11	tissue repair	1.6	0.2699	0.3511	7.8	0.0007	0.0115	3.2	0.0084	0.0176	#	1.1	0.1870		
100051067	*RGS2*	regulator of G protein signaling 2	tissue growth	1.5	0.0113	0.0206	2.7	0.0000	0.0000	1.8	0.0004	0.0011	$	2.9	0.0009	0.0639	
100033887	*S100A6*	S100 calcium binding protein A6	calcium handling	8.9	0.0000	0.0000	4.6	0.0000	0.0000	0.5	0.0000	0.0001	$	2.2	0.0009	0.0639	
100050682	*SORBS2*	sorbin and SH3 domain containing 2	cytoskeletal	4.0	0.0000	0.0000	6.9	0.0000	0.0000	1.6	0.0159	0.0311	$	5.2	0.0010	0.0639	(24–27)
100053029	*SPP1*	secreted phosphoprotein 1	integrin binding	31.3	0.0000	0.0000	24.5	0.0000	0.0000	0.8	0.2696	0.3627	$	4.3	0.0040	0.0840	
100059332	*TCEAL7*	transcription elongation factor A like 7	other	0.8	0.4201	0.5079	2.7	0.0006	0.0101	4.1	0.0000	0.0000	#	2.3	0.0157		
100065098	*TMEM108*	transmembrane protein 108	microtubule, cytoskeletal	1.2	0.4261	0.5136	3.8	0.0000	0.0002	3.1	0.0001	0.0002	#	4.9	0.0011		
100146229	*TRIM16*	tripartite motif containing 16	autophagy	1.7	0.0005	0.0011	2.4	0.0000	0.0000	1.4	0.0218	0.0412	$	2.5	0.0009	0.0639	
100052052	*TTL*	tubulin tyrosine ligase	microtubule, cytoskeletal	1.7	0.0015	0.0031	2.7	0.0000	0.0000	1.6	0.0021	0.0050	$	2.8	0.0010	0.0639	
100033838	*UCHL1*	ubiquitin C-terminal hydrolase L1	neural	0.4	0.0000	0.0000	1.2	0.0514	0.2394	4.7	0.0000	0.0000	$	2.1	0.0028	0.0808	

The fold differences (diff), *P* values, and false discovery rate (FDR) are displayed. #Genes that were significantly greater (log2FC > 1, FDR < 0.05) in the MTJ vs. both the muscle and tendon fractions; $genes that were observed to be significantly greater (log2FC > 1, FDR < 0.1) than expected (based on relative contribution from tendon and muscle tissue). Significant FDR values alone (regardless of fold difference) are displayed in bold font. Source data: Supplemental Fig. S3 (24); Supplemental Fig. S1 (25); Supplemental Fig. S3 (26); Supplemental Fig. S2 (27); Table 1. (15). BMP, bone morphogenetic protein; ECM, extracellular matrix; MTJ, myotendinous junction.

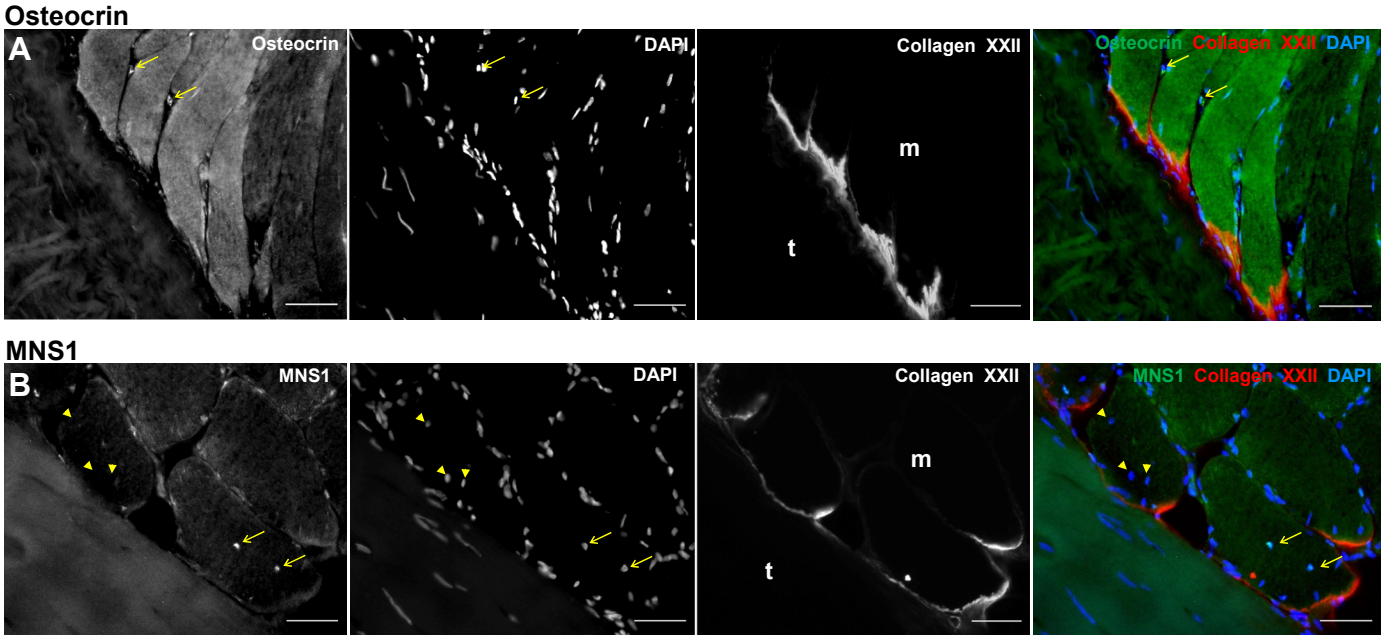

Figure 7. Microscopy images of osteocrin (*A*) and MNS1 (*B*) staining in human MTJ. Muscle (m) and tendon (t) are seen on either side of the MTJ. Single grayscale images are displayed with a merged image to the *right*. Osteocrin labeled the membrane of some mononuclear cells (arrows point to examples) in addition to some immunoreactivity for the muscle fiber cytoplasm. MNS1 was observed to stain some (arrows indicate examples), but not all (see arrowheads for examples) myonuclei. Scale bar = 50 $_m$m. MNS1, meiosis-specific nuclear structural protein 1; MTJ, myotendinous junction.

muscle, but an association with FGF7 and the MTJ has been found by snRNAseq in mice (25, 27), in line with our data.

In addition to periostin and other known components of the MTJ (COL22A1, NCAM1, and NES), we identified three previously undescribed proteins of the human MTJ: lactase, MNS1, and osteocrin. Osteocrin (also known as musclin) was observed to stain the muscle fiber cytoplasm in addition to what appeared to be mononuclear cells between muscle fibers and at the muscle-tendon interface. Osteocrin is a member of the natriuretic peptide family and is known to regulate bone formation and dendritic branching as well as

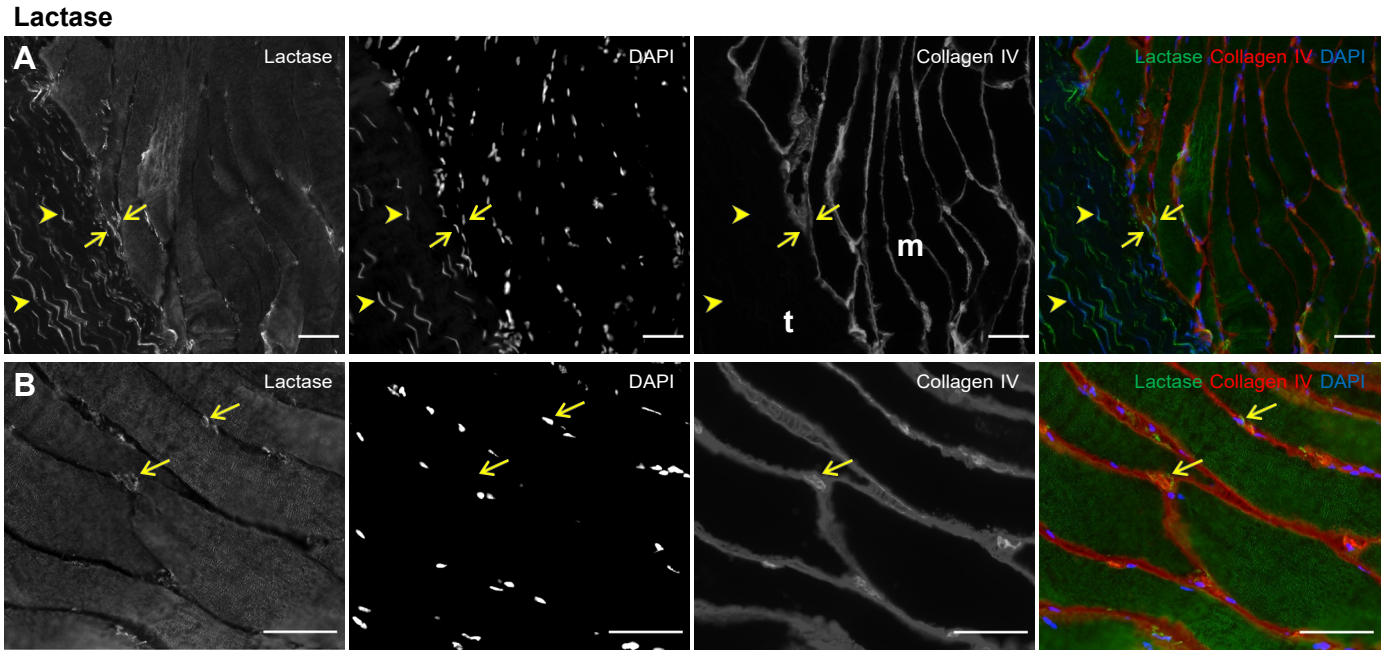

Figure 8. Microscopy images of lactase (*A*, *B*) staining in human MTJ. Muscle (m) and tendon (t) are seen on either side of the MTJ in *A*, whereas the images in *B* are captured further away from the MTJ. Single grayscale images are displayed with a merged image to the *right*. Lactase was observed in the membrane of mononuclear cells near the MTJ (examples indicated by arrows), in the tendon tissue (arrowheads point to examples), as well as between the muscle fibers (*B*), some of which were associated with capillaries (collagen IV). Scale bar = 50 $_m$m. MTJ, myotendinous junction.

myogenesis and T cell activity (50). Osteocrin is produced by skeletal muscle (51), is responsive to exercise (52), and overexpression of osteocrin has been reported to prevent muscle atrophy in cachexic mice (53). Furthermore, osteocrin has been linked to browning of adipose tissue (54), which is potentially related to our recent observations of adipocytes at the muscle-tendon interface in human hamstring tissue (55). Together these studies suggest a role for osteocrin specifically in the domain of skeletal muscle fibers close to the MTJ.

Lactase (LCT) was expressed to a higher degree in MTJ than muscle and tendon and has not been previously described at the MTJ, with its presence close to the MTJ confirmed by immunofluorescence. Small cells expressing lactase were found between muscle fibers and in the tendon tissue adjacent to the inserting muscle fibers. Lactase is produced by the microvilli-coated epithelial cells of the intestines, where it splits lactose in the process of digestion (56), and it has not yet been described in skeletal muscle-tendon tissue, where it possibly plays a role in metabolism. Similarly, MNS1, another MTJ component identified in the current study, has received very little attention and is not known to be associated with the muscle-tendon complex. It is related to nuclear morphology during meiosis (in spermatogenesis) (57), which may be a relevant function in relation to our observation of MNS1 being present in myonuclei near the MTJ. Myonuclei in this region are more often positioned centrally in the fiber than in the midregion (30), and it is possible they are subjected to different patterns of mechanical strain as force is transferred from the muscle to the tendon. With regard to alternative roles for MNS1, loss-of-function mutations in humans have been linked to left-right patterning defects and male infertility (58). Studies in MNS1 knockout mice reveal its importance for motile ciliary functions and microtubule organization (59), which are particularly important during development and potentially also at the MTJ.

Immune cell genes were also strongly represented in the RNAseq data, e.g., CD52, RAG2, ANKS1B, CXADR, and ALCAM. Although we have documented the presence of CD68^{+} macrophages at the human MTJ, and an increase in cell number after 4 wk of heavy resistance training (22), other immune cell types have so far not been shown to be implicated in the MTJ. Thus, the expression of genes related to B cell and T cell activity opens up possible new roles for additional immune cells in remodeling and injury-repair of the MTJ.

The ECM-related genes initially selected for RT-PCR (COMP, COL1A, COL3A, COL22A1) were found to be expressed at higher levels in the MTJ than in muscle, as expected. Tenomodulin (TNMD), which is normally considered a phenotypical indicator of a tendon (60–62), was also expressed to a greater degree at the MTJ when compared with muscle, but surprisingly muscle and tendon levels were similar. Tenomodulin is believed to be expressed by tenocytes and involved in the proliferation of these cells, primarily during growth and development but it is also important for tendon healing and remodeling following injury and exercise (63–66). Scleraxis, another widely used marker of tendons, did not display high expression levels in the tendon, and in fact both MTJ and muscle demonstrated higher mRNA levels for scleraxis than the tendon. This is likely to be related to scleraxis as a marker for developing or growing tendons (60–62), and it is probably downregulated in the adult tendon where the protein turnover is low (6). ITGA7 demonstrated a pattern similar to scleraxis and is believed to be important for strength of the adhesion between actin filaments and laminin in the basal lamina surrounding the muscle fibers (67–69). The presence of tenomodulin and scleraxis at the MTJ has not previously been reported, but given the high plasticity of the MTJ and the susceptibility to strain injuries in this region, it is possible that they are present to aid in remodeling of the connective tissue and secure optimal repair following injury (66). Interestingly, a matricellular regulator of ECM, fat metabolism, and angiogenesis, Angiopoietin-like-4 (ANGPTL4) was found to be expressed at higher levels in tendon tissue versus both MTJ and muscle, in line with earlier findings of an important role for ANGPTL4 in angiogenesis in stretched tendon (70).

Only 13 of our 61 MTJ genes identified by RNAseq have been reported in the MTJ gene data sets of the recent snRNAseq studies in mice (24–27). Of the handful of genes actually shown to be expressed at the MTJ (by FISH), *Tigd4* (26), and *Adamts20* (27) were not detected in our data set. *Ebf1* (26) was detected, however, but not significantly enriched at the MTJ. The reason for this rather low concordance is unclear, indeed it is challenging to even compare these two fundamentally different approaches. Potential differences in the MTJ of mice and larger mammals may exist, or it is possible that the nature of snRNAseq measuring largely only pre-mRNA, compared with the more mature mRNA detected by RNAseq, is behind this discrepancy. It is also worth noting that snRNAseq is carried out on nuclei collected from whole muscle, rather than the tissue-specific regions prepared in the current study and MTJ nuclei tend to be classified based on the expression of COL22A1 rather than their location in the tissue. Furthermore, in some cases, only the myonuclei were analyzed by snRNAseq (26), which will generate different sets of gene clusters than when nuclei from nonmuscle cells are included, illustrating the importance of tissue context in interpreting cluster-based data. Potentially, even more difficult to reconcile are differences in our MTJ data and data acquired by proteomics (15, 71) and earlier studies identifying proteins common to the MTJ and costameres, such as talin and vinculin (72, 73). For example, COL5A3 was recently reported to be expressed at the MTJ of mouse soleus muscle according to proteomics analysis of one sample of pooled muscles, although immunofluorescence could not confirm specificity for the MTJ (15). However, we did not detect COL5A3 in our data set. For the costameric proteins, talin and vinculin (72, 73), it is possible the mRNA for these proteins was expressed in the muscle fraction to a degree that a relative significant enrichment could not be detected in the MTJ fraction. An interesting issue is whether mRNAs are produced ubiquitously within a muscle fiber and transported to the MTJ or are produced exclusively by nuclei locally at the MTJ. It is possible that if we had included more targets in our PCR analysis, such as talin and vinculin, we might have observed differences between the tissue fractions. In general, it is important to highlight that our RNAseq data represent five biological replicates and a conservative statistical analysis was applied. In the first approach, the 43 genes identified at the MTJ only represent genes demonstrating at

least twofold greater levels than both the muscle and tendon tissue fractions, according to FDR-adjusted *P* values. Further work, at the gene expression and protein levels, is clearly required to reconcile the differences observed with these various methodological approaches.

In conclusion, through an unbiased approach, we identified 48 novel MTJ genes using RNA sequencing. As well as genes involved in ECM, adhesion, tissue regeneration, and development, neural and immune cell genes were strongly represented. In addition, we demonstrate for the first time, to our knowledge, the presence of periostin, osteocrin, lactase, and MNS1 in the human MTJ by immunofluorescence. Future work could focus on obtaining cleaner MTJ tissue since our MTJ fraction represents tendon on one side of the MTJ and muscle on the other side enriched in myofiber tips as they terminate at the muscle-tendon interface. Furthermore, many mononuclear cells in this region remain to be identified. A limitation of our study is that the physiological function of the mRNAs identified to be enriched at the MTJ was not determined, either in the context of maintenance or repair of this complex tissue interface. Indeed, it is possible that different genes would be identified during conditions of loading or repair, in contrast tox the maintenance state studied in the present study. Given that, much of our understanding of the development, composition, and repair of the MTJ is based on elegant studies performed in animals, as reviewed elsewhere (14, 16, 74), there is a need for the development of suitable standardized models for studying repair of the human MTJ to address the clinical problem of (recurring) muscle strain injury in athletes.

SUPPLEMENTAL DATA

Supplemental Figs. S1–S3, S4 (*A* and *B*), S5, and S6: https://doi.org/10.6084/m9.figshare.14748216.v1.

ACKNOWLEDGMENTS

Anja Jokipii-Utzon is warmly acknowledged for excellent technical work. We gratefully acknowledge the Novo Nordisk Foundation (No. 0064829), Bispebjerg and Frederiksberg Hospital, Aase and Einar Danielsen's Foundation, and International Olympic Committee for providing financial support to this study.

GRANTS

This study was supported by Novo Nordisk Foundation Grant 0064829 (to A.L.M.), Bispebjerg and Frederiksberg Hospital grant (to A.L.M.), Aase and Einar Danielsen's Foundation grant (to M.R.K.), and International Olympic Committee grant (to M.R.K. and M.K.). H. Carstensen was generously funded by The Independent Research Fund Denmark [Grant No. Danmarks Frie Forskningsfond (DFF)-7017-00050] and M. Koch by the German Research Foundation Deutsche Forschungsgemeinschaft Research Unit FOR 2722.

DISCLOSURES

No conflicts of interest, financial or otherwise, are declared by the authors.

AUTHOR CONTRIBUTIONS

J.R.J., P.S., R.B.S., R.B., H.C., M.R.K., M.K., and A.L.M. conceived and designed research; J.R.J., R.B.S., R.B., and H.C. performed experiments; J.R.J. and P.S. analyzed data; J.R.J., P.S., M.K., M.R.K., M.K., and A.L.M. interpreted results of experiments; J.R.J., P.S., and A.L.M. prepared figures; J.R.J., P.S., M.K., and A.L.M. drafted manuscript; J.R.J., P.S., R.B.S., R.B., H.C., M.K., M.R.K., M.K., and A.L.M. edited and revised manuscript; J.R.J., P.S., R.B.S., R.B., H.C., M.K., M.R.K., M.K., and A.L.M. approved final version of manuscript.

REFERENCES

1. Baker BA. An old problem: aging and skeletal-muscle-strain injury. *J Sport Rehabil* 26: 180–188, 2017. doi:10.1123/jsr.2016-0075.
2. Hagglund M, Walden M, Ekstrand J. Previous injury as a risk factor for injury in elite football: a prospective study over two consecutive seasons. *Br J Sports Med* 40: 767–772, 2006. doi:10.1136/bjsm.2006.026609.
3. Reurink G, Goudswaard GJ, Tol JL, Almusa E, Moen MH, Weir A, Verhaar JA, Hamilton B, Maas M. MRI observations at return to play of clinically recovered hamstring injuries. *Br J Sports Med* 48: 1370–1376, 2014. doi:10.1136/bjsports-2013-092450.
4. Silder A, Sherry MA, Sanfilippo J, Tuite MJ, Hetzel SJ, Heiderscheit BC. Clinical and morphological changes following 2 rehabilitation programs for acute hamstring strain injuries: a randomized clinical trial. *J Orthop Sports Phys Ther* 43: 284–299, 2013. doi:10.2519/jospt.2013.4452.
5. Wangensteen A, Tol JL, Witvrouw E, Van Linschoten R, Almusa E, Hamilton B, Bahr R. Hamstring reinjuries occur at the same location and early after return to sport: a descriptive study of MRI-confirmed reinjuries. *Am J Sports Med* 44: 2112–2121, 2016. doi:10.1177/0363546516646086.
6. Heinemeier KM, Schjerling P, Heinemeier J, Magnusson SP, Kjaer M. Lack of tissue renewal in human adult Achilles tendon is revealed by nuclear bomb (14)C. *FASEB J* 27: 2074–2079, 2013. doi:10.1096/fj.12-225599.
7. Heinemeier KM, Schjerling P, Heinemeier J, Moller MB, Krogsgaard MR, Grum-Schwensen T, Petersen MM, Kjaer M. Radiocarbon dating reveals minimal collagen turnover in both healthy and osteoarthritic human cartilage. *Sci Transl Med* 8: 346ra390, 2016. doi:10.1126/scitranslmed.aad8335.
8. Karlsen A, Soendenbroe C, Malmgaard-Clausen NM, Wagener F, Moeller CE, Senhaji Z, Damberg K, Andersen JL, Schjerling P, Kjaer M, Mackey AL. Preserved capacity for satellite cell proliferation, regeneration, and hypertrophy in the skeletal muscle of healthy elderly men. *FASEB J* 34: 6418–6436, 2020. doi:10.1096/fj.202000196R.
9. Mackey AL, Brandstetter S, Schjerling P, Bojsen-Moller J, Qvortrup K, Pedersen MM, Doessing S, Kjaer M, Magnusson SP, Langberg H. Sequenced response of extracellular matrix deadhesion and fibrotic regulators after muscle damage is involved in protection against future injury in human skeletal muscle. *FASEB J* 25: 1943–1959, 2011. doi:10.1096/fj.10-176487.
10. Mackey AL, Kjaer M. The breaking and making of healthy adult human skeletal muscle in vivo. *Skelet Muscle* 7: 24, 2017. doi:10.1186/s13395-017-0142-x.
11. Mackey AL, Magnan M, Chazaud B, Kjaer M. Human skeletal muscle fibroblasts stimulate in vitro myogenesis and in vivo muscle regeneration. *J Physiol* 595: 5115–5127, 2017. doi:10.1113/JP273997.
12. Mackey AL, Rasmussen LK, Kadi F, Schjerling P, Helmark IC, Ponsot E, Aagaard P, Durigan JL, Kjaer M. Activation of satellite cells and the regeneration of human skeletal muscle are expedited by ingestion of nonsteroidal anti-inflammatory medication. *FASEB J* 30: 2266–2281, 2016. doi:10.1096/fj.201500198R.
13. Charvet B, Guiraud A, Malbouyres M, Zwolanek D, Guillon E, Bretaud S, Monnot C, Schulze J, Bader HL, Allard B, Koch M, Ruggiero F. Knockdown of col22a1 gene in zebrafish induces a muscular dystrophy by disruption of the myotendinous junction. *Development* 140: 4602–4613, 2013. doi:10.1242/dev.096024.
14. Charvet B, Ruggiero F, Le Guellec D. The development of the myotendinous junction. A review. *Muscles Ligaments Tendons J* 2: 53–63, 2012.
15. Jacobson KR, Lipp S, Acuna A, Leng Y, Bu Y, Calve S. Comparative analysis of the extracellular matrix proteome across the

myotendinous junction. *J Proteome Res* 19: 3955–3967, 2020. doi:10.1021/acs.jproteome.0c00248.
16. Jakobsen JR, Krogsgaard MR. The myotendinous junction- a vulnerable companion in sports. A narrative review. *Front Physiol* 12: 635561, 2021. doi:10.3389/fphys.2021.635561.
17. Narayanan N, Calve S. Extracellular matrix at the muscle - tendon interface: functional roles, techniques to explore and implications for regenerative medicine. *Connect Tissue Res* 62: 53–71, 2020. doi:10.1080/03008207.2020.1814263.
18. Scott RW, Arostegui M, Schweitzer R, Rossi FMV, Underhill TM. Hic1 defines quiescent mesenchymal progenitor subpopulations with distinct functions and fates in skeletal muscle regeneration. *Cell Stem Cell* 25: 797–813.e9, 2019. doi:10.1016/j.stem.2019.11.004.
19. Tidball JG. Force transmission across muscle cell membranes. *J Biomech* 24 Suppl 1: 43–52, 1991. doi:10.1016/0021-9290(91)90376-X.
20. Tidball JG, Lin C. Structural changes at the myogenic cell surface during the formation of myotendinous junctions. *Cell Tissue Res* 257: 77–84, 1989. doi:10.1007/BF00221636.
21. Koch M, Schulze J, Hansen U, Ashwodt T, Keene DR, Brunken WJ, Burgeson RE, Bruckner P, Bruckner-Tuderman L. A novel marker of tissue junctions, collagen XXII. *J Biol Chem* 279: 22514–22521, 2004. doi:10.1074/jbc.M400536200.
22. Jakobsen JR, Mackey AL, Knudsen AB, Koch M, Kjaer M, Krogsgaard MR. Composition and adaptation of human myotendinous junction and neighboring muscle fibers to heavy resistance training. *Scand J Med Sci Sports* 27: 1547–1559, 2017. doi:10.1111/sms.12794.
23. Miyamoto-Mikami E, Kumagai H, Kikuchi N, Kamiya N, Miyamoto N, Fuku N. eQTL variants in COL22A1 are associated with muscle injury in athletes. *Physiol Genomics* 52: 588–589, 2020. doi:10.1152/physiolgenomics.00115.02020.
24. Chemello F, Wang Z, Li H, McAnally JR, Liu N, Bassel-Duby R, Olson EN. Degenerative and regenerative pathways underlying Duchenne muscular dystrophy revealed by single-nucleus RNA sequencing. *Proc Natl Acad Sci USA* 117: 29691–29701, 2020. doi:10.1073/pnas.2018391117.
25. Dos Santos M, Backer S, Saintpierre B, Izac B, Andrieu M, Letourneur F, Relaix F, Sotiropoulos A, Maire P. Single-nucleus RNA-seq and FISH identify coordinated transcriptional activity in mammalian myofibers. *Nat Commun* 11: 5102, 2020. doi:10.1038/s41467-020-18789-8.
26. Kim M, Franke V, Brandt B, Lowenstein ED, Schowel V, Spuler S, Akalin A, Birchmeier C. Single-nucleus transcriptomics reveals functional compartmentalization in syncytial skeletal muscle cells. *Nat Commun* 11: 6375, 2020. doi:10.1038/s41467-020-20064-9.
27. Petrany MJ, Swoboda CO, Sun C, Chetal K, Chen X, Weirauch MT, Salomonis N, Millay DP. Single-nucleus RNA-seq identifies transcriptional heterogeneity in multinucleated skeletal myofibers. *Nat Commun* 11: 6374, 2020. doi:10.1038/s41467-020-20063-w.
28. Patterson-Kane JC, Firth EC. The pathobiology of exercise-induced superficial digital flexor tendon injury in thoroughbred racehorses. *Vet J* 181: 79–89, 2009. doi:10.1016/j.tvjl.2008.02.009.
29. Ekstrand J, Hagglund M, Walden M. Epidemiology of muscle injuries in professional football (soccer). *Am J Sports Med* 39: 1226–1232, 2011. doi:10.1177/0363546510395879.
30. Jakobsen JR, Jakobsen NR, Mackey AL, Koch M, Kjaer M, Krogsgaard MR. Remodeling of muscle fibers approaching the human myotendinous junction. *Scand J Med Sci Sports* 28: 1859–1865, 2018. doi:10.1111/sms.13196.
31. R Core Team. R: A language and environment for statistical computing. R Foundation for Statistical Computing, Vienna, Austria. 2020. https://www.R-project.org.
32. van der Maaten LJP, Hinton G. Visualizing high-dimensional data using t-SNE. *J Mach Learn Res* 9: 2579–2605, 2008.
33. Liao Y, Smyth GK, Shi W. The R package Rsubread is easier, faster, cheaper and better for alignment and quantification of RNA sequencing reads. *Nucleic Acids Res* 47: e47, 2019. doi:10.1093/nar/gkz114.
34. Love MI, Huber W, Anders S. Moderated estimation of fold change and dispersion for RNA-seq data with DESeq2. *Genome Biol* 15: 550, 2014. doi:10.1186/s13059-014-0550-8.
35. Luo W, Friedman MS, Shedden K, Hankenson KD, Woolf PJ. GAGE: generally applicable gene set enrichment for pathway analysis. *BMC Bioinformatics* 10: 161, 2009. doi:10.1186/1471-2105-10-161.
36. Korotkevich G, Sukhov V, Sergushichev A. Fast gene set enrichment analysis (Preprint). *bioRxiv*, 2019. doi:10.1101/060012.
37. Schubert W, Zimmermann K, Cramer M, Starzinski-Powitz A. Lymphocyte antigen Leu-19 as a molecular marker of regeneration in human skeletal muscle. *Proc Natl Acad Sci USA* 86: 307–311, 1989. doi:10.1073/pnas.86.1.307.
38. Soendenbroe C, Heisterberg MF, Schjerling P, Karlsen A, Kjaer M, Andersen JL, Mackey AL. Molecular indicators of denervation in aging human skeletal muscle. *Muscle Nerve* 60: 453–463, 2019. doi:10.1002/mus.26638.
39. Carlsson L, Li Z, Paulin D, Thornell LE. Nestin is expressed during development and in myotendinous and neuromuscular junctions in wild type and desmin knock-out mice. *Exp Cell Res* 251: 213–223, 1999. doi:10.1006/excr.1999.4569.
40. Vaittinen S, Lukka R, Sahlgren C, Rantanen J, Hurme T, Lendahl U, Eriksson JE, Kalimo H. Specific and innervation-regulated expression of the intermediate filament protein nestin at neuromuscular and myotendinous junctions in skeletal muscle. *Am J Pathol* 154: 591–600, 1999. doi:10.1016/S0002-9440(10)65304-7.
41. Lubinska L, Zelena J. Acetylcholinesterase at muscle-tendon junctions during postnatal development in rats. *J Anat* 101: 295–308, 1967.
42. Miledi R, Zelena J. Sensitivity to acetylcholine in rat slow muscle. *Nature* 210: 855–856, 1966. doi:10.1038/210855a0.
43. Mos W, Maslam S, van Raamsdonk W, Kilarski W, de Jager S. Acetylcholinesterase and acetylcholine receptor histochemistry on end plate regions, myotendinous junctions, and sarcolemma in the axial musculature of three teleost fish species. *Acta Histochem* 72: 39–53, 1983. doi:10.1016/S0065-1281(83)80007-5.
44. Jozsa L, Balint J, Kannus P, Jarvinen M, Lehto M. Mechanoreceptors in human myotendinous junction. *Muscle Nerve* 16: 453–457, 1993. doi:10.1002/mus.880160503.
45. Nakamoto T, Matsukawa K. Muscle mechanosensitive receptors close to the myotendinous junction of the Achilles tendon elicit a pressor reflex. *J Appl Physiol (1985)* 102: 2112–2120, 2007. doi:10.1152/japplphysiol.01344.2006.
46. Latroche C, Weiss-Gayet M, Muller L, Gitiaux C, Leblanc P, Liot S, Ben-Larbi S, Abou-Khalil R, Verger N, Bardot P, Magnan M, Chretien F, Mounier R, Germain S, Chazaud B. Coupling between myogenesis and angiogenesis during skeletal muscle regeneration is stimulated by restorative macrophages. *Stem Cell Reports* 9: 2018–2033, 2017. doi:10.1016/j.stemcr.2017.10.027.
47. Ozdemir C, Akpulat U, Sharafi P, Yıldız Y, Onba.,sılar I, Kocaefe C. Periostin is temporally expressed as an extracellular matrix component in skeletal muscle regeneration and differentiation. *Gene* 553: 130–139, 2014. doi:10.1016/j.gene.2014.10.014.
48. Zhao T, Zhao W, Chen Y, Li VS, Meng W, Sun Y. Platelet-derived growth factor-D promotes fibrogenesis of cardiac fibroblasts. *Am J Physiol Heart Circ Physiol* 304: H1719–H1726, 2013. doi:10.1152/ajpheart.00130.2013.
49. Zhao W, Zhao T, Huang V, Chen Y, Ahokas RA, Sun Y. Platelet-derived growth factor involvement in myocardial remodeling following infarction. *J Mol Cell Cardiol* 51: 830–838, 2011. doi:10.1016/j.yjmcc.2011.06.023.
50. Moffatt P, Thomas GP. Osteocrin–beyond just another bone protein? *Cell Mol Life Sci* 66: 1135–1139, 2009. doi:10.1007/s00018-009-8716-3.
51. Nishizawa H, Matsuda M, Yamada Y, Kawai K, Suzuki E, Makishima M, Kitamura T, Shimomura I. Musclin, a novel skeletal muscle-derived secretory factor. *J Biol Chem* 279: 19391–19395, 2004. doi:10.1074/jbc.C400066200.
52. Subbotina E, Sierra A, Zhu Z, Gao Z, Koganti SR, Reyes S, Stepniak E, Walsh SA, Acevedo MR, Perez-Terzic CM, Hodgson-Zingman DM, Zingman LV. Musclin is an activity-stimulated myokine that enhances physical endurance. *Proc Natl Acad Sci USA* 112: 16042–16047, 2015. doi:10.1073/pnas.1514250112.
53. Re Cecconi AD, Forti M, Chiappa M, Zhu Z, Zingman LV, Cervo L, Beltrame L, Marchini S, Piccirillo R. Musclin, a myokine induced by aerobic exercise, retards muscle atrophy during cancer cachexia in mice. *Cancers (Basel)* 11: 1541, 2019. doi:10.3390/cancers11101541.

54. Jeremic N, Chaturvedi P, Tyagi SC. Browning of white fat: novel insight into factors, mechanisms, and therapeutics. *J Cell Physiol* 232: 61–68, 2017. doi:10.1002/jcp.25450.
55. Jakobsen JR, Jakobsen NR, Mackey AL, Knudsen AB, Hannibal J, Koch M, Kjaer M, Krogsgaard M. Adipocytes are present at human and murine myotendinous junctions. *Transl Sports Med* 4: 223–230, 2021. doi:10.1002/tsm2.212.
56. Sahi T. Hypolactasia and lactase persistence. Historical review and the terminology. *Scand J Gastroenterol Suppl* 202: 1–6, 1994. doi:10.3109/00365529409091739.
57. Furukawa K, Inagaki H, Naruge T, Tabata S, Tomida T, Yamaguchi A, Yoshikuni M, Nagahama Y, Hotta Y. cDNA cloning and functional characterization of a meiosis-specific protein (MNS1) with apparent nuclear association. *Chromosome Res* 2: 99–113, 1994. doi:10.1007/BF01553489.
58. Ta-Shma A, Hjeij R, Perles Z, Dougherty GW, Abu Zahira I, Letteboer SJF, Antony D, Darwish A, Mans DA, Spittler S, Edelbusch C, Cindrić S, Nöthe-Menchen T, Olbrich H, Stuhlmann F, Aprea I, Pennekamp P, Loges NT, Breuer O, Shaag A, Rein AJJT, Gulec EY, Gezdirici A, Abitbul R, Elias N, Amirav I, Schmidts M, Roepman R, Elpeleg O, Omran H. Homozygous loss-of-function mutations in MNS1 cause laterality defects and likely male infertility. *PLoS Genet* 14: e1007602, 2018. doi:10.1371/journal.pgen.1007602.
59. Zhou J, Yang F, Leu NA, Wang PJ. MNS1 is essential for spermiogenesis and motile ciliary functions in mice. *PLoS Genet* 8: e1002516, 2012. doi:10.1371/journal.pgen.1002516.
60. Jo CH, Lim HJ, Yoon KS. Characterization of tendon-specific markers in various human tissues, tenocytes and mesenchymal stem cells. *Tissue Eng Regen Med* 16: 151–159, 2019. doi:10.1007/s13770-019-00182-2.
61. Shukunami C, Takimoto A, Nishizaki Y, Yoshimoto Y, Tanaka S, Miura S, Watanabe H, Sakuma T, Yamamoto T, Kondoh G, Hiraki Y. Scleraxis is a transcriptional activator that regulates the expression of Tenomodulin, a marker of mature tenocytes and ligamentocytes. *Sci Rep* 8: 3155, 2018. doi:10.1038/s41598-018-21194-3.
62. Shukunami C, Takimoto A, Oro M, Hiraki Y. Scleraxis positively regulates the expression of tenomodulin, a differentiation marker of tenocytes. *Dev Biol* 298: 234–247, 2006. doi:10.1016/j.ydbio.2006.06.036.
63. Dex S, Alberton P, Willkomm L, Sollradl T, Bago S, Milz S, Shakibaei M, Ignatius A, Bloch W, Clausen-Schaumann H, Shukunami C, Schieker M, Docheva D. Tenomodulin is required for tendon endurance running and collagen I fibril adaptation to mechanical load. *EBioMedicine* 20: 240–254, 2017. doi:10.1016/j.ebiom.2017.05.003.
64. Dex S, Lin D, Shukunami C, Docheva D. Tenogenic modulating insider factor: systematic assessment on the functions of tenomodulin gene. *Gene* 587: 1–17, 2016. doi:10.1016/j.gene.2016.04.051.
65. Docheva D, Hunziker EB, Fassler R, Brandau O. Tenomodulin is necessary for tenocyte proliferation and tendon maturation. *Mol Cell Biol* 25: 699–705, 2005. doi:10.1128/MCB.25.2.699-705.2005.
66. Lin D, Alberton P, Caceres MD, Volkmer E, Schieker M, Docheva D. Tenomodulin is essential for prevention of adipocyte accumulation and fibrovascular scar formation during early tendon healing. *Cell Death Dis* 8: e3116, 2017. doi:10.1038/cddis.2017.510.
67. Burkin DJ, Wallace GQ, Nicol KJ, Kaufman DJ, Kaufman SJ. Enhanced expression of the alpha 7 beta 1 integrin reduces muscular dystrophy and restores viability in dystrophic mice. *J Cell Biol* 152: 1207–1218, 2001. doi:10.1083/jcb.152.6.1207.
68. Guo C, Willem M, Werner A, Raivich G, Emerson M, Neyses L, Mayer U. Absence of alpha 7 integrin in dystrophin-deficient mice causes a myopathy similar to Duchenne muscular dystrophy. *Hum Mol Genet* 15: 989–998, 2006. doi:10.1093/hmg/ddl018.
69. Hakim CH, Burkin DJ, Duan D. Alpha 7 integrin preserves the function of the extensor digitorum longus muscle in dystrophin-null mice. *J Appl Physiol (1985)* 115: 1388–1392, 2013. doi:10.1152/japplphysiol.00602.2013.
70. Mousavizadeh R, Scott A, Lu A, Ardekani GS, Behzad H, Lundgreen K, Ghaffari M, McCormack RG, Duronio V. Angiopoietin-like 4 promotes angiogenesis in the tendon and is increased in cyclically loaded tendon fibroblasts. *J Physiol* 594: 2971–2983, 2016. doi:10.1113/JP271752.
71. Can T, Faas L, Ashford DA, Dowle A, Thomas J, O'Toole P, Blanco G. Proteomic analysis of laser capture microscopy purified myotendinous junction regions from muscle sections. *Proteome Sci* 12: 25, 2014. doi:10.1186/1477-5956-12-25.
72. Frenette J, Tidball JG. Mechanical loading regulates expression of talin and its mRNA, which are concentrated at myotendinous junctions. *Am J Physiol Cell Physiol* 275: C818–C825, 1998. doi:10.1152/ajpcell.1998.275.3.C818.
73. Tidball JG. Desmin at myotendinous junctions. *Exp Cell Res* 199: 206–212, 1992. doi:10.1016/0014-4827(92)90425-8.
74. Charvet B, Malbouyres M, Pagnon-Minot A, Ruggiero F, Le Guellec D. Development of the zebrafish myoseptum with emphasis on the myotendinous junction. *Cell Tissue Res* 346: 439–449, 2011. doi:10.1007/s00441-011-1266-7.

A single bout of eccentric exercise increases the gene expression of nestin and osteocrin in human myotendinous junctions

Jens R. Jakobsen[1], Peter Schjerling[2,3], Michael Kjær[2,3], Abigail L. Mackey[2,3,4], Michael R. Krogsgaard[1].

[1]Section for Sports Traumatology M51, Department of Orthopaedic Surgery, Copenhagen University Hospital, Bispebjerg and Frederiksberg, Denmark*

[2]Institute of Sports Medicine Copenhagen, Department of Orthopedic Surgery, Copenhagen University Hospital - Bispebjerg and Frederiksberg, Copenhagen, Denmark*

[3]Center for Healthy Aging, Department of Clinical Medicine, University of Copenhagen, Denmark

[4]Xlab, Center for Healthy Aging, Department of Biomedical Sciences, Faculty of Health and Medical Sciences, University of Copenhagen, Copenhagen, Denmark

*Departments are part of IOC Research Center Copenhagen.

Corresponding author
Jens Rithamer Jakobsen
Section of Sports Traumatology, M51, department of Orthopaedic Surgery M
Bispebjerg and Frederiksberg Hospital
Nielsine Nielsens Vej 3
Copenhagen 2400 NV
Denmark
Tel: (+45) 3863 5639
Email: jensjakobsendk@gmail.com

Conflict of Interest
The authors have declared that no conflict of interest exists.

Abstract

Background: The myotendinous junction (MTJ) as a specialized interface for force transmission between muscle and tendon has a unique transcriptional activity and is highly susceptible to strain injury. Eccentric exercise reduces the risk for these injuries. Knowledge about the human MTJ is limited, in particular in relation to gene expression and the effect of eccentric exercise on the tissue.

Methods: 30 humans were randomized to a single bout of eccentric exercise 1 week prior to tissue sampling or no exercise (control). Samples were collected from the semitendinosus in connection with reconstruction of the anterior cruciate ligament and were divided into fractions containing muscle, MTJ and tendon, respectively. The concentrations of macrophages and satellite cells were counted, and the expression of genes previously known to be active at the MTJ were analysed by RT-qPCR.

Results: The expression of NES and OSTN mRNA were significantly increased in the MTJ and tendon fractions in the exercise group. Many genes earlier identified at the MTJ (COL22A1, POSTN, ADAMTS8, MNS1, NCAM1) were confirmed to be significantly higher expressed in the MTJ compared to muscle and

tendon but they were unaffected by exercise. In the eccentric exercise bout group there was an increase in the number of macrophages, but not satellite cells, in the muscle tissue near the MTJ.

Conclusion: Eccentric exercise leads to increased expression of nestin and osteocrin in human semitendinosus MTJ but does not induce proliferation of satellite cells near the MTJ. The increase in nestin and osteocrin indicates that they could be of interest in the understanding of how the MTJ adapts to eccentric exercise.

Introduction

It is necessary that the interface between skeletal muscle fibers and tendon, the myotendinous junction (MTJ), has a structure that supports force transmission between the two tissues. Clinically, the MTJ is the site of strain injuries, which are among the most common injuries within a wide range of sports (Orchard and Seward, 2002; Ekstrand et al., 2011; Eirale et al., 2013). Eccentric training effectively prevents these injuries, suggesting that there is an adaptive potential of the MTJ in reaction to this type of exercise (Arnason et al., 2008; Petersen et al., 2011; Seagrave et al., 2014; Van Der Horst et al., 2015; Al Attar et al., 2017). Most studies on this have focused on the ultrastructural morphology of the muscle membrane (Kojima et al., 2008; Curzi et al., 2012, 2016; Jacob et al., 2019) but in recent years the molecular basis of this interface has experienced increasing interest (Calve et al., 2020; Dos Santos et al., 2020; Jakobsen et al., 2020, 2021; Kim et al., 2020; Petrany et al., 2020). Myonuclei with specific transcriptional activity different from other myonuclei have been identified at the MTJ, and this confirmed that the MTJ is a unique region in skeletal muscle. However, only very little is known about the effects of eccentric exercise on the cellular and transcriptional activity at the MTJ.

A few studies have shown increases in mRNA for integrin alpha 7, talin and vinculin following eccentric loading regimes, suggesting a cytoskeletal adaptation to eccentric exercise(Frenette and Côté, 2000; Boppart et al., 2008). Integrin alpha 7 is located in the muscle membrane and at the MTJ where it links with vinculin and talin, providing a connection between actin from the last sarcomere and collagen fibrils in the tendon (Matsumura and Campbell, 1994). Animal models have shown that upregulation of integrin alpha 7 counteracts some of the reduction in muscle force caused by absence of dystrophin, suggesting a protective effect of this integrin type (Burkin et al., 2001; Hakim et al., 2013). At the MTJ this integrin type links with collagen XXII, which is specifically located at the MTJ and has been shown to be important for strength and integrity of the MTJ (Charvet et al., 2013) It has further been suggested that increases in proteins, such as integrin alpha 7, at the MTJ lead to an increased strength of the tissue, reducing the risk of strain injuries, and that these adaptations are stimulated by eccentric exercise (Frenette and Côté, 2000; Boppart et al., 2006, 2008).
However, earlier studies were made on whole muscle and not isolated MTJ tissue. Isolation of the MTJ is particularly important in relation to these cytoskeletal proteins, since many of them are present along the myofiber, attaching laterally to the endomysium through costameres (Pardo et al., 1983; Mondello et al., 1996; Passerieux et al., 2007).

A recent study demonstrated a feasible method for dividing a sample into muscle, MTJ and tendon fractions (Jakobsen et al., 2021). Here a panel of genes and proteins concentrated at the MTJ from horses was reported(Jakobsen et al., 2021). Among these were osteocrin which has been speculated to be involved in the mitochondrial adaptation to exercise as well as the intermediate filament protein nestin which has previously been described at the MTJ in animals (Carlsson et al., 1999; Vaittinen et al., 2001; Subbotina et al., 2015). The specific function of nestin is not fully elucidated, but the general function of the

intermediate filaments in general is to link the myofibrils with the muscle membrane (Small et al., 1992). Nestin is thought to be related to regeneration of skeletal muscle, and its presence at the MTJ could indicate that is has a role in the high rate of remodeling, which seen in the muscle fibers at the MTJ (Vaittinen et al., 2001; Lindqvist et al., 2017; Jakobsen et al., 2018a).

A single study has investigated the cellular activity at the MTJ following resistance exercise and shown a higher concentrations of macrophages but not satellite cells near the MTJ following 4 weeks of exercise (Jakobsen et al., 2017). It was speculated that the absence of increase in satellite cell quantity could be due to a high demand for satellite cells at the MTJ since this is known as a region with a high rate of remodeling of the muscle fibers and therefore potentially also a region with a high demand for satellite cell activity.

Using the recently described method to isolate tissue of the MTJ from muscle and tendon tissue (Jakobsen et al., 2021), the current study aim to investigate the effects of a single bout of heavy eccentric exercise in humans on gene expression in muscle, MTJ and tendon Furthermore, the current study aim at analyzing the effect of eccentric exercise on the concentration of satellite cells and macrophages at the MTJ and in tendon.

Methods

Participants

Humans with rupture of the anterior cruciate ligament of the knee and scheduled for reconstructive surgery with a hamstring-tendon graft were invited to participate in the study. Resistance exercise involving the hamstring for a period of 3 months prior to inclusion was not allowed. Smokers and subjects with BMI > 30 were excluded due to possible effects on mRNA expression. Thirty subjects were enrolled and randomized to either the control group, which did not perform any exercise, or the training group, which performed one session of eccentric exercise 7 days before the scheduled surgery. Five subjects (3 exercise, 2 controls) were excluded following randomization for reasons not related to the study (Cancelled surgery, tendon rupture during surgery, additional knee trauma preventing exercise participation), leaving 14 controls (4 females and 10 males, mean age 28.5 ±7.2, BMI 24.1± 1.6) and 11 exercised (5 females, 6 males, mean age 28.2 ±5.2, BMI 28.2 ± 1.7). All volunteers gave written informed consent before inclusion. The human tissue was obtained from ACL-patients, as previously described (Jakobsen et al., 2017). The study was approved by The Research Ethics Committees of the Capital Region of Denmark (ref. H-3-2010-070) and performed according to the standards set by the Declaration of Helsinki.

Exercise intervention

The training program was designed to eccentrically load the hamstring muscles and included the exercises: Nordic Hamstring, lying leg curl and stiff-legged deadlift (See supplemental file for detailed description). All of which consisted of 3 sets of 6-8 repetitions performed until exhaustion with 2 minutes between each set.

Tissue collection

The semitendinosus was harvested from all participants and the tendon was used as graft for the ACL-reconstruction. Excess tissue from the semitendinosus, containing muscle, tendon and MTJ was used in this project. Multiple samples from each subject were cut from the excess tissue and placed on a plastic stick with the tendon placed at the bottom as flat as possible before embedding in Tissue-Tek and freezing in liquid nitrogen-cooled isopentane.

From each subject one sample was prepared for RT-qPCR. First, the samples were divided into the various fractions (muscle, MTJ and tendon), using a recently described method (Jakobsen et al., 2021): the samples were placed in a cryostat and sectioned. By placing the tendon at the bottom, the first sections contained pure muscle tissue and were collected as the muscle fraction in tubes for further processing. Control sections were mounted before and after collecting sections for tubes. By visually inspecting the control sections and the samples it was noted when the MTJ was reached. Sections containing a mixture of muscle and tendon i.e. MTJ, were collected as the MTJ fraction. Following that, the tendon fraction was collected. From three subjects all muscle tubes (7 tubes) were included to analyze the difference in gene expression in muscle with varying distance from the MTJ.

For immunohistochemical evaluation another sample from each subject was placed in the cryostat so that each section would contain both tendon, MTJ and cross-sectionally cut muscle fibers. 10 µm thick sections were mounted on glass-slides and stored at -80 degrees.

Immunofluorescence

To investigate the cellular response to exercise, sections from all subjects were stained with antibodies against CD56 (Neural Cell Adhesion molecule (NCAM)) to label satellite cells, and against CD68 to label macrophages as described previously (Jakobsen et al., 2016, 2018). Briefly, sections were incubated with the following primary antibodies: Mouse anti-CD68(cat. No. M0718 Dako Denmark A/S, Glostrup, Denmark) diluted 1:500, mouse-anti CD56(cat.no. 34770; Becton Dickinson, San Jose, California, USA) in 1:50, rabbit anti-laminin (Cat. No. Z0097 Dako, Denmark A/S, Glostrup, Denmark) in 1:500, guinea-pig anti-collagen XXII (A kind gift from Manuel Koch, University of Cologne, Germany) in 1:1000.
Primary antibodies were labelled with the following secondary antibodies: Alexa Fluor 488 goat anti-mouse, Alexa Fluor 568 goat anti-guinea pig, and Alexa Fluor 647 goat anti-rabbit (Molecular Probes cat. no. A11029, A11075, A21076, respectively; Invitrogen A/S)

The following antibody combinations were used: 1. CD68, Collagen XXII and laminin. 2. CD56, Collagen XXII and laminin.

Image analysis

Images were acquired using an Olympus BX51 microscope with a digital camera mounted on top (Olympus DP71, Olympus Deutschland GmbH, Hamburg, Germany), controlled by the software Cell^F (Olympus Soft

Imaging Solutions, GmbH, Münster, Germany). Since each section couldn't fit into one image, several images were stitched together using a previously developed macro for ImageJ to stitch 3 channels. Satellite cells and macrophages were counted manually in ImageJ by a person blinded to the intervention. A satellite cell was defined as a CD56-positive cell located inside of laminin+ muscle membrane and containing a nucleus seen as DAPI-staining (figure 4). A cell located outside of the capillaries and between muscle fibers showing both immunoreactivity towards CD68 and DAPI staining was counted as a macrophage (figure 5).

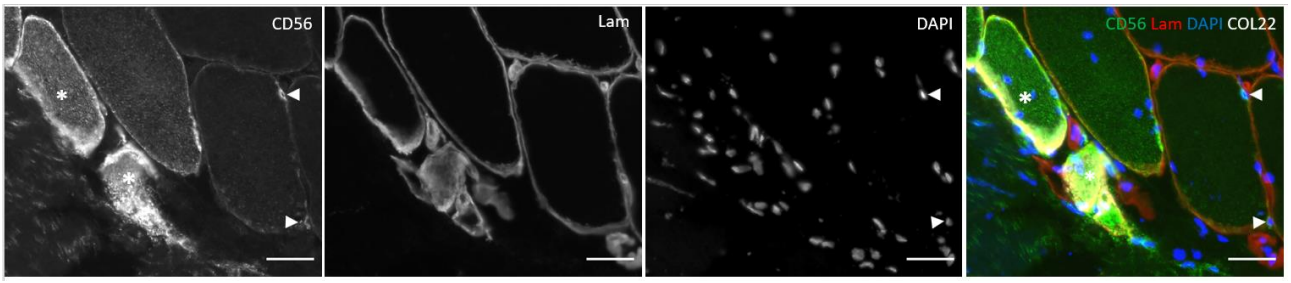

Figure 4: Satellite cells in muscle
The figure shows representable images of satellite cells (arrows) in relation to muscle fibers as well as CD56+ muscle fibers (Asterix) near the collagen XXII labelled MTJ. The first three images are single channel images showing each staining and the last image is a combination of the three + the collagen XXII staining. Scale bars are 50 µm.

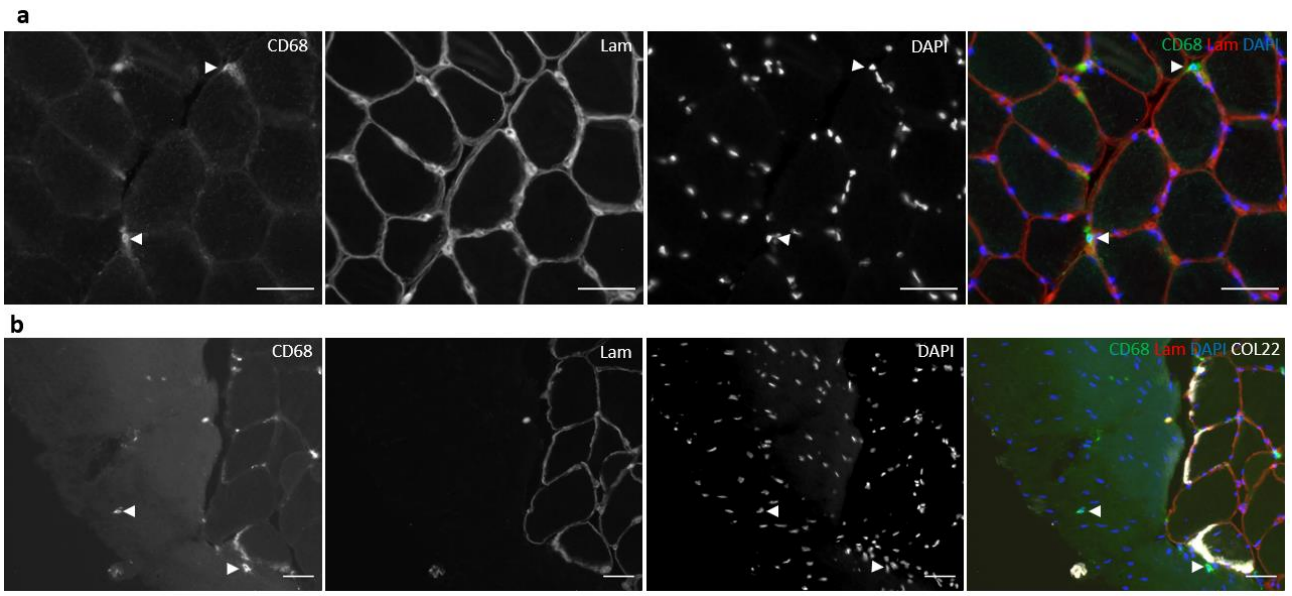

Figure 5: Macrophages in muscle and tendon
The figure shows representable images of CD68 staining of muscle and tendon. Panel a shows macrophages in relation to skeletal muscle fibers (arrows) while panel b shows macrophages in tendon (arrows). The first three images are single channel images showing each staining and the last image is a combination of the three + the collagen XXI staining.
Scale bars are 50 µm.

The number of satellite cells are expressed relative to the total number of muscle fibers on the given section, which were counted manually.
The number of macrophages are expressed relative to both number of muscle fibers but also area of muscle and area of tendon. The measurements of area were manually measured using ImageJ. In 3 trained subjects (all female) a large number of necrotic and regenerating muscle fibers were seen. This affected the ability to properly identify macrophageas illustrated in figure 6. macrophagein muscle were therefore not counted for these subjects. Satellite cells were counted for the persons with necrotic muscle fibers but were excluded before running the statistics since they were clear outliers and probably not reflecting a normal physiological response to exercise.

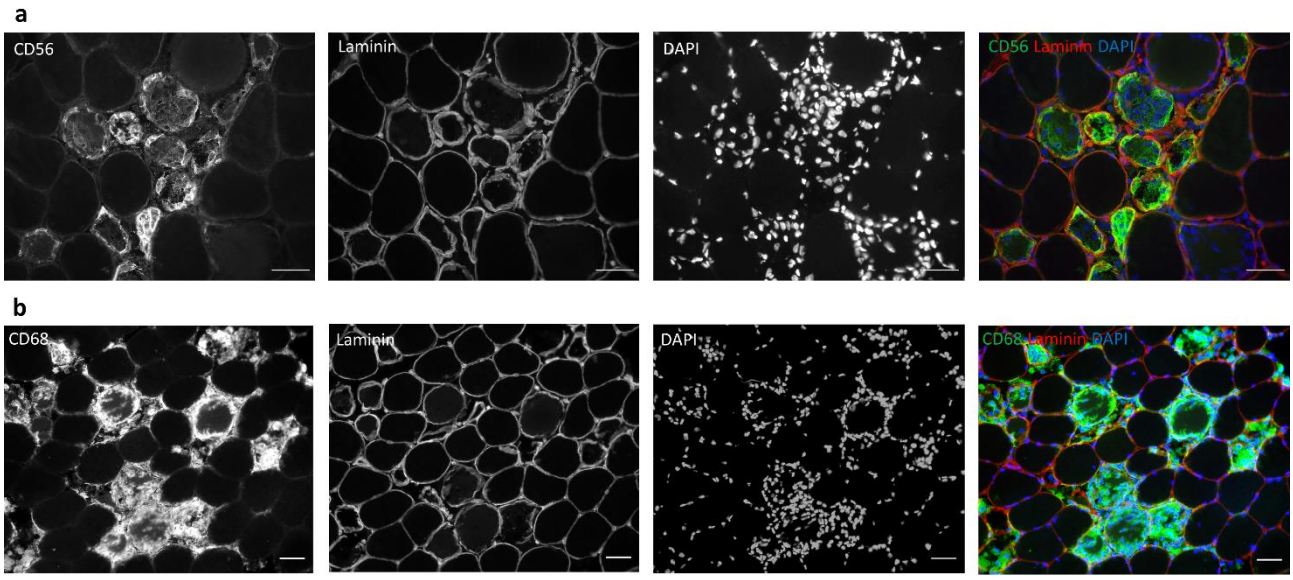

Figure 6: Necrosis and remodeling of skeletal muscle fibers
The figure shows a panel of images showing cross-sections of skeletal muscle fibers from an exercised subject that was undergoing remodeling/reformation and necrosis, respectively. In figure a) the muscle fibers that were newly formed or under remodeling were indicated by the CD56 staining. The muscle fiber membrane was labelled with laminin and the nuclei with DAPI. To the right is a merged image of all three channels showing muscle fibers with strong immunoreactivity against CD56 and a very high number of infiltrating cells/nuclei.
In Figure b the necrotic muscle fibers are indicated with a CD68 staining which labels macrophages. While the muscle membrane was still intact, seen by the laminin staining, lots of macrophages were seen to infiltrate and fill up the cytoplasm in some of the muscle fibers.
Scale bars are 50 µm.

RNA extraction

Approx. 200-300 cryo sections of 10 µm from the embedded tissue were homogenized in 1 mL of TriReagent (Molecular Research Center, Cincinnati, OH, USA) containing five stainless steel balls of 2.3 mm in diameter (BioSpec Products, Bartlesville, Oklahoma, USA) by shaking in a FastPrep®-24 instrument (MP Biomedicals, Illkirch, France) at speed level 4 for 15 s. Following homogenization, bromo-chloropropane

was added in order to separate the samples into an aqueous and an organic phase. Following isolation of the aqueous phase, RNA was precipitated using isopropanol. The RNA pellet was then washed in ethanol and subsequently dissolved in 10 µL RNAse-free water. Total RNA concentrations were determined using RiboGreen assay (R11490, Invitrogen, Naerum, Denmark).

Real-time RT-PCR

100 ng total RNA was converted into cDNA in 20 µL using the OmniScript reverse transcriptase (Qiagen, California, USA) and 1 µM poly-dT (Invitrogen, Naerum, Denmark) according to the manufacture's protocol (Qiagen). For each target mRNA, 0.25 µL cDNA was amplified in a 25 µL SYBR Green polymerase chain reaction (PCR) containing 1 × Quantitect SYBR Green Master Mix (Qiagen) and 100 nM of each primer (**Table PRIMERS**). The amplification was monitored real time using the MX3005P Real-time PCR machine (Stratagene, California, USA). The Ct values were related to a standard curve made with known concentrations of DNA oligonucleotides (Ultramer^{TM} oligos, Integrated DNA Technologies, Inc., Leuven, Belgium) with a DNA sequence corresponding to the sequence of the expected PCR product. The specificity of the PCR products was confirmed by melting curve analysis after amplification. Originally, RPLP0 mRNA was chosen as internal control (supplements). However, as described in results, instead tissue volume was used for normalization to make tendon and muscle more comparable. Tissue volume (3 ± 2sd mm^3) was estimated from the area of the control sections and the number of 10 µm sections. Data are shown relative to the geometric mean of the muscle samples from control subjects. LCT was only detected in 6 samples (4 muscle, 2 MTJ) and only just above one molecule in the PCR and therefore not included in the quantifications. However, sequencing of the PCR product confirmed LCT identity.

Table PRIMERS:

mRNA	Genbank ID	Sense	Antisense
RPLP0	NM_053275.3	GGAAACTCTGCATTCTCGCTTCCT	CCAGGACTCGTTTGTACCCGTTG
GAPDH	NM_002046.4	CCTCCTGCACCACCAACTGCTT	GAGGGGCCATCCACAGTCTTCT
MYH2 (MHCIIA)	NM_017534.5	TTGCTGAGTCCCAGGTGAACAA	TTTGTGCCTGTCTTCAGTCATTCC
MYH3 (MHCemb)	NM_002470.3	CGGATATCGCAGAATCTCAAGTCAA	CTCCAGAAGGGCTGGCTCACTC
COL22A1	NM_152888.2	CGAGATGGGACCCCCTGGAA	CAGCTGGTCCTGTCTCCCCTTG
NCAM1	NM_000615.6	ATTGCGGTCAACCTGTGTGGAA	CCACGATGGGCTCCTTGGACT
POSTN	NM_006475.3	CAGCAGACACACCTGTTGGAAATG	ACAGTCACGGGGATTTCTTTGAAGG
NES	NM_006617.2	GAGAACTCCCGGCTGCAAACAC	GGCTCAGGACTGGGAGCAAAGA
MNS1	NM_018365.4	GAAGAGCGTCGCCAACAATTCC	CCTTTGCTGCAACTGCCACTCTT
OSTN	NM_198184.2	CCCCATGGATCGGATTGGTAGA	GCTGTGACATTTCACCCAAGGAAG
ADAMTS8	NM_007037.6	GGGGGAGGAGCGAGTTCAAAG	ACACACTGGCCACGGACACAGA
ITGA7	NM_002206.3	GCATGTCTGGGGCCGTCTCT	GACAATCACTTCCAGGGACTTCACA
COL1A1	NM_000088.3	GGCAACAGCCGCTTCACCTAC	GCGGGAGGTCTTGGTGGTTTT
COL3A1	NM_000090.3	CACGGAAACACTGGTGGACAGATT	ATGCCAGCTGCACATCAAGGAC
TENC	NM_002160.3	CAGCCAAGATCCAGGCACTCAA	GTCCTTGGGGAAGGGGTACAGG
TNMD	NM_022144.3	GAAGCGGAAATGGCACTGATGA	TGAAGACCCACGAAGTAGATGCCA
COMP	NM_000095.3	TGACAACTGTCCCCAGAAGAGCAAC	TTGATCGCTGTCACAAGCATCTCC
LCT	NM_002299.4	TCCCAGCGGGAAGAAACAGACC	TCCATCGCACTCCAAACTGTGTATC

Statistics

Unpaired t-test was used for the analysis of satellite cells and macrophages in muscle. However, due to large variation and the presence of 1, 2 or 3 cells in some of the tendon samples the risk of stochastic variation was present as well as a non-normalized distribution of data. Therefore, Mann-Whitney U-test was chosen for these results.

To analyze the effect of exercise on the gene expression at the MTJ, data from real-time RT-PCR was first normalized to RPLP0 and relative the mean value of control muscle (shown in supplemental file) but due to the low number of cells in tendon this normalization was not found to be representative for the actual gene expression in the tissue. Instead, to take into account the large difference in number of cells/nuclei in muscle and tendon, data was normalized to tissue volume and expressed relative to the mean of control muscle. Data from the 3 participants with a high number of necrotic muscle fibers, identified as fibers showing immunoreactivity against CD68, were excluded from both the cell counting and the RT-qPCR analysis due to the high number of necrotic muscle fibers potentially affecting the results.
Two-way repeated measures ANOVA was performed with tissue and exercise as the two factors using log-transformed values. Since the variance in the data wasn't evenly distributed between muscle, MTJ and tendon, they were split into two separate analysis comparing first muscle vs MTJ and then MTJ vs tendon.

The level of significance was set to < 0.05.

SigmaPlot 13.0 was used to run all the statistics and graphs are made in GraphPad Prism 9.0

Results

Macrophages and satellite cells

A significant increase in the concentration of macrophages were seen in the exercised muscles compared to control, both number of cells relative to number of muscle fibers and relative to muscle area (Figure 7b-c). From the three subjects excluded from the analysis, 10-18 % of the muscle fibers were identified as necrotic (figure 6). In the samples from the other subjects two (1 exercised and 1 control) had 0.2 % necrotic muscle fibers where none were seen in the rest of the samples.

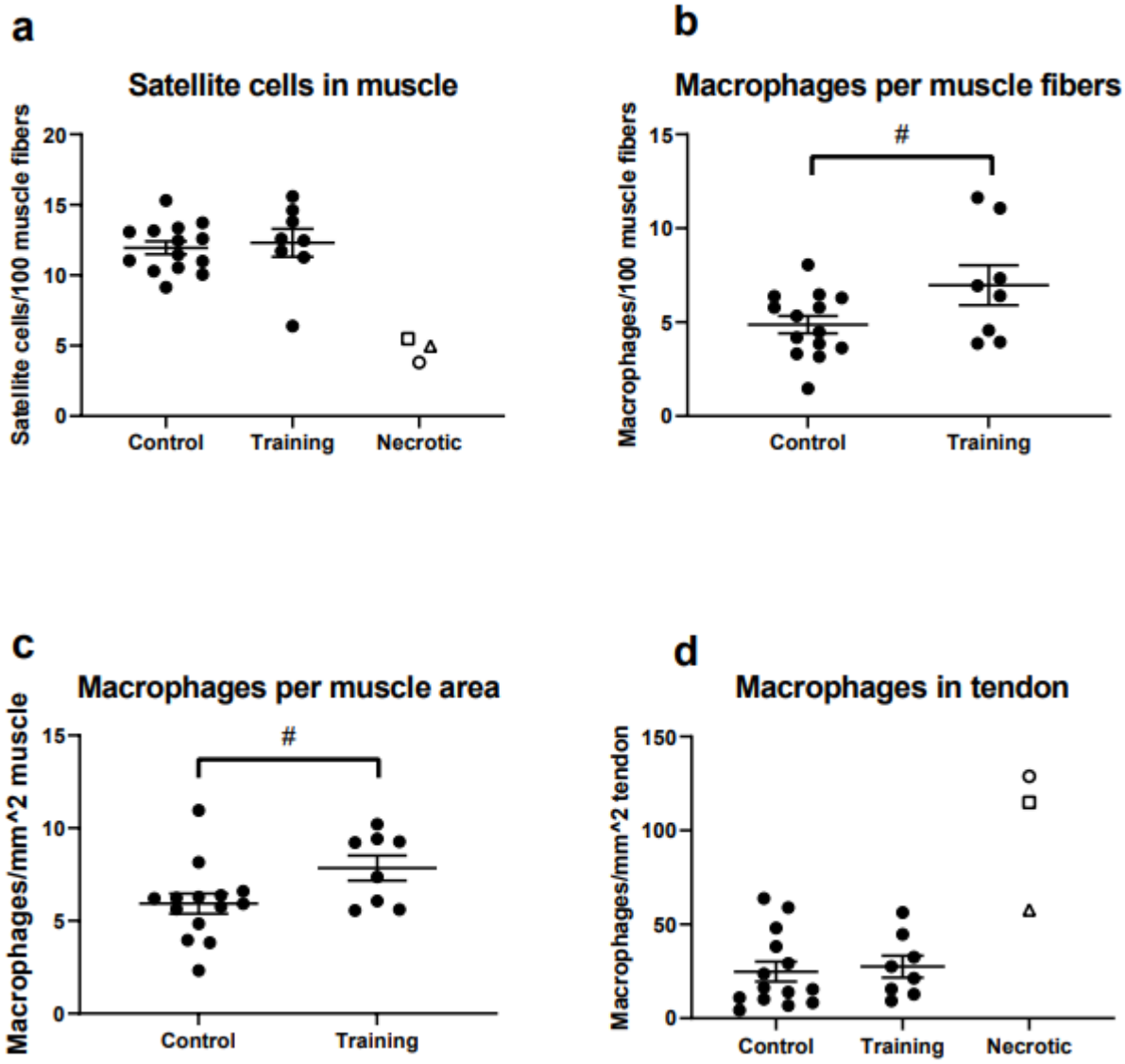

Figure 7: Satellite cells and macrophages in muscle and tendon.
The diagrams show the number of satellite cells in muscle and macrophages in muscle and tendon in the training and control groups. Individual values are indicated with a circle and mean for each group is presented as a line with SEM. The open circles in a and d represents the participants who had a high number of necrotic and regenerating fibers. These were not included in the statistics.
a. Satellite cells per 100 muscle fibers in muscle. b. Macrophages per 100 muscle fibers
c. Macrophages per mm^2 muscle. D. Macrophages per mm^2 tendon.

No significant differences were seen for the number of macrophages in tendon, nor satellite cells in muscle following training (p=0.718). In control MTJ's a mean of 11.9 (± 1.7) satellite cells were seen per 100 fibers whereas in the acute exercised MTJ's a mean of 12.3 (± 2.8) satellite cells were seen in the muscle (Figure 7a).

RT-qPCR

The effect of exercise and tissue were compared between muscle versus MTJ as well as MTJ versus tendon (see figure 8). To exclude any potential confounding effects, samples from the three subjects showing a high degree of muscle fibers undergoing necrosis were excluded from the statistics but are shown in figure 8 as separate values.

A significant effect of exercise was seen for NES (P=0.040) and OSTN (P=0.037) in the MTJ and tendon, where the expression values were higher in the exercised samples than in control, but no interaction between tissue and exercise was found. No other effects of exercise were seen.
Comparing muscle versus MTJ a significant effect of tissue was seen for all targets except GAPDH. Most of the chosen targets, except MYH2, COL1A1, TENC, TNMD and COMP, were significantly higher expressed in the MTJ fraction compared to tendon.

From three subjects all collected fractions (7 muscle, 1 MTJ and 1 tendon fraction) were analyzed to illustrate the gene expression change relative to the distance to the MTJ (Figure 9). Most of the targets decreased with increasing distance to the MTJ and tendon.

a

Gene expression relative to tissue volume
Muscle vs MTJ

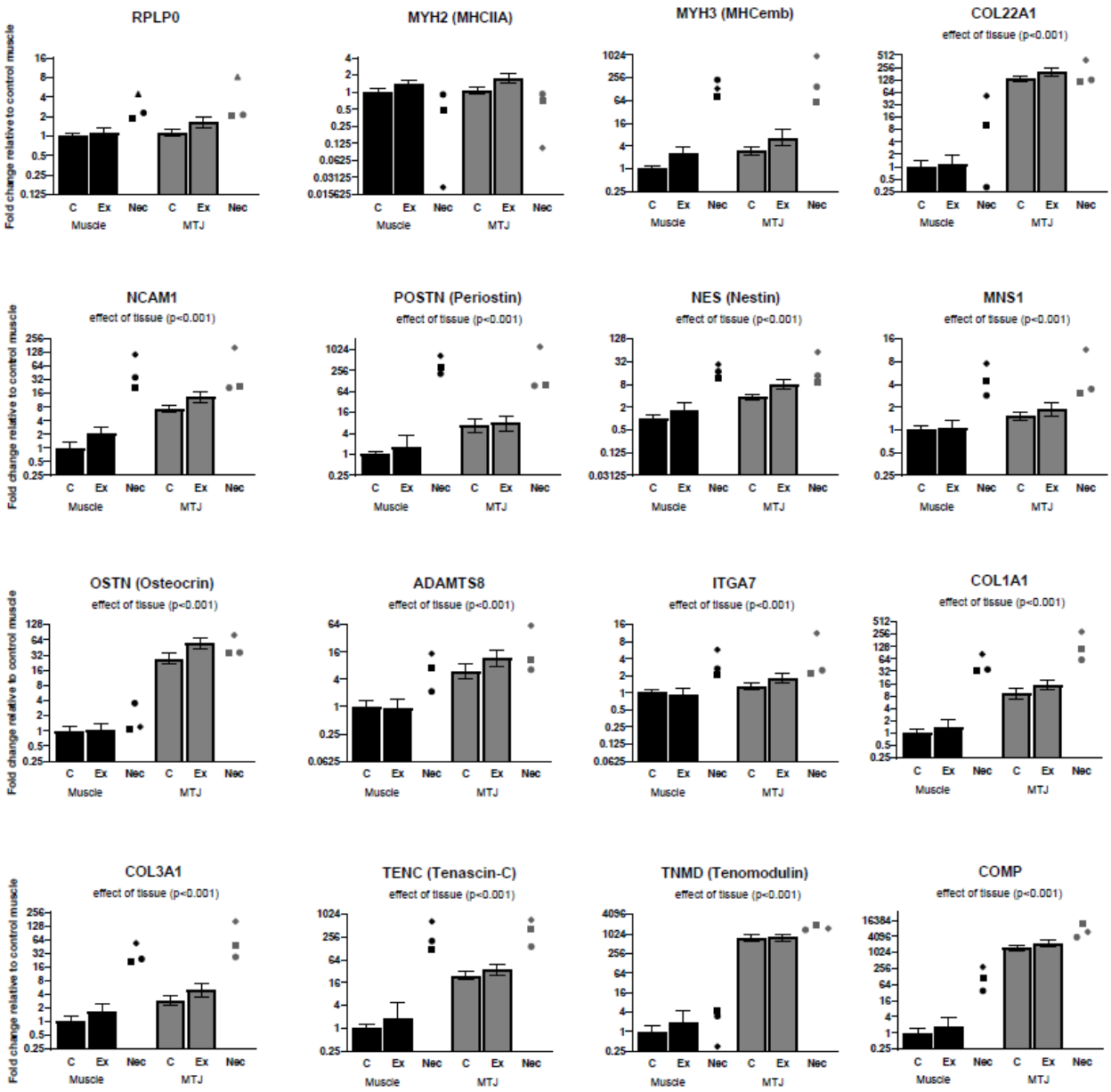

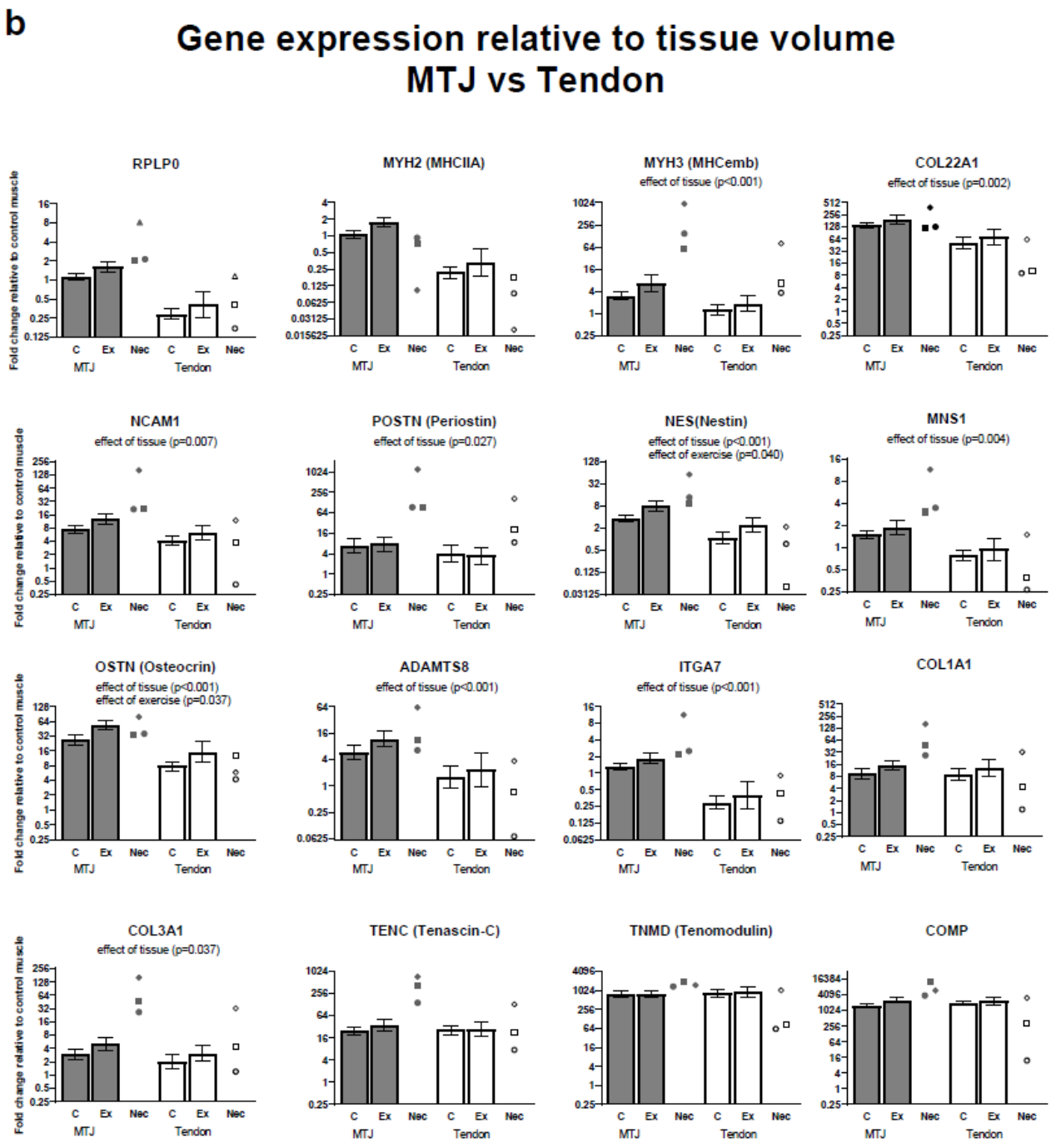

Figure 8: Results of RT-PCR analysis

The graph shows the mRNA expression of the selected genes in muscle vs MTJ (a) and MTJ vs tendon (b). All data are normalized to tissue volume and expressed relative to control muscle. Two-way repeated measures ANOVA was performed to analyze the effects of tissue and exercise. P-values from this test are inserted under each gene name. Data shown as geometric mean ± back-transformed SEM. Three subjects were excluded from the analysis due to a high number of necrotic fibers. Individual values from these subjects are shown separately for all targets. Each subject is represented by a specific symbol.

Due to large difference in the expression values between targets and to optimally illustrate the expression for each mRNA target the y-axis are different between targets.

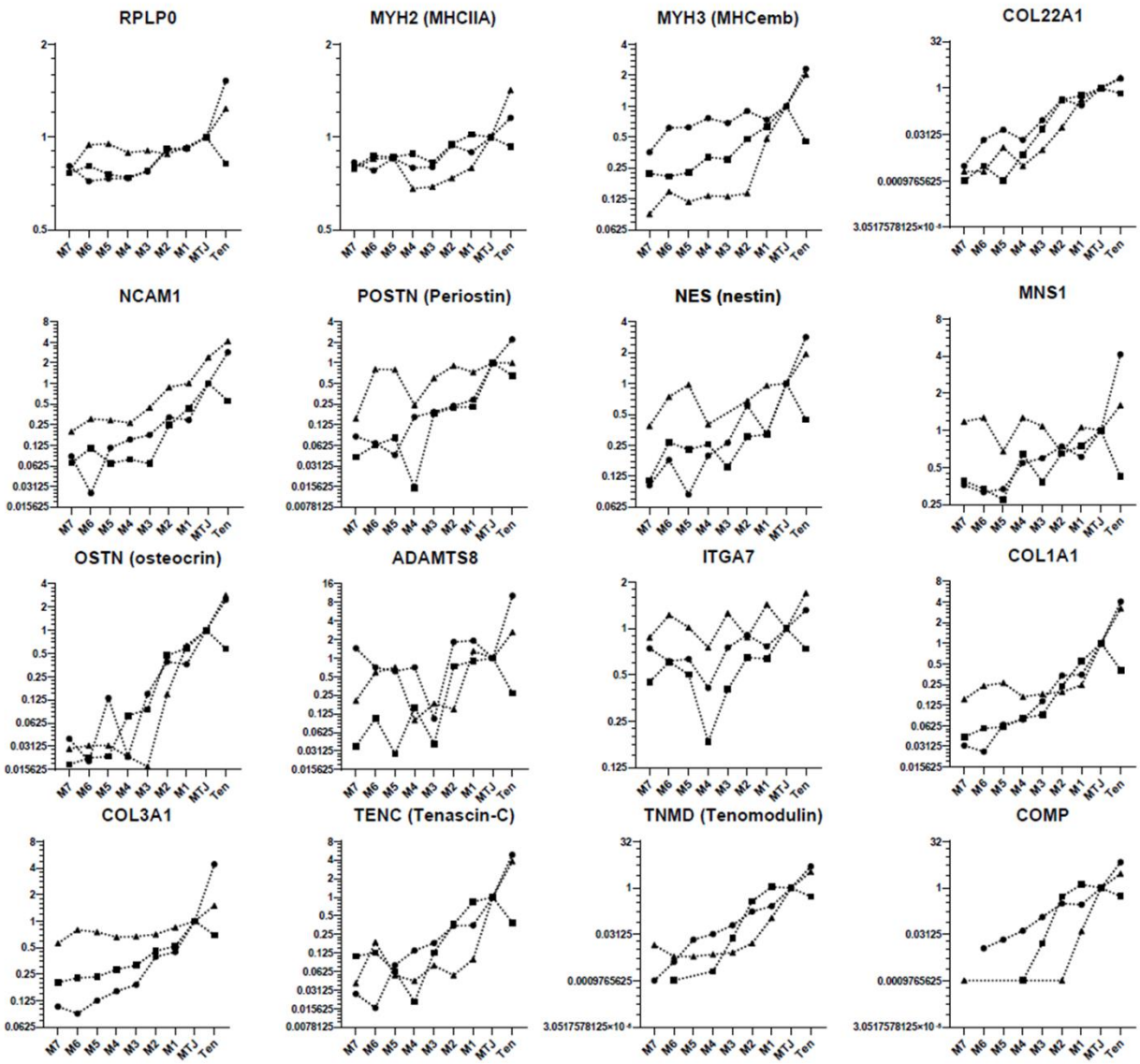

Figure 9: Differences in gene expression depending on distance from MTJ

The graph shows RT-PCR values for tissue fractions collected from 3 subjects. "M1-7" represents muscle fractions collected in varying distance from MTJ with "Muscle 7" being furthest from the MTJ and "M1" being closest to the MTJ. The data was normalized to RPLP0 and expressed relative to the mean MTJ values.

Discussion

This is the first study to evaluate gene expression and cellular response after a single bout of eccentric exercise compared to control in muscle, tendon and MTJ from the human semitendinosus. The main findings were that samples from the group performing a single bout of eccentric exercise showed higher expression of nestin and osteocrin at the MTJ as well as a significant infiltration of macrophages in the muscle near the MTJ, seven days after exercise.

Previous clinical studies have shown positive effects of heavy eccentric exercise on the incidence of strain injuries, which occur at the MTJ and are particularly frequent in hamstring MTJs (Noonan and Garrett, 1992; Tidball et al., 1993; Ekstrand et al., 2011; Petersen et al., 2011; Van Der Horst et al., 2015).

Nestin, an intermediate filament protein, was found to be both higher expressed in the MTJ and tendon fraction in the exercise group as well as higher in the MTJ than general muscle. The presence of nestin at the MTJ has been described in previous studies, in which it has also been found to be important for embryonic development of the MTJ and neuromuscular junctions (Carlsson et al., 1999; Vaittinen et al., 2001). However, it is also expressed in non-muscle cells such as neuroepithelial stem cells (Lendahl et al., 1990) and rapid dividing cancer cells such as small cell lung cancer and prostate cancer cells (Kleeberger et al., 2007; Takakuwa et al., 2013). In general muscle nestin is suggested to be involved in proliferation and muscle regeneration(Vaittinen et al., 1999, 2001; Sahlgren et al., 2006) and has been shown to be upregulated following muscle injury suggesting that it has a potential role in muscle regeneration (Lindqvist et al., 2017; Singh et al., 2017). The current findings of an increase in expression of nestin in the MTJ following exercise suggests that nestin could be involved in the regeneration of the MTJ following unaccustomed exercise. Based on our findings it can be hypothesized that nestin is involved in the adaptive response following eccentric exercise, leading to a stronger MTJ and a lower risk for strain injury.

Another recently identified MTJ-related gene, osteocrin, was also found with higher expression in the group performing exercise, in both MTJ and tendon. Osteocrin is a natriuretic peptide which has previously been studied in relation to bone, hence the name, but is also named “musclin” in skeletal muscle research (Moffatt and Thomas, 2009). Its specific function in skeletal muscle is currently unknown, but some studies suggest that it could be involved in glucose metabolism, mitochondrial genesis or oxidative capacity (Nishizawa et al., 2004; Subbotina et al., 2015; Jeremic et al., 2017; Shimomura et al., 2021). The latter proposal was based on a study showing increase in the protein concentration of osteocrin following aerobic exercise as well as an impaired oxidative capacity in osteocrin-knockout mice (Subbotina et al., 2015). None of these studies have intendedly examined osteocrin in the MTJ but used whole muscles in which the specific content of MTJ is unknown. Therefore, the specific role for OSTN at the MTJ is still uncertain, but it could be speculated, that since the MTJ has been shown to be a region with high degree of remodeling of muscle fibers, osteocrin is involved in the metabolic processes that are necessary for muscle remodeling. Interestingly, adipocytes have previously been shown to be present at the MTJ (Jakobsen et al., 2020) and since osteocrin has been suggested to be involved in browning of adipose tissue, the high concentration of adipocytes at MTJ could potentially be the reason for the high expression of osteocrin at the MTJ (Jeremic et al., 2017). However, it has not been confirmed whether the adipocytes seen at the MTJ are white, beige or brown, nor is it known whether the increased expression of osteocrin following exercise would lead to a browning of the adipocytes at the MTJ.

In previous studies increases in TENC, ITGA7, COL1A1 and COL3A1 were demonstrated in muscle tissue following an exercise bout but was seen to be unaffected by exercise in the current study (Hyldahl et al., 2015; Jensen et al., 2020). This difference could in part be due to differences in time of sampling post-

exercise and the fact that different muscles were analyzed. The collection of samples 7 days post-exercise in the current study was chosen based on our previous knowledge from human vastus lateralis muscles where satellite cells and macrophages are seen to reach their maximum concentration around this time-point after an exercise bout. However, it is a compromise since some mRNA's are known to increase very rapidly following exercise, i.e. Tenascin-C and ITGA7 (Fluck et al., 2000; Boppart et al., 2008), whereas others are upregulated over a longer period of time, i.e. COL1A1 and COL3A1 (Hyldahl et al., 2015; Jensen et al., 2020). EMG studies have shown that the chosen exercises are effective in targeting the semitendinosus muscle (Bourne et al., 2017; Hegyi et al., 2018; Boyer et al., 2021). Together with the finding of infiltration of macrophages in the trained muscles this suggests that the lack of increase in COL1A1 and COL3A1 was not due to the semitendinosus muscles not being loaded heavily enough. In fact, the exercise regimen was so hard for three of our participants, that extensive necrosis of the muscle fibers appeared (figure 6).

Despite the infiltration of macrophages, the number of satellite cell were unaffected by the exercise bout which confirms the findings from a previous study examining the human semitendinosus MTJ(Jakobsen et al., 2018b). Satellite cells are muscle progenitor cells with the unique ability of re-entering cell cycle to form new muscle fibers and to provide the muscle fibers with additional myonuclei. In the resting muscle satellite cells are thought to be quiescent but following injury and/or exercise the satellite cells are activated and proliferate to support the repair and regeneration of the muscle fibers (Crameri et al., 2004; Kadi et al., 2005). An increased number of satellite cells has been seen both acutely, 24-48 hours after exercise (Dreyer et al., 2006), and 8 days later suggesting that the lack of increase in satellite cells seen in the current study is not related to the time of sampling (Crameri et al., 2004). However, we investigated the semitendinosus muscle, in contrast to most previous studies, in which vastus lateralis was used, and there might also be differences between the MTJ region and body of the muscle. There is a high degree of remodeling at the MTJ, and it could be speculated that the lack of increase in the satellite cell pool at the MTJ is not due to absence of proliferation of satellite cells, but instead a dynamic phenomenon where the newly formed daughter cells fuse quickly after being formed, by which they do not add to the number of satellite cells.

When comparing the gene expression between the tissue fractions most of the targets were highest expressed at the MTJ. All targets except GAPDH was found to be higher expressed in the MTJ fraction compared to muscle. Interestingly, that also included MNS1, OSTN, POSTN, NES and ADAMTS8, all of which have recently been identified to be highly expressed at the MTJ from horse muscles by RNA-sequencing (Jakobsen et al., 2021) and confirmed by immunohistochemistry. These targets were also higher expressed in the MTJ compared to tendon and could therefore be important in the future studies of the MTJ. LCT was also among the targets identified at the horse MTJ by RNA-seq. In the current study the presence of lactase was also examined and was found in samples from some subjects, but not all and not exclusively in MTJ fractions. Interestingly, this confirms that lactase is in fact seen in muscle and MTJ in some subjects. The fact that it is only seen in some subjects could indicate that it is expressed in cells, potentially immune-cells, "travelling" through the skeletal muscle, and therefore they appear in some subjects randomly.

Surprisingly, MYH2 (MHCIIA) was expressed to similar extent in both the MTJ and tendon fraction. MHCIIA is to our knowledge not related to tendon and its presence in the tendon samples could therefore indicate that the tendon fraction has been contaminated with muscle fibers to some degree. This contamination was confirmed by looking at the control sections mounted on glass-slides before collecting tissue for RT-qPCR where it was seen that for many of the tendon sections some muscle fibers were still present among the tendon substance. In that light the tendon fraction should not be considered as pure tendon.

To investigate how the gene expression, differ between different areas of muscle depending on the distance from MTJ, all sectioned tissue fractions from three subjects were analyzed (Seven muscle regions with varying distance from the MTJ, one MTJ and one tendon fraction). For most of the targets a clear tendency was seen where the expression increased the closer the muscle fiber was to the MTJ. While this confirms that many of the selected targets are higher expressed in the MTJ than in muscle, it also implies that measurements on samples close to the MTJ should be interpreted with caution. Interestingly, the genes of some of the proteins thought to be unique for MTJ, such as COL22A1 were also seen in the muscle fractions some distance from the MTJ. While this could be explained by some myonuclei producing this mRNA at some distance from the MTJ and then transport it to the MTJ, it could also indicate that the mRNA is produced near the MTJ but then to a small degree diffuse in the muscle cytoplasm away from the junction. However, this can only apply to the mRNA's produced by myonuclei, such as COL22A1.

In conclusion, we found that a single bout of eccentric exercise seemed to lead to an increased expression of nestin and osteocrin in the MTJ and tendon parts of samples from muscle, MTJ and tendon components. Genes which have recently be identified to be highly expressed in horse MTJ (NES, OSTN, ADAMTS8, POSTN and MNS1) were all confirmed to be higher expressed in the human MTJ compared to muscle. Altogether these findings indicate that increases in nestin and osteocrin are induced by eccentric exercise and suggests that these proteins could be important in the adaptive response at the MTJ following eccentric exercise.

References:

Al Attar, W. S. A., Soomro, N., Sinclair, P. J., Pappas, E., and Sanders, R. H. (2017). Effect of Injury Prevention Programs that Include the Nordic Hamstring Exercise on Hamstring Injury Rates in Soccer Players: A Systematic Review and Meta-Analysis. *Sport. Med.* 47, 907–916. doi:10.1007/s40279-016-0638-2.

Arnason, A., Andersen, T. E., Holme, I., Engebretsen, L., and Bahr, R. (2008). Prevention of hamstring strains in elite soccer: an intervention study. *Scand J Med Sci Sport.* 18, 40–48. doi:10.1111/j.1600-0838.2006.00634.x.

Boppart, M. D., Burkin, D. J., and Kaufman, S. J. (2006). Alpha7beta1-integrin regulates mechanotransduction and prevents skeletal muscle injury. *Am. J. Physiol. Cell Physiol.* 290, C1660-5. doi:10.1152/ajpcell.00317.2005.

Boppart, M. D., Volker, S. E., Alexander, N., Burkin, D. J., and Kaufman, S. J. (2008). Exercise promotes alpha7 integrin gene transcription and protection of skeletal muscle. *Am. J. Physiol. Regul. Integr. Comp. Physiol.* 295, R1623-30. doi:10.1152/ajpregu.00089.2008.

Bourne, M. N., Duhig, S. J., Timmins, R. G., Williams, M. D., Opar, D. A., Al Najjar, A., et al. (2017). Impact of the Nordic hamstring and hip extension exercises on hamstring architecture and morphology: Implications for injury prevention. *Br. J. Sports Med.* 51, 469–477. doi:10.1136/bjsports-2016-096130.

Boyer, A., Hug, F., Avrillon, S., and Lacourpaille, L. (2021). Individual differences in the distribution of activation among the hamstring muscle heads during stiff-leg Deadlift and Nordic hamstring exercises. *J. Sports Sci.*, 1–8. doi:10.1080/02640414.2021.1899405.

Burkin, D. J., Wallace, G. Q., Nicol, K. J., Kaufman, D. J., and Kaufman, S. J. (2001). Enhanced expression of the alpha 7 beta 1 integrin reduces muscular dystrophy and restores viability in dystrophic mice. *J. Cell Biol.* 152, 1207–18.

Calve, S., Jacobson, K. R., Lipp, S., Acuna, A., Leng, Y., and Bu, Y. (2020). Comparative analysis of the extracellular matrix proteome across the myotendinous junction. *J. Proteome Res.* 19, 3955–3967. doi:10.1021/acs.jproteome.0c00248.

Carlsson, L., Li, Z., Paulin, D., and Thornell, L. E. (1999). Nestin is expressed during development and in myotendinous and neuromuscular junctions in wild type and desmin knock-out mice. *Exp. Cell Res.* 251, 213–223. doi:10.1006/excr.1999.4569.

Charvet, B., Guiraud, A., Malbouyres, M., Zwolanek, D., Guillon, E., Bretaud, S., et al. (2013). Knockdown of col22a1 gene in zebrafish induces a muscular dystrophy by disruption of the myotendinous junction. *Development* 140, 4602–4613. doi:10.1242/dev.096024.

Crameri, R. M., Langberg, H., Magnusson, P., Jensen, C. H., Schrøoder, H. D., Olesen, J. L., et al. (2004). Changes in satellite cells in human skeletal muscle after a single bout of high intensity exercise. *J. Physiol.* 558, 333–340. doi:10.1113/jphysiol.2004.061846.

Curzi, D., Salucci, S., Marini, M., Esposito, F., Agnello, L., Veicsteinas, A., et al. (2012). How physical exercise changes rat myotendinous junctions: an ultrastructural study. *Eur J Histochem* 56, e19. doi:10.4081/ejh.2012.19.

Curzi, D., Sartini, S., Guescini, M., Lattanzi, D., Di Palma, M., Ambrogini, P., et al. (2016). Effect of Different Exercise Intensities on the Myotendinous Junction Plasticity. *PLoS One* 11, e0158059. doi:10.1371/journal.pone.0158059.

Dos Santos, M., Backer, S., Saintpierre, B., Izac, B., Andrieu, M., Letourneur, F., et al. (2020). Single-nucleus RNA-seq and FISH identify coordinated transcriptional activity in mammalian myofibers. *Nat. Commun.* 11. doi:10.1038/s41467-020-18789-8.

Dreyer, H. C., Blanco, C. E., Sattler, F. R., Schroeder, E. T., and Wiswell, R. A. (2006). Satellite cell numbers in young and older men 24 hours after eccentric exercise. *Muscle Nerve* 33, 242–53. doi:10.1002/mus.20461.

Eirale, C., Farooq, A., Smiley, F. a., Tol, J. L., and Chalabi, H. (2013). Epidemiology of football injuries in Asia: A prospective study in Qatar. *J. Sci. Med. Sport* 16, 113–117. doi:10.1016/j.jsams.2012.07.001.

Ekstrand, J., Hägglund, M., and Waldén, M. (2011). Epidemiology of muscle injuries in professional football (soccer). *Am. J. Sports Med.* 39, 1226–1232. doi:10.1177/0363546510395879.

Fluck, M., Tunc-Civelek, V., and Chiquet, M. (2000). Rapid and reciprocal regulation of tenascin-C and tenascin-Y expression by loading of skeletal muscle. *J Cell Sci* 113 (Pt 2, 3583–3591.

Frenette, J., and Côté, C. H. (2000). Modulation of structural protein content of the myotendinous junction following eccentric contractions. *Int. J. Sports Med.* 21, 313–320. doi:10.1055/s-2000-3774.

Hakim, C. H., Burkin, D. J., and Duan, D. (2013). Alpha 7 integrin preserves the function of the extensor digitorum longus muscle in dystrophin-null mice. *J. Appl. Physiol.* 115, 1388–1392. doi:10.1152/japplphysiol.00602.2013.

Hegyi, A., Péter, A., Finni, T., and Cronin, N. J. (2018). Region-dependent hamstrings activity in Nordic hamstring exercise and stiff-leg deadlift defined with high-density electromyography. *Scand. J. Med. Sci. Sports* 28, 992–1000. doi:10.1111/sms.13016.

Hyldahl, R. D., Nelson, B., Xin, L., Welling, T., Groscost, L., Hubal, M. J., et al. (2015). Extracellular matrix remodeling and its contribution to protective adaptation following lengthening contractions in human muscle. *FASEB J.* 29, 2894–2904. doi:10.1096/fj.14-266668.

Jacob, C. D. S., Rocha, L. C., Neto, J. P., Watanabe, I. S., and Ciena, A. P. (2019). Effects of physical training on sarcomere lengths and muscle-tendon interface of the cervical region in an experimental model of menopause. *Eur. J. Histochem.* 63, 131–135. doi:10.4081/ejh.2019.3038.

Jakobsen, J. R., Jakobsen, N. R., Mackey, A. L., Knudsen, A. B., Hannibal, J., Koch, M., et al. (2020). Adipocytes are present at human and murine myotendinous junctions. *Transl. Sport. Med.*, tsm2.212. doi:10.1002/tsm2.212.

Jakobsen, J. R., Jakobsen, N. R., Mackey, A. L., Koch, M., Kjaer, M., and Krogsgaard, M. R. (2018a). Remodeling of muscle fibers approaching the human myotendinous junction. *Scand. J. Med. Sci. Sport.* doi:10.1111/sms.13196.

Jakobsen, J. R., Jakobsen, N. R., Mackey, A. L., Koch, M., Kjaer, M., and Krogsgaard, M. R. (2018b). Remodeling of muscle fibers approaching the human myotendinous junction. *Scand. J. Med. Sci. Sports*. doi:10.1111/sms.13196.

Jakobsen, J. R., Mackey, A. L., Knudsen, A. B., Koch, M., Kjaer, M., and Krogsgaard, M. R. (2016). Composition and adaptation of human myotendinous junction and neighboring muscle fibers to heavy resistance training. *Scand. J. Med. Sci. Sports*. doi:10.1111/sms.12794.

Jakobsen, J. R., Mackey, A. L., Knudsen, A. B., Koch, M., Kjær, M., and Krogsgaard, M. R. (2017). Composition and adaptation of human myotendinous junction and neighboring muscle fibers to heavy resistance training. *Scand. J. Med. Sci. Sport.* 27. doi:10.1111/sms.12794.

Jakobsen, J. R., Schjerling, P., Svensson, R. B., Buhl, R., Carstensen, H., Koch, M., et al. (2021). RNA-sequencing and immunofluorescence of the myotendinous junction of mature horses and humans. *Am. J. Physiol. Physiol.* doi:10.1152/AJPCELL.00218.2021.

Jensen, S. M., Bechshøft, C. J. L., Heisterberg, M. F., Schjerling, P., Andersen, J. L., Kjaer, M., et al. (2020). Macrophage Subpopulations and the Acute Inflammatory Response of Elderly Human Skeletal Muscle to Physiological Resistance Exercise. *Front. Physiol.* 11. doi:10.3389/fphys.2020.00811.

Jeremic, N., Chaturvedi, P., and Tyagi, S. C. (2017). Browning of White Fat: Novel Insight Into Factors, Mechanisms, and Therapeutics. *J. Cell. Physiol.* 232, 61–68. doi:10.1002/jcp.25450.

Kadi, F., Charifi, N., Denis, C., Lexell, J., Andersen, J. L., Schjerling, P., et al. (2005). The behaviour of satellite cells in response to exercise: What have we learned from human studies? *Pflugers Arch. Eur. J. Physiol.* 451, 319–327. doi:10.1007/s00424-005-1406-6.

Kim, M., Franke, V., Brandt, B., Lowenstein, E. D., Schöwel, V., Spuler, S., et al. (2020). Single-nucleus transcriptomics reveals functional compartmentalization in syncytial skeletal muscle cells. *Nat. Commun.* 11. doi:10.1038/s41467-020-20064-9.

Kleeberger, W., Bova, G. S., Nielsen, M. E., Herawi, M., Chuang, A. Y., Epstein, J. I., et al. (2007). Roles for the stem cell-associated intermediate filament nestin in prostate cancer migration and metastasis. *Cancer Res.* 67, 9199–9206. doi:10.1158/0008-5472.CAN-07-0806.

Kojima, H., Sakuma, E., Mabuchi, Y., Mizutani, J., Horiuchi, O., Wada, I., et al. (2008). Ultrastructural changes at the myotendinous junction induced by exercise. *J Orthop Sci* 13, 233–239. doi:10.1007/s00776-008-1211-0.

Lendahl, U., Zimmerman, L. B., and McKay, R. D. G. (1990). CNS stem cells express a new class of intermediate filament protein. *Cell* 60, 585–595. doi:10.1016/0092-8674(90)90662-X.

Lindqvist, J., Torvaldson, E., Gullmets, J., Karvonen, H., Nagy, A., Taimen, P., et al. (2017). Nestin contributes to skeletal muscle homeostasis and regeneration. *J. Cell Sci.* 130, 2833–2842. doi:10.1242/jcs.202226.

Matsumura, K., and Campbell, K. P. (1994). Dystrophin-glycoprotein complex: Its role in the molecular pathogenesis of muscular dystrophies. *Muscle Nerve* 17, 2–15. doi:10.1002/mus.880170103.

Moffatt, P., and Thomas, G. P. (2009). Osteocrin - Beyond just another bone protein? *Cell. Mol. Life Sci.* 66, 1135–1139. doi:10.1007/s00018-009-8716-3.

Mondello, M. R., Bramanti, P., Cutroneo, G., Santoro, G., Di Mauro, D., and Anastasi, G. (1996). Immunolocalization of the costameres in human skeletal muscle fibers: confocal scanning laser microscope investigations. *Anat. Rec.* 245, 481–7. doi:10.1002/(SICI)1097-0185(199607)245:3<481::AID-AR4>3.0.CO;2-V.

Nishizawa, H., Matsuda, M., Yamada, Y., Kawai, K., Suzuki, E., Makishima, M., et al. (2004). Musclin, a Novel Skeletal Muscle-derived Secretory Factor. *J. Biol. Chem.* 279, 19391–19395. doi:10.1074/jbc.C400066200.

Noonan, T. J., and Garrett, W. E. (1992). Injuries at the myotendinous junction. *Clin. Sports Med.* 11, 783–806.

Orchard, J., and Seward, H. (2002). Epidemiology of injuries in the Australian Football League, seasons 1997-2000. *Br. J. Sports Med.* 36, 39–44. doi:10.1136/bjsm.36.1.39.

Pardo, J. V., D'Angelo Siliciano, J., and Craig, S. W. (1983). A vinculin-containing cortical lattice in skeletal muscle: Transverse lattice elements ('costameres') mark sites of attachment between myofibrils and sarcolemma. *Proc. Natl. Acad. Sci. U. S. A.* 80, 1008–1012. doi:10.1073/pnas.80.4.1008.

Passerieux, E., Rossignol, R., Letellier, T., and Delage, J. P. (2007). Physical continuity of the perimysium from myofibers to tendons: involvement in lateral force transmission in skeletal muscle. *J Struct Biol* 159, 19–28. doi:10.1016/j.jsb.2007.01.022.

Petersen, J., Thorborg, K., Nielsen, M. B., Budtz-Jorgensen, E., and Holmich, P. (2011). Preventive effect of eccentric training on acute hamstring injuries in men's soccer: a cluster-randomized controlled trial. *Am J Sport. Med* 39, 2296–2303. doi:10.1177/0363546511419277.

Petrany, M. J., Swoboda, C. O., Sun, C., Chetal, K., Chen, X., Weirauch, M. T., et al. (2020). Single-nucleus RNA-seq identifies transcriptional heterogeneity in multinucleated skeletal myofibers. *Nat. Commun.* 11. doi:10.1038/s41467-020-20063-w.

Sahlgren, C. M., Pallari, H. M., He, T., Chou, Y. H., Goldman, R. D., and Eriksson, J. E. (2006). A nestin scaffold links Cdk5/p35 signaling to oxidant-induced cell death. *EMBO J.* 25, 4808–4819. doi:10.1038/sj.emboj.7601366.

Seagrave, R. A., Perez, L., McQueeney, S., Toby, E. B., Key, V., and Nelson, J. D. (2014). Preventive Effects of Eccentric Training on Acute Hamstring Muscle Injury in Professional Baseball. *Orthop. J. Sport. Med.* 2, 2325967114535351. doi:10.1177/2325967114535351.

Shimomura, M., Horii, N., Fujie, S., Inoue, K., Hasegawa, N., Iemitsu, K., et al. (2021). Decreased muscle-derived musclin by chronic resistance exercise is associated with improved insulin resistance in rats with type 2 diabetes. *Physiol. Rep.* 9. doi:10.14814/phy2.14823.

Singh, D. P., Lonbani, Z. B., Woodruff, M. A., Parker, T. J., Steck, R., and Peake, J. M. (2017). Effects of topical icing on inflammation, angiogenesis, revascularization, and myofiber regeneration in skeletal muscle following contusion injury. *Front. Physiol.* 8, 93. doi:10.3389/fphys.2017.00093.

Small, J. V., Fürst, D. O., and Thornell, L. -E (1992). The cytoskeletal lattice of muscle cells. *Eur. J. Biochem.* 208, 559–572. doi:10.1111/j.1432-1033.1992.tb17220.x.

Subbotina, E., Sierra, A., Zhu, Z., Gao, Z., Koganti, S. R. K., Reyes, S., et al. (2015). Musclin is an activity-stimulated myokine that enhances physical endurance. *Proc. Natl. Acad. Sci. U. S. A.* 112, 16042–

16047. doi:10.1073/pnas.1514250112.

Takakuwa, O., Maeno, K., Kunii, E., Ozasa, H., Hijikata, H., Uemura, T., et al. (2013). Involvement of intermediate filament nestin in cell growth of small-cell lung cancer. *Lung Cancer* 81, 174–179. doi:10.1016/j.lungcan.2013.04.022.

Tidball, J. G., Salem, G., and Zernicke, R. (1993). Site and mechanical conditions for failure of skeletal muscle in experimental strain injuries. *J. Appl. Physiol.* 74, 1280–1286. doi:10.1152/jappl.1993.74.3.1280.

Vaittinen, S., Lukka, R., Sahlgren, C., Hurme, T., Rantanen, J., Lendahl, U., et al. (2001). The expression of intermediate filament protein nestin as related to vimentin and desmin in regenerating skeletal muscle. *J. Neuropathol. Exp. Neurol.* 60, 588–597. doi:10.1093/jnen/60.6.588.

Vaittinen, S., Lukka, R., Sahlgren, C., Rantanen, J., Hurme, T., Lendahl, U., et al. (1999). Specific and innervation-regulated expression of the intermediate filament protein nestin at neuromuscular and myotendinous junctions in skeletal muscle. *Am. J. Pathol.* 154, 591–600. doi:10.1016/S0002-9440(10)65304-7.

Van Der Horst, N., Smits, D. W., Petersen, J., Goedhart, E. A., and Backx, F. J. G. (2015). The Preventive Effect of the Nordic Hamstring Exercise on Hamstring Injuries in Amateur Soccer Players: A Randomized Controlled Trial. *Am. J. Sports Med.* 43, 1316–1323. doi:10.1177/0363546515574057.

Supplemental files:

Description of exercise program:

The training program included three eccentric hamstring exercises; The Nordic Hamstring, lying leg curl and stiff-legged deadlift. All of which consisted of 3 sets of 6-8 repetitions performed until exhaustion with 2 minutes between each set. In addition to the hamstring exercises, the participants also did two exercises targeting the quadriceps muscles in order to train both the front and back thigh muscles. The seated leg extension and leg press was included and completed between the hamstring exercises in order to give the participants a longer break from the very intensive eccentric work. Therefore, the participants were also instructed to perform these exercises with an intensity that still felt comfortable.

In addition to the hamstring exercises, the participants also performed two exercises targeting the quadriceps muscles in order to train both the front and back thigh muscles. The seated leg extension and leg press was included and completed between the hamstring exercises in order to give the participants a longer break from the very intensive eccentric work. Therefore, the participants were also instructed to perform these exercises with an intensity that still felt comfortable.

The Nordic Hamstring exercise was performed as previously described with heels fixed under a step-bench and knees placed on a foam mat (Jakobsen et al., 2017) (Figure 1). From here the participants leaned forward with the hips as straight as possible until they were unable to control the movement and fell to the floor. They were instructed to avoid lifting themselves up again using their hamstrings and instead raising

themselves back up using their arms.

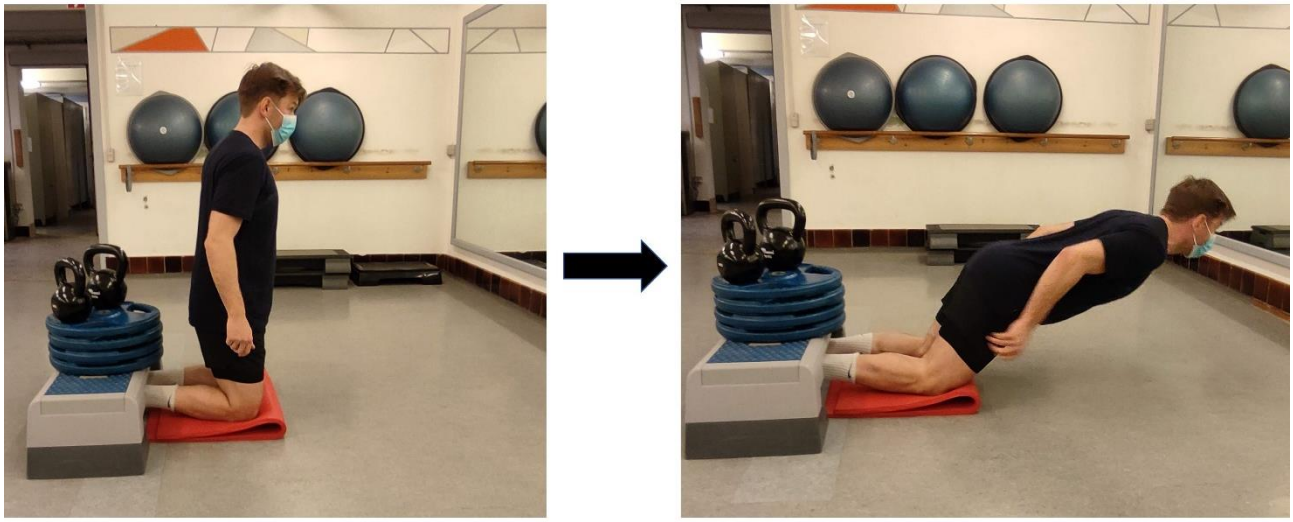

Figure 1: Nordic Hamstring exercise.
To perform the Nordic Hamstring exercise the participants tugged their heels under a step-bench (left image) and from here slowly lowered their upper-body towards the floor while contracting the hamstring muscles until they were unable to give hold and drifted to the floor.

The lying leg curl was performed unilaterally in a Prone Leg Curl machine from Technogym (Figure 2). Following a light set to get accustomed to the machine and find the right position of the leg, a concentric 1 repetition max (RM) test was done. This was used as indicator of the load for the subsequent eccentric sets. To make the exercise purely eccentric the pad was lifted by the instructor and the participant was told to flex their injured knee until their heel reached the pad. From here the instructor slowly released the pad so the weight was put on the heel of the participant, who subsequently slowly lowered the pad until full stretch of the knee. An effort was made to do this slowly, so that each repetition lasted around 6 seconds. In the bottom position the pad was again lifted by the instructor and the second repetition performed. The weight was initially set to the concentric 1RM but was adjusted (increased or decreased) so the participant was able to perform three sets of 6-8 repetitions to exhaustion.

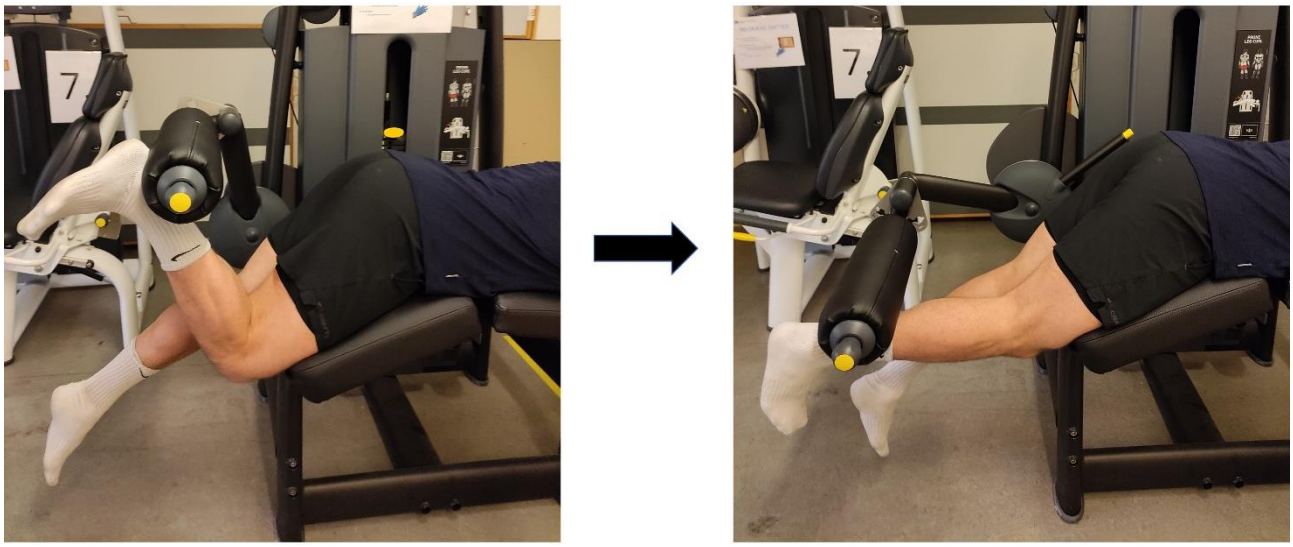

Figure 2: Unilateral eccentric lying leg curl.
The image to the left shows the starting position in the unilateral eccentric lying leg curl exercise. Prior to the image the pad had been lifted by the instructor. From the starting position the participant slowly lowered the pad until the knee is stretched.

The last exercise was the stiff-legged deadlift. (Figure 3) A barbell was arranged in height so that the participants could reach it with their hands while keeping their knees almost fully extended and their lower back straight and close to parallel to the floor. The participants started the lift by bending their knee and lifting the bar to a standing position as they would do in a regular deadlift. By allowing them to bend the knee the concentric movement was easier for the hamstrings and back muscles and a heavier weight could be lifted. From here they slowly lowered the bar towards the ground keeping their knees close to full extension and their back straight until the bar was back in the starting position. The weights were adjusted so that all sets were performed to exhaustion while keeping a proper form.

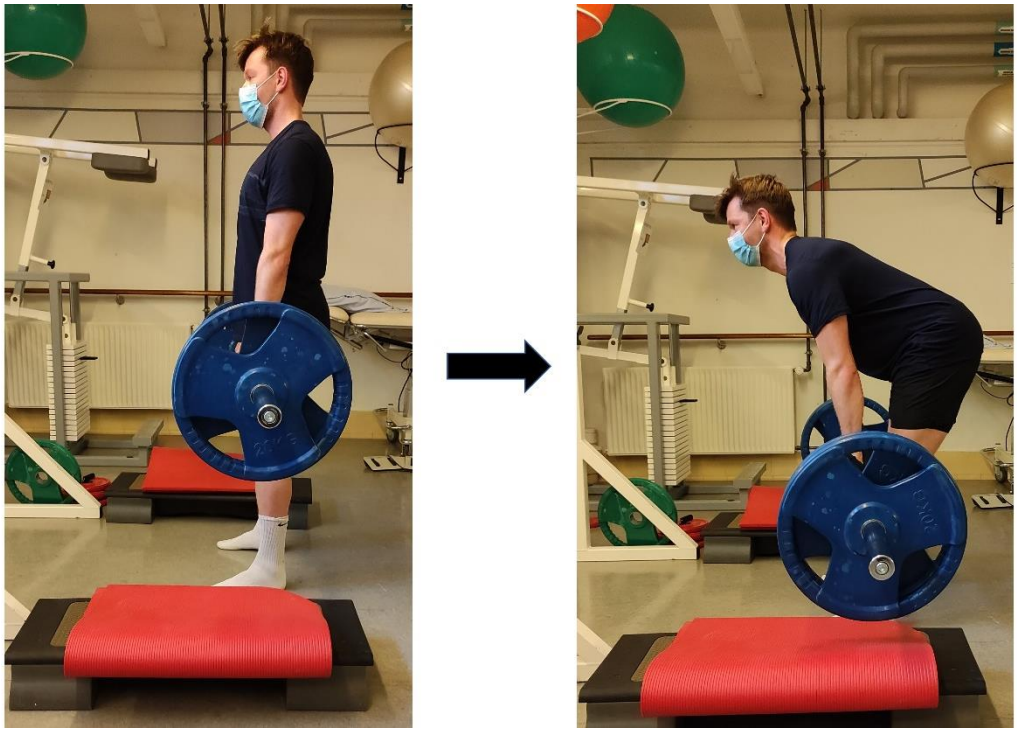

Figure 3: Stiffed-leg deadlift.
From a standing position (left image) the participant slowly lowered the bar while keeping his legs almost straight and a neutral spine until the weights reached the boxes (right image). Prior to the left image the participant has lifted the bar from the boxes making sure he bends his knees to use his quadriceps and take some of the load off the hamstrings in the concentric movement.

qRT-PCR data relative to RPLP0:

a

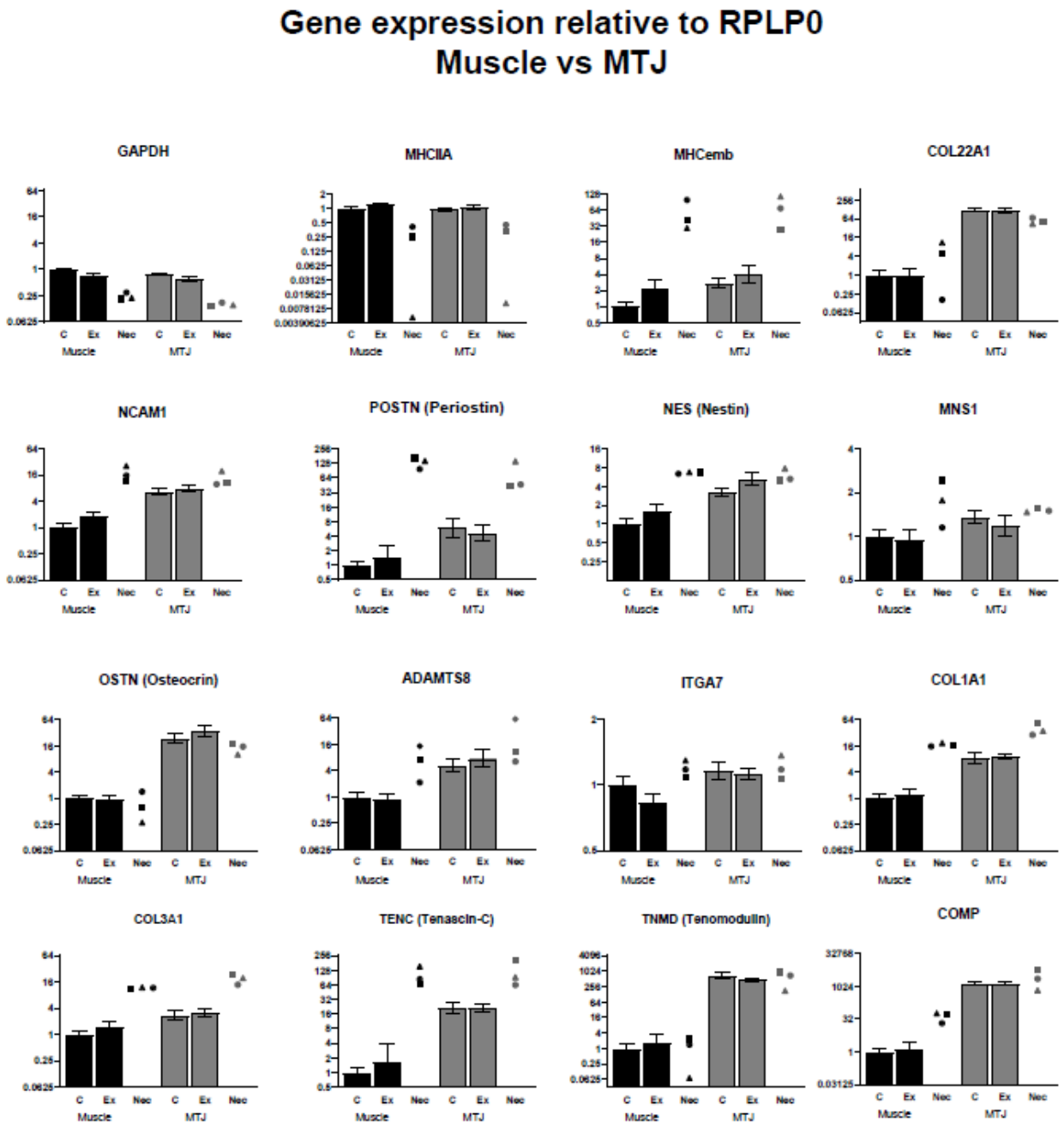

b

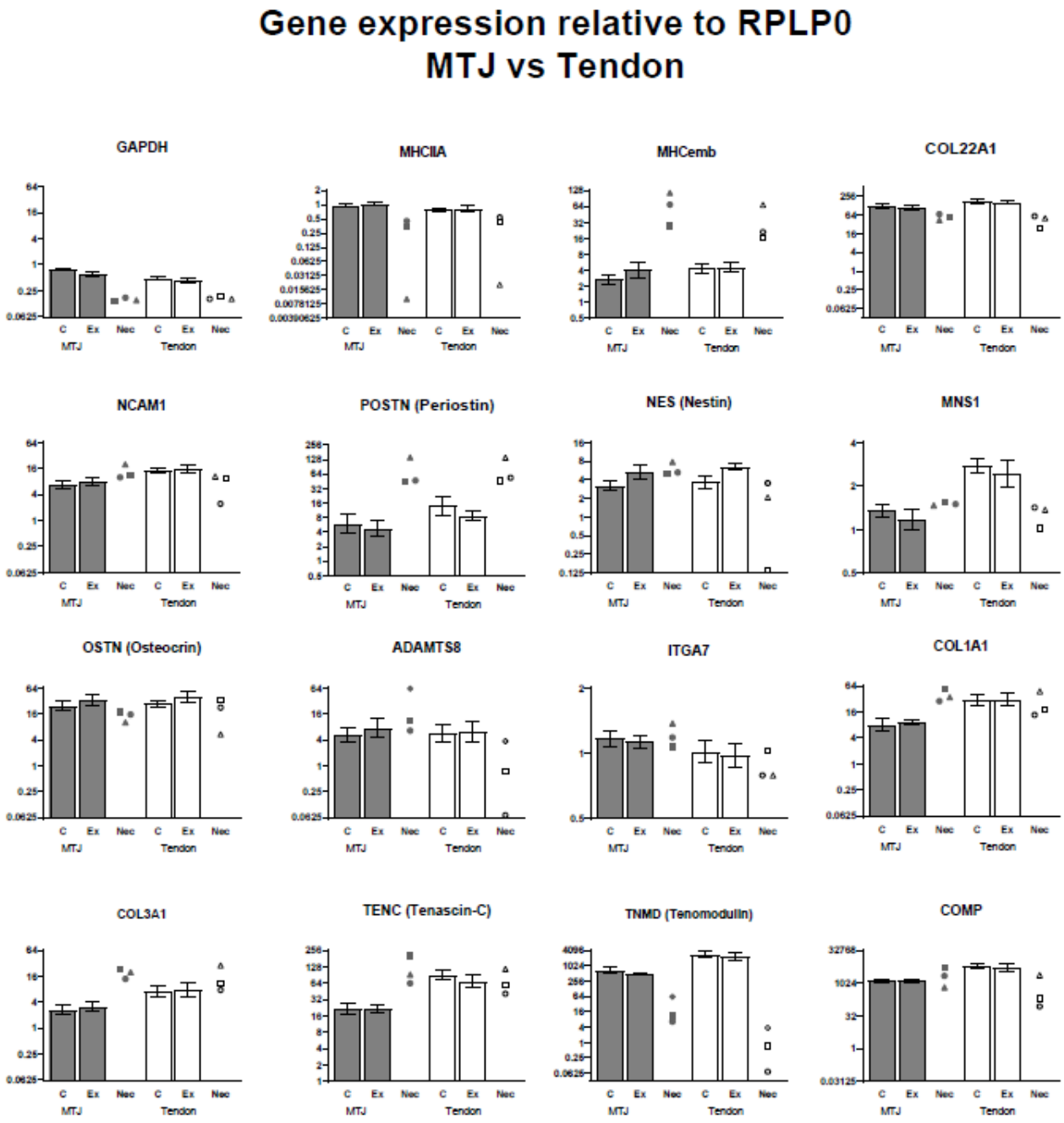

The graph shows the mRNA expression of the selected genes in muscle vs MTJ (a) and MTJ vs tendon (b) normalized to RPLP0 and expressed relative to control muscle. Data shown as geometric mean ± back-transformed SEM. Individual values from three subjects with a high proportion of necrotic muscle fibers are shown as open circles. Due to large difference in the expression values between targets and to optimally illustrate the expression for each mRNA target the y-axis are different between targets.